Three and four dimensional computed tomographic angiography of free and pedicled flaps: investigating the vascular territories

Wong, Corrine Jui Yin

THREE AND FOUR DIMENSIONAL COMPUTED TOMOGRAPHIC ANGIOGRAPHY OF FREE AND PEDICLED FLAPS: INVESTIGATING THE VASCULAR TERRITORIES

Corrine Jui Yin Wong, M.B.B.S., M.R.C.S.

A thesis submitted in accordance with the requirements for the degree of Doctorate of Medicine, University of London

July 2011

Centre for Cutaneous Research
St. Bartholomew's and The Royal London
School of Medicine and Dentistry
Queen Mary and Westfield College
University of London

Dedicated to my husband Michael Watkins, whose love and support I treasure.

Acknowledgements

I am grateful to Mr. Simon Myers for his help, support and guidance through the sometimes murky waters of manuscript-/ thesis-writing; to Professor Harshad Navsaria for giving me the opportunity to explore the field of research; to Dr. Rod Rohrich and Dr. Spencer Brown for letting me use the UT Southwestern Medical Center Department of Plastic Surgery Research as a base and resource for my studies; and to Dr. Michel Saint-Cyr, whose torrent of ideas and wealth of knowledge basically gave birth to my studies and saw them to maturity.

Abstract

In plastic surgery, flap reconstruction has been utilised to repair defects in every part of the body, in an effort to restore form and function to patients. The basis of every flap is its blood supply, therefore this series of studies investigates the vascular territory of named arteries, veins and even perforators, utilizing computer tomography (CT) and TeraRecon software. The latter two is technology which allows appreciation of vascular flow in 3D and 4D (dynamic studies), whereas previous studies of vascularity has only been static and in 2D. Vascular anatomy studies were performed using fresh cadavers. Perforator flaps on the anterior trunk studied were the internal mammary artery perforator (IMAP) flap, the transverse rectus abdominis musculocutaneous (TRAM) flap, the deep inferior epigastric artery perforator (DIEP) flap and the superficial inferior epigastric artery (SIEA) flap. Posterior trunk flaps included the posterior intercostal artery perforator flap, the lumbar artery perforator flap and the superior gluteal artery perforator (SGAP) flap. In the upper extremity, we studied the supraclavicular artery perforator flap. In the lower extremity, we studied the gracilis musculocutaneous flap. Trends and characteristics are noted in the vascular analyses, and four major principles drawn are discussed in the last chapter.

Contents

List of Tables

List of Figures

Page

Chapter 2

Chapter 3

Chapter 4

Chapter 5

Video Figure Legend

2.1.1

Injection of an IMAP in ICS 2 shows flow traveling in a transverse direction

2.1.2

Injection of an IMAP in ICS 3 shows flow traveling in an infero-lateral direction

2.2.1

Perfusion of right deep inferior epigastric artery (in full width TRAM flap). A dominant medial row perforator is demonstrated, as perfusion extends from zone I to zone II, then finally zone III.

2.2.2

Perfusion of left deep inferior epigastric artery (in full width TRAM flap). A dominant lateral row perforator is demonstrated, as perfusion extends from zone I to zone III, then finally zone II.

2.2.3

Injection of contrast into a single medial row deep inferior epigastric artery perforator. Contrast traveled earlier to zone II, which had a greater area of perfusion compared to zone III

2.2.4

Injection of contrast into a single lateral row deep inferior epigastric artery perforator. Contrast traveled earlier to zone III, which had a greater area of perfusion compared to zone II

2.4.1

Injection of contrast into a superior gluteal artery perforator perfuses the whole flap

2.4.2

Lateral view of video 2.4.1. Recurrent flow into the adjacent perforator is demonstrated via the subdermal plexus (bottom layer)

3.1

Injection of contrast into a supraclavicular artery flap

3.2

Injection of contrast into another supraclavicular flap. Contrast is seen entering and filling adjacent perforators' vascular territory

CHAPTER 1

Introduction

History

Manchot, Salmon, Taylor, McCormack and others have been instrumental in increasing our knowledge of the vascular anatomy of the skin and deeper tissues (e.g. fascia, bone, etc.) of the body[1-8]. Perforator flaps represent the latest descendent in a line of evolution that begun with the random-pattern flap. The random pattern flap, which by definition lacked an axial arteriovenous system, was constrained by rigorous length-to-width ratios to ensure viability. These flaps were used as local and tube pedicled flaps, and it was not until Milton in 1970 revealed in the pig model that flaps made under similar conditions of blood supply survived to the same length regardless of width, and that the only effect of decreasing width is to decrease the chance of a pedicle containing a large vessel. The axial pattern flap, coined by 1972 McGregor and Jackson in their classic description of the groin flap and first introduced by Bakamjian in the description of the deltopectoral flap, represented the next milestone in flap development. In was in the 1970’s that the works of Manchot, which had lain untranslated in German since 1889, were discovered, revealing that many axial flaps were based on vessels that had already been described by him, as well as the concept that each cutaneous artery supplied a discrete skin vascular territory. Manchot had completed his work in only six months whilst a medical student, and submitted it for a competition arranged by the medical faculty of the University of Strasbourg. Musculocutaneous flaps were first described by Ger and by Orticochea in 1972, and rapidly became popular due to their reliability and wide arcs of rotation. Descriptions of their vascular territories were later provided by McCraw et al, and by Mathes and Nahai. In 1981 Pontén reported his series of flaps on the lower leg, noting that inclusion of the deep fascia achieved length-to-width ratios in excess of 2.5:1 in an area where local skin flaps had previously been unsuitable. The anatomical basis for these flaps was soon described by Haertsch, Barclay et al., and by Cormack and Lamberty. In 1980 Taylor set out to reappraise the work of Manchot, and in 1982 through a communication with Lamberty in 1982 learnt of the works of Salmon which had been written in 1936 but which remained untranslated in French. Salmon's monumental work was a reappraisal of the work of Manchot using radiography. Although Salmon had noted that the presence of arterial territories both within the skin and muscle, it was in 1987 that Taylor and Palmer published their work on defining the vascular territories of source arteries, introducing the concept of angiosomes, three-dimensional anatomic territories supplied by a source artery that spans between the skin and bone, which has proven invaluable in flap design.

In 1984 Song et al. had described their clinical experience with the 'septocutaneous artery flap' from the anterolateral, anteromedial, and posterior thigh. The perforator flap concept was introduced by Kroll and Rosenfield in 1988 in their description new type of flap based on unnamed perforators located near the midline of the lower back region for low posterior midline defects. They noted that such flaps combined the superior blood supply of the myocutaneous flap with the lack of donor-site morbidity of a skin flap. The beginning of the perforator flap area was crystalised in 1989 when Koshima and Soeda described an inferior epigastric artery skin flap without rectus abdominis muscle pedicled on the muscle perforators and the proximal inferior deep epigastric artery for the reconstruction of floor of the mouth and groin defects. They noted that a large flap without muscle could survive on a single muscle perforator, and the perforator flap era had begun.

Advantages of perforator flaps over musculocutaneous flaps include reduced morbidity to the form and function of the donor site by preservation of the underlying muscle, often leading to faster recovery, and the ability to tailor the flap to reconstruct exactly the tissues that are missing at the recipient site. Musculocutanoeus flaps tend to cause bulkiness at the recipient site and when denervated may atropy at an unpredictable rate, leading to poor aesthetic results. A perforator flap may also be thinned either as a one- or two-stage procedure allowing contouring of shallow defects that is not possible with a musculcutanous flap. There is also freedom of orientation of the pedicle, and a longer pedicle than can be achieved with the parent musculocutaneous flap.

The vast majority of anatomical vascular studies in the past have used lead oxide injection and two-dimensional radiography to determine vascular territories. Although lead oxide treated specimens provide excellent images, limitations of this methodology include only allowing 2- dimensional analysis, and gives static images. In contrast three and four dimension radiography can provide not only qualitative data on vascular anatomy, but information on the direction and path of blood flow through the tissue planes of an injected flap. Three dimensional anatomy is defined as an appraisal of the perforator vasculature in the sagittal, coronal and transverse views whereas four-dimensional anatomy refers to sequential images produced by repeated scanning as contrast flows through the flap. This results in a video of simulated flap perfusion.

Although Taylor and Palmer have been instrumental in increasing our knowledge of vascular anatomy via the angiosome concept, this theory is based on the vascular supply of source arteries[4-6]. In the present era of perforator flaps, interest has shifted from the source artery to the perforator itself. A further consideration is to determine the dynamic vascular properties of perforator flaps. Whole body static imaging (as illustrated in Taylor et al.'s studies) does not provide an accurate description of a single perforator's vascular distribution and flow characteristics. In order to truly understand and determine a single perforator's vascular territory, this perforator must be cannulated and injected. Knowledge of the axiality of blood flow, connections with adjacent perforators and contribution to the subdermal plexus and fascia are all vital when designing perforator flaps.

Aims and Objectives

1. To measure the vascular territories of selected vessels (arteries, veins and perforators)
2. To define the anatomical structure of vessels with the use of 3D CT angiography
3. To investigate the perfusion characteristics of selected vessels using 4D CT angiography
4. To define arterial "perforasomes" in the body in order to better guide perforator flap design in clinical use.

Materials and Methods (General)

Vascular anatomy studies were performed using fresh cadavers which were acquired through the Willed Body Program at the University of Texas Southwestern Medical Center. The cadavers were less than a week old and were kept in a cold facility when not being utilized for the development of flaps. Several studies would be undwerway simultaneously, so multiple flaps were harvested from a single cadaver.

Dissection of all vessels was performed under loupe magnification. Injection of a dilute methylene blue solution through all the vessels defined their course, and allowed identification of any leaking in the periphery of the flap or under surface of the flap.

Perforator flaps on the anterior trunk studied were the internal mammary artery perforator (IMAP) flap, the transverse rectus abdominis musculocutaneous (TRAM) flap, the deep inferior epigastric artery perforator (DIEP) flap and the superficial inferior epigastric artery (SIEA) flap. Posterior trunk flaps included the posterior intercostal artery perforator flap, the lumbar artery perforator flap and the superior gluteal artery perforator (SGAP) flap. In the upper extremity, we studied the supraclavicular artery perforator flap. In the lower extremity, we studied the gracilis musculocutaneous flap.

All surgical landmarks relevant to flap design were marked, and each perforator flap was dissected based on the largest perforator originating from its own main source pedicle. Following flap dissection, the vessel was cannulated using a 24 gauge butterfly catheter (0.7 mm in diameter, BD Insyte, Becton-Dickinson S,A, Madrid Spain). Methylene blue solution was infiltrated into the flap to identify vascular leaks which were then either coagulated using bipolar or ligated using silk sutures. The use of surgical clips was avoided to prevent CT angiography artifact.

Dynamic Computer Tomographic Scan Protocol: 4D-CTA

Four dimensional CTA is similar to 3D-CTA but with the added 4^{th} element of time. Flaps were scanned with contrast medium injected simultaneously during a pre-determined time interval in order to appreciate the characteristics and distribution of vascular perfusion. In contrast, 3D CT angiography involves scanning flaps which have already been pre-injected and results in a static image only.

Prior to scanning, each flap was set on individual styrofoam trays and secured with sutures at key points at the periphery, to maintain their shape and orientation as the flap is scanned at 30° from vertical. To minimize scanning slices needed for each flap the CT gantry is tilted at 30° and the flaps on their styrofoam trays are set on a custom-built platform that 'presents' the flap at 30° to the CT scanner (as opposed to laying it flat on the table, which would require many more helical scans). The flaps were also placed skin downward to avoid pressure on the pedicle and to minimize the risk of increased resistance during vascular imaging and perfusion. Iodinated contrast (Isovue^{R}, Bracco Diagnostics) was heated to 37° C (to reduce viscosity) prior to filling a syringe. The volumes of contrast medium required for flap imaging range from 2 ml to 5 ml, depending on flap size.

Single vessel/perforator injections were carried out with a Harvard precision pump (PHD 2000, Harvard Apparatus, Inc.) running at 0.5ml/minute, and the flap subjected to dynamic CT scanning using a GE Lightspeed sixteen slice scanner (General Electric, Milwaukee, WI) set to perform 0.625 mm slices using a 0.5 second rotation time. Each scan was set to 80 kVp and current ran at 300 mA. Scans were repeated at 0.125ml increments (every 15 seconds) for the first 1 ml, then at 0.5ml increments (every 60 seconds) for the next 2-4 ml, thus giving us progressive CT images over time[9-12].

Static Computer Tomographic Scan Protocol: 3D-CTA

A barium-gelatin mixture was prepared by warming 100ml of normal saline to 40°C, and adding 3g of gelatin while stirring continuously. This was followed by slowly adding 40g of barium sulphate[13]. This solution is then injected into the investigated perforator artery using the Harvard precision pump running at 1 ml/min until the vascular tree is saturated (previously repaired leaks will start to leak and have to be re-cauterized or ligated). The flaps were then frozen for at least 24 hours prior to CT scanning.

Powerful visualization tools are needed to take full advantage of the high-resolution multi-phase volumetric datasets. We used the AquariusNET server and thin client application (TeraRecon, Inc, San Mateo, CA) which manages up to 28,000 CT slices simultaneously and allowed viewing of three- and four-dimensional images. The volume rendering function allowed us to produce clear and accurate images of the simulated flaps. Manipulation of static three-dimensional images from different angles (with the mouse) enabled us to clearly visualize branching patterns of perforators as well as the characteristics of their linking vessels. The dynamic images demonstrated the axiality or preferential direction of flow. Certain functions such as measurement of area allowed us to compare marked out areas of flap perfusions.

CHAPTER 2

Trunk

2.1 CHEST: Internal Mammary Artery Perforator (IMAP) Flap

Introduction

Although free tissue transfer methods have been added to the head and neck reconstruction armamentarium, local or regional flaps are still widely used as there is good tissue match in terms of color, texture and thickness, and they can present relatively rapid options in otherwise compromised patients. These include the deltopectoral, pectoralis major, trapezius and latissimus dorsi flaps. The deltopectoral flap was once the workhorse for head and neck reconstruction[14, 15], although its use was limited by a high rate of flap necrosis[16, 17], the need for skin grafting of the donor site, and the dog-ear created by its pedicle. The pectoralis major flap tends to be bulky and can result in a poor cosmetic outcome for both donor and recipient sites.

Since the description of the perforator flap concept by Koshima, new types of perforator flaps have been described for neck reconstruction including the supraclavicular flap[18, 19] and the internal mammary artery perforator (IMAP) flap. The IMAP flap has been reported in the reconstruction of tracheostomas[20] and the anterior neck[21, 22]. It replaces the deltopectoral flap in its indications while avoiding the disadvantages of this flap.

Previous anatomical studies of the internal mammary artery perforators have reported the number, location and sizes of the IMAPs[21, 23-25]. Ink injection studies have been carried out either on the internal mammary artery[24] or the perforators themselves[21]. These reflect the cutaneous territory of the perforators, but are unable to demonstrate the characteristics of the vessels within the tissue, or the communication either between adjacent perforators or between an IMAP and another artery such as the lateral thoracic artery.

Although Yu[20] and Vesely *et al*[21] speculated that there communications existed between the perforators in differing intercostals spaces, this has never been proven. In this study, we employed innovative three- and four-dimensional CT angiographic methods to precisely visualize the arterial and venous vascular anatomy of each perforator as well as the "axiality" of their perfusion.

Materials and Methods

Eleven hemichest adipo-cutaneous flaps were harvested from six fresh adult cadavers. One cadaver was male, and the rest were female. One hemichest was excluded from this study as there was an implanted cardiac device placed in the subcutaneous tissue close to the midline in the second and third rib area. We were unable to elevate the pectoral fascia whole with the flaps, as the thin fascia was found to be quite adherent to the underlying muscle. As such, all our flaps were dissected in a suprafascial plane. The margins of the adipo-cutaneous flap were the inferior border of the clavicle, midline of the chest, costal margin and mid-axillary line (Figure 2.1.1).

Specimen dissection was performed under loupe magnification, in a plane superficial to the thin pectoral fascia. We recorded the distance of each IMAP from the sternal edge, the number of perforators per hemichest and measured their external diameter. The perforator arteries/veins were individually cannulated with a 24 gauge catheter.

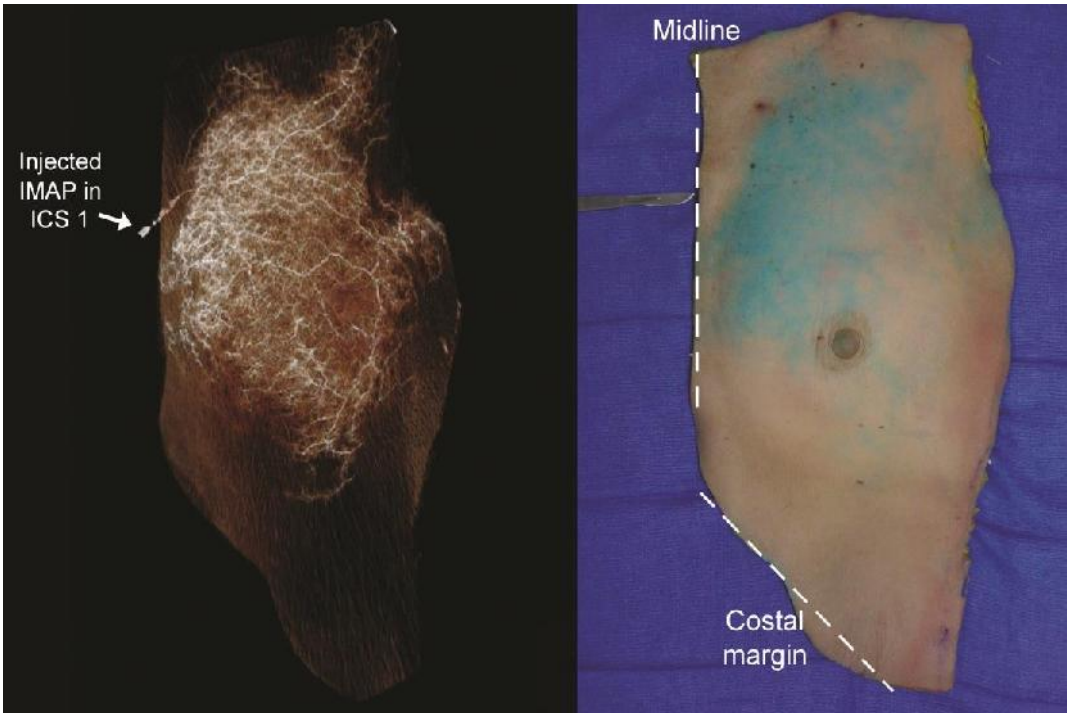

Figure 2.1.1 *Adipo-cutaneous flap of the chest is delineated by the inferior border of the clavicle, midline of the chest, costal margin, and mid-axillary line. Both pictures show the same flap, where the IMAP in intercostal space (ICS) 1 is injected with contrast on the left (3D CT scan), and methylene blue dye on the right (photograph-scalpel shows the level of the IMAP injected).*

Results

Eleven hemichest flaps were raised from six fresh cadavers. We were unable to elevate the pectoral fascia whole with the flaps, as the thin fascia was found to be quite adherent to the underlying muscle.

Each hemichest flap had one to three IMAP perforators, most commonly in intercostals spaces (ICS) 1, 2 and 3. We found that the number of perforators tended to be symmetrical, but not necessarily their locations (e.g. cadaver 2, where there were three perforators on both sides, but on the left side, the perforators were in intercostals spaces 1, 2 and 3, whereas on the right side, the perforators were located in intercostals spaces 2, 3 and 4). A total of twenty-six IMAPs were dissected, and nineteen of the perforator arteries as well as six perforator veins were injected with contrast for analysis of vascular territory (Table 2.1.1).

The mean perforator diameter for IMAPs in ICS-1 was 1.50mm (range 1.0-2.2mm), ICS 2 was 1.83mm (range 1.3-2.4mm) and ICS-3 was 1.47mm (range 1.3-1.7mm). The mean horizontal and vertical dimensions of the vascular territories are recorded in Table 2.1.2 using the measuring tool on the TeraRecon software.

Table 2.1.1

Internal mammary artery perforators identified - recorded intercostals space (ICS) and distance from sternal edge

Cadaver	1		2		3		4		5		6	
Hemichest	L	R	L	R	L	R	L	R	L	R	L	R
ICS† (mm from sternal edge)	1 (7)*	1 (0)	1 (10)	2 (0)*	2 (5)*	2 (10)*	n/a	1 (15)*	2 (9.3)*	1 (0)	1 (6.7)*	1 (0)*
			2 (0)	3 (26)*	6 (25)	6 (0)*		3 (55)*	3 (0)*	3 (32)	2 (5.2)*	2(0)*
			3 (37)	4 (0)	7 (0)			5 (12)			3 (0)	3 (0)

† ICS = Intercostal space
∗ Communicates with lateral thoracic artery

Table 2.1.2

Characteristics of internal mammary artery perforators and their vascular territories according to location (intercostal space)

IMAP in intercostal space	1	2	3	6	7
Number of perforators injected	6	6	5	1	1
Mean horizontal length of vascular territory (mm)	183	198	164	229*	163
Mean vertical length of vascular territory (mm)	221	271	219	288*	172
Mean diameter of perforator (mm)	1.5	1.83	1.47	1.3	0.8
Mean distance from sternal edge (mm)	5.5	4.2	21	0	0

*Lateral thoracic artery forms a ‘bridge’ between perforators’ territory, hence enlarging vascular territory of IMAP in ICS 6

Perforator arteries (arterial perforasomes)

Injection of single internal mammary perforators demonstrated large vascular territories (Table 2.1.3). Internal mammary artery perforators in ICS-1 perfused to the level of the clavicle and lateral mammary fold (LMF) in all cases and to the level of the xiphisternum one-third of the time. Internal mammary artery perforators in ICS-2 had a territory reaching the clavicle and xiphisternum in four out of six cases, and the LMF in all cases (Figure 2.1.2). Internal mammary artery perforators in ICS-3 only reached the clavicle in 40%, the xiphisternum in 60% and the LMF in 80% of cases. The IMAP in ICS-6 was found to perfused a large territory, as the lateral thoracic artery acted as a 'bridge' between its territory and that of the IMAP in ICS-2, thus giving it an even larger territory than any other IMAP (Figure 2.1.8 and Table 2.1.2). It did not reach the level of the clavicle, but did extend to the level of the xiphisternum and the LMF. The IMAP in ICS-7 had a territory reaching the xiphisternum, but not to the LMF or clavicle.

In our series, all of the IMAPs injected (18 out of 19) almost always perfused the nipple-areolar complex (NAC) including those in ICS-6 and ICS-7. The one IMAP that did not perfuse the NAC originated from ICS 1.

Table 2.1.3

Vascular territories of IMAPs according to their intercostals level

Extends to	Level of clavicle	Level of xiphisternum	NAC*	Lateral mammary fold	Lat Thor comm†
ICS 1 (n=6)	6/6	2/6	5/6	6/6	3/6
ICS 2 (n=6)	4/6	4/6	6/6	6/6	5/6
ICS 3 (n=5)	2/5	3/5	5/5	4/5	3/5
ICS 6 (n=1)	0/1	1/1	1/1	1/1	1/1
ICS 7 (n=1)	0/1	1/1	1/1	0/1	0/1

* NAC= Nipple areolar complex

† Communicates with the lateral thoracic artery

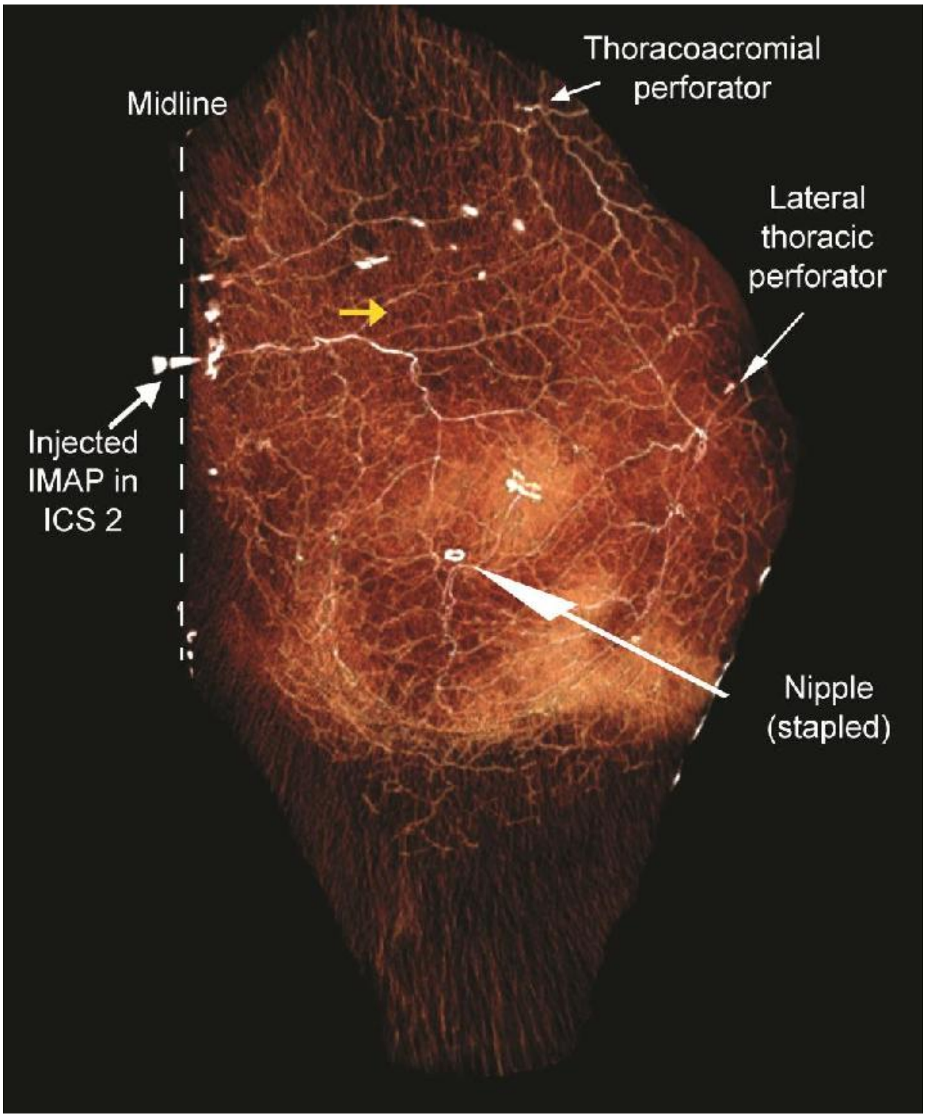

Figure 2.1.2 *3D CT scan of a flap where the IMAP in ICS 2 was injected with contrast. The vascular territory is found to encompass the nipple (stapled), and extends to the levels of the xiphisternum, clavicle and lateral mammary fold. Linking vessels are shown to communicate with perforators of the thoracoacromial and lateral thoracic artery. Yellow arrow shows direction of flow.*

Linking vessels

The phenomenon of linking vessels between adjacent IMAP(s) as well as linking vessels between the IMAP(s) and the lateral thoracic artery could explain why a single perforator can vascularize an adipo-cutaneous flap which is extensive in both its superior-inferior and medial-lateral dimensions. The linking vessels between adjacent IMAPs can be proximal to the pedicle of the flap (Figure 2.1.3) or distal (Figure 2.1.4). We have also found linking vessels between IMAPs and branches of the lateral thoracic artery (Figure 2.1.3, 2.1.7 and 2.1.8).

These communicating vessels were located at the subdermal level - indirect linking vessels, which we define as those that have to go through the subdermal plexus and reach the adjacent perforator through recurrent flow (Figure 2.1.5), or direct linking vessels which we determine to be midway between the dermis and the pectoral fascia (Figure 2.1.6).

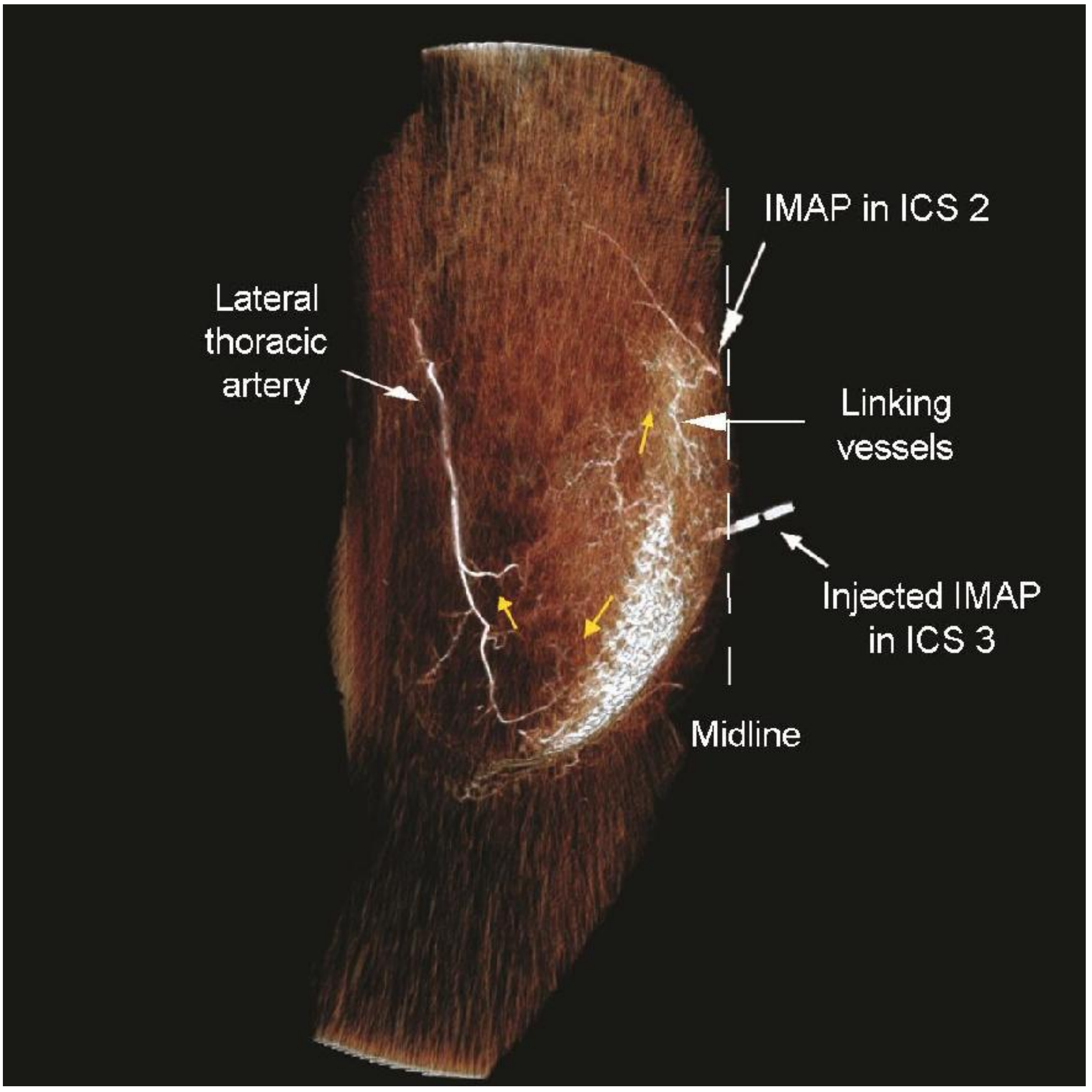

Figure 2.1.3 *3D CT scan of a flap where the IMAP in ICS 3 was injected with contrast. Linking vessels are found between adjacent IMAPs, located crania to the pedicle of the flap. Yellow arrows show direction of flow.*

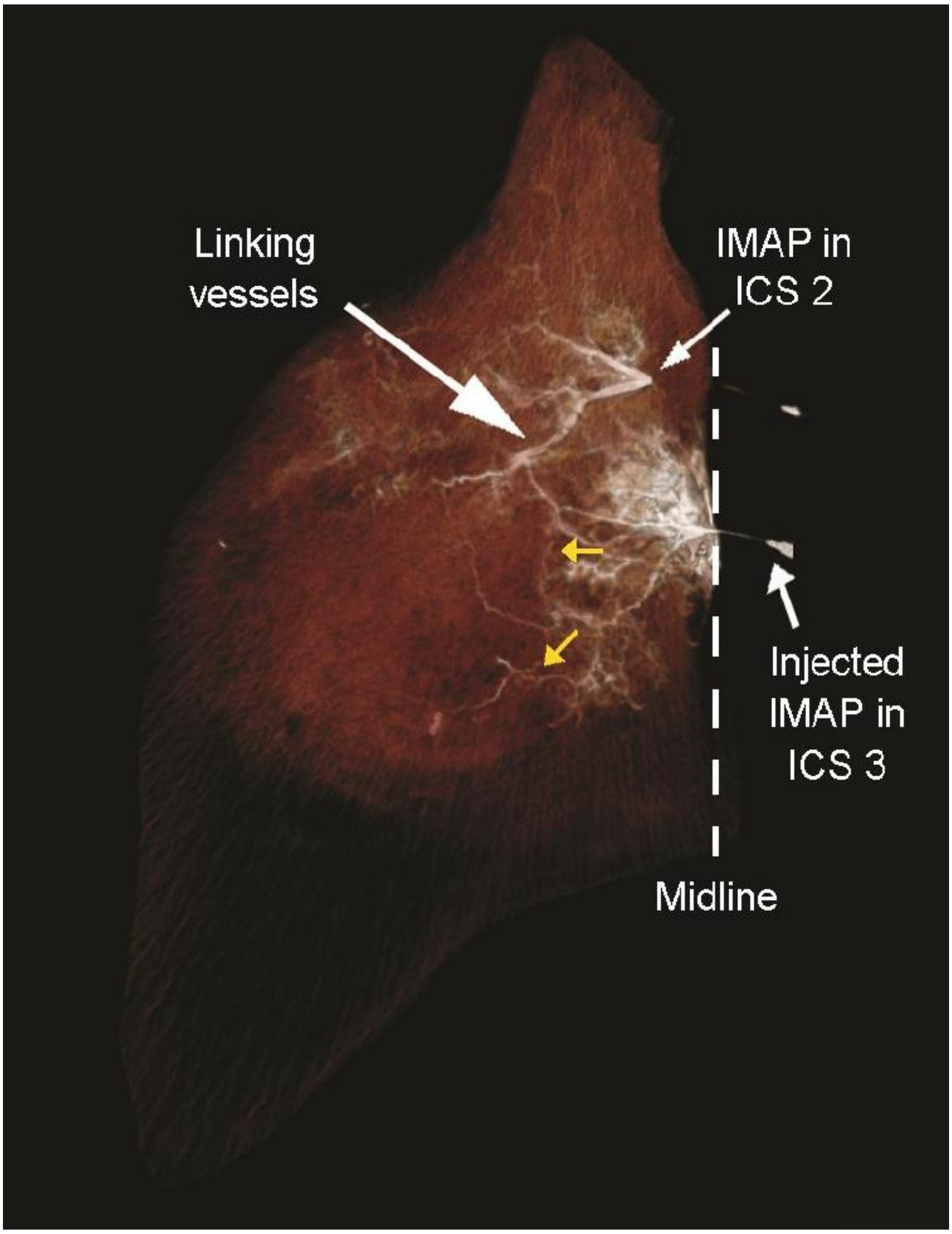

Figure 2.1.4 *3D CT scan of a flap where the IMAP in ICS 3 was injected with contrast. Linking vessels are found between adjacent IMAPs, located distal to the pedicle of the flap. Yellow arrows show direction of flow.*

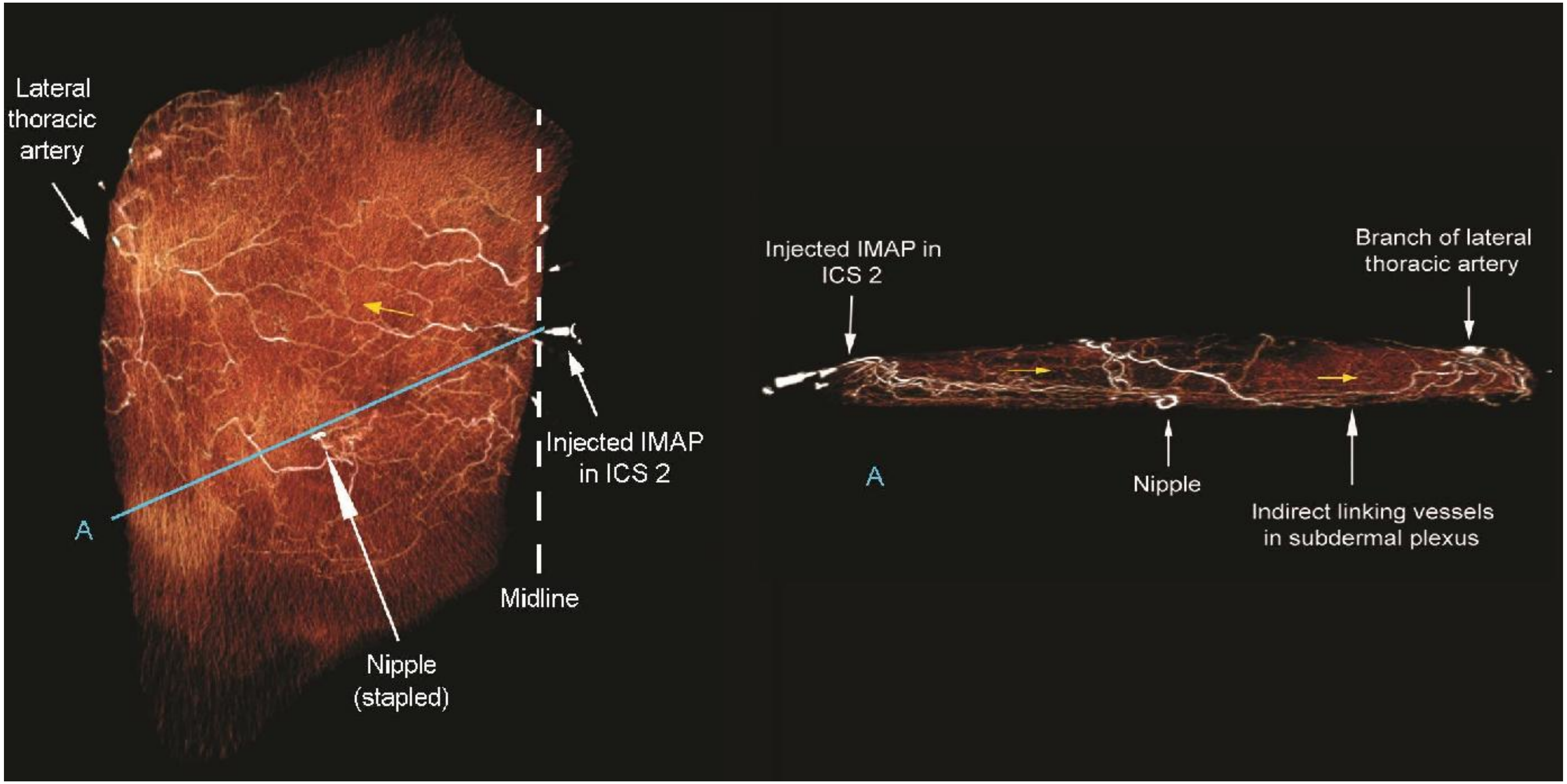

Figure 2.1.5 *3D CT scan of a flap where the IMAP in ICS 2 was injected with contrast. Left: AP view of flap. Right: Oblique-transverse view of flap, corresponding to line A. Indirect linking vessels between the IMAP and the lateral thoracic artery are found at the subdermal level. Yellow arrows show direction of flow.*

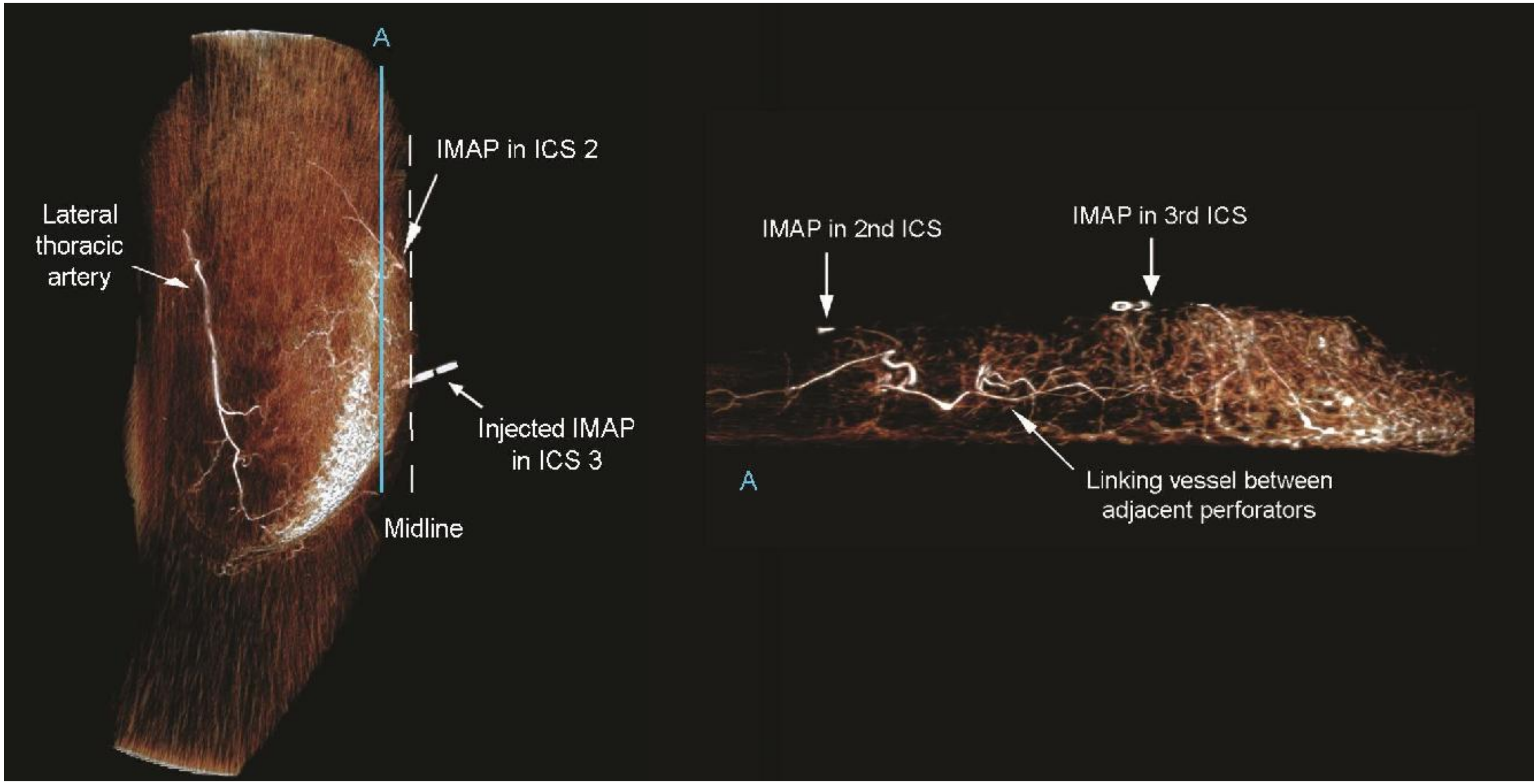

Figure 2.1.6 *3D CT scan of a flap where the IMAP in ICS 3 was injected with contrast. Left: AP view of flap. Right: Sagittal view of flap, corresponding to line A. Direct linking vessels between adjacent perforators (IMAPs in ICS 2 and 3) are located midway between the dermis and the pectoral fascia.*

Relationship with the lateral thoracic artery

Internal mammary artery perforators were found to communicate with the lateral thoracic artery in twelve of our flaps. Linking vessels between the IMAPs and the lateral thoracic artery are located at and around the nipple-areolar complex (Figure 2.1.7). These were also found to be at two levels, the subdermal level (Figure 2.1.5) and midway between the dermis and pectoral fascia (Figure 2.1.7). In a few cases, the lateral thoracic artery was found to 'bridge' the vascular territories of IMAPs (Figure 2.1.8) thus enlarging the vascular territory of each IMAP even more.

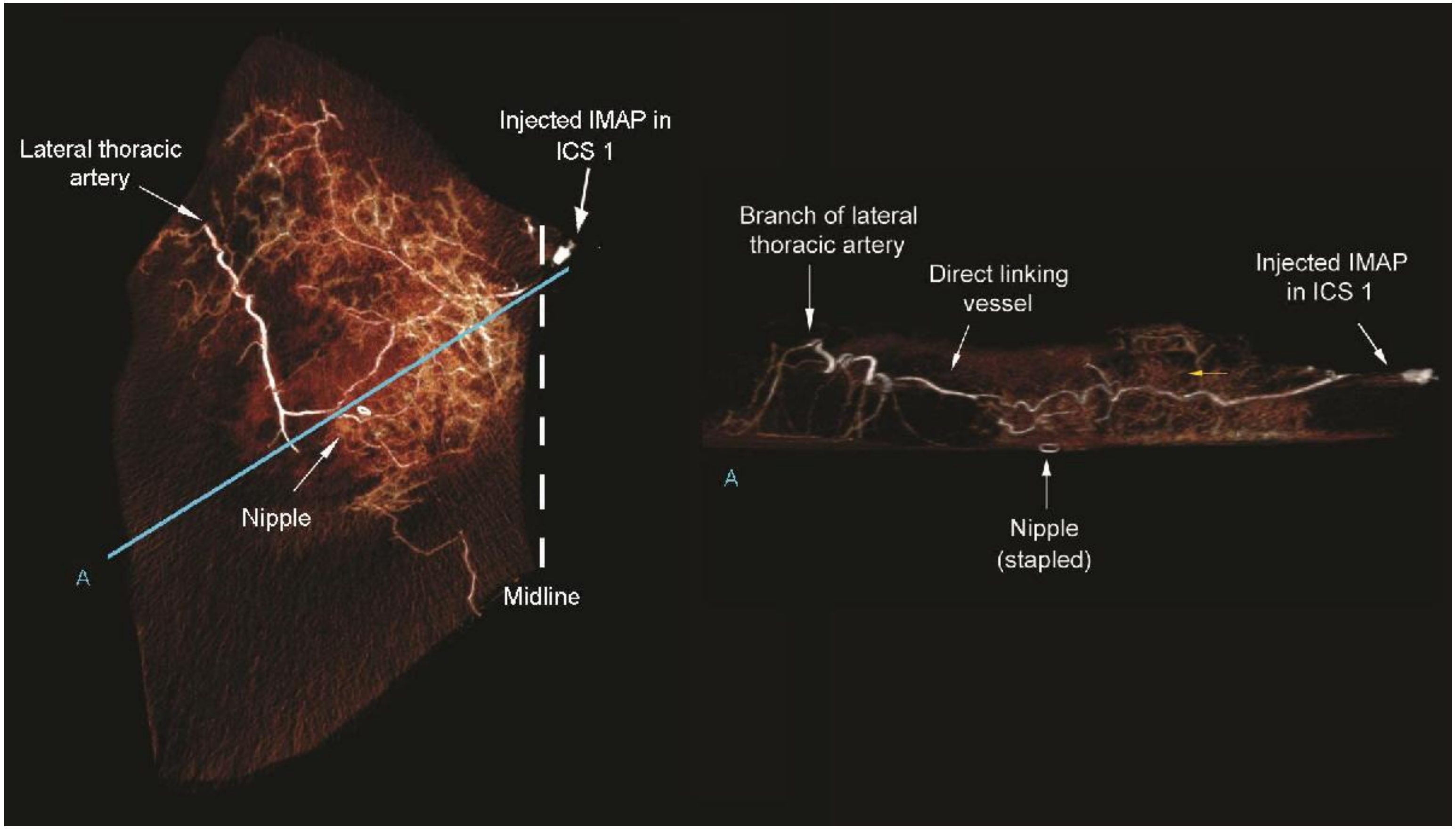

Figure 2.1.7 *3D CT scan of a flap where the IMAP in ICS 1 was injected with contrast. Left: AP view of flap. Linking vessels between the IMAPs and the lateral thoracic artery are located around the nipple (stapled). Right: Oblique-transverse view of flap, corresponding to line A. Direct linking vessels between the IMAP and the lateral thoracic artery are found midway between dermis and pectoral fascia. Yellow arrow shows direction of flow.*

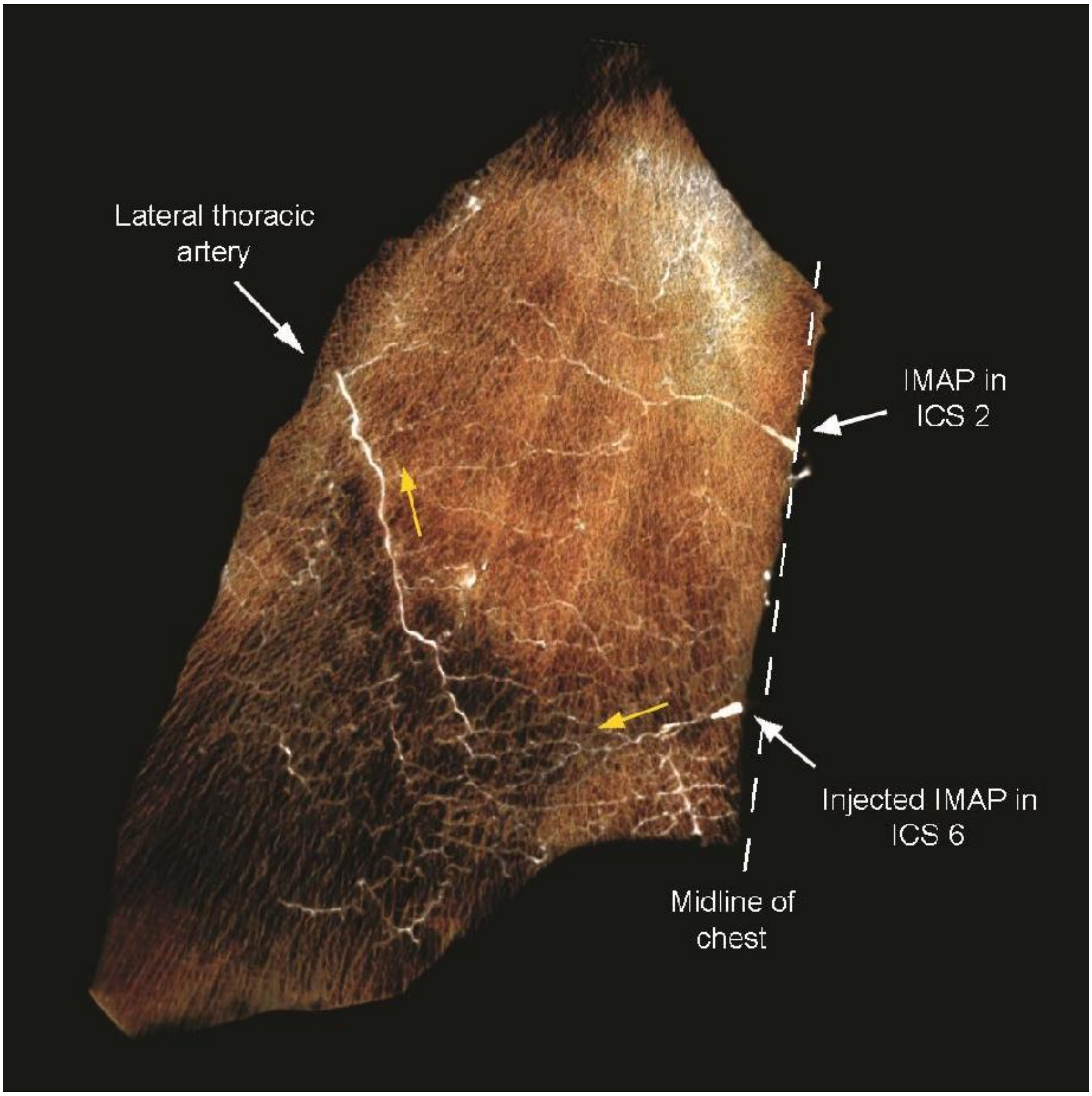

Figure 2.1.8 *3D CT scan of a flap where the IMAP in ICS 6 was injected with contrast. The lateral thoracic artery was found to 'bridge' the vascular territories of IMAPs in ICS 6 and ICS 2, thus further enlarging both perforasomes.*

Perforator veins (venous perforasomes)

Six perforator veins in our series were injected. When a perforator vein was injected, the vascular territory it encompassed was similar to that of its accompanying perforator artery but could be larger than the artery's territory (Figures 2.1.9 and 2.1.10). Also, the perforator veins were found to communicate with the lateral thoracic vein in all six cases. The venous system was found to be mostly at the subdermal level (Figure 2.1.10).

Axiality of flow

When the superior IMAPs were injected (ICS 1-2), the linking vessels were found to be orientated in a transverse fashion (Figure 2.1.9). However, when the inferior IMAPs (ICS 3-7) were injected, the orientation of the linking vessels took a more infero-lateral orientation (Figure 2.1.8). From the four dimensional CT angiography performed, we elucidated that the axiality of blood flow of the IMAP flap was lateral if an IMAP in ICS 1 or 2 were used, and infero-lateral if an IMAP in ICS 3 and below were used (Videos 2.1.1-2.1.2).

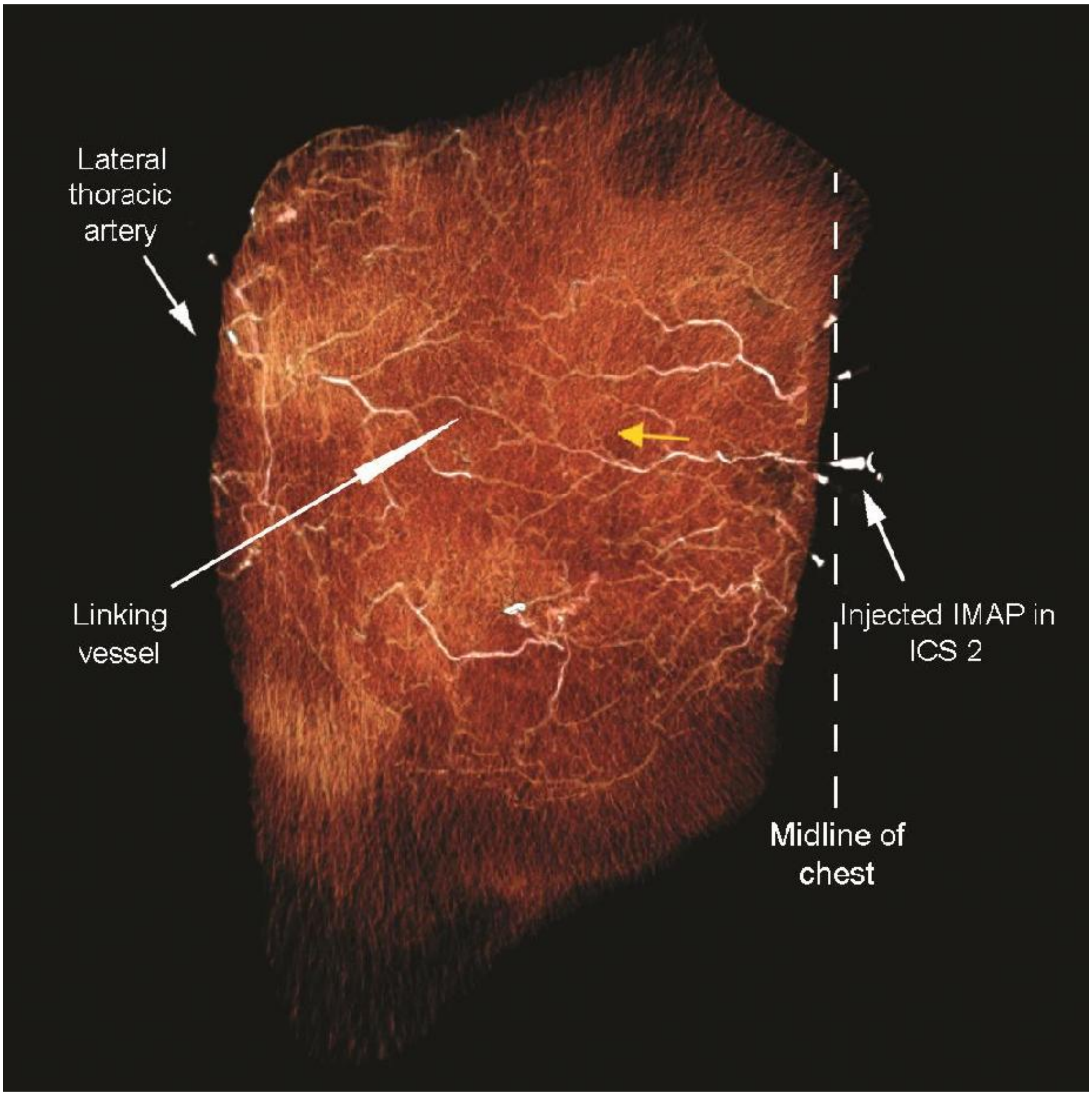

Figure 2.1.9 *3D CT scan of a flap where the IMAP (artery) in ICS 2 was injected with contrast. Yellow arrows show direction of flow.*

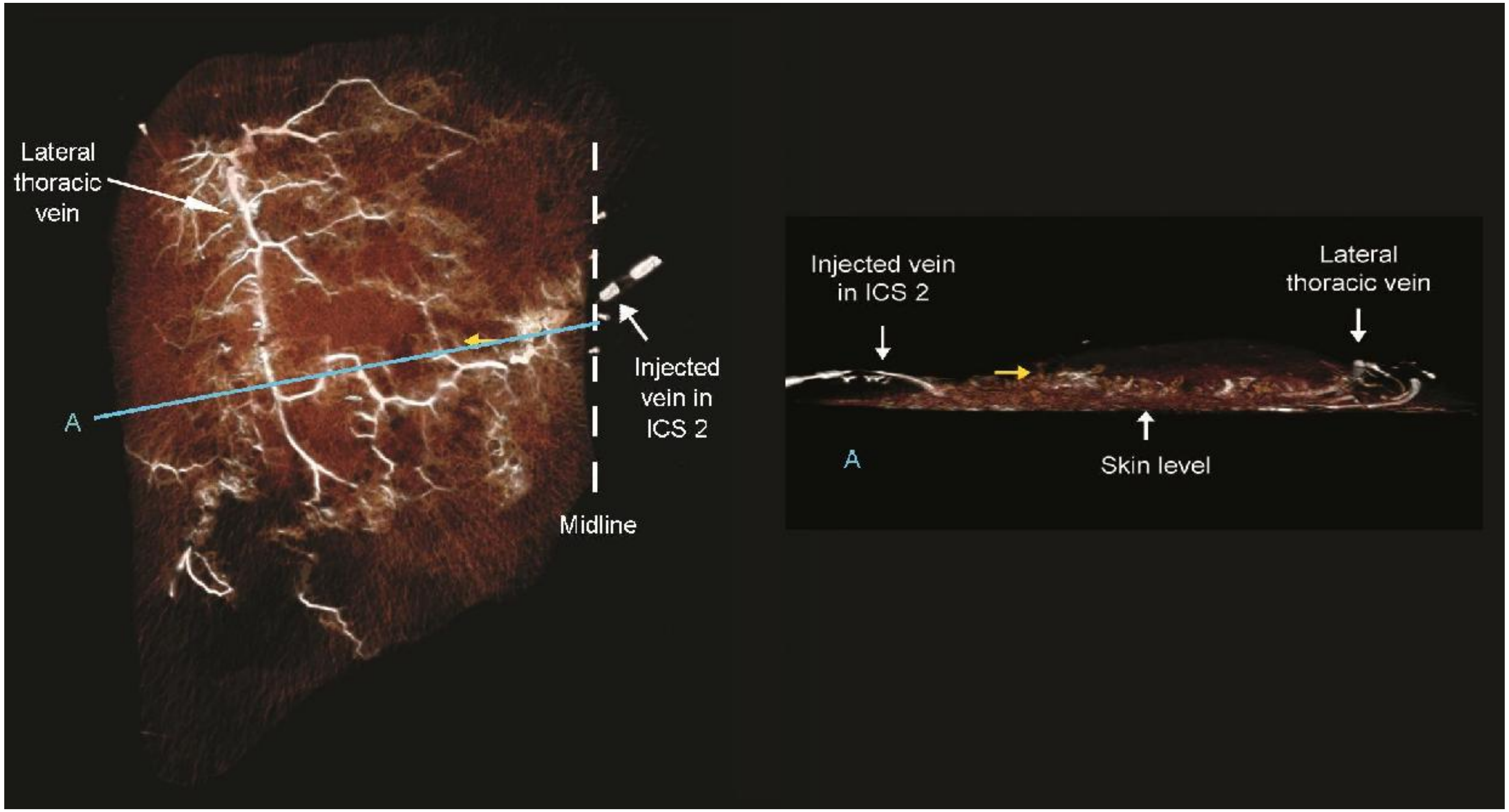

Figure 2.1.10 *3D CT scan of the same flap in 10a where the corresponding vein in ICS 2 was injected with contrast. Left: AP view of flap. The venous vascular territory was found to be similar to that of the accompanying perforator artery but may be larger than the artery's territory. Communication with the lateral thoracic vein was found in all six cases. Right: Transverse view of flap, corresponding to line A. The venous system is found to be mostly at the subdermal level. Yellow arrow shows direction of flow.*

Discussion

This technique enables clear visualization of the whole vascular tree in a three-dimensional manner (e.g. lateral view demonstrates branching patterns of vessels re. Figures 2.1.5 – 2.1.7, 2.1.10). This allows us to analyze the direct relationship of these vessels with respect to different levels of the skin, specifically the dermis. The four-dimensional aspect demonstrates the dynamic study of flow in the vascular territory. This shows us which part of the flap is perfused first, and which part of the skin receives the greatest blood flow.

The IMAP flap has demonstrated reliability, versatility, freedom of arc of rotation (Figure 2.1.11), neck coverage with skin of similar texture and pigmentation with sensory innervation, as well as a primary closure of the donor site [20-22]. Strategies to increase its arc of rotation have included division of the fibers of pectoralis major cephalad to the pedicle[20], and excision of a portion of the costal cartilage of the second rib[21]. Bilateral IMAP flaps can be used to reconstruct a large central defect of the neck[21] and pre-expansion can also be used to maximize IMAP flap size and coverage surface.[18]

This study focuses on the arterial and venous vascular territory of single perforators, (which we have termed arterial and venous perforasomes), coming off the internal mammary artery, which constitute the medial vascular supply of the anterior chest/ breast (Figure 2.1.12). Marcus[26] and Palmer[24] found that the internal mammary artery was dominant over the lateral thoracic artery with regards to vascularity of the breast in 68-74% of their cases. The largest and most frequently found IMAP has been reported to be in the second or third intercostals spaces [24, 25].

The phenomenon of linking vessels between adjacent perforators/arteries is an important finding. This explains how perfusion extends to the vascular territory of nearby perforators, and how perfusion is maintained all the way to the distal periphery of the flap. In effect, one perforator can increase its own vascular territory by 'sharing' the territory of another perforator, and vice versa, if the flap were to be based on the other perforator. This also demonstrates collateral flow in the pectoral region, and hence the ability to minimize devastating effects of any ischaemic insult.

The lateral thoracic artery was prominent in many of our flaps. Linking vessels between the lateral thoracic artery and the IMAPs allows it to serve as a 'bridge' in the lateral thoracic area. Hence, theoretically, if a large flap is needed it may be wise to include the lateral thoracic artery to ensure perfusion to the distal edges.

The level at which these linking vessels were found (subdermal and between dermis and fascia) indicates that an IMAP flap can be raised on a level superficial to the pectoral fascia safely. As the venous system was also found to be at a superficial level, problems with flap congestion will likely be minimized if elevation of the flap occurred at this recommended level. Thinning of the flap should not go beyond halfway through the thickness of the flap.

Based on the axiality of perfusion of the IMAPs, the orientation of the flap should be transverse if based on IMAPs in ICS 1-2, and transverse or diagonal in the infero-lateral direction if based on ICS 3 and below.

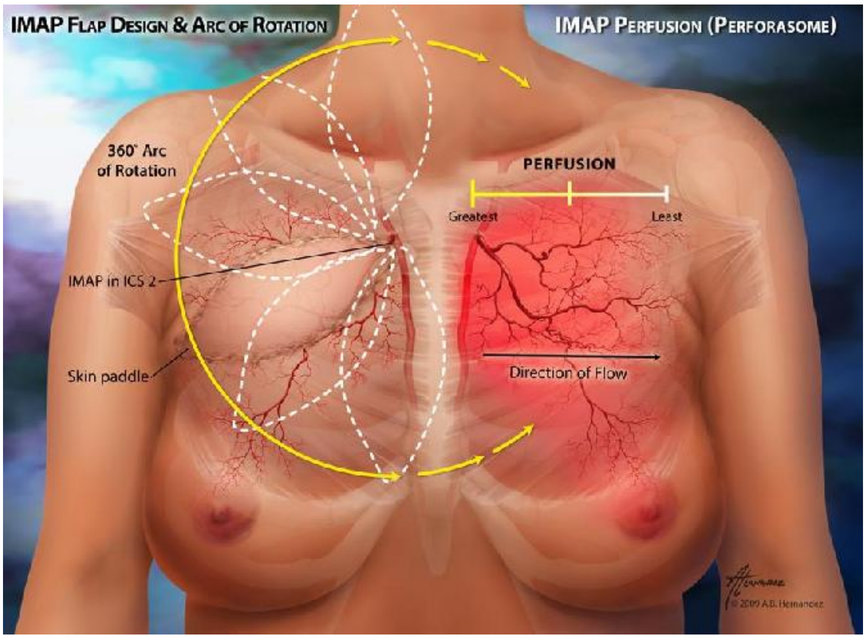

Figure 2.1.11 *Left: Arc of rotation of IMAP flap, based perforator in ICS 2. Flaps may reach the neck and even down to xiphoid level. Right: Perforasome of the IMAP in ICS 2.*

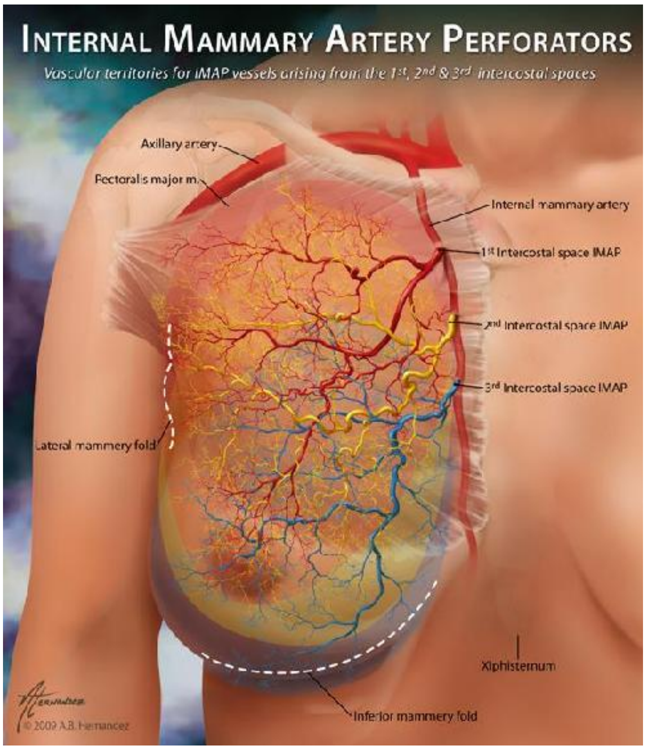

Figure 2.1.12 *Vascular territories/ Perforasomes of IMAPs in the 1st, 2nd and 3rd intercostals spaces.*

Conclusion

With 3D, 4D CT angiographic techniques, we have elucidated the arterial and venous perforasomes of the internal mammary artery perforators with respect to their intercostals spaces, the level of their linking vessels, and the relationship between the IMAP and lateral thoracic artery. We have demonstrated the dimensions of the IMAP flap, and recommended the safe level of flap dissection/thinning and orientation of the skin paddle. The flaps raised may be able to reconstruct areas between the neck and down to the xiphoid level (Fig 2.1.11)

This contributes to our knowledge of the IMAP flap, which remains an important option in reconstruction of the head and neck region.

2.2 ABDOMEN: Transverse Rectus Abdominis Musculocutaneous (TRAM), Pedicled TRAM, Muscle-sparing TRAM, Deep Inferior Epigastric Artery Perforator (DIEP) and Superficial Inferior Epigastric Artery (SIEA) Flaps

Abdominal Study I

A Comparison of the Commonly Used Abdominal Flaps in Breast Reconstruction - Transverse Rectus Abdominis Musculocutaneous (TRAM), Pedicled TRAM, Muscle-sparing TRAM, Deep Inferior Epigastric Artery Perforator (DIEP) and Superficial Inferior Epigastric Artery (SIEA) Flaps

Introduction

The use of abdominal tissue for autologous breast reconstruction has been long and widely practiced. It is an ideal source, as most patients who develop breast cancer are at an age when they also have excessive abdominal fat and skin. Autologous breast reconstruction has many advantages over implant reconstruction including reduced risks of infection, capsular contracture, and a more natural and aesthetically pleasing breast.

Holstrom first described the free transverse rectus abdominis myocutaneous (TRAM) flap in 1979 for breast reconstruction[27]. In 1982, Hartrampf popularized the pedicled TRAM flap, based on the superior epigastric artery[28]. However, the superior epigastric artery has been shown to be the secondary blood supply to the tissue of the anterior abdominal wall[6, 28-32]. Currently, the inferior, rather than the superior epigastric pedicle plays the dominant role in abdominal tissue transfer in autologous breast reconstruction.

From the free TRAM flap, attempts to minimize donor site morbidity (e.g. abdominal bulge and hernia) led to the development of the muscle-sparing TRAM flap and deep inferior epigastric perforator (DIEP) flap. Koshima and Soeda described the inferior epigastric artery skin flap for reconstruction of the floor of the mouth and groin defects[33], but it was Allen and Treece who first used the DIEP flap for breast reconstruction[34], and this has now become common practice in many Plastic Surgical units.

The perfusion of the transverse abdominal flap was studied by Scheflan and Dinner[35, 36], but became better known after Hartrampf published his work on the TRAM flap[28]. However, the classic Hartrampf zones II and III were demonstrated by Holm *et al* to be reversed[37] using fluorescent perfusion techniques. This gave significant weight to the suggestion that blood flow from the pedicle travels to the ipsilateral side before crossing the midline.

In this study, we compare the vascular territories of the pedicled TRAM, full width TRAM, muscle-sparing TRAM, DIEP (medial or lateral row perforator) and superficial inferior epigastric artery (SIEA) flaps utilizing three and four- dimensional CT angiography. The sequential images also allow us to re-appraise the four zones of vascularity.

Materials and Methods

Nine transverse abdominal flaps were harvested from fresh adult cadavers acquired through the Willed Body Program at the University of Texas Southwestern Medical Center, and two specimens were harvested from abdominoplasty procedures after informed consent.

The margins of all the skin paddles were the anterior superior iliac spines, the supra-pubic crease, and 2cm superior to the umbilicus. Four cadaveric abdominal flaps were studied with respect to two pedicled TRAMs, two full width TRAMs, two muscle-sparing TRAMs and two DIEP flaps each. One of these also had an SIEA flap studied. Five other cadaver flaps were used to study superficial inferior epigastric artery (SIEA) flaps. The abdominoplasty specimens were cannulated and irrigated with heparinised saline prior to the perfusion studies. With these tissues, six single-perforator DIEP flaps were simulated as the three medial row perforators and three lateral row perforators were cannulated. In total, forty-three flap perfusions were simulated with CT angiography. We studied seven pedicled TRAM flaps (superior epigastric artery injected), eight full width TRAM flaps (deep inferior epigastric artery injected), four lateral muscle-sparing TRAM flaps (deep inferior epigastric artery injected, medial perforators ligated), four medial muscle-sparing TRAM flaps (deep inferior epigastric artery injected, lateral perforators ligated), seven medial perforator DIEP flaps (medial deep inferior epigastric artery perforator injected), seven lateral perforator DIEP flaps (lateral deep inferior epigastric artery perforator injected- see Figure 2.2.1) and six SIEA flaps (superficial inferior epigastric artery injected).

Specimen dissection was performed under loupe magnification. Each cadaveric flap was accompanied by full width and full length bilateral rectus muscle.

Injection of a dilute methylene blue solution through the artery according to the type of flap studied enabled all vascular leaks to be sealed, either through bipolar diathermy or suture ligation.

In studying the cadaveric specimens, we first simulated the perfusion of the pedicled TRAM, where the superior epigastric artery was cannulated and injected with contrast medium and subjected to dynamic CT scanning. The process was repeated with cannulation of the deep inferior epigastric artery for a full width TRAM. For a muscle-sparing TRAM, either the lateral or medial row perforators were perfused. The simulation of a DIEP flap was performed by injecting a single perforator (either lateral or medial row perforator). For a SIEA flap, the superficial epigastric artery was injected.

In between the sets of perfusion studies, the flap was irrigated with saline to remove remnant contrast medium. Previous experimental studies have shown that multiple washouts did not affect the diameter or vascular territories of the vessels within the flap[9, 12].

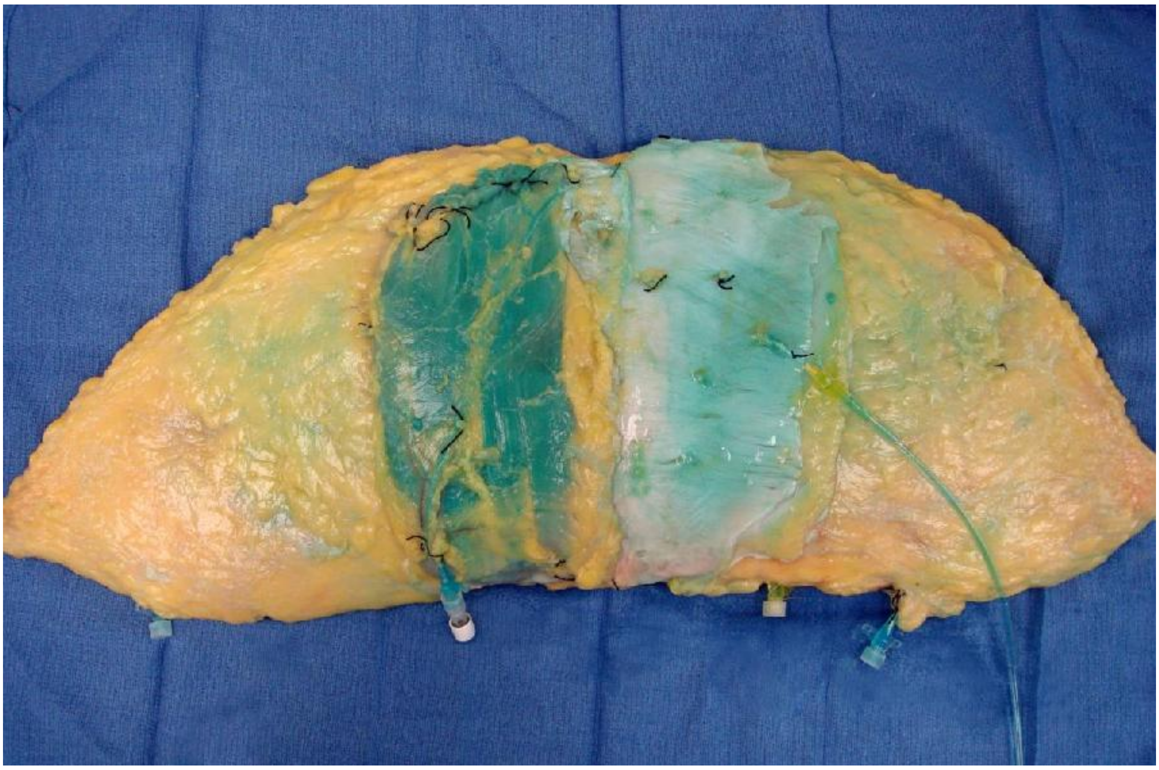

Figure 2.2.1 *Photograph of cadaveric DIEP flap, where the lateral perforator on the right side is cannulated and attached to tubing. The left rectus muscle is still intact, whereas the left had been removed.*

Results

The perfusion of a total of forty-three flaps was simulated. The area of the vascular territory of each individual flap in mm^2 using the measuring tool on TeraRecon and as a percentage of the corresponding skin paddle is tabulated in Table 2.2.1. The mean areas of the different types of flaps are summarized in Table 2.2.2 and Graph 2.2.

The pedicled TRAM flap (Figure 2.2.2) is found to have the smallest vascular territory, with a mean of 32.6 ± 13.1% of the skin paddle perfused. Two sample difference of means of pedicled TRAM versus full width TRAM gave a $p<0.03$.

The full width TRAM (Figure 2.2.3) had a mean of 48.4 ± 12.6% skin paddle perfused, which is comparable to the medial row-perfused muscle-sparing TRAM (Figure 2.2.4), which had a mean of 45.7 ±5.3% skin paddle perfusion ($p<0.70$). The lateral-row perfused muscle-sparing TRAM (Figure 2.2.5) had a reduced area, with a mean of 43.2 ± 7.9% ($p<0.47$ when compared to full width TRAM).

The DIEP flap which utilizes the medial row perforator (Figure 2.2.7) has a wider area of perfusion with a mean of 44.6 ±11.0% ($p<0.55$, medial DIEP vs. full TRAM) compared to one which is perfused by a lateral row perforator (Figure 2.2.6), with a mean of 32.9 ±2.9% ($p<0.007$ lateral DIEP vs. full TRAM, $p<0.02$ lateral DIEP vs. medial DIEP).

The SIEA flap (Figure 2.2.8) has a mean of 33.3 ±6.7% area perfused, which is comparable to a lateral perforator DIEP flap ($p<0.94$). Not only do they have a similar size of vascular territory, they also have a tendency to stay in one hemi-abdomen.

Vascular flow between zones of perfusion (I-IV) can be explained by the linking vessels which communicate between the perforators (Figures 2.2.9-2.2.10) as well as recurrent flow via the subdermal plexus (Figures 2.2.11- 2.2.12).

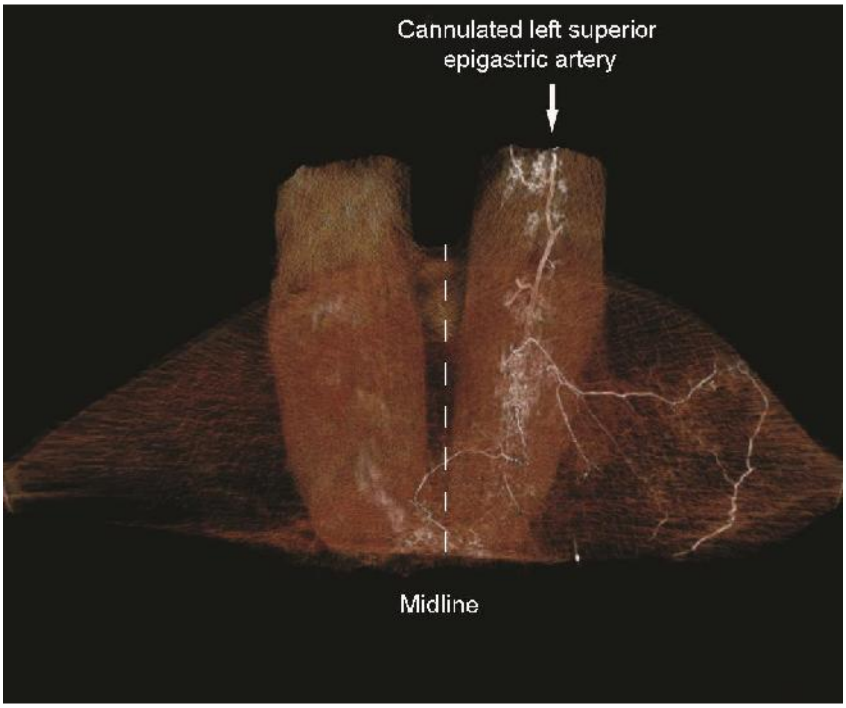

Figure 2.2.2 *Pedicled TRAM flap. Left superior epigastric artery injected with contrast.*

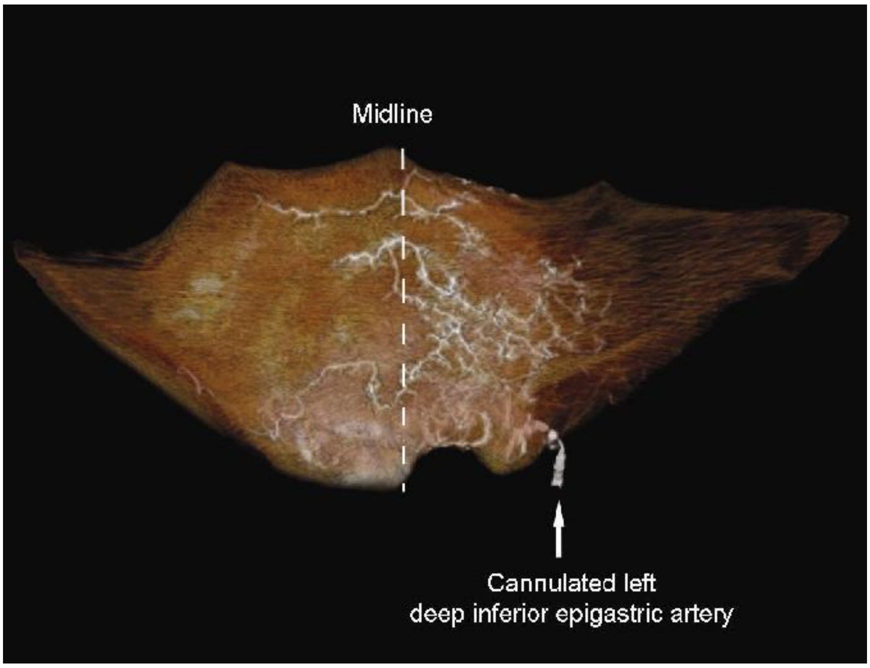

Figure 2.2.3 *Full width TRAM flap. Left deep inferior epigastric artery injected with contrast.*

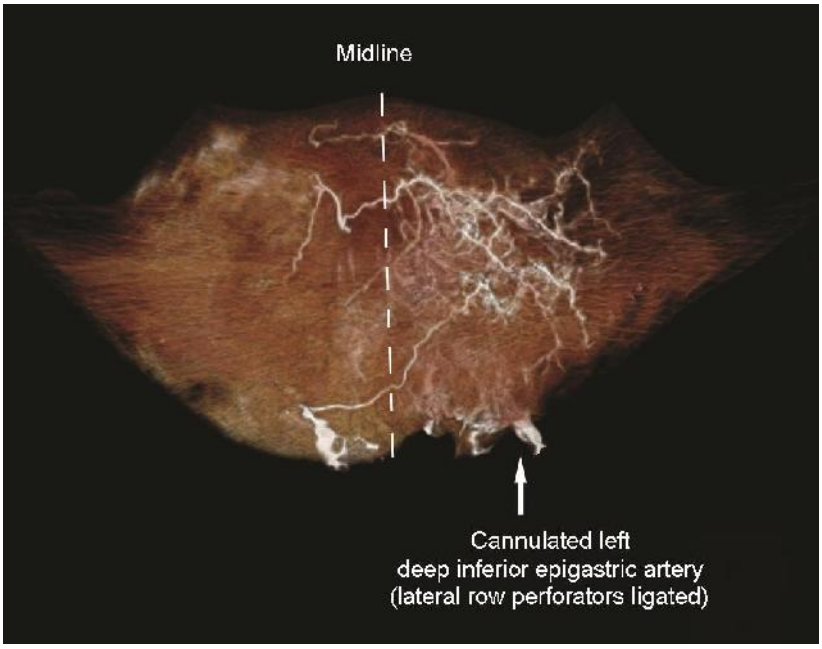

Figure 2.2.4 *Muscle-sparing TRAM flap (medial row perforators perfused). Left deep inferior epigastric artery injected with contrast after ligation of the lateral row perforators.*

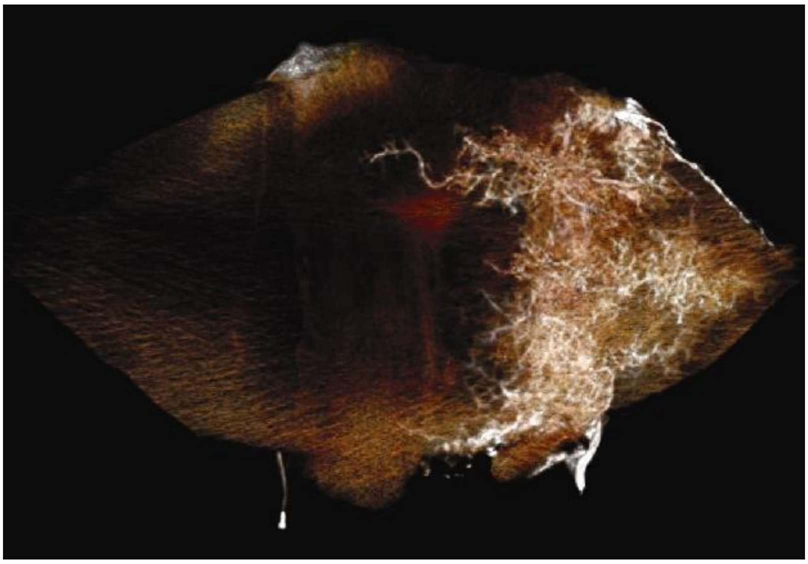

Figure 2.2.5 *Muscle-sparing TRAM flap (lateral row perforators perfused). Left deep inferior epigastric artery injected with contrast after ligation of the medial row perforators.*

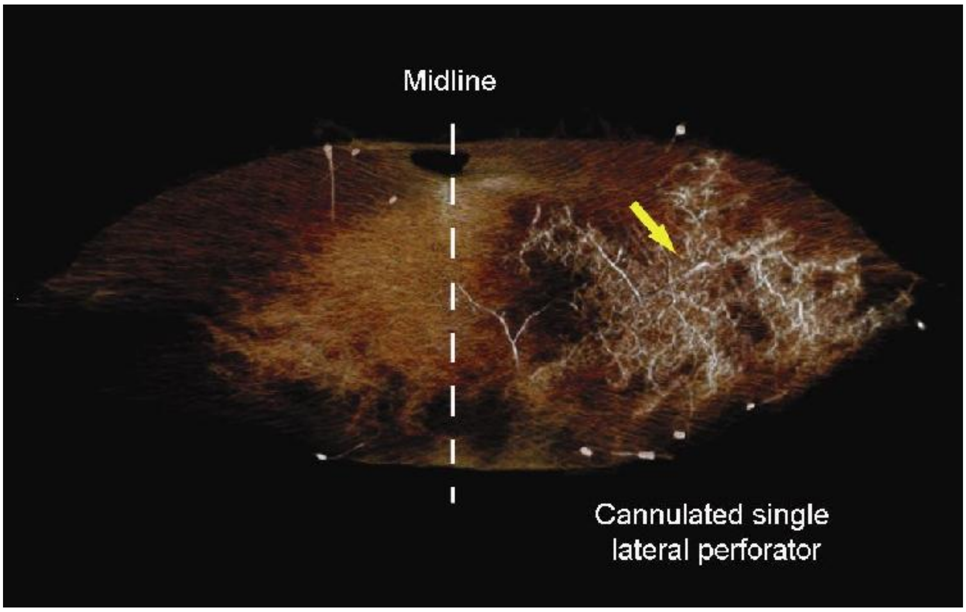

Figure 2.2.6 *DIEP flap (lateral perforator-based). Single lateral row perforator injected with contrast (yellow arrow).*

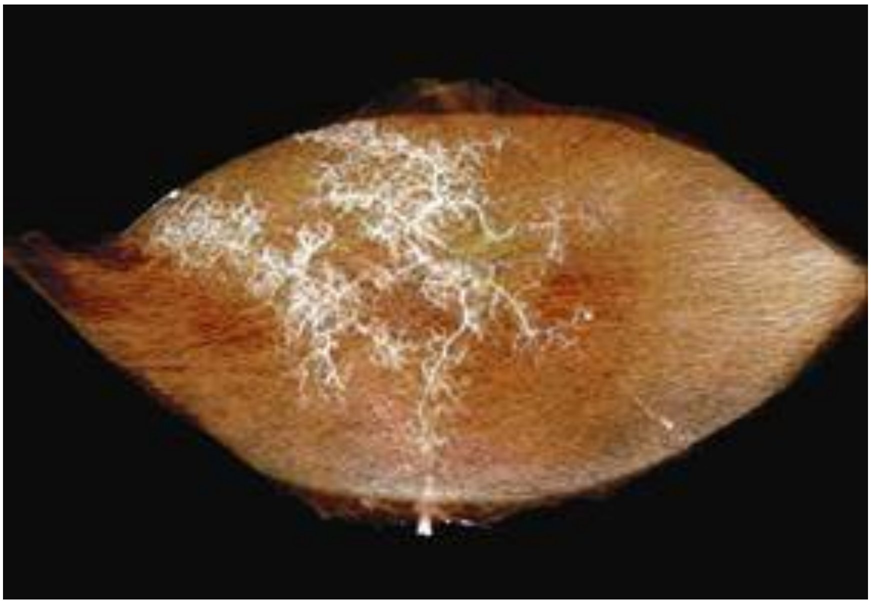

Figure 2.2.7 *DIEP flap (medial perforator-based). Single medial row perforator injected with contrast.*

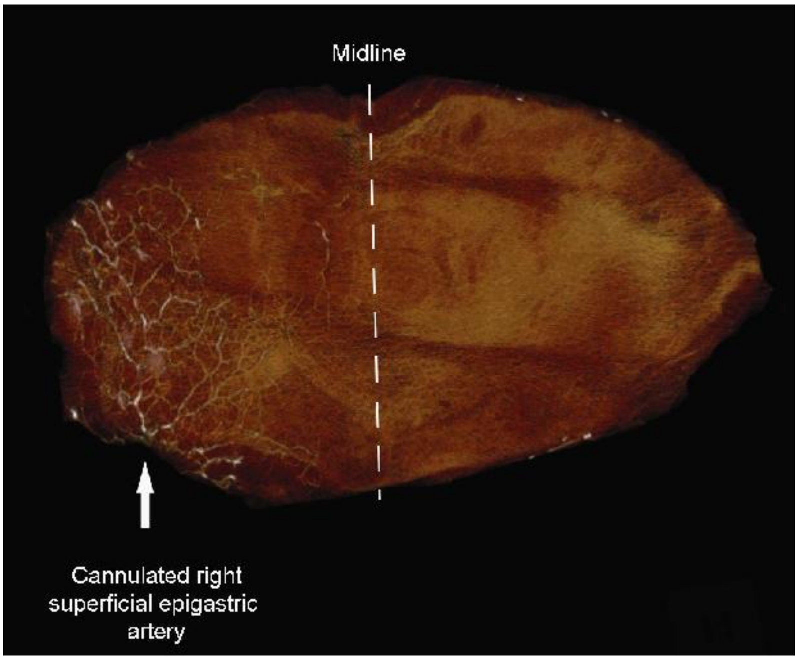

Figure 2.2.8 *SIEA flap. Right superficial inferior epigastric artery injected with contrast.*

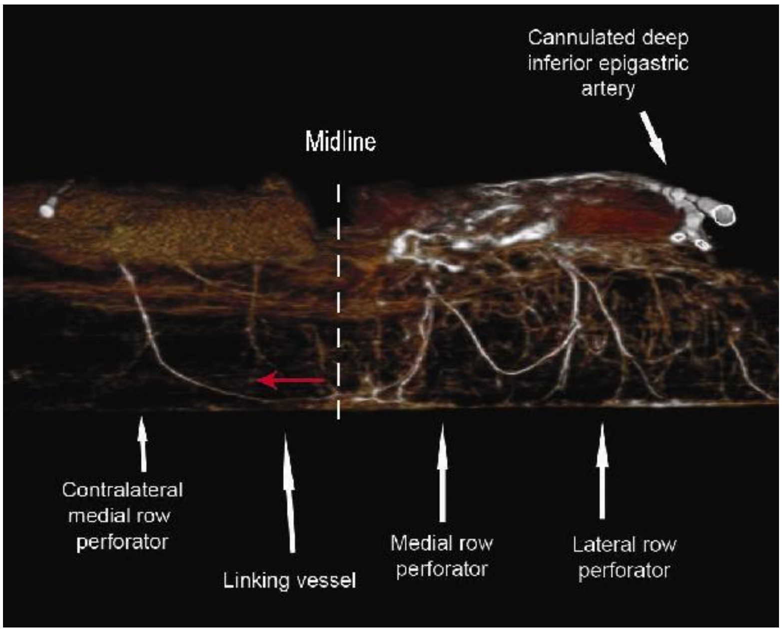

Figure 2.2.9 *Lateral view of muscle-sparing TRAM flap. Linking vessels between perforator complexes are shown, crossing the midline. Note direction of flow (red arrow).*

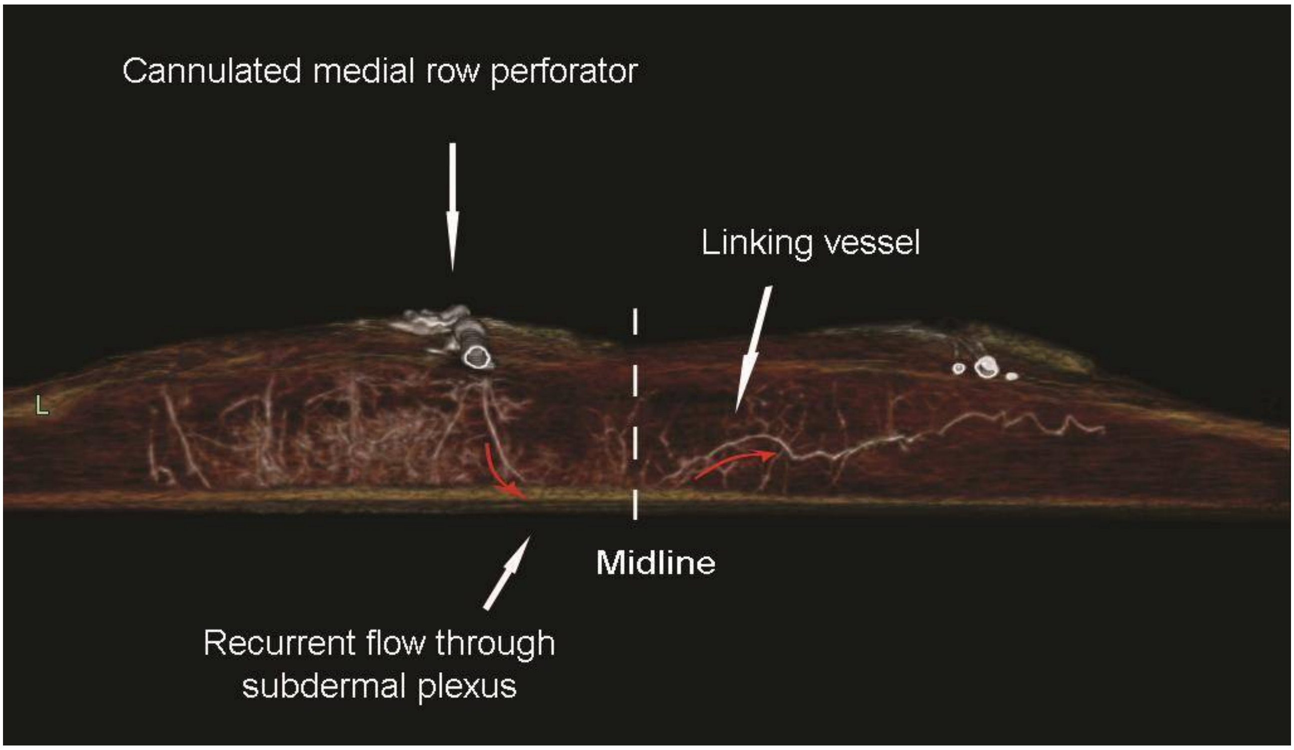

Figure 2.2.10 *Lateral view of DIEP flap. Linking vessels between perforator complexes are shown, crossing the midline. Note direction of flow (red arrows).*

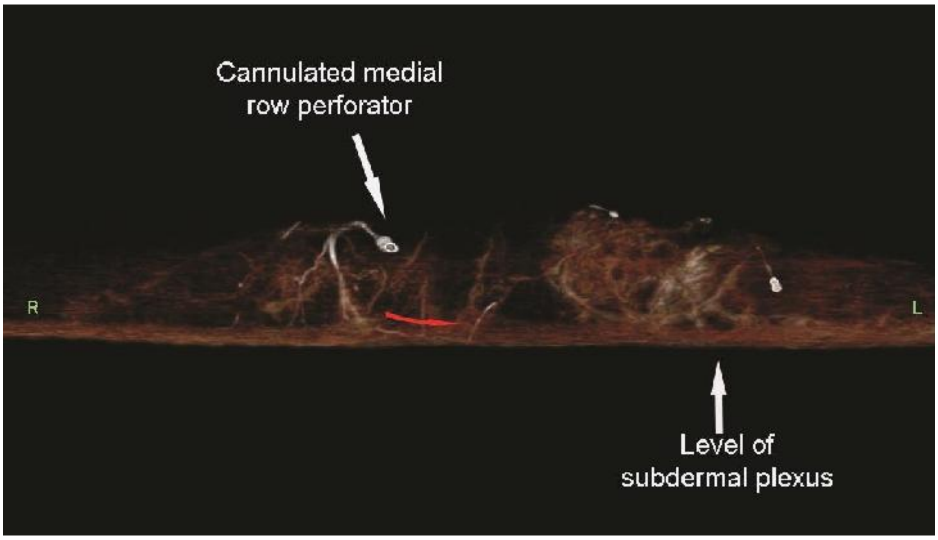

Figure 2.2.11 *0.25ml of contrast injected into a perforator of a DIEP flap. Note direction of flow (red arrow).*

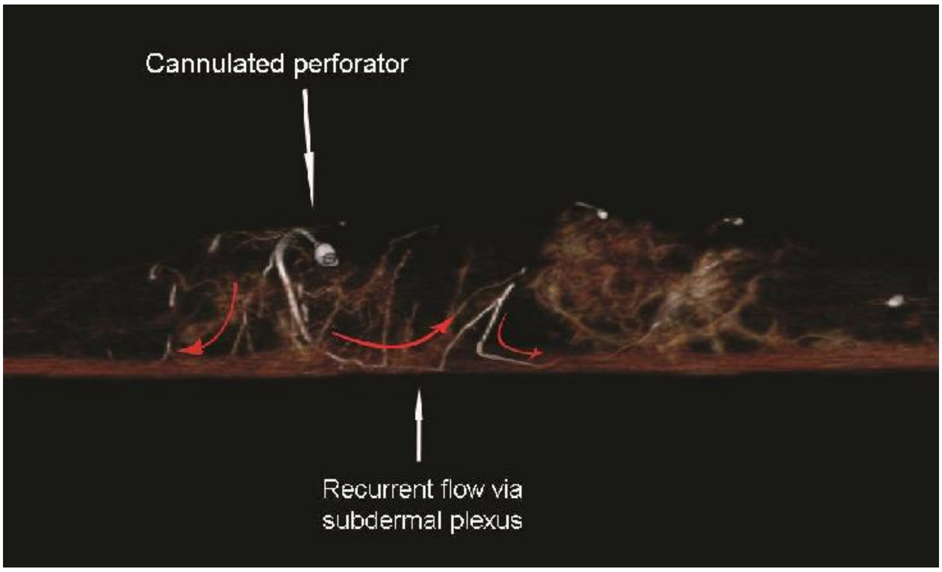

Figure 2.2.12 *0.4ml of contrast injected into the same perforator of the DIEP flap above. Linking vessels demonstrate recurrent flow from the subdermal plexus to the deeper tissues, before flowing superficially and away from the primary perforator (red arrows).*

Table 2.2.1. Vascular territory according to flap type

	Specimen 1 +	Specimen 2 +	Specimen 3 +	Specimen 4 +	Specimen 5 +	Specimen 6 +	Specimen 7 +	Specimen 8 +	Specimen 9 +	Specimen 10 *		Specimen 11 *
Areas of skin paddle (mm^2)	34591.4	69071.1	43766.1	34632.1	62578.8	43689.6	46352.5	50969.4	68457.2	44877.5		64408.8
Pedicled TRAM (mm^2)/ % of skin paddle	6904.1/ 20.0	17753.4/ 25.7	23087.1/ 52.8	10486.6/ 30.3	n/a	n/a	n/a	n/a	n/a	n/a	n/a	n/a
	n/a	22133.3/ 32.0	20929.8/ 47.8	6733.3/ 19.4	n/a	n/a	n/a	n/a	n/a	n/a	n/a	n/a
Full width TRAM (mm^2)/ % of skin paddle	12448.5/ 36.0	23863.3/ 34.5	27324.8/ 62.4	18672.0/ 53.9	n/a	n/a	n/a	n/a	n/a	n/a	n/a	n/a
	14448.5/ 41.8	24763.4/ 35.9	25629.8/ 58.6	22088.7/ 63.8	n/a	n/a	n/a	n/a	n/a	n/a	n/a	n/a
Lateral muscle-sparing TRAM (mm^2)/ % of skin paddle	11542.6/ 33.4	28958.6/ 41.9	19687.1/ 45.0	18174.7/ 52.5	n/a	n/a	n/a	n/a	n/a	n/a	n/a	n/a
Medial muscle-sparing TRAM (mm^2)/ % of skin paddle	14648.4/ 42.3	29408.5/ 42.6	19388.5/ 44.3	18523.3/ 53.5	n/a	n/a	n/a	n/a	n/a	n/a	n/a	n/a
Lateral perforator DIEP (mm^2)/ % of skin paddle	11377.3/ 32.9	25894.2/ 37.5	12585.6/ 28.8	10785.9/ 31.1	n/a	n/a	n/a	n/a	n/a	16069.6/ 35.8	14864.4/ 33.1	20248.3/ 31.4
Medial perforator DIEP (mm^2)/ % of skin paddle	11619.4/ 33.6	23307.3/ 33.7	25426.5/ 58.0	15395.9/ 44.5	n/a	n/a	n/a	n/a	n/a	27311.4/ 60.9	17434.1/ 38.8	27281.4/ 42.4
SIEA (mm^2)/ % of skin paddle	n/a	18049.1/ 26.1	n/a	n/a	15451.1/ 24.7	15997.1/ 36.6	18782.4/ 40.5	16616.9/ 32.6	26998.2/ 39.4	n/a	n/a	n/a

+ Cadaver specimen

*Abdominoplasty specimen

Table 2.2.2. Summary of vascular territory according to flap type

	Pedicled TRAM	Full width TRAM	Muscle-sparing TRAM (lateral row)	Muscle-sparing TRAM (medial row)	DIEP (lateral perforator)	DIEP (medial perforator)	SIEA
No. of flaps	7	8	4	4	7	7	6
% of paddle	20	36	33.4	42.3	32.9	33.6	26.1
	25.7	41.8	41.9	42.6	37.5	33.7	24.7
	32.0	34.5	52.5	53.5	31.1	44.5	36.6
	30.3	35.9	45.0	44.3	35.8	60.9	40.5
	19.4	53.9			33.1	38.8	32.6
	52.8	63.8			31.4	42.4	39.4
	47.8	62.4			28.8	58.0	
		58.6					
avg % of paddle (SD)	32.6 (13.1)	48.4 (12.6)	43.2 (7.9)	45.7 (5.3)	32.9 (2.9)	44.6 (11.0)	33.3 (6.7)

Graph 2.2

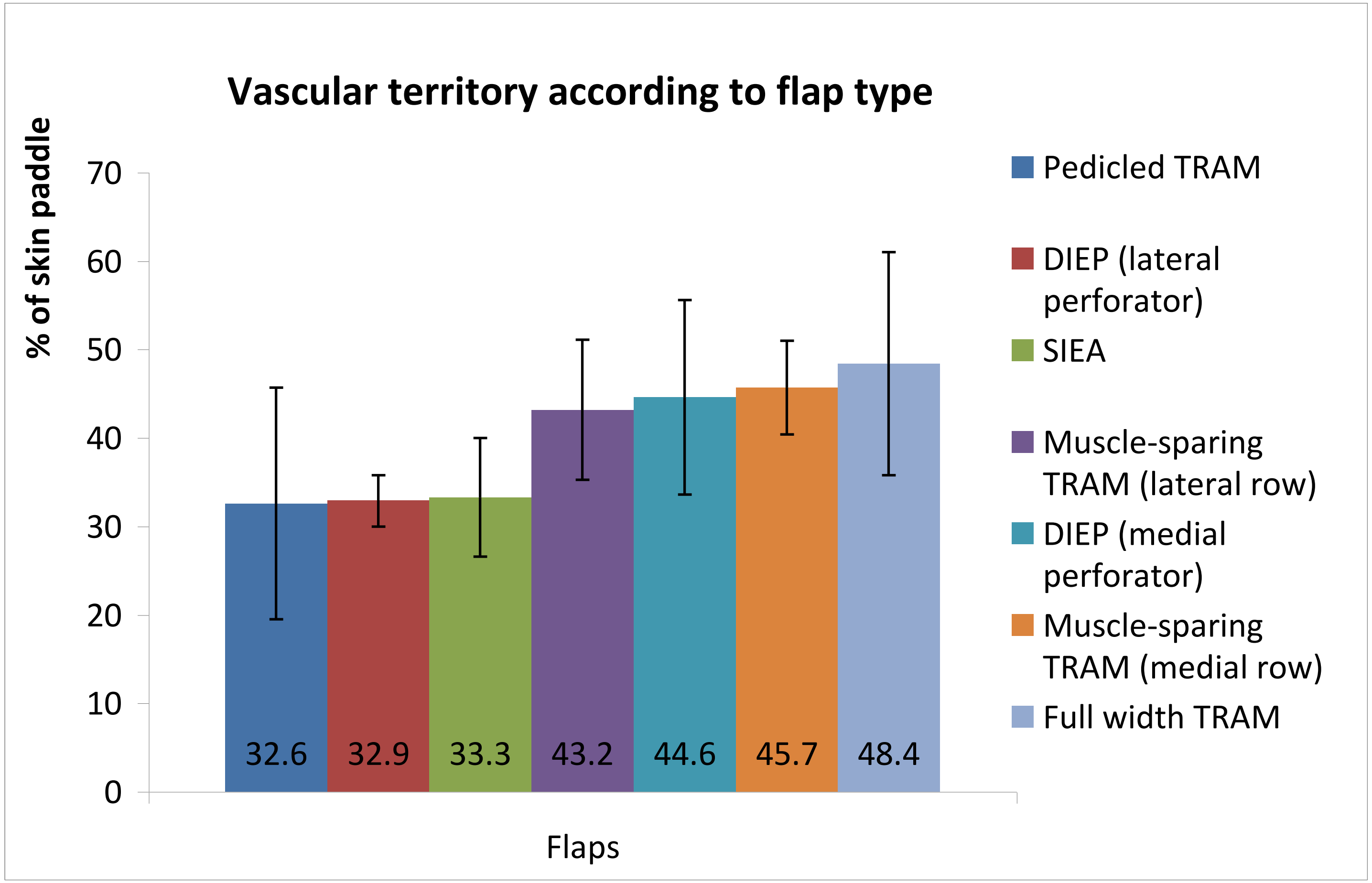

Vascular territory according to flap type
% of skin paddle
70
60
50
40
30
20
10
0
32.6
32.9
33.3
43.2
44.6
45.7
48.4
Flaps
Pedicled TRAM
DIEP (lateral perforator)
SIEA
Muscle-sparing TRAM (lateral row)
DIEP (medial perforator)
Muscle-sparing TRAM (medial row)
Full width TRAM

4D CT angiography

In full width TRAM flaps (i.e. both medial and lateral row perforators still present), we found that vascular perfusion from zone I to zone II (contralateral medial zone) or zone III (ipsilateral lateral zone) depends on perforator dominance. If the medial row perforator is dominant, then zone I perfuses to zone II earlier and more intensely than zone III (Figure 2.2.13, video 2.2.1). If the lateral row perforator is dominant, then zone III is perfused before and more so than zone II (Fig. 2.2.14, video 2.2.2). In muscle-sparing TRAM (n=8) and DIEP flaps (n=14), the perfusion depends on whether the perforators are medial or lateral row. In a similar story as above, those based on medial row perforators have zone II perfusing earlier and more intensely than zone III. If the lateral row perforator is utilised, then zone III is perfused before and more so than zone II.

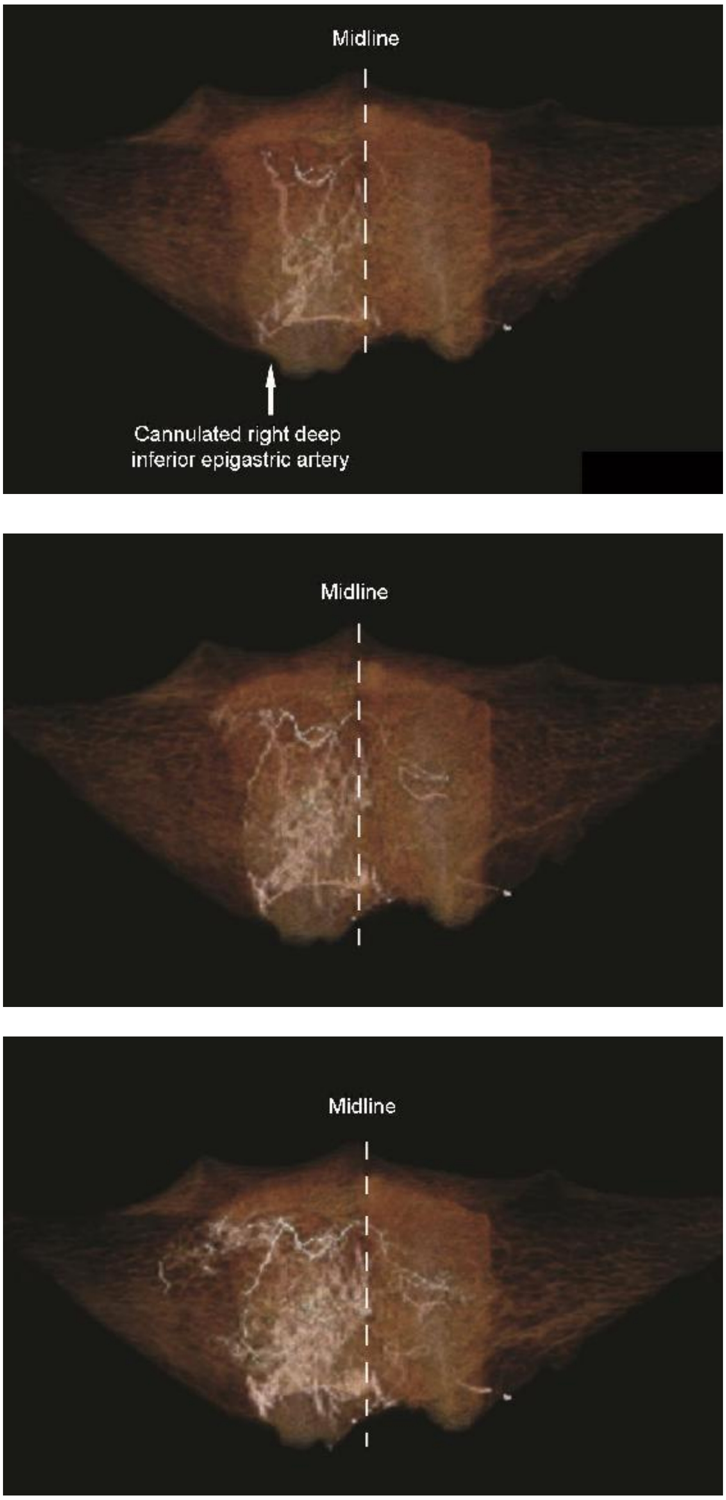

Figure 2.2.13 *Perfusion of right deep inferior epigastric artery (in full width TRAM flap). (Top) At initial stage, only zone I is perfused. (Middle) Perfusion of right deep inferior epigastric artery (in full width TRAM flap). At middle stage, zones I and II are perfused, demonstrating a dominant medial row perforator. (Bottom) Perfusion of right deep inferior epigastric artery (in full width TRAM flap). At late stage, zones I, II and III are perfused.*

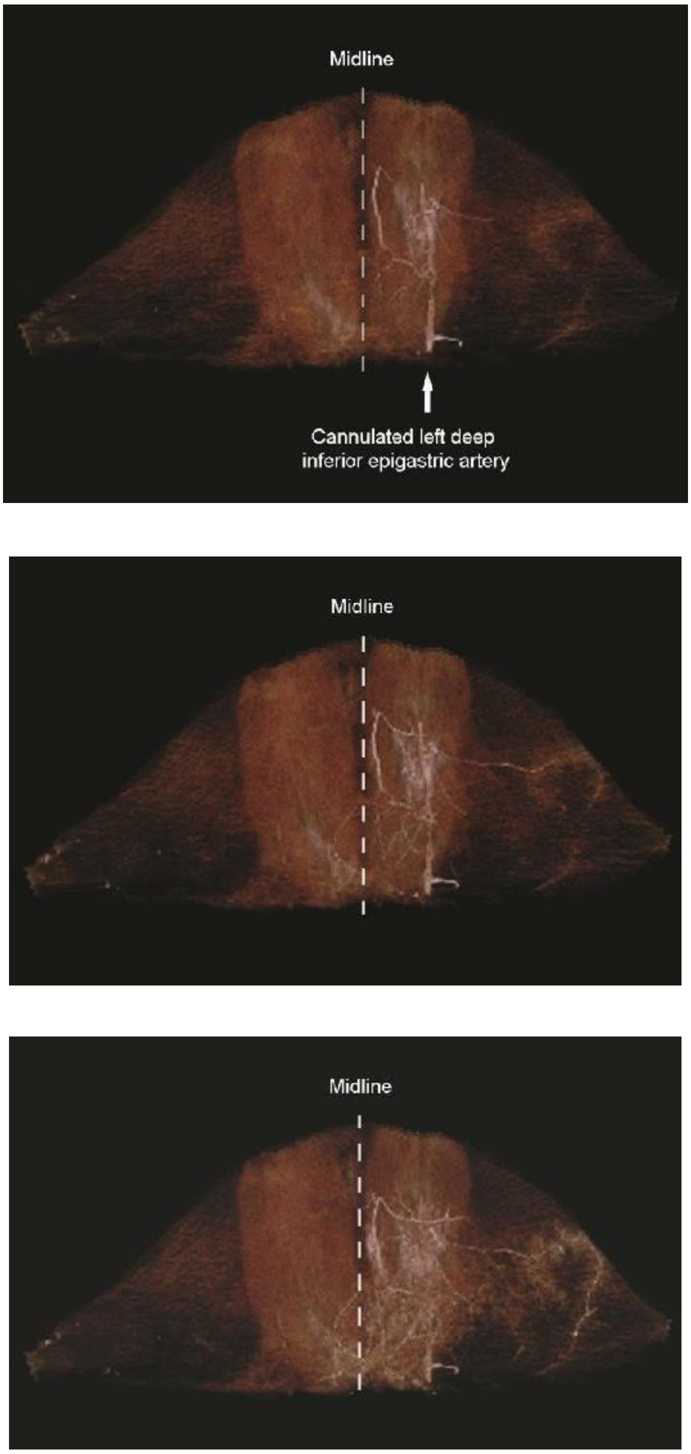

Figure 2.2.14 *Perfusion of left deep inferior epigastric artery (in full width TRAM flap). (Top) At initial stage, only zone I is perfused. (Middle) Perfusion of left deep inferior epigastric artery (in full width TRAM flap). At middle stage, zones I and III are perfused, demonstrating a dominant lateral row perforator. (Bottom) Perfusion of left deep inferior epigastric artery (in full width TRAM flap). At late stage, zones I, II and III are perfused.*

Discussion

We have found that perfusion studies involving cadaveric tissue underestimate the extent of vascular territory *in vivo*. Even so, this study gives us an idea of how the lower abdominal flaps perfuse with respect to the named artery/perforator investigated.

The superior epigastric artery has been acknowledged to be the secondary blood supply to the tissue of the anterior abdominal wall[6, 28-32]. Although no microsurgery is necessary, it has been suggested that the pedicled TRAM has a rate of partial necrosis approaching 25% and fat necrosis rate of up to 27%[38, 39]. Comparatively, TRAM, muscle-sparing TRAM and DIEP flaps which utilize the deep inferior epigastric artery have failure rates quoted to be 1-4%, and fat necrosis rates of 4-16%[40-44]. This is supported by the fact that the caliber of the superior epigastric artery is considerably smaller than that of the deep inferior epigastric artery, and our findings of the vascular territory of a pedicled TRAM being about 60% of the territory of a full width TRAM flap.

The full width TRAM flap and muscle-sparing medial row TRAM flap were shown to have comparable areas of perfusion (46-48%). Therefore, we recommend the use of the muscle-sparing TRAM flap as opposed to the full width TRAM, to reduce the risk of donor site morbidity.

The DIEP flap based on a medial perforator has a perfusion area of 44.6%, and is reduced to 32.9% if based on a lateral perforator, which is a smaller area compared to both types of TRAM flaps. Kroll's study in 2000 implied that DIEP flaps have a less robust blood supply than free TRAM flaps[41], as he found higher rates of partial flap loss and fat necrosis in the former compared to the latter. For TRAM flaps, the partial failure rate was 2.2%, and a fat necrosis rate of 12.9%. For DIEP flaps, in selected patients, the partial failure rate was 8.7% and fat necrosis rate was 17.4%. Whether the DIEP flaps were based on lateral or medial row perforators was not specified, so the author's conclusion would concur with our results if most of the DIEP flaps were based on lateral row perforators. The DIEP flaps harvested in this study were all based on a single perforator. We realize that the DIEP flap's vascular territory could be potentially increased if two or more perforators were also selected.

We found that the vascular territory of a DIEP flap based on a lateral row perforator was similar to that of the superficial inferior epigastric artery (SIEA) flap, in that the vascular territories tend to reside in one hemi-abdomen. Studies have been performed to advocate the use of the lateral branch of the deep inferior epigastric artery in DIEP flap harvesting. It is more frequently dominant, and tends to run a more rectilinear course, allowing for easier dissection[45, 46]. However, we recommend using the medial row perforators if a larger flap (encroaching zones III and IV) is needed. Blondeel noted in a clinical series that all flaps with compromised vascularisation of zone IV were perfused by lateral row perforators, and therefore advised that the use of medial row perforators is imperative if zone IV is required[47]. Therefore, if a large breast reconstruction is required then we recommend harvesting a medial row perforator DIEP flap, or a muscle-sparing TRAM flap, to secure a larger area of perfusion. If a small volume breast is to be reconstructed, where only a hemi-abdominal flap is required, then a lateral row perforator DIEP flap or SIEA flap may be a better option.

Holm *et al.* performed perfusion studies which demonstrated that Hartrampf zones II and III should be reversed[37]. They stated that Hartrampf's concept was erroneous and that "perfusion of the vascular territories across the midline was always delayed and less intensive than in the territories on the ipsilateral side". This elegant study was well carried out, but its bold statement does not always hold true. With 4D CT angiography, we found that within a full TRAM flap, perfusion from zone I can spread either to zone II or zone III, depending on perforator dominance. In Holm's study, only 2 out of 15 flaps utilized just the medial row perforators, and 8 used only lateral row perforators (the rest had both medial and lateral row perforators). Itoh and Arai's anatomical study showed that the lateral branch of the deep inferior epigastric artery is more frequently dominant compared to the medial branch[45], therefore, Holm's results are not surprising.

Our studies show that if the medial row perforator is dominant within a full TRAM flap, zone II is perfused before zone III (Figure 2.2.13, video 2.2.1) and if the lateral row perforator is dominant, zone III is perfused before zone II (Figure 2.2.14, video 2.2.2). This demonstrates that both Hartrampf and Holm's concepts are correct, and that no rule is absolute.

This first study led to our next abdominal study, which was to compare medial perforators versus lateral perforators within a DIEP flap.

Conclusion

Vascular territories of commonly used abdominal flaps for breast reconstruction in increasing size are: pedicled TRAM flap, lateral row perforator DIEP flap, SIEA flap, lateral row muscle-sparing TRAM flap, medial row perforator DIEP flap, medial row muscle-sparing TRAM flap and full width TRAM flap (Graph 2.2). The last three flaps have comparable areas of perfusion, therefore we recommend using a muscle-sparing TRAM to decrease the risk of donor site morbidity. To ensure perfusion of the distal part (zones III and IV) of a DIEP flap, selection of a medial row perforator is recommended. The extension of perfusion within a full TRAM flap from zone I to zone II or III will depend on perforator dominance.

Abdominal Study II

Comparison of Lateral vs. Medial Perforators of the Deep Inferior Epigastric Artery: Vascular Study and Clinical Implications

INTRODUCTION

The deep inferior epigastric artery perforator (DIEP) flap has held and continues to hold an important role in free autologous tissue breast reconstruction. It provides autologous tissue for breast reconstruction without sacrificing the underlying rectus muscle with minimal risks of bulge or hernia formation[42, 48]. The literature is replete with DIEP series comparing flap results, fat necrosis, and clinical outcomes[41, 42, 44, 49, 50]. One of the major problems is that not all DIEP flaps are alike, and a proper classification system based on zones of perfusion is required in order to make a meaningful comparison between the different flaps.

The perfusion of the transverse abdominal flap was studied by Scheflan and Dinner[35, 36], but became better known after Hartrampf published his work on the TRAM flap[28]. Since then, other authors have provided detailed anatomical studies of the deep inferior epigastric arterial system[29, 31, 51]. In 2006, the classic Hartrampf zones II and III were demonstrated by Holm *et al* to be reversed[37] using fluorescent perfusion techniques. This gave significant weight to the suggestion that blood flow from the pedicle travels to the ipsilateral side before crossing the midline.

We hypothesize that the zones of perfusion of the DIEP flap differ greatly based on whether a lateral row perforator versus a medial row perforator is selected. Increased knowledge of the lateral and medial row perforator vascular anatomy may have a significant impact on flap design and in turn help decrease flap related complications. We tested this hypothesis using three and four- dimensional

CT angiography, which has been previously utilized in other vascular anatomical studies[9, 11, 12, 52].

MATERIALS AND METHODS

A total of thirty-six DIEP flaps were simulated for this study. These flaps were harvested from eighteen fresh cadavers from the University of Texas Willed Body Program. A total of 14 single lateral row perforators versus 22 medial row perforators were injected with contrast in order to determine the vascular territory in the zones of perfusion. All dissections were performed under loupe magnification, and a 23-gauge catheter was used to cannulate all selected perforators (Figure 2.2.18). Dilute methylene blue dye was used to inject each perforator to identify vascular leakage points, which were subsequently ligated with bipolar cautery or with silk suture. The single most dominant perforator was selected in all cases. The dominant perforator was determined to be the largest perforator in the DIEP flap, by examination of the external diameter of perforators directly upon dissection of the rectus muscle. Flaps were then submitted to static and dynamic CT scan imaging.

Using the TeraRecon Aquarius workstation, we measured the area of perfusion of each flap and the mean vascular territory of medial perforators was compared to that of lateral perforator using the Student's t-test. The mean percentage of zones II and III perfusion between medial and lateral perforators were compared using the Kruskal-Wallis test.

RESULTS

The results of our study are summarized in Table 2.2.3. All our simulated DIEP flaps are based on single perforators.

Table 2.2.3

Medial vs. lateral perforators of a DIEP flap: Comparison of areas of perfusion.

Perforator injected	n =	Mean vascular territory/ cm^2	Mean area of zone II perfused/ cm^2	Mean % of zone II perfused	Mean area of zone III perfused/ cm^2	Mean % of zone III perfused
Medial	22	296.4*	93.1	65.8†	122.3	43.9†
Lateral	14	195.6*	5.2	4.8†	95.3	85.2†

* $p < 0.008$ using Student's t-test

† $p < 0.01$ using Kruskal-Wallis test

Medial Row Perforators

Twenty-two medial perforator DIEP flaps were used in this study. The mean vascular territory for a medial perforator DIEP flap injected with contrast was 296cm^2 (p<0.008 when compared to vascular territory of lateral perforator). The branches of the medial row perforator were seen to be directed both laterally and medially, and crossed the midline in all cases. The vascular territories of these flaps were more centralized compared to those perfused by a lateral perforator. Large-diameter linking vessels were found to connect perforators within the same medial row (Figure 2.2.15). The injected medial perforators connected with contralateral medial row perforators (across the midline) through the indirect linking vessels via the subdermal plexus (Figures 2.2.16 and 2.2.17). Moon and Taylor also noted that crossover of the midline is predominantly in the subdermal plexus[31]. Medial row and lateral row perforators within the same hemi-abdomen were connected via both direct and indirect linking vessels (Figure 2.2.17).

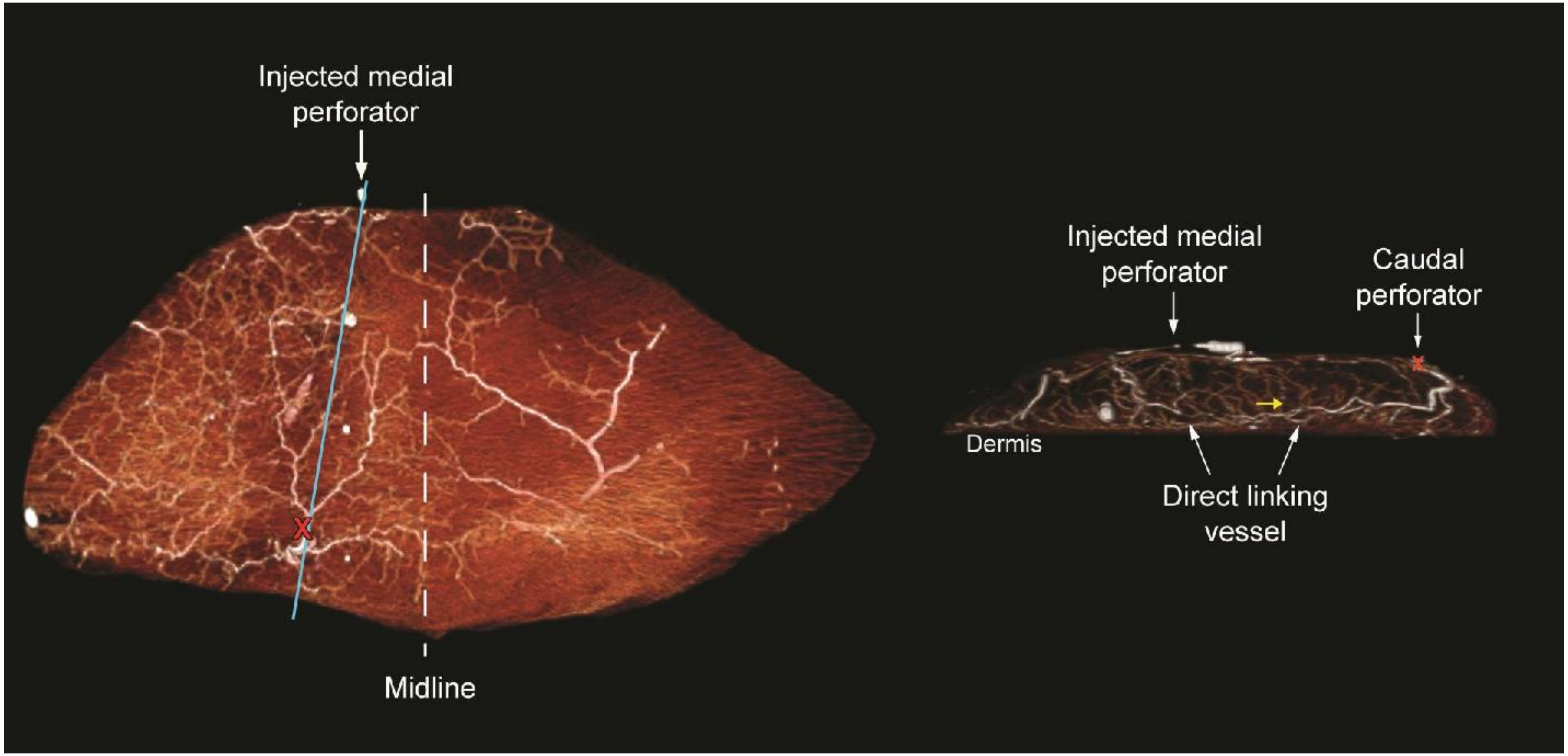

Figure 2.2.15 *3D CT angiogram of a medial perforator DIEP flap. Left: Antero-posterior (AP) view; Right: Sagittal view of flap, corresponding to blue line in AP view. Direct linking vessels connect perforators within the same medial row. X marks a perforator caudal to the injected medial one. Yellow arrow shows direction of flow.*

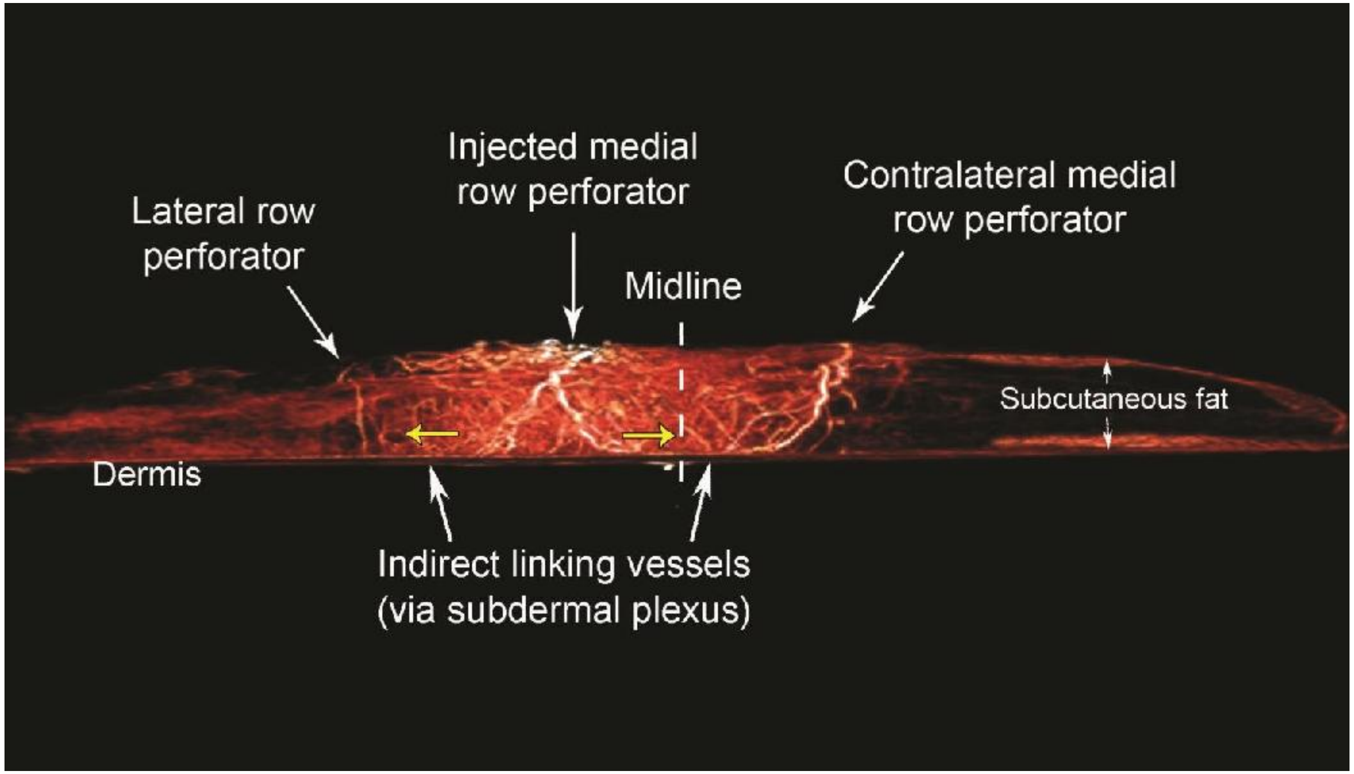

Figure 2.2.16 *3D CT angiogram of a medial perforator DIEP flap, transverse view. Injected medial perforator connected to the contralateral medial row perforator through indirect linking vessels via the subdermal plexus. Yellow arrows show direction of flow.*

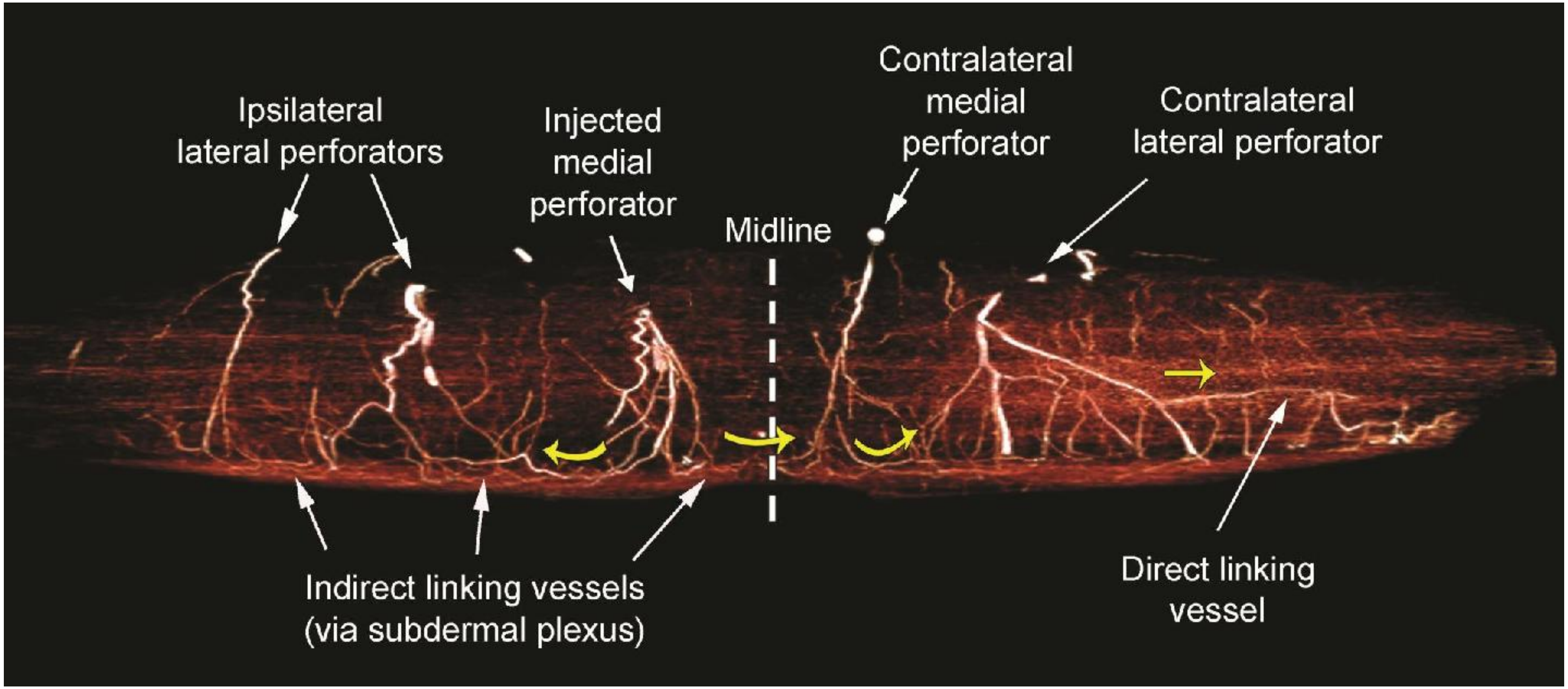

Figure 2.2.17 *3D CT angiogram of a medial perforator DIEP flap, transverse view. Medial row and lateral row perforators within the same hemi-abdomen were connected via both direct and indirect linking vessels. Contrast traveled across the midline via indirect linking vessels via the subdermal plexus. Yellow arrows show direction of flow.*

Lateral Row Perforators

Fourteen lateral perforator DIEP flaps were analyzed. The mean vascular territory of a DIEP flap when a lateral row perforator was injected was 196cm^2. Perfusion was found to be more lateralized, and very few of these flaps crossed the midline (3 out of 14). Contrast injected into a lateral perforator tended to stay in one hemi-abdomen (Figure 2.2.18). Again, large-diameter linking vessels were found to connect perforators within the same lateral row perforators, and both direct and indirect linking vessels were found to communicate between perforators of the same hemi-abdomen (Figure 2.2.19).

We found that for both lateral and medial perforators, indirect linking vessels (through the subdermal plexus) outnumber direct linking vessels, which implies that perfusion occurs mostly at the superficial level of the skin.

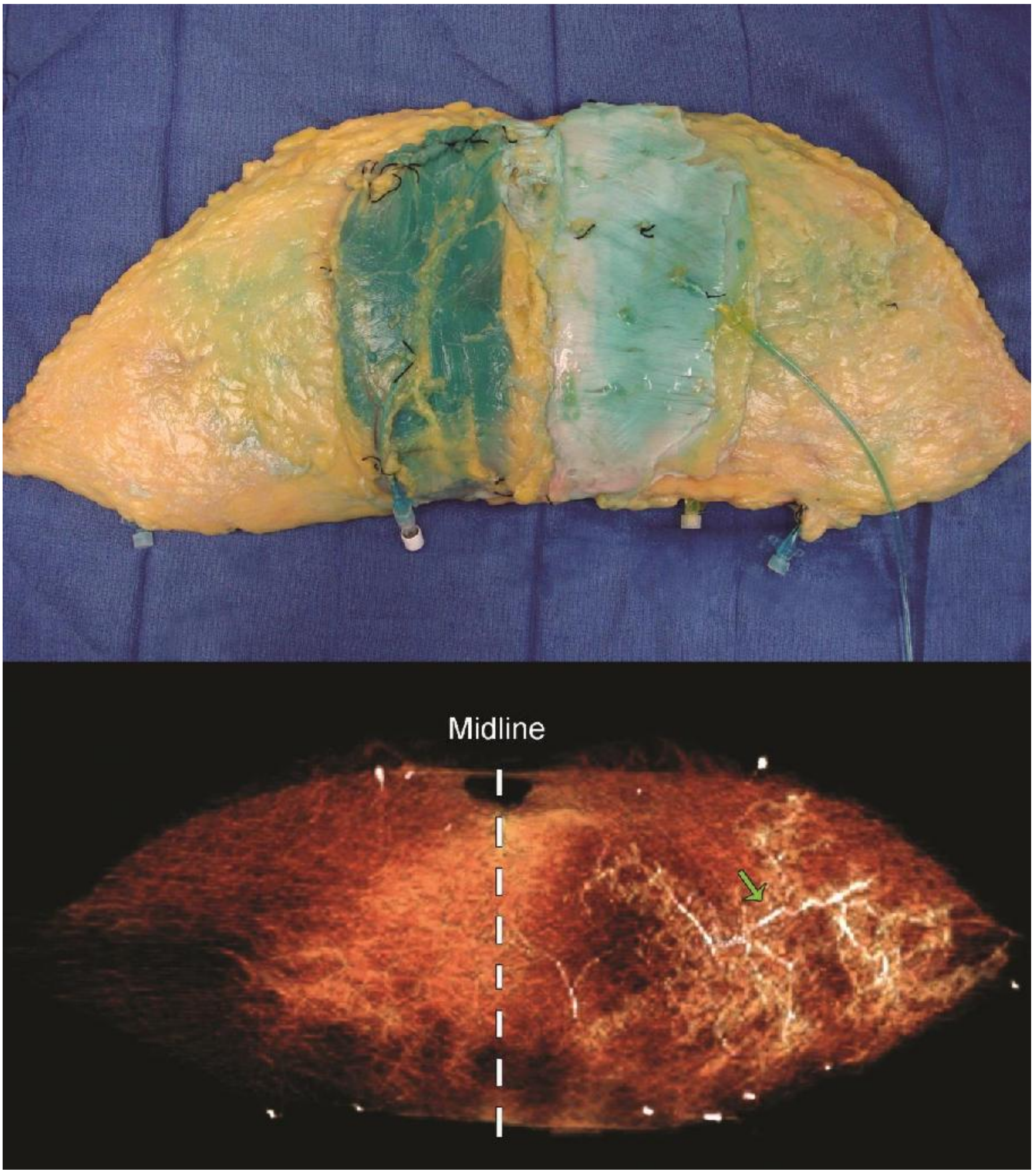

Figure 2.2.18 *(Above:)Photograph of cadaveric DIEP flap where right lateral perforator is cannulated and injected with contrast. (Below): 3D CT angiogram of flap. Arrow shows the location of lateral row perforator injected with contrast. Perfusion tends to stay in one hemi-abdomen.*

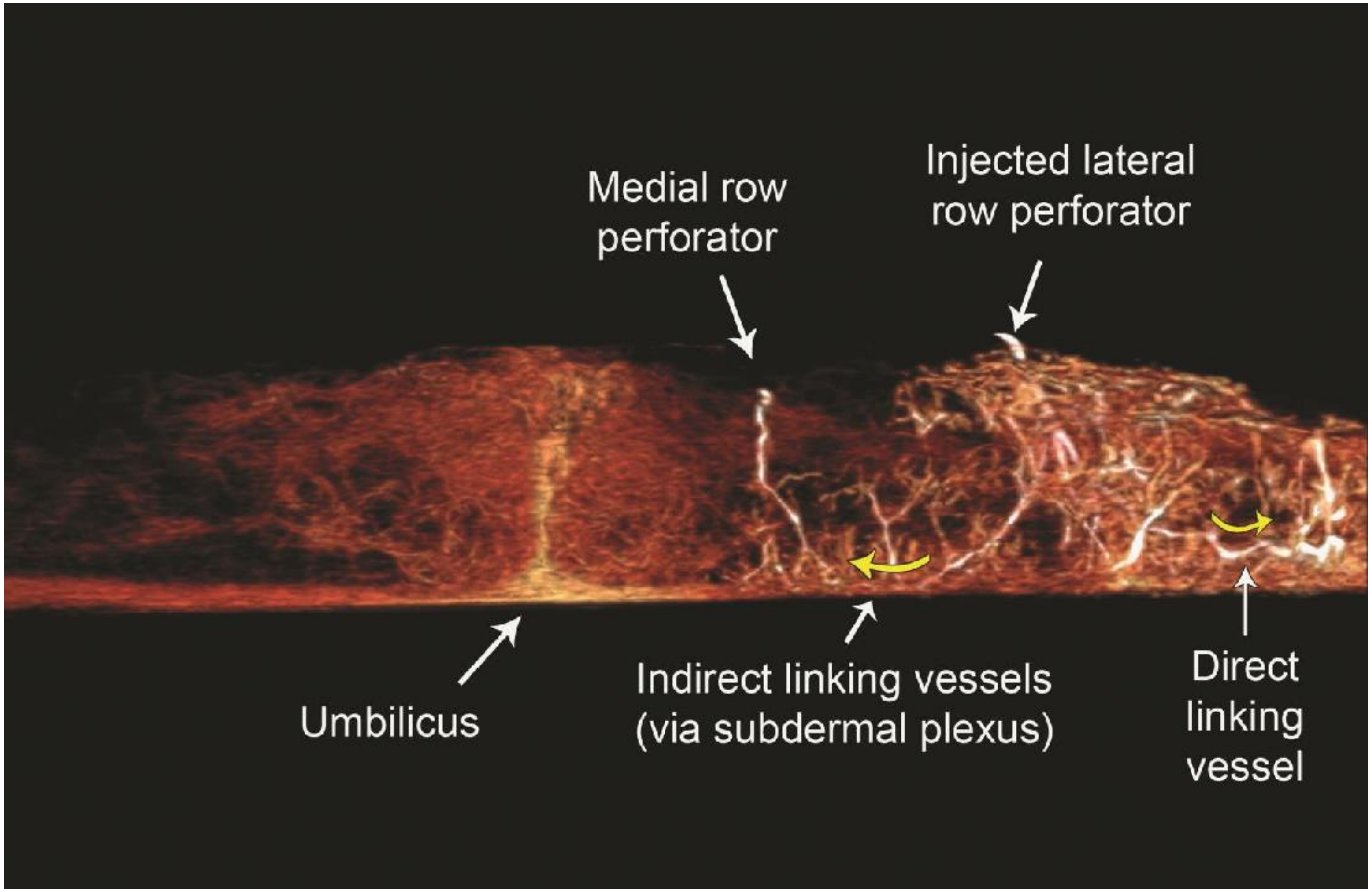

Figure 2.2.19 *3D CT angiogram of a lateral perforator DIEP flap, transverse view. Both direct and indirect linking vessels were found to communicate between perforators of the same hemi-abdomen. Contrast rarely crossed the midline. Yellow arrows show direction of flow.*

Zones of Perfusion

In a medial perforator DIEP flap, the mean percentage of Hartrampf zone II perfused was 65.8% compared to 4.8% for a lateral perforator DIEP flap. For Hartrampf zone III, a medial perforator injection had only 43.9% compared to 85.2% for a lateral perforator ($p < 0.01$) (Graph 2.3). Five medial perforator flaps had vascular territories encroaching zone IV, whereas none of the lateral perforator flaps did.

In our 4D CT investigations, we found that flow of contrast for a medial perforator DIEP traveled earlier to Hartrampf zone II and had a greater area of vascularity compared to Hartrampf zone III (Figure 2.2.20, Video 2.2.3). The lateral perforator DIEP flaps had earlier and greater contrast flow into Hartrampf zone III compared to Hartrampf zone II (Figure 2.2.21, Video 2.2.4).

Graph 2.3 *Comparison of zone II and III perfusion according to perforator (medial versus lateral).*

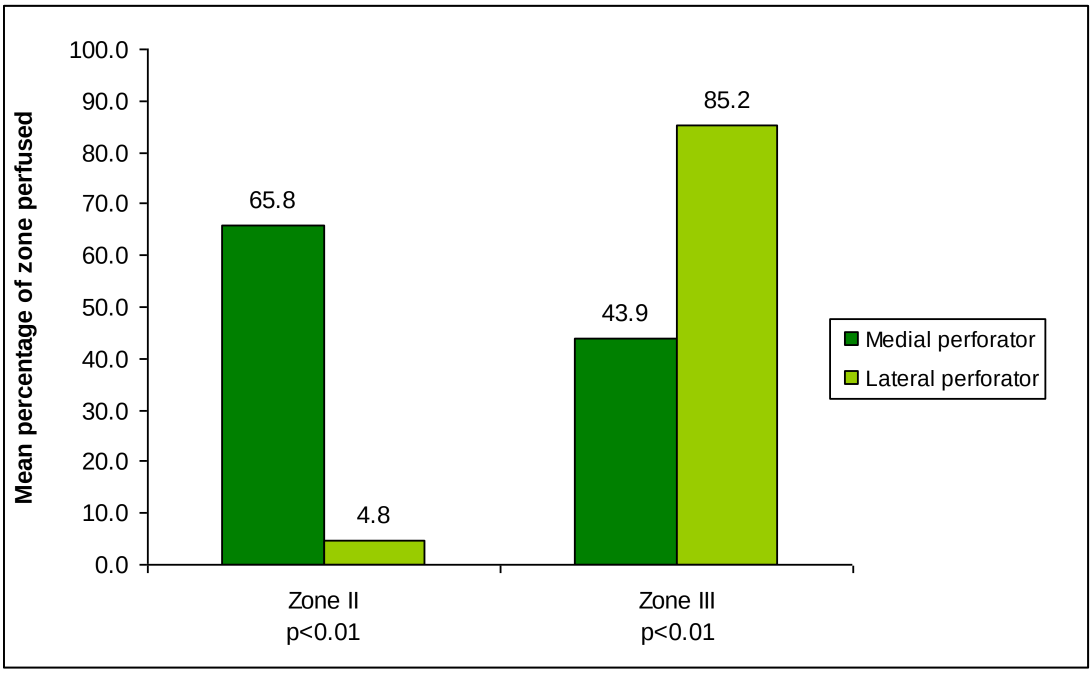

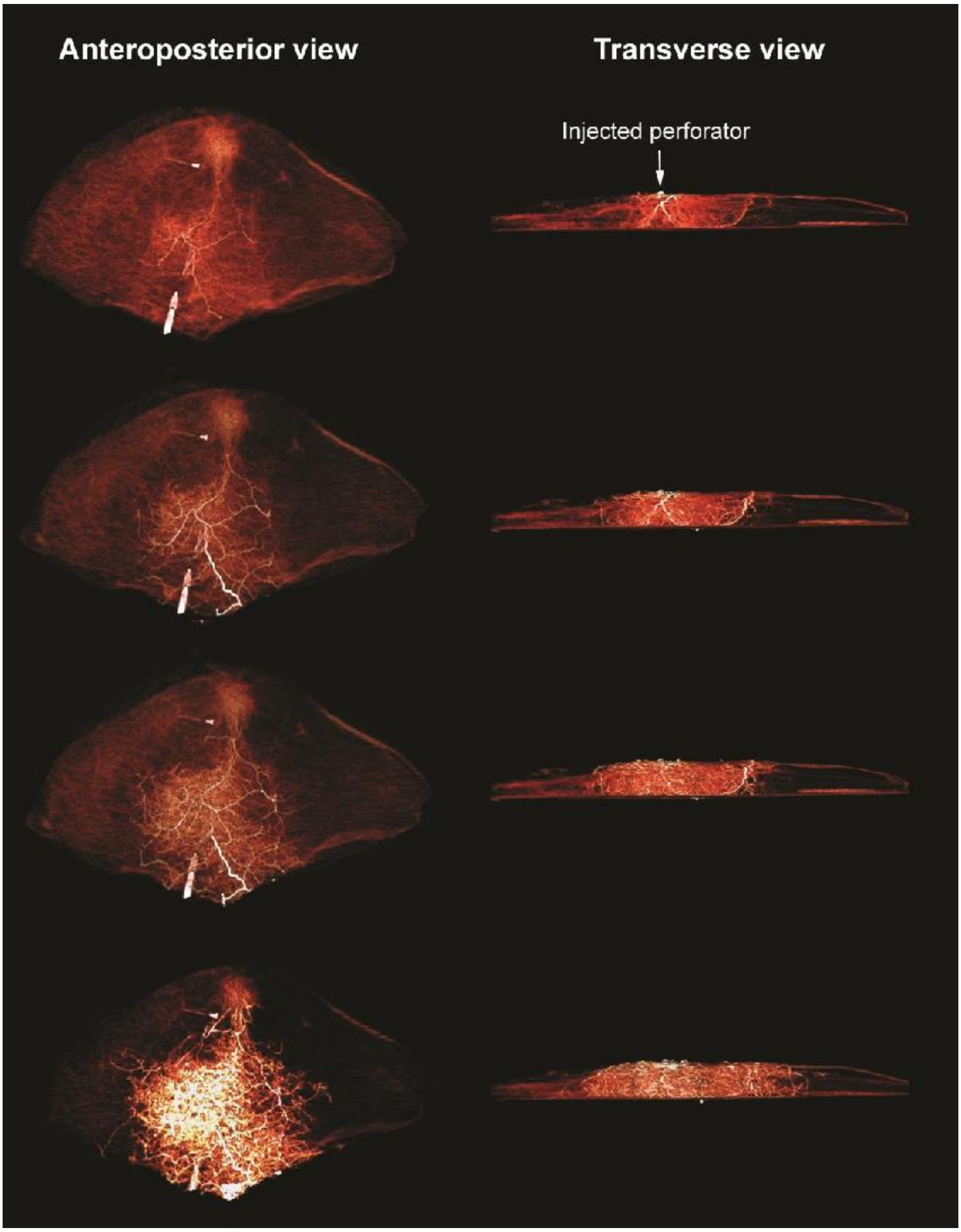

Figure 2.2.20 *4D CT angiogram demonstrating perfusion of a medial perforator DIEP flap. Left: Antero-posterior view; Right: Transverse view. Flow of contrast traveled earlier to zone II and had a greater area of vascularity, compared to zone III.*

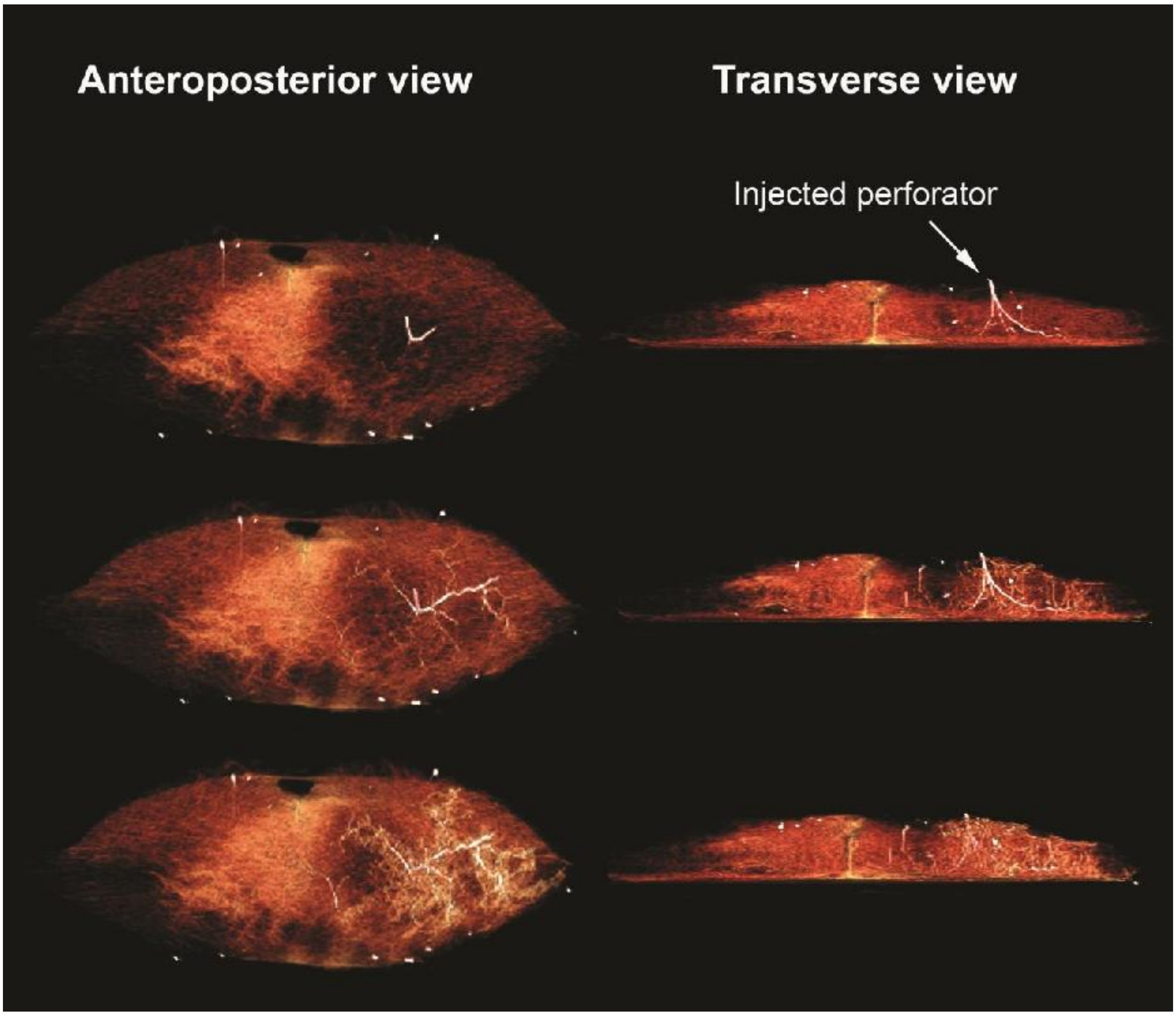

Figure 2.2.21 *4D CT angiogram demonstrating perfusion of a lateral perforator DIEP flap. Left: Antero-posterior view; Right: Transverse view. There was earlier and greater contrast flow into zone III compared to zone II.*

DISCUSSION

This methodology does not pretend to mimic physiological conditions and cannot account for aspects such as vasoconstriction and physiological shunting. Actual vascularity may be quite different in a physiological situation, where nervous, hormonal and local controls of the vessels come into play. This merely gives us a means of comparing two different types of perforators using identical experimental conditions.

We found that anatomical vascular imaging always underestimates the true clinical vascular perfusion area (many surgeons will attest to harvesting lateral perforator DIEP flaps which were larger than a hemi-abdomen without complications). Therefore, larger vascular territories can be anticipated in a clinical arena. Medial and lateral row perforators offer distinct and stereotypical zones of perfusion that have a significant impact on flap design and harvesting. When considering a lateral row-based perforator flap, vascularity was found to rarely cross the midline in our anatomical cadaver CT studies. We propose that this was due to a higher number of communicating vessels needed to cross the midline, compared to a flap based on a medial perforator (Figure 2.2.22).

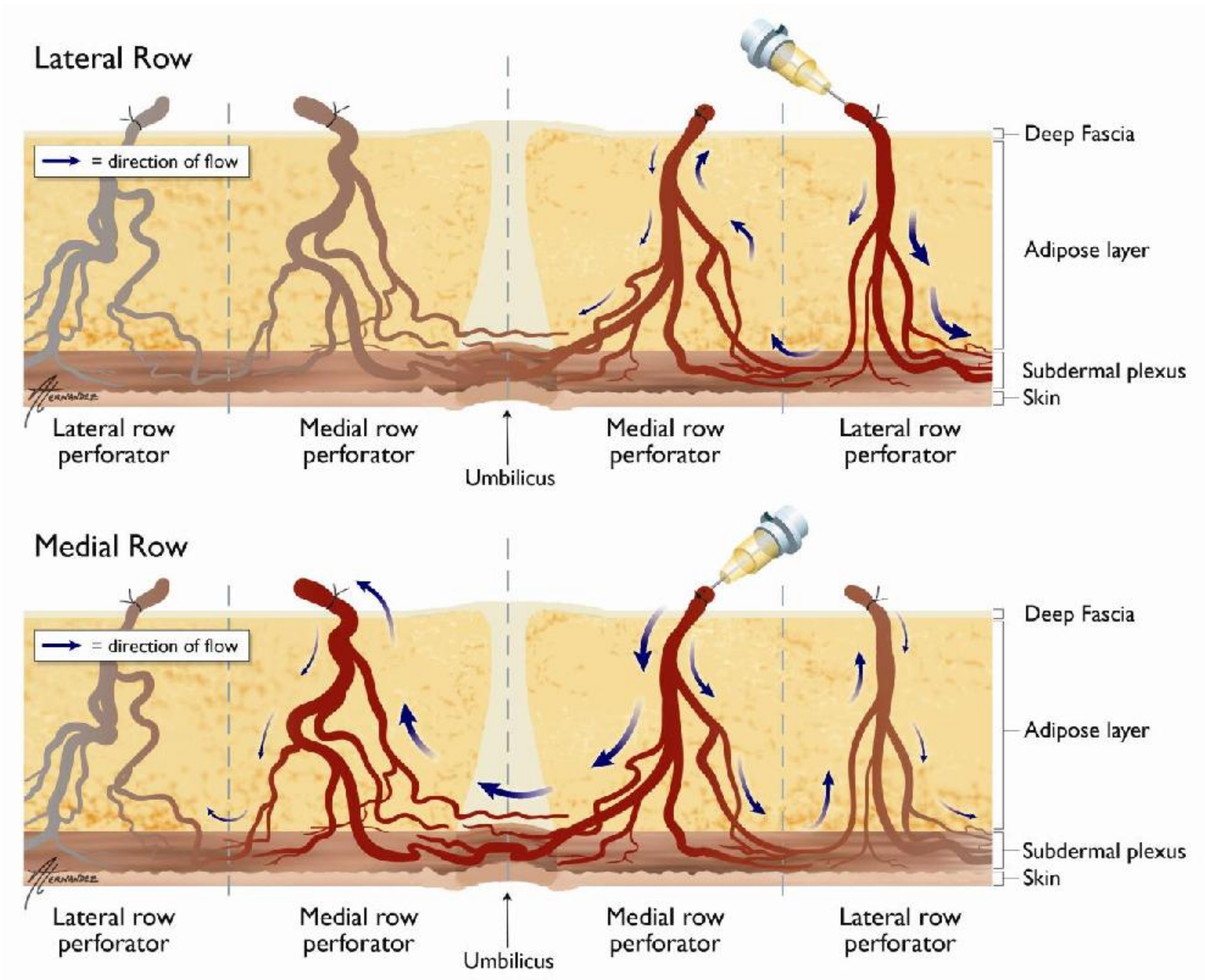

Figure 2.2.22 *Illustration of contrast flow in a DIEP flap. Top: Lateral row perforator injected. At least 2 sets of linking vessels need to be crossed to reach the midline; Bottom: Medial row perforator injected. Less linking vessels are required to cross the midline thus contrast flows into zone II more easily, hence a more centralized perfusion.*

When planning a large breast reconstruction, a medial row perforator or a combination of medial and lateral perforators (muscle-sparing TRAM or TRAM flap) should be considered. If a single medial row perforator is selected, the vascular territory is larger, and more centralized compared to a lateral row perforator-based flap. Therefore, both tips of the flap are subjected to a higher risk of ischemia (Figure 2.2.23). We routinely discard the distal third or half of Hartrampf zone III and half or all of zone IV when selecting a medial row single perforator DIEP flap.

Lateral row perforators are simple to harvest and when found close to the lateral edge of the rectus muscle, they follow a more direct vertical orientation when passing through the muscle to the lateral division of the deep inferior epigastric artery and vein. Studies have been performed to advocate the use of the lateral row perforators in DIEP flap harvesting. The lateral branch is frequently wider, and tends to run a more rectilinear course, allowing for easier and speedier dissection[45, 46]. Lateral row perforators used in a hemiabdominal flap have more of a central position, and have less risk of partial flap necrosis of the most distal ipsilateral tip of the flap. Therefore, hemiabdominal flaps tend to be safely harvested based on a single lateral row perforator (Figure 2.2.24), and this can be used in small to medium breast reconstructions. It is also very useful for bilateral breast reconstruction.

In Abdominal Study I, we found that the free TRAM flap, which has both medial and lateral perforators, had the largest vascular territory amongst the commonly used abdominal flaps for breast reconstruction, and perfused Hartrampf zones I, II and III[53].

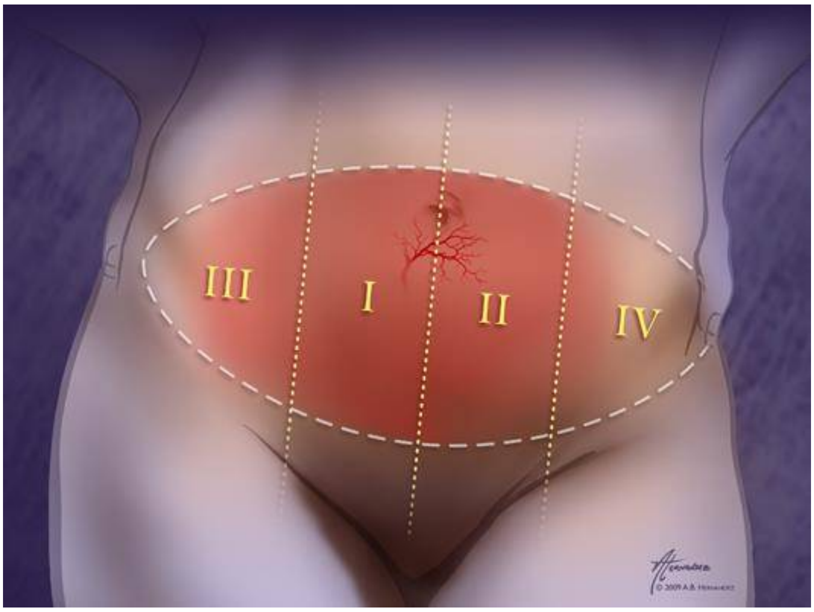

Figure 2.2.23 *Illustration of a medial perforator DIEP flap, where perfusion is more centralized and has a bigger vascular territory. These are useful for large breast reconstructions.*

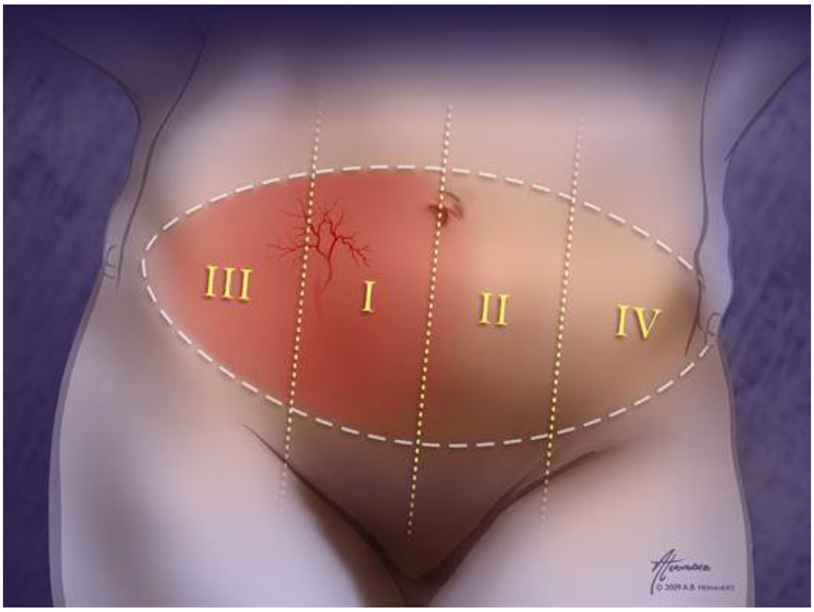

Figure 2.2.24 *Illustration of a lateral perforator DIEP flap, where perfusion is more lateralized. These are useful for small to moderate-sized, and bilateral breast reconstructions.*

Reappraisal of the Zones of Perfusion

Holm *et al.* performed perfusion studies which demonstrated that Hartrampf zones II and III should be reversed. They stated that Hartrampf's concept was erroneous and that "perfusion of the vascular territories across the midline was always delayed and less intensive than in the territories on the ipsilateral side". This elegant study was well carried out, but its bold statement does not always hold true. In Holm's study, only 2 out of 15 flaps utilized just the medial row perforators, and 8 used only lateral row perforators (the rest had both medial and lateral row perforators).

Based on our 3D, 4D CT angiographic studies, contrast flow from a medial perforator perfused Hartrampf zone II earlier and more so than Hartrampf zone III. The resultant area of vascularity of Hartrampf zone II is greater than in Hartrampf zone III. Therefore, flaps based on a single medial row perforator are shown to be more centralized, and follow Hartrampf's classification of perfusion zones, with zone II being the contralateral medial region of a transverse abdominal flap. Zone III is ipsilateral to zone I and zone IV is ipsilateral to zone II (Figure 2.2.25).

In contrast, perfusion for a lateral perforator DIEP is more lateralized. Contrast travelled to Hartrampf zone III earlier and had a greater area of vascularity compared to Hartrampf zone II. Therefore, this perfusion pattern follows Holm's classification, and zones II and III should be in reverse order (Figure 2.2.26). Holm's zone II corresponds to the area ipsilateral to zone I, and Holm's zone III should now be the contralateral medial region, in the same hemi-abdomen with zone IV.

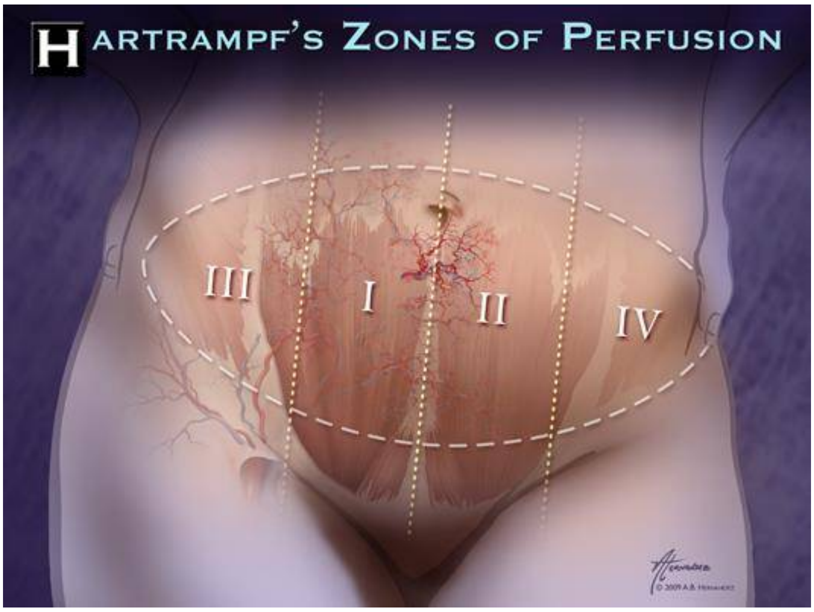

Figure 2.2.25 *Medial perforator DIEP flaps follow Hartrampf zones of perfusion. Zone II is on the contralateral hemi-abdomen.*

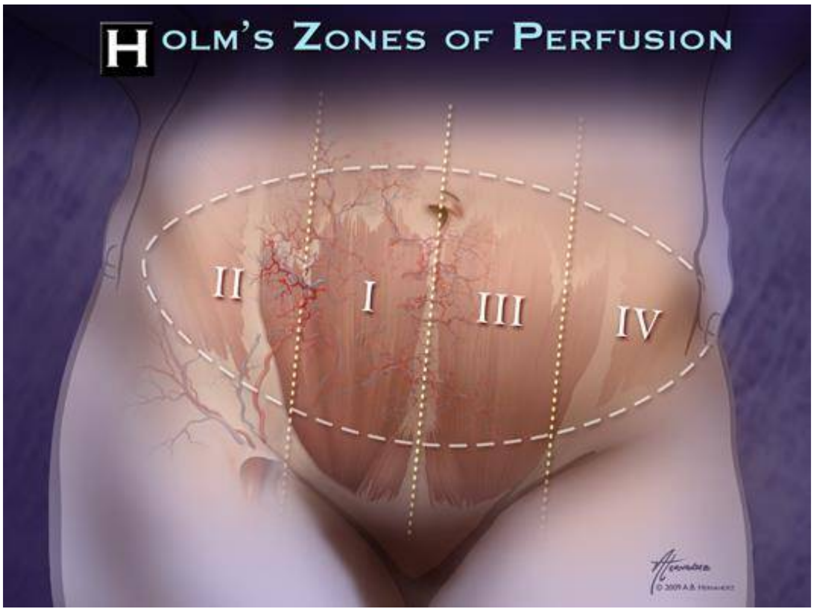

Figure 2.2.26 *Lateral perforator DIEP flaps follow Holm's zones of perfusion. Zone II is on the ipsilateral hemi-abdomen.*

Still, regardless of perforator location, the largest perforator should always be selected during a flap harvest. The deep inferior epigastric artery flap has allowed a significant decrease in donor site morbidity and can provide an aesthetic breast reconstruction which is comparable to all other abdominal donor site flaps. Thorough knowledge of the vascular anatomy of medial or lateral-based perforators is crucial for safe flap design and harvesting and can help minimize the risks of postoperative fat necrosis and partial flap necrosis. In a recent meta-analysis, the risk of fat necrosis in DIEP flaps was reported to be twice that of TRAM flaps[54]. This is likely due to improper knowledge of the vascular anatomy of lateral versus medial row-based perforators. Both of these perforator types will have distinct vascular territories, and this should be respected during DIEP flap harvesting in order to avoid such complications.

Our study demonstrates that the perfusion characteristics of a medial row perforator differ significantly from that of a lateral row-based perforator. Therefore, each perforator has its own distinct vascular territory, which has been termed a ‘perforasome’[55]. This may also explain why there are significant differences in the literature regarding fat necrosis and DIEP flap complications. Numerous series mention their complications by combining both lateral and medial row-based perforator DIEP flaps. Therefore, if meaningful comparison is to be made, medial row perforator DIEP flaps need to be compared with medial row perforator DIEP flaps, and likewise with lateral row perforator DIEP flaps. We acknowledge that a limitation of this study is the focus on only single perforator DIEP flaps, as we were investigating the vascular territory of single perforators. Clinically, although some DIEP flaps are based on 2 or more perforators, many DIEP flaps are based on single perforators, so we believe the findings from this study are still valid.

Of course in these modern times, when we require a large abdominal-based free flap, we employ techniques such as turbo-charging or use bipedicled flaps.

Conclusion

DIEP flaps based on medial row perforators will have a different vascular territory compared to those based on lateral perforators. Increased knowledge of the vascular anatomy and zones of perfusion of both these perforator types will likely help decrease flap-related complications such as fat necrosis, and partial flap loss. This in general will yield better patient outcome and decreased morbidity in the reconstructive process.

2.3 BACK: Posterior Intercostal Artery Perforator and Lumbar Artery Perforator Flaps

Nine complete hemiback flaps were harvested to analyze the vascular anatomy of the posterior dorsal intercostal artery perforator flap. The margins were the level of C7 superiorly, mid-axillary line laterally, mid-back medially and T12 inferiorly.

The whole lumbar skin (no incision through midline) was harvested from the level of T12 to the level of the iliac crest to study the lumbar artery perforators (four flaps). The lateral intercostal artery perforator flaps (six flaps) were analyzed using the same technique.

Perforators in both thoracic (posterior intercostal artery perforators) and lumbar (lumbar artery perforators) were cannulated and injected with contrast for CT scanning and analysis.

Results

Linking vessels between adjacent perforators were demonstrated. Injection of contrast into one perforator shows communication between adjacent perforators (Figures 2.3.1 and 2.3.2). The injection of a single perforator was frequently found to perfuse a large area. Perfusion from a perforator between the midline and mid-axillary line can perfuse the superior or inferior halves of a hemiback flap (Figure 2.3.3).

Linking vessels in the trunk are commonly directed perpendicular to the midline and follow an oblique transverse direction, parallel to the cutaneous dermatomes (Figure 2.3.4).

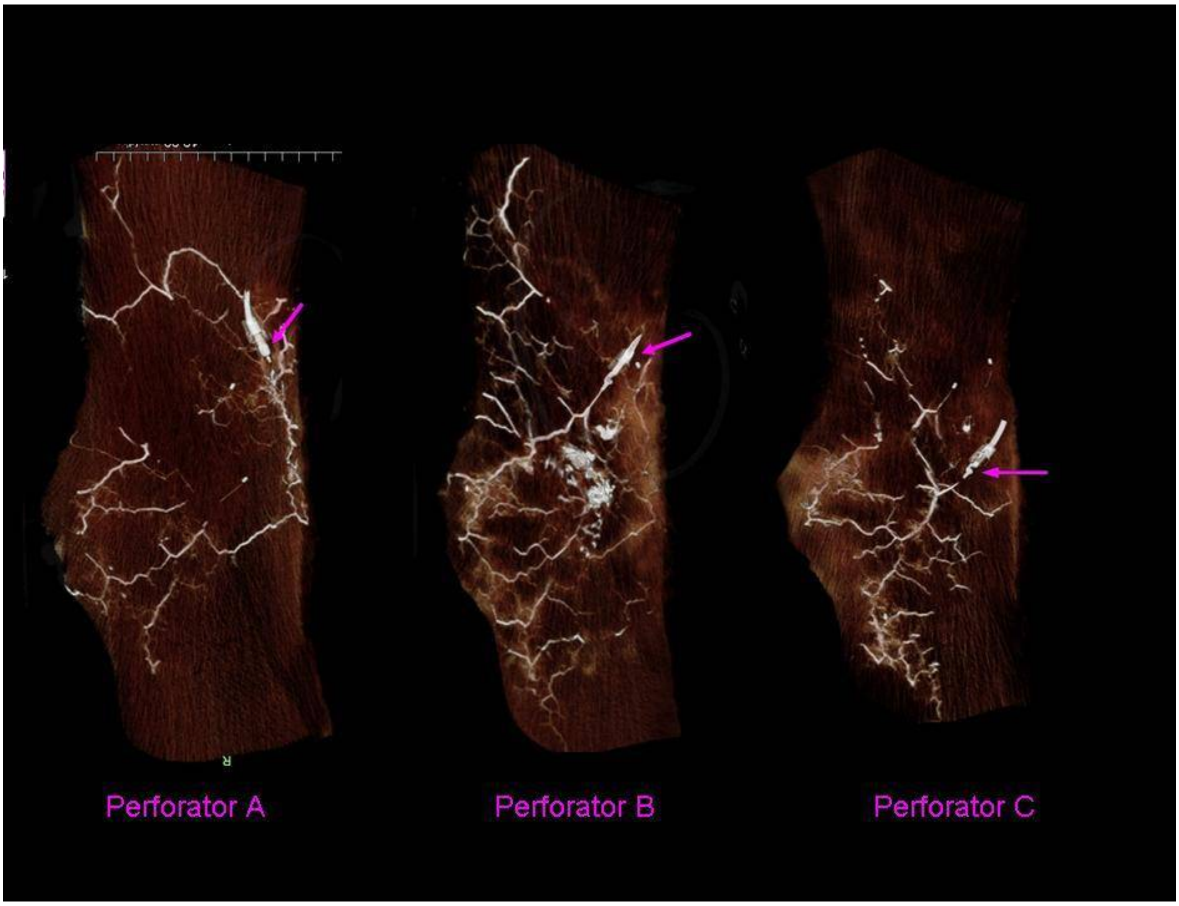

Figure 2.3.1 *Perforators A, B and C are adjacent posterior intercostal perforators on a hemiback flap. (Left) Injection of Perforator A shows communication with Perforator B. (Middle) Injection of Perforator B demonstrates connection with both Perforators A and C. (Right) Injection of Perforator C shows communication with Perforator B but not Perforator A.*

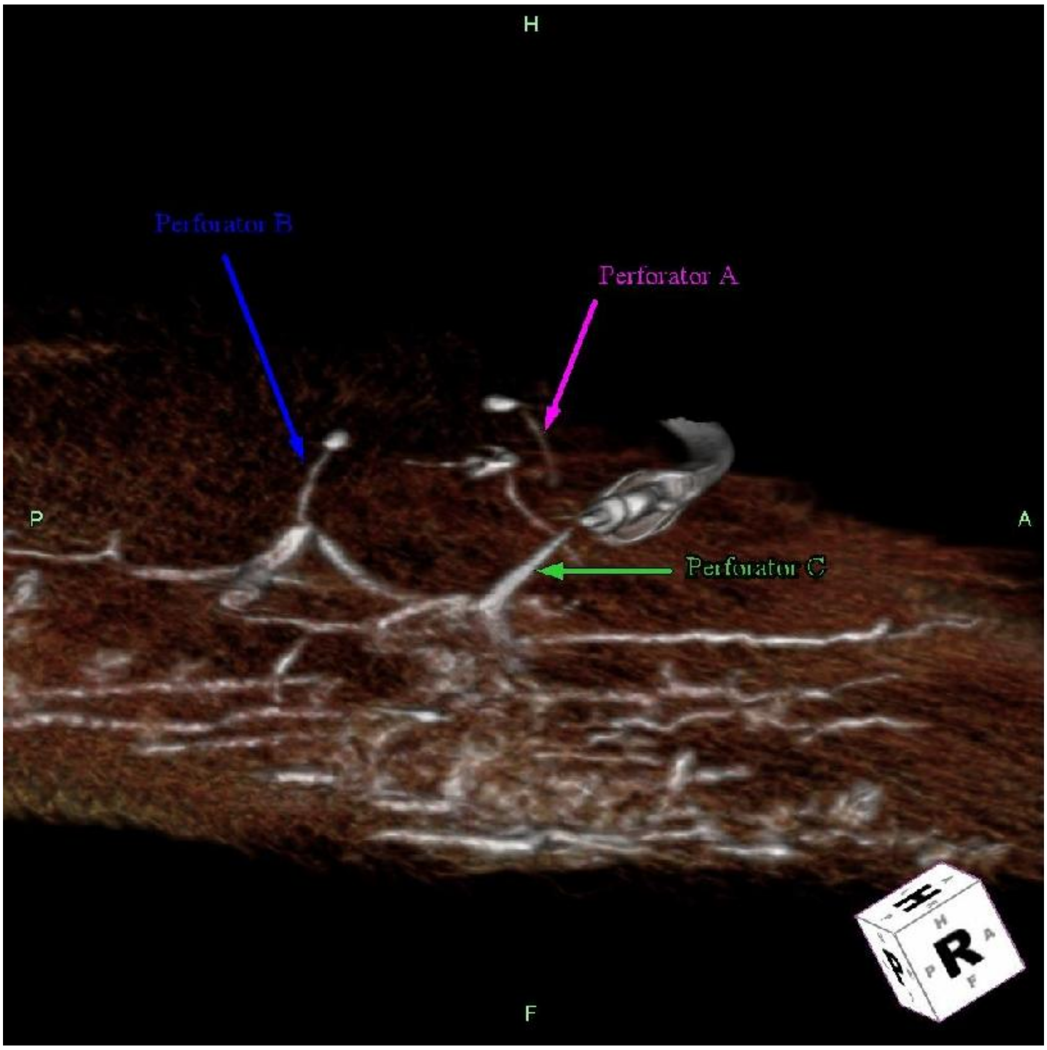

Figure 2.3.2 *Oblique view of hemiback flap above, demonstrating Perforators A, B and C. Note: Cube of orientation in right bottom corner. R=right, H=head, F=foot, A=anterior, P=posterior*

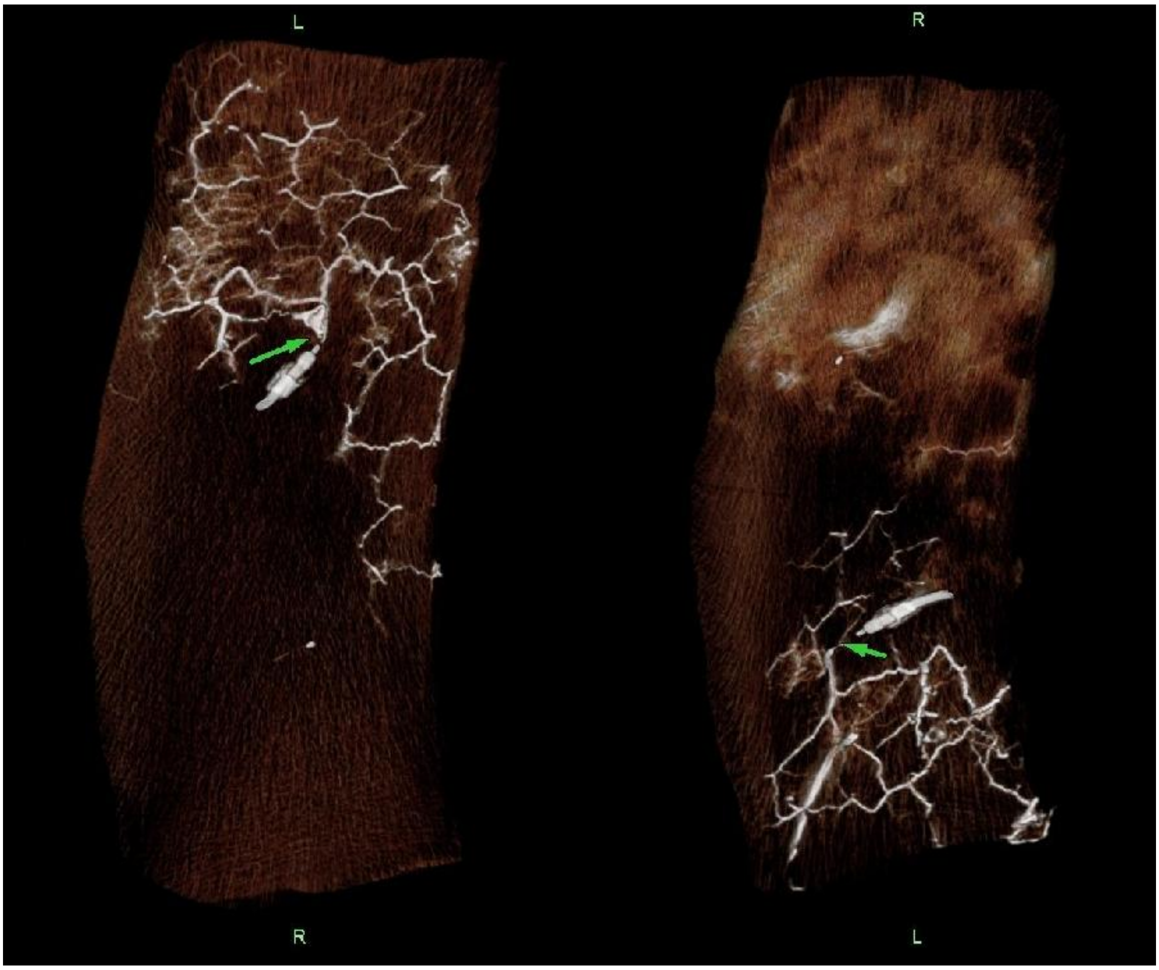

Figure 2.3.3 *(Left) A superior posterior intercostal perforator between the midline and mid-axillary line perfused the superior half of this hemiback flap. (Right) An inferior posterior intercostal perforator between the midline and mid-axillary line perfused the inferior half of the same flap.*

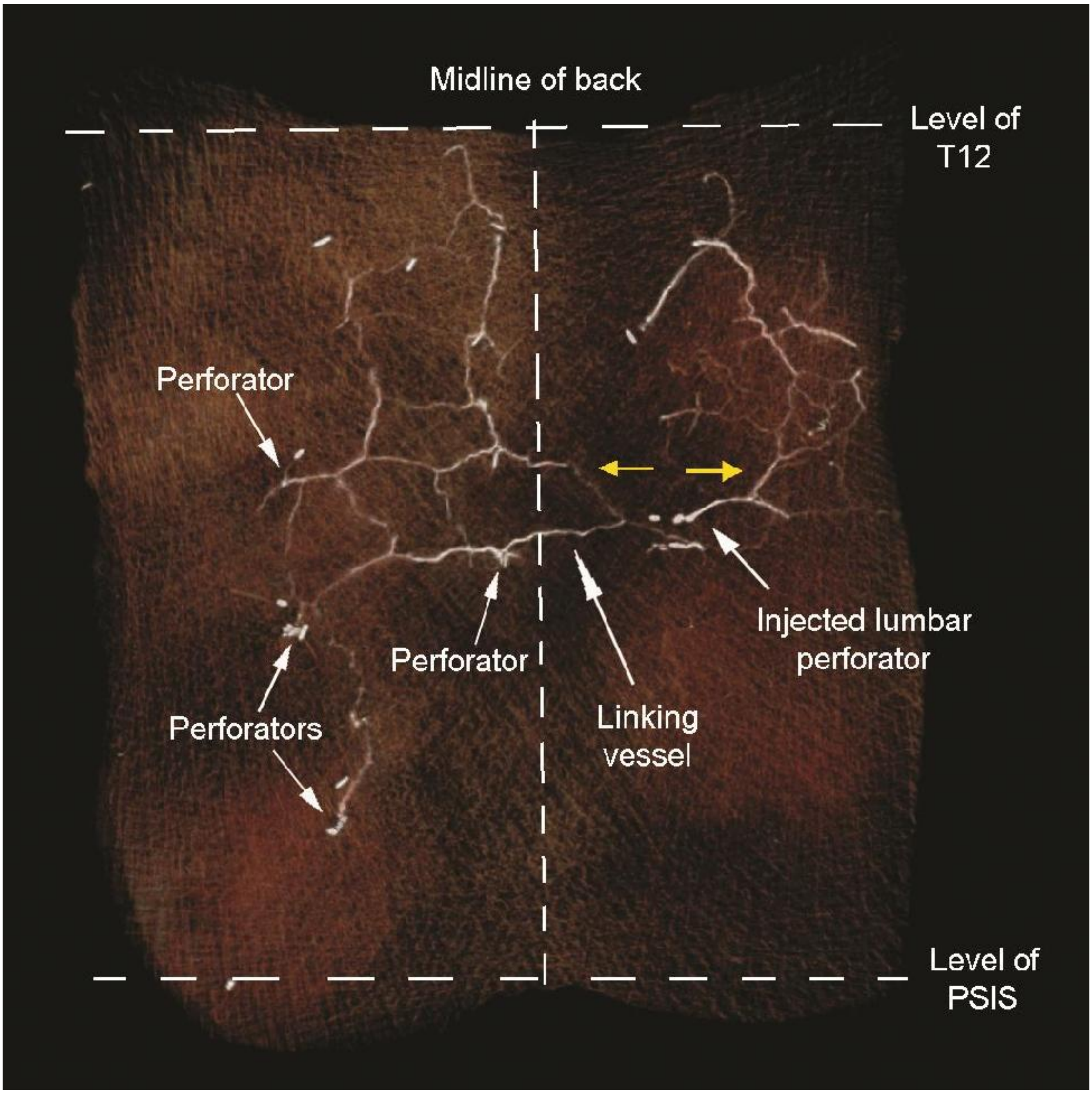

Figure 2.3.4 *Whole lumbar skin from T12 level to posterior superior iliac spine (PSIS). Lumbar perforator injected with contrast, and was found to perfuse across the midline, as well as ipsilaterally in a transverse direction. Yellow arrows show direction of flow.*

2.4 GLUTEAL REGION: Superior Gluteal Artery Perforator (SGAP) Flap

For the gluteal region, four SGAP skin flaps were harvested. On a line connecting the greater trochanter with the posterior superior iliac spine, the perforators were located in the area of the medial to middle third. Centered around this region, an elliptical skin paddle was harvested, with the tips at the midline and the iliac crest. The skin island measures approximately 8 to 12 cm width and 25 to 30 cm length. The largest perforator for each flap was cannulated and subsequently subjected to CT scanning.

Results

Two of the SGAP flaps demonstrated good perfusion of the whole flap (Figures 2.4.1). However, the other two SGAP flaps were harvested from a cadaver with a sacral pressure sore, and showed no perfusion in the region encompassed by the sore (Figures 2.4.2 and 2.4.3). 4D CT angiography demonstrated perfusion travelling bi-directionally, i.e. medially and laterally (Video 2.4.1)

Lateral views show linking vessels within the subdermal plexus connecting adjacent perforators (Figure 2.4.4, Video 2.4.2)

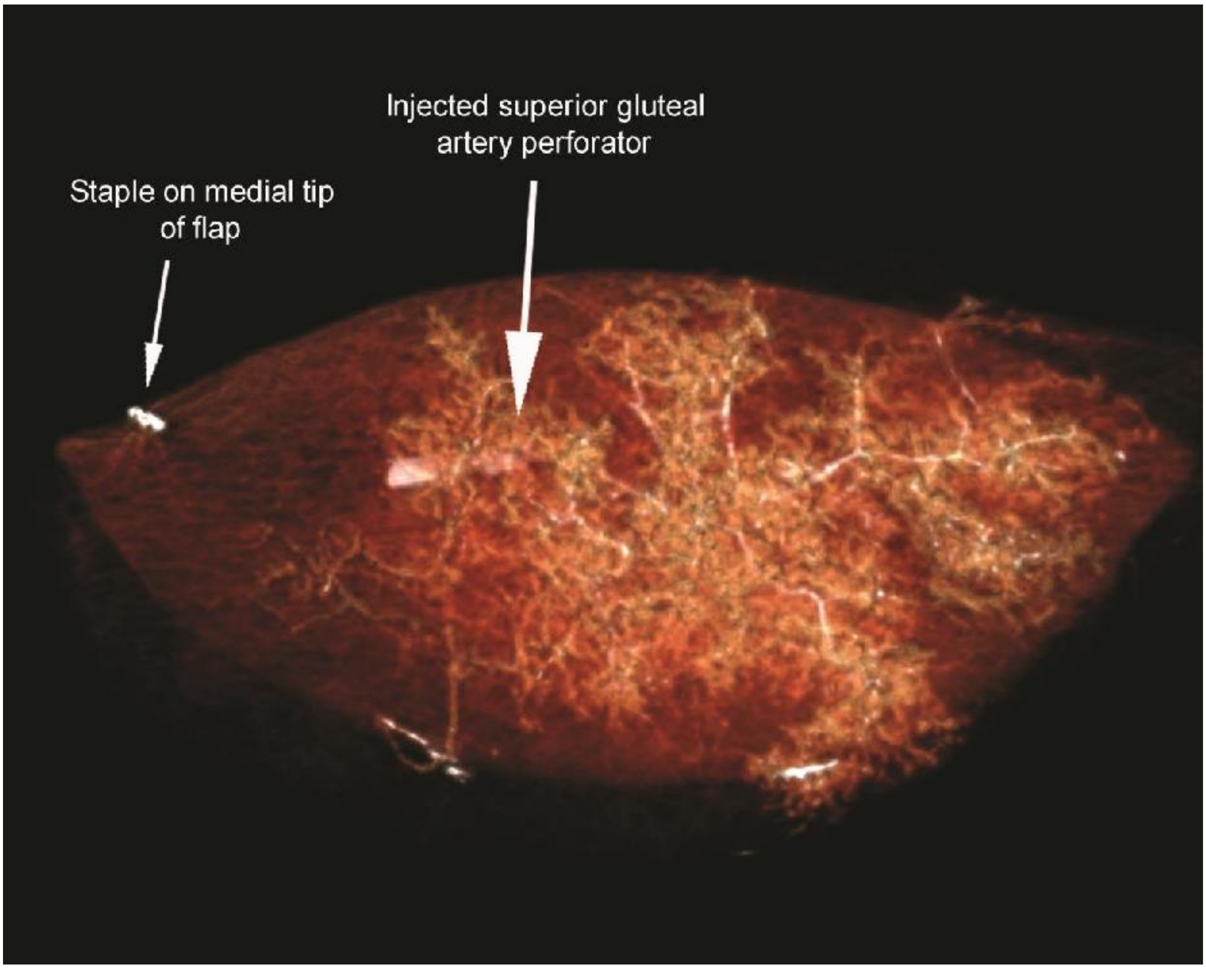

Figure 2.4.1 *Superior gluteal artery perforator (SGAP) flap showing good perfusion.*

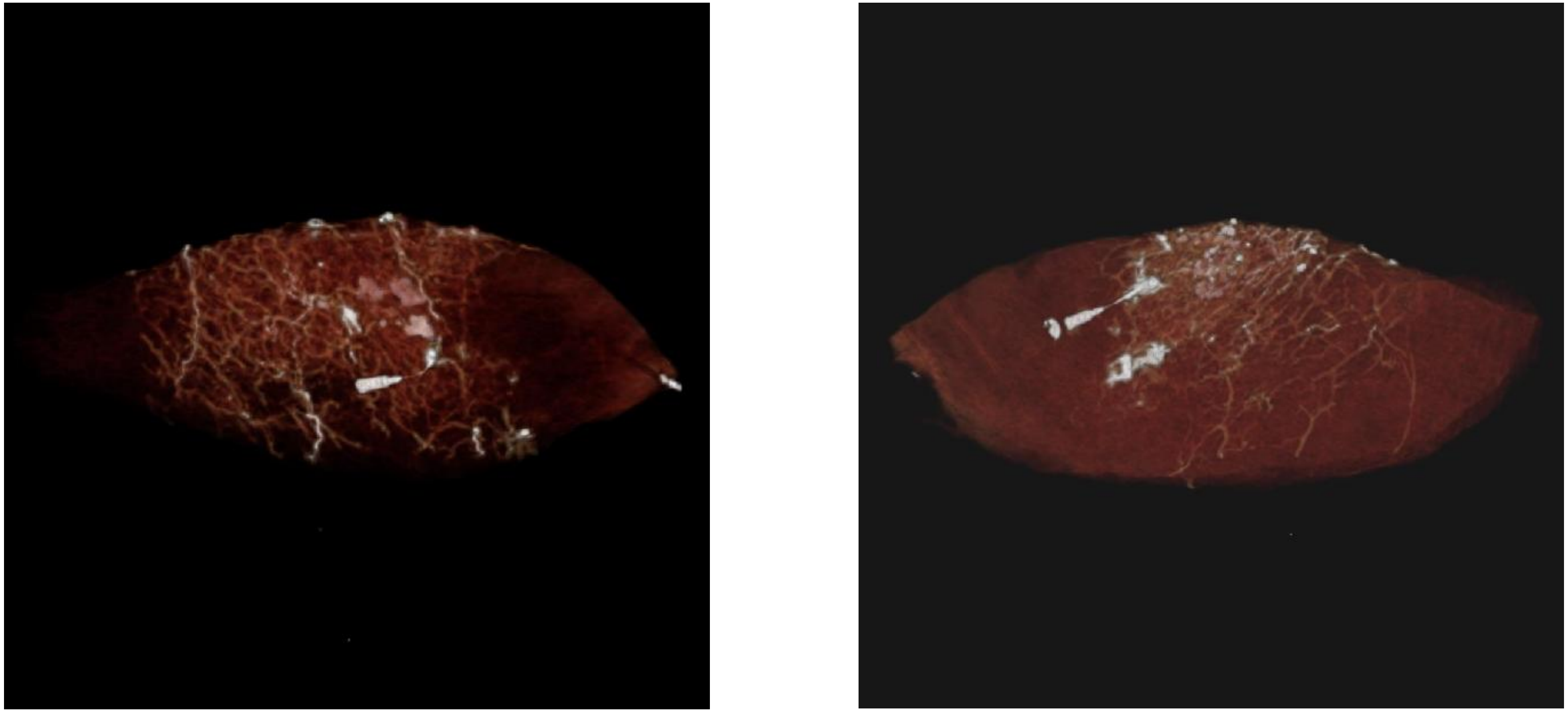

Figures 2.4.2 and 2.4.3 *SGAP flaps from a cadaver with a sacral pressure sore. Note the lack of perfusion in the midline*

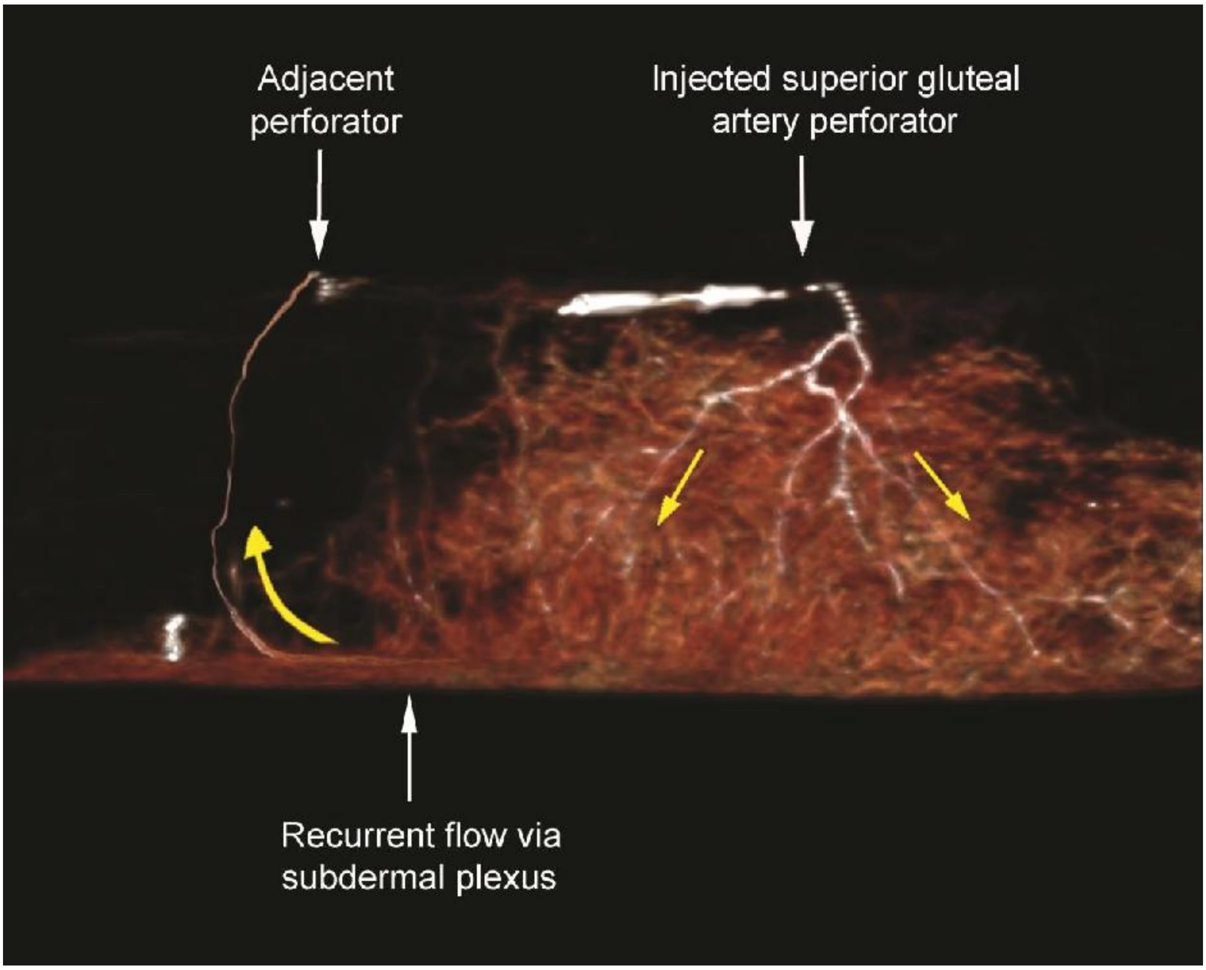

Figure 2.4.4 *Lateral view of flap in Figure 2.4.1. Indirect linking vessels within the subdermal plexus connect adjacent perforators. Yellow arrows show direction of flow.*

Discussion

As we shift towards increased use of single perforator based flap reconstructions, knowledge of individual perforator vascular anatomy supercedes that of source artery vascular anatomy. Each perforator has its own vascular territory called a perforasome which carries a multi-directional flow pattern which is highly variable and complex. These perforasomes are linked to one another by linking vessels. These numerous vascular connections confer further protection from ischaemia and vascular injury in the case of trauma. In the back, the orientation of linking vessels appears to be transverse, thus skin paddle orientation should also be transverse. These linking vessels make it possible to harvest large perforator flaps based on a single perforator. We believe that when a perforator flap is harvested all muscle and cutaneous branches from the source artery are ligated which results in hyperperfusion of the selected perforator. Increased vascular filling pressures clinically dilate the perforator itself and allow extensive inter-perforator flow via opening and recruitment of additional linking vessels. These linking vessels, both direct and indirect, are subject to higher than normal filling pressures and are able to capture additional adjacent perforator vascular territories (perforasomes).

CONCLUSION

Each perforator holds a unique vascular territory (perforasome). Every perforator has a potential to become either a pedicle or free perforator flap depending on the size of the source artery. As a result, this allows a myriad of perforator flap designs which can be tailored to better reconstruct defects. The reconstructive surgeon now has more options in replacing like with like. Local flap alternatives become more plentiful and flap design is limited only by the availability of clinically relevant perforators close to the defect for pedicle perforator flaps. Free-style perforator flap options are only limited by the size and length of their respective source artery and vein.

CHAPTER 3

Upper Limb

3.1 Supraclavicular Artery Island (SAI) Flap

Introduction

Oropharyngeal oncologic resections often results in complex wounds requiring the use of local, regional, or free tissue transfer to return form and function. Microvascular free tissue transfer revolutionized reconstructive surgery in the head and neck by providing more flap options to reliably replace tissue defects with minimal donor site morbidity. However they require technical expertise as well as an increased operative time. Local flaps often are not of adequate size and regional flaps are bulky and associated with increased donor site morbidity.

In 1949, the first clinical application of a flap from the shoulder ("Charretera" or acromial flap) was performed by Kazanjian and Converse.[56] Charretera, in Spanish, means the shoulder area where honors are bestowed on military personnel. In 1979, the first anatomical studies were performed by Mathes and Vasconez who described the vascular territory and clinical applications for head and neck reconstruction[57]. The flap was renamed the cervicohumeral flap. In 1983, Lamberty and Cormack named a vessel cephalad to the clavicular insertion of the trapezius muscle the supraclavicular artery[58] (Figure 3.1.1). Since its use, the flap has been controversial because of the reported incidence of distal flap necrosis (Luce)[59]. Beginning in the 1990's, Pallua *et al* "rediscovered" this flap and popularized its use by performing detailed anatomical studies examining the vascularity of what is known today as the supraclavicular island flap[18, 19, 60]. Although the supraclavicular artery island (SAI) flap has been shown to be a versatile regional flap for head and neck reconstruction, the vascular anatomy is still poorly understood. In this study, the vascular anatomy of this flap is examined using computed tomographic (CT) angiography which to date has not been performed.

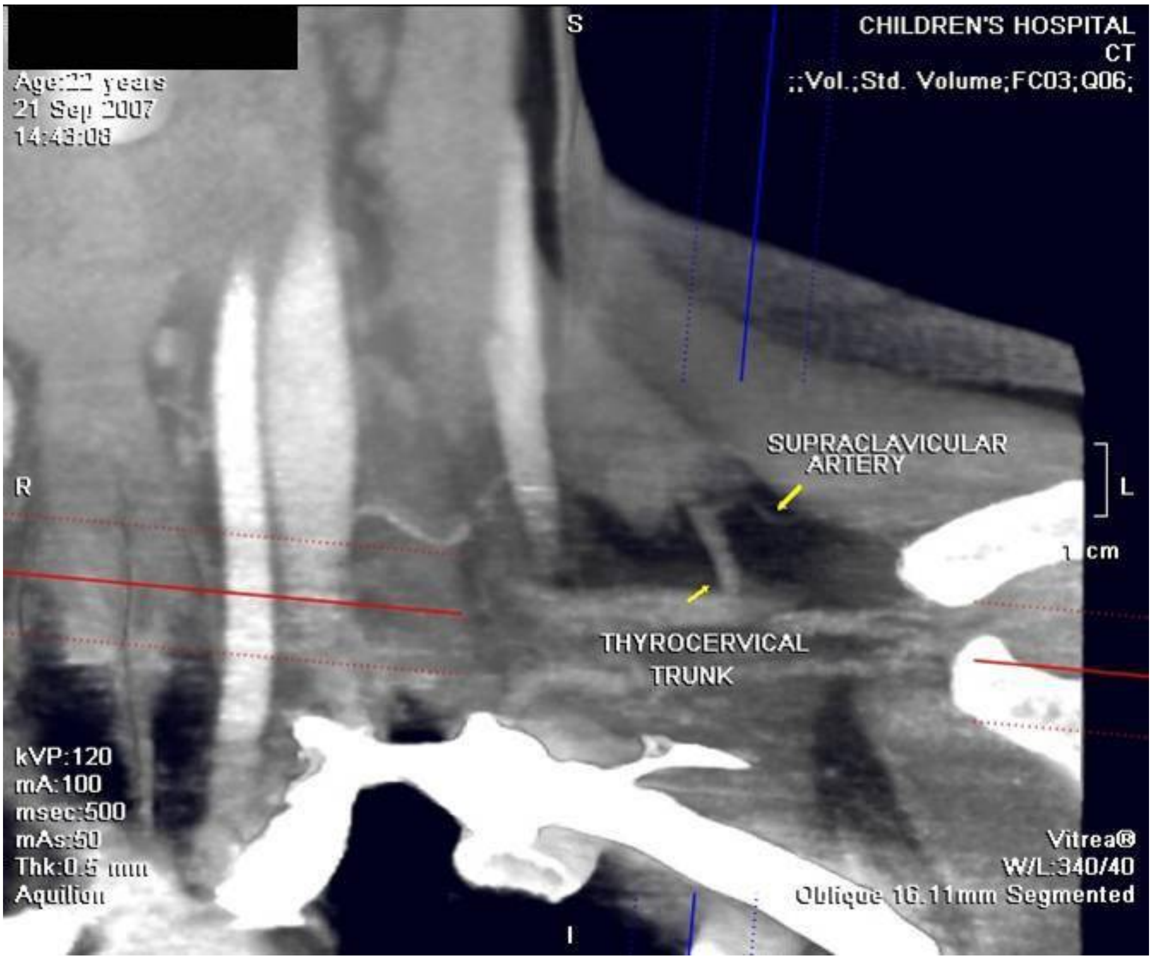

Figure 3.1.1. *CT angiogram of patient demonstrating the supraclavicular artery branching from the thyrocervical trunk.*

Materials and Methods

Ten supraclavicular flaps were harvested from fresh adult cadavers acquired through the Willed Body Program at the University of Texas Southwestern Medical Center. The adipo-cutaneous paddle was incised over the proximal half of the lateral upper arm (overlying the deltoid muscle) and shoulder joint, with the proximal portion of the flap extending to the area superior to the lateral third of the clavicle. The supraclavicular artery which perfuses the flap was dissected out in the proximal portion of the flap. It was usually found to be superior to the lateral third of the clavicle.

Specimen dissection was performed under loupe magnification. Injection of a dilute methylene blue solution through the supraclavicular artery enabled all vascular leaks to be sealed, either through bipolar diathermy or suture ligation.

Results

The SAI flaps were found to have a mean length of 24.2cm and mean width of 8.7cm. The mean area measured 152.8cm^2. Mean diameter of the supraclavicular artery was 1.33mm. It was found 3.6 ± 0.8cm above the clavicle and 8.6 ± 0.3cm from the sternoclavicular junction. The supraclavicular artery was found to perfuse the whole skin paddle in nine flaps (Figures 3.1.2 and 3.1.3). One of the flaps was perfused only 50% (Figure 3.1.4). In this case the pedicle artery was found to be much smaller than the other flap pedicles (0.7mm).

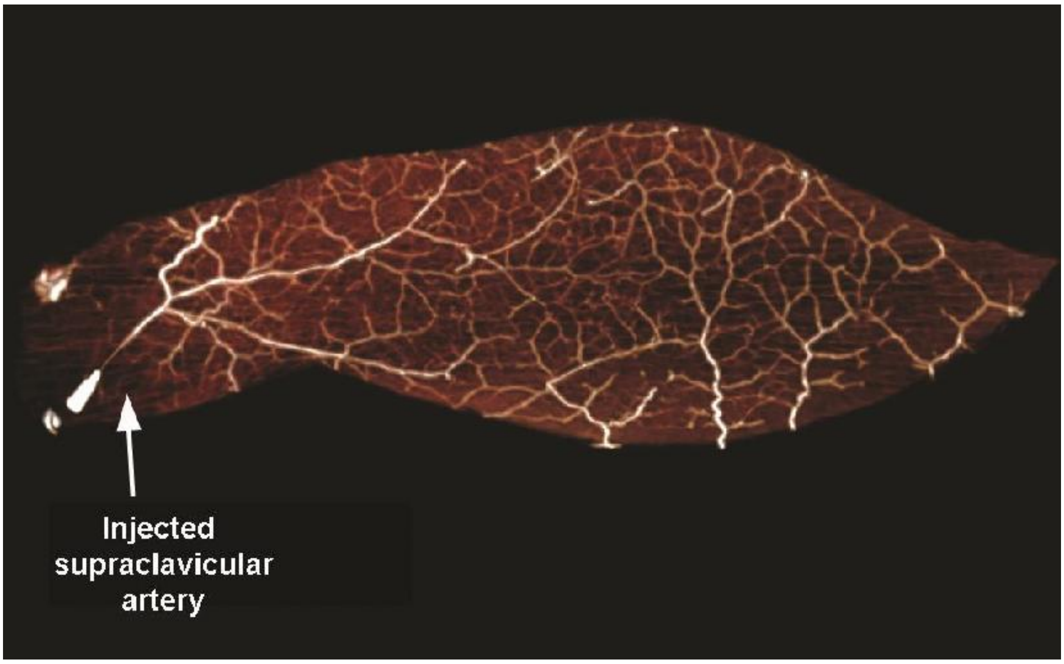

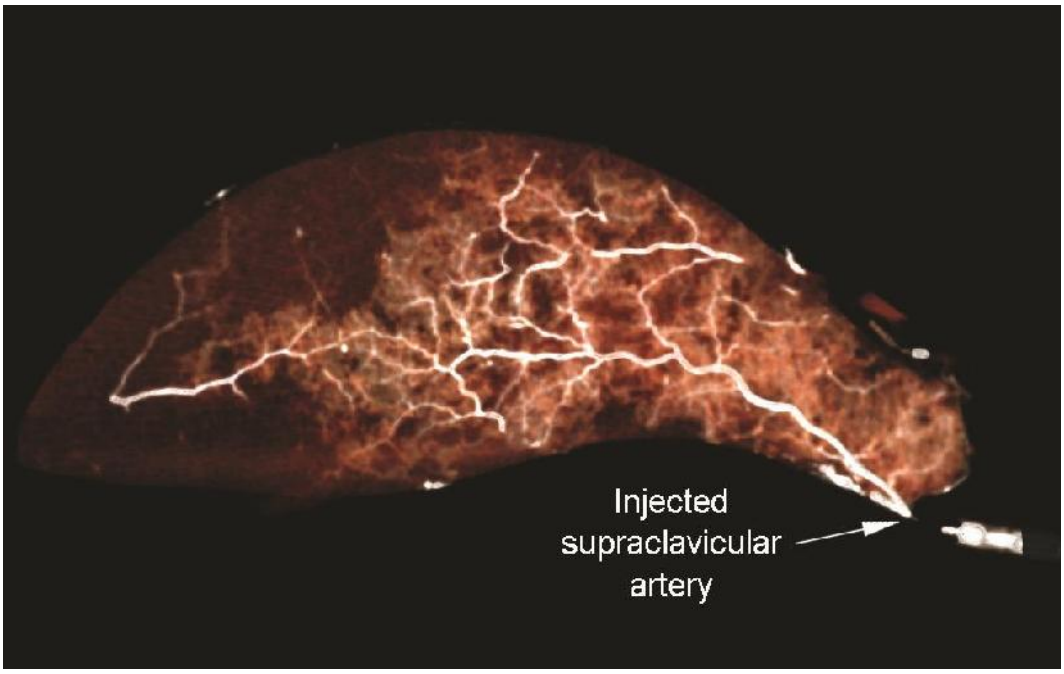

3.1.2 and 3.1.3 *3D CT angiograms of supraclavicular flaps (AP view). Both demonstrate almost 100% flap perfusion.*

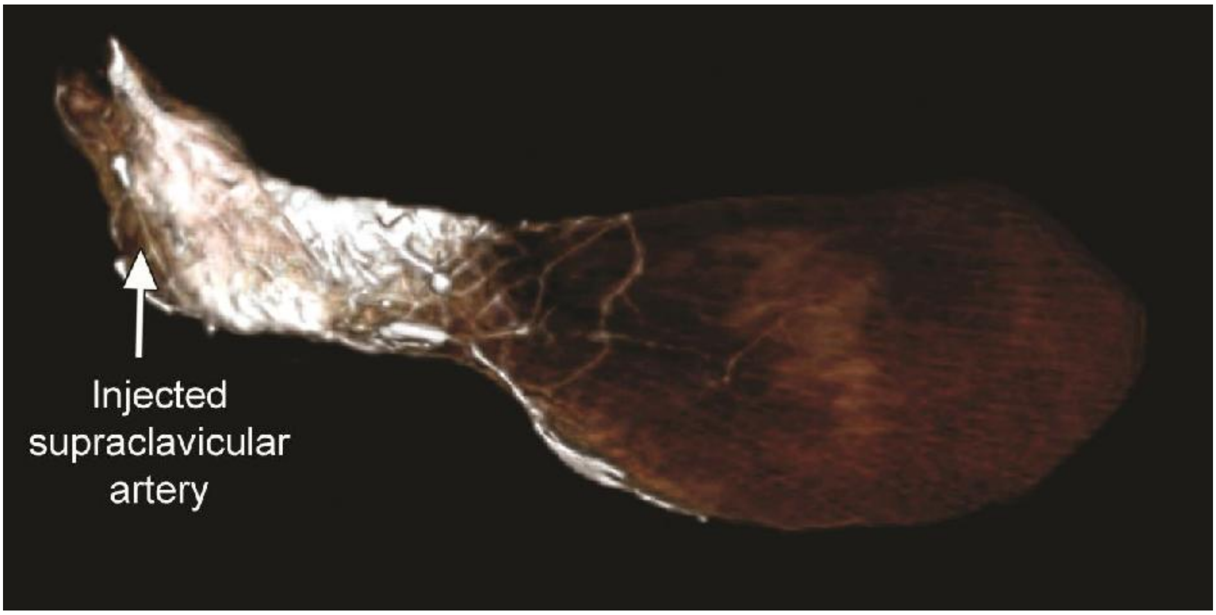

Figure 3.1.4 *3D CT angiogram of a supraclavicular flap, AP view. This flap was perfused only 50% upon contrast injection.*

Direct linking vessels as well as recurrent flow via the subdermal plexus were found to convey the flow of contrast between adjacent perforators (Figure 3.1.5, 3.1.6 and 3.1.7). This allows the capture of adjacent areas through an inter-perforator flow mechanism. This explains how perfusion is maintained all the way to the distal periphery of the flap.

Perfusion follows the axiality of linking vessels, and these linking vessels follow the axiality of the limb. This is demonstrated in 4D (Videos 3.1.1 and 3.1.2).

We have found that perfusion studies involving cadaveric tissue underestimate the extent of vascular territory *in vivo*. Therefore, clinically, the flap could possibly be extended to beyond the margins of the deltoid muscle in most cases.

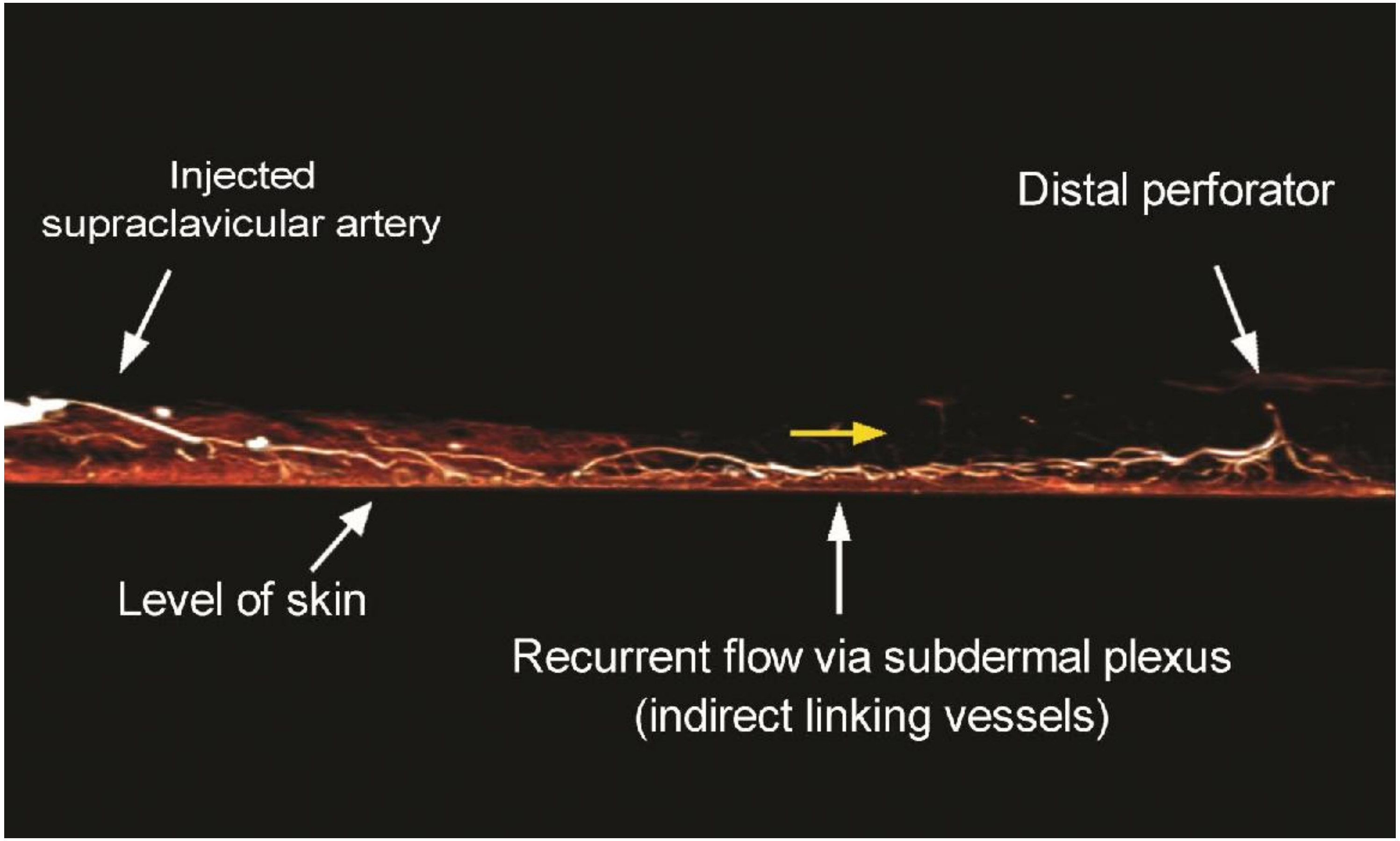

Figure 3.1.5 *Lateral view of supraclavicular flap. Communication between adjacent perforators demonstrated through recurrent flow via subdermal plexus. Yellow arrow shows the direction of flow.*

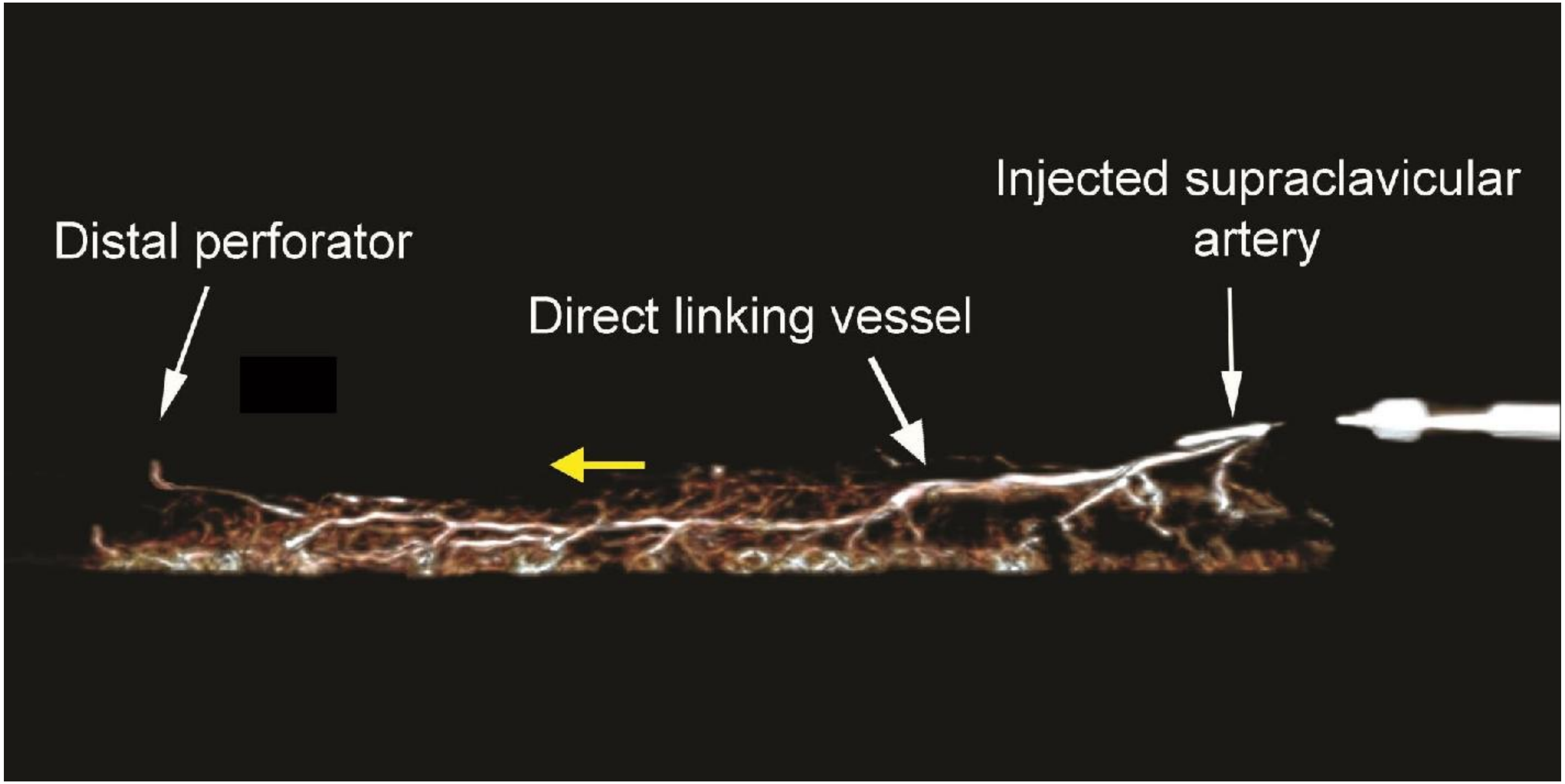

Figure 3.1.6 *Lateral view of supraclavicular flap demonstrating direct linking vessels between perforators. Yellow arrow shows the direction of flow.*

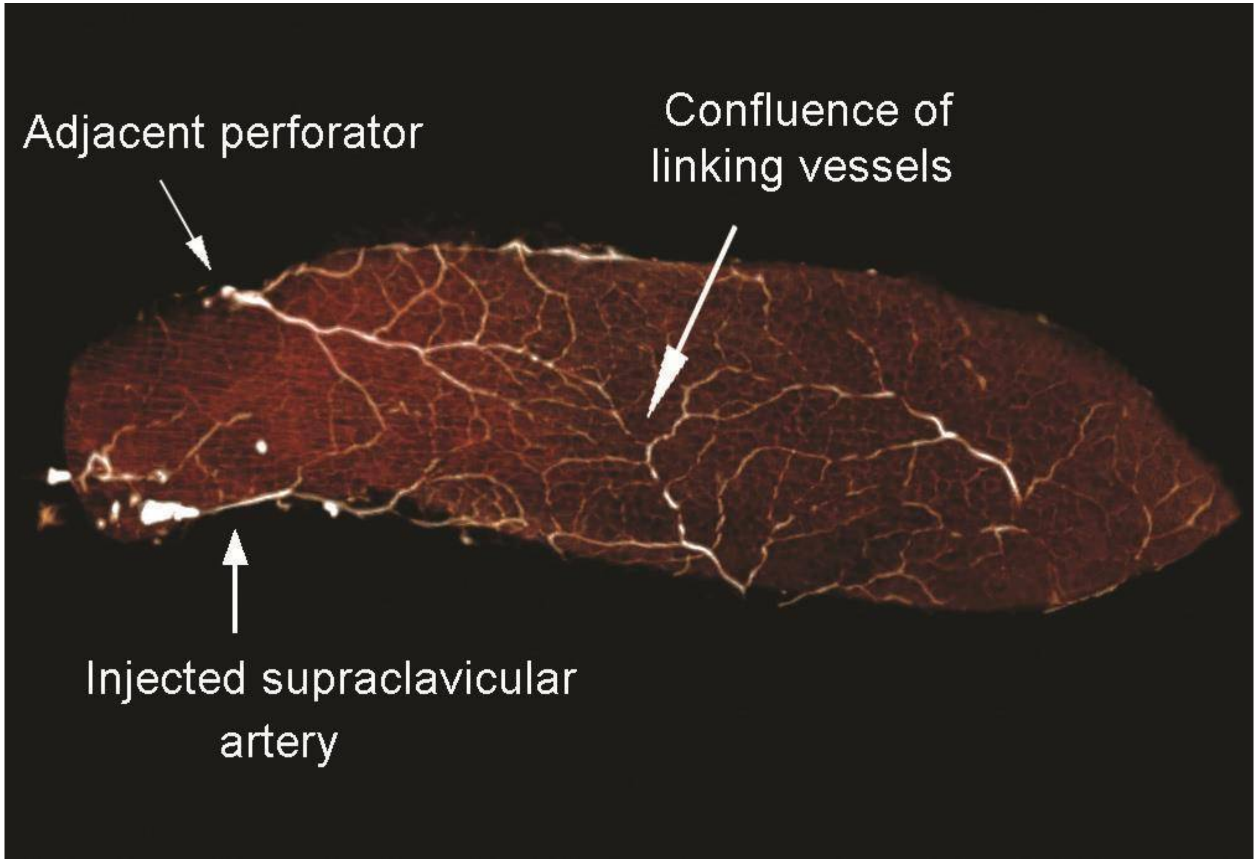

Figure 3.1.7 *Linking vessels are found to communicate between adjacent perforators.*

Discussion

The supraclavicular artery is a branch of the transverse cervical artery. Less frequently, the supraclavicular artery may arise from the suprascapular artery which may be smaller. The arterial vessel averages 1.0 to 1.5 mm in diameter and is constantly joined by one or two major concomitant veins. Lamberty[61] found this vessel constantly in 30 fresh cadavers examined as the superficial branch of the superficial transverse cervical artery - later named the supraclavicular artery.

An elegant anatomical dissection study was performed by Abe *et al*[62]. They showed that the supraclavicular artery mean diameter varied from 1.1-1.5mm, pedicle length ranged from 1-7 cm, and was present 80% of the time (N=55). Two-thirds of the vessels were found not to have crossed the clavicle. The venous drainage is usually via the accompanying transverse cervical vein.

Pallua *et al*[19] studied the supraclavicular artery in 19 cadavers. In all specimens they found the supraclavicular artery to arise 3-4 cm from the origin of the transverse cervical artery. Examination of the skin landmarks revealed that the artery exited 3.0 ± 0.7 cm above the clavicle at a distance of 8.2 ± 1.7 cm from the sternoclavicular joint and approximately 2.1 ± 0.9 cm dorsal to the sternocleidomastoid muscle. The mean diameter of the artery was 0.15 ± 0.034 cm. They used India ink to demonstrate which skin region is supplied by the supraclavicular artery. In all cases, the vascular territory extended from the supraclavicular region to the shoulder cap. They noted that the distal part of the angiosome is on the ventral surface of the deltoid muscle. The area of this angiosome ranged from 10 cm in width and 22 cm in length to 16 x 30 cm.

Three- and four-dimensional CT angiography have been used to investigate the anatomy and perfusion of various other flaps in the axial, coronal, and sagittal views in cadaveric flaps[9, 11, 12]. No studies to date have evaluated the vascular anatomy of this flap using CT angiography. Our results show that with an adequately sized supraclavicular artery, the entire flap is based on its flow. We have also shown the distal part of the flap is dependent on inter-perforator flow from direct linking vessels and recurrent flow via the subdermal plexus.

The phenomenon of recurrent flow through the subdermal plexus was first noted by Moon and Taylor in the transverse abdominal adipocutaneous paddle perfused by the deep superior epigastric artery[31], and was seen by Alkureishi *et al*. in their study of the arterial anatomy of the anterolateral thigh flap in specimens following diaphanization[63]. Saint-Cyr's study on the anterolateral thigh perforator flap is the first study in which it has been demonstrated dynamically, and it appears to be an important mechanism of flap perfusion[12]. This supports the perforasome theory, where the perforasome is defined as the vascular territory of a single perforator and perfusion of a flap is conveyed through these methods of inter-perforator communications[55].

A weakness of this study is the use of cadaveric flaps. From prior cadaveric perfusion studies we know that the vascular territory is most likely underestimated. However, the dynamic three-dimensional imaging method used in this study more closely models *in vivo* effects than has been achievable previously. The margins of the flap could likely be extended to beyond that of the deltoid muscle. The 4D CT angiograms demonstrating the injection of the supraclavicular artery (Videos 3.1.1 and 3.1.2) showed the direction of flow as away from the trunk (proximal to distal), highlighted by the orientation of the larger vessels. The density of the capillaries filled with contrast was interpreted as areas of optimal perfusion, and were more frequently found in the proximal regions of the flaps.

Recently, Ma *et al*[64], investigated a pectorally extended supraclavicular flap. Microangiograms of their flap showed that there were extensive anastomoses with perforators of the thoracoacromial artery and the second and third perforators of the internal thoracic arteries. Their vascular territory flap extended to a width of 18 cm and a length of 20 cm.

The supraclavicular artery island flap has been successfully used for difficult facial reconstruction cases providing acceptable results without using microsurgical techniques. Its utility has been demonstrated in reconstructing a variety of head and neck oncologic defects which normally require traditional regional or free flaps. In our study we are able to provide a better understanding of the vascularisation of this flap.

CHAPTER 4

Lower Limb

4.1 Transverse Musculocutaneous Gracilis (TMG) Flap

Introduction

There are currently multiple options for breast reconstruction. Possible autologous tissue transfers include latissimus dorsi (LD), transverse rectus abdominal myocutaneous (TRAM)[28], deep inferior epigastric perforator (DIEP)[34, 65], superficial inferior epigastric artery (SIEA)[66], superior gluteal artery perforator (SGAP)[67, 68], inferior gluteal artery perforator (IGAP)[68, 69] and lumbar artery perforator flaps[70]. The transverse myocutaneous gracilis (TMG) flap has gained popularity, especially in Europe, because of its many advantages[71, 72]. These include a reliable vascular anatomy, a faster and simpler dissection compared to other flaps, no need for patient repositioning, minimal donor function loss and since the transverse orientation of the flap was described[73], a discrete scar which also helps to lift the medial thigh.

However, major disadvantages of the gracilis flap include the lower flap volume compared to abdominal- and gluteal-based flaps, and reported unreliability of the more caudal regions of the skin paddle if a vertically-orientated flap were harvested. Traditionally, the gracilis flap has only been used to reconstruct small to moderate-sized breasts. Modifications to increase this have included harvesting the flap from a more posterior location, to recruit the bulkier posterior thigh tissue[74-76]. In addition, Fattah *et al* have also taken to undermining the skin and recruiting the superficial fat of the thigh distal to the inferior border of the transverse skin paddle. Peek *et al* described the vertically-orientated extended gracilis perforator flap (which precludes the gracilis muscle) which is made possible by preserving the intramuscular connection between the major and minor pedicles, thus recruiting the neighbouring angiosome of the minor pedicle[77]. Vega *et al* have included a vertical portion to form an L-shaped flap in their bid for a larger gracilis flap[78]. The heaviest flaps have been reported to be 420 to 576g[76, 79]. Volumes of 180 to 550cc have been recorded by Schoeller[75]. The largest skin paddles were 30 x 10cm[75, 79]. Even with these maneuvers, surgeons still occasionally have to resort to 'doubling up' bilateral TMG flaps for one breast to make up sufficient volume[75, 76].

Our study utilizes three-dimensional CT angiography, barium-gelatin solution and anatomical dissection to ascertain the vascular territory of the major pedicle of the gracilis muscle. This will tell us if extension beyond the traditional margins of the TMG flap is possible to increase its volume.

Methods and Materials

Ten circumferential thigh adipo-cutaneous flaps attached to the gracilis muscle were harvested from fresh adult cadavers acquired through the Willed Body Program at the University of Texas Southwestern Medical Center. An incision was made in the mid-lateral thigh, and the flap was harvested from lateral to medial (for both anterior and posterior). The margins of the adipo-cutaneous flap are the midlateral thigh, groin crease, gluteal crease and superior patella. Specimen dissection was performed under loupe magnification. The minor pedicle of the gracilis was ligated. Parameters recorded during dissection included diameter of major and minor vascular pedicles, length of pedicles, distance of pedicles from pubis and number and locations of cutaneous perforators. Thigh width was defined as the length between the mid-lateral and mid-medial lines of each thigh.

The major pedicles were cannulated and injected with a dilute methylene blue solution to enable all vascular leaks to be sealed, either through bipolar diathermy or suture ligation. After we were satisfied with the repair of leaks, the major pedicle was then injected with contrast and subjected to 3D CT scanning.

Comparison of vascularity extension from mid-medial thigh anteriorly and posteriorly was calculated using the paired student's t-test on Microsoft Excel.

Weight and Volume

After CT scanning, the flaps were incised to include only tissue that was perfused with contrast. This was done firstly by viewing the images and measuring the extent of the vascular territory from the major pedicle, and then whilst making incisions, looking out for the white barium-gelatin contrast still in the tissue vasculature (contrast is solidified after freezing). This 'perfused' tissue was then measured for weight and volume.

Results

The mean muscle length was 35.4cm. The mean muscle widths at the major and minor pedicles were 5.4cm and 2.7cm respectively. The recorded measurements of the major and minor pedicles are summarized in Table 4.1.

Table 4.1

Measurements of the major and minor pedicles of the gracilis muscle

	Major pedicle	Minor pedicle
n=	10	10
Distance from pubis/ cm SD (range)	8.57 0.76 (7.6-9.8)	23.32 1.11 (21.8-26.0)
Mean length of pedicle/ cm SD (range)	6.69 0.48 (6.0-7.4)	4.09 0.78 (3.3-5.3)
Mean arterial diameter/ mm SD (range)	2.24 0.32 (2.0-2.8)	1.55 0.33 (0.9-1.9)
Mean venous diameter/ mm SD (range)	2.33 0.29 (2.0-2.8)	1.83 0.12 (1.7-2.0)

The minor pedicle of the gracilis was found to have a common arterial input with a large pedicle of the sartorius in all cases (Figure 4.1.1).

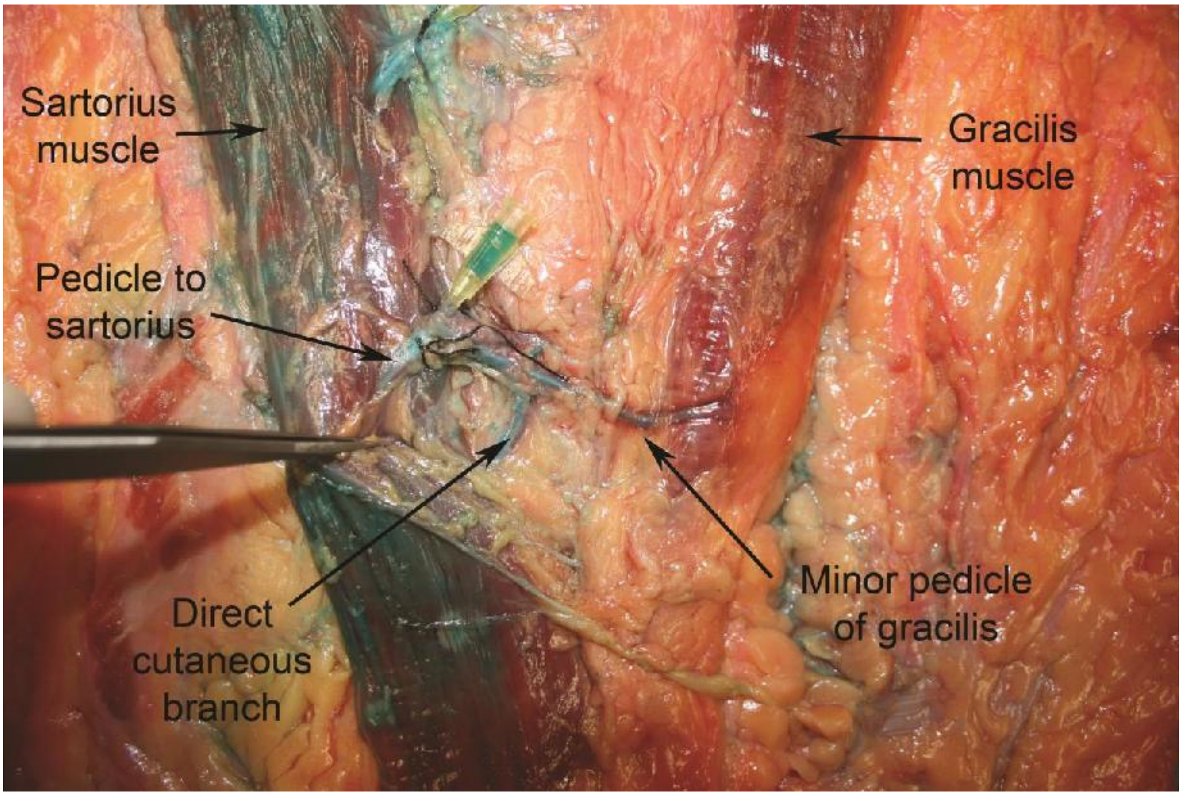

Figure 4.1.1 *Photograph of cadaveric anterior thigh tissue, including sartorius and gracilis muscles. The minor pedicle of the gracilis was found to have a common arterial input with a large pedicle of the sartorius in all cases.*

A total of 43 perforators were dissected, with median of 4 cutaneous perforators per flap, range 3-8 (Table 4.2).

Table 4.2

Perforators dissected (MC=musculocutaneous, SC=septocutaneous)

Flap	No. of perforators	MC	SC
1	8	4	4
2	3	3	0
3	4	4	0
4	3	1	2
5	3	2	1
6	4	3	1
7	6	4	2
8	3	3	0
9	5	3	2
10	4	3	1
Total	43	30	13

The mean external diameter of the perforators was 0.61mm. Locations of the perforators that are 0.5mm or larger are mapped out in Figure 4.1.2 (n=26).

The majority of the musculocutaneous perforators 0.5mm or larger were found at 14-45% of the relative length of the gracilis muscle (0 is origin of muscle from pubic tubercle) and 7-38mm from the anterior border of the gracilis. The septocutaneous perforators were found anterior to the gracilis muscle (0 on the y-axis of Figure 2) and were located at 24-74% of the relative length of the gracilis muscle.

Tissue perfused with contrast had a mean weight of 573g (range 313-812g) and volume of 617ml (range 330-850ml).

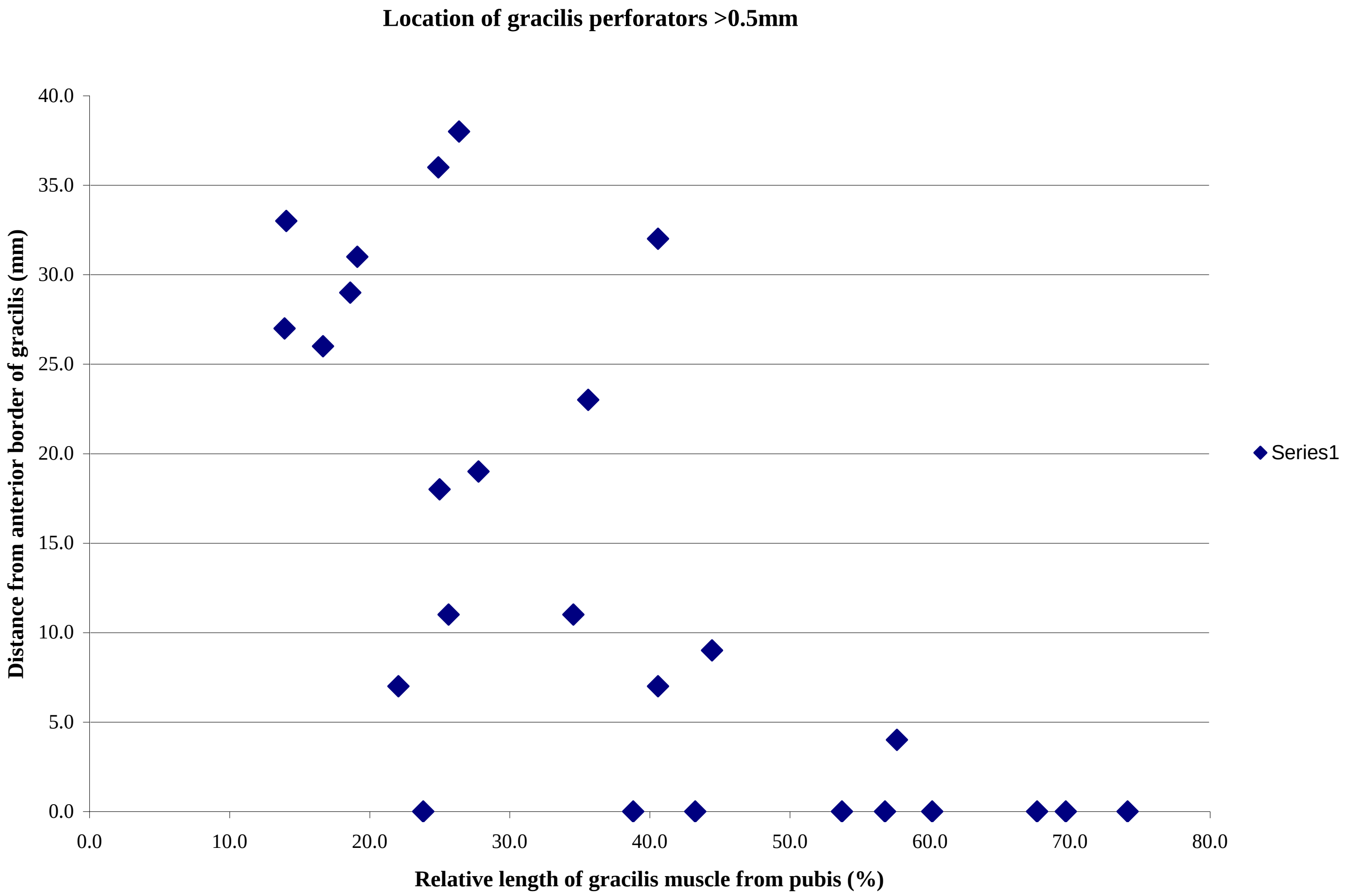

Figure 4.1.2 Location *of gracilis perforators that are 0.5mm or larger (n=26). X-axis refers to distance from pubis, as a relative length of the gracilis. Y-axis refers to the distance from the anterior border of the gracilis muscle (perforators located at 0 are septocutaneous).*

3D CT Angiography

3D images from contrast injection of the major gracilis pedicle showed a cutaneous vascular territory that extended more posteriorly than anteriorly (Figures 4.1.3 to 4.1.6). The extent of cutaneous perfusion on the posterior thigh was found to be a mean of 65% of the thigh width. Maximum was 95% of posterior thigh width. In comparison, contrast perfusion in the anterior thigh was found to extend to merely 38% of the thigh width, $p < 0.05$ (Table 4.3).

Table 4.3

Extent of cutaneous perfusion based on injection of contrast into major gracilis pedicle.

Flap	Thigh width*/mm	Extent of perfusion† on posterior thigh/mm	Extent of perfusion† on anterior thigh/mm	Posterior perfusion as percentage of thigh width‡	Anterior perfusion as percentage of thigh width‡
1	267	167	88	62.8	33.2
2	215	157	147	72.9	68.2
3	198	124	60	62.6	30.5
4	193	96	53	49.9	27.3
5	215	205	96	95.3	44.7
6	272	166	100	61.0	36.8
7	301	131	103	43.5	34.4
8	287	173	111	60.3	38.7
9	218	158	82	72.5	37.5
10	248	170	78	68.6	31.2
Mean	241.4	154.8	91.8	64.9	38.2

***** Thigh width was defined as the length between the mid-lateral and mid-medial lines of each thigh.
† Transversely, medial to lateral direction
‡ $p<0.05$, using the paired student's t-test

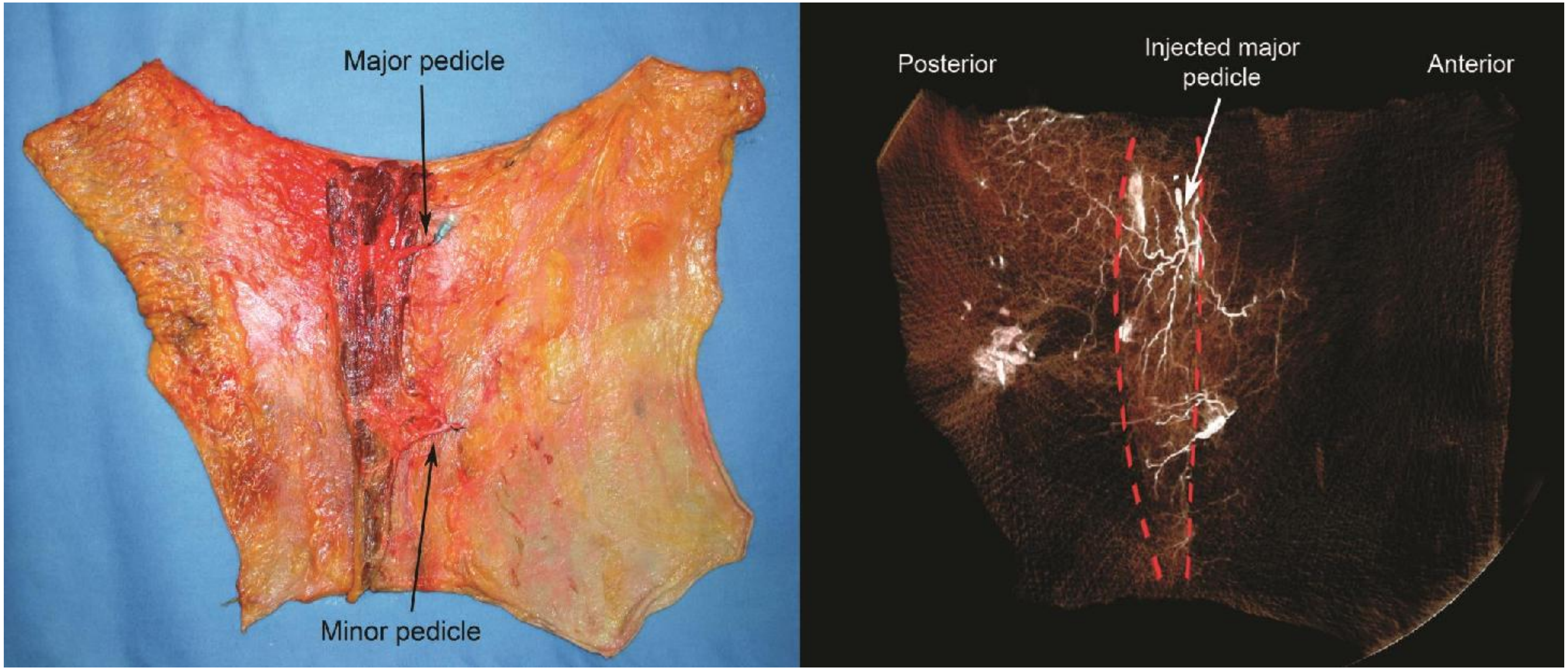

Figure 4.1.3 *Left: Photograph of cadaveric circumferential thigh tissue, including the gracilis muscle. The margins of the flap are the midlateral thigh, groin crease, gluteal crease and superior patella. Right: 3D CTA image of the flap. The red dotted lines depict the margins of the gracilis muscle. Contrast injection of the major gracilis pedicle showed a cutaneous vascular territory that extended more posteriorly than anteriorly.*

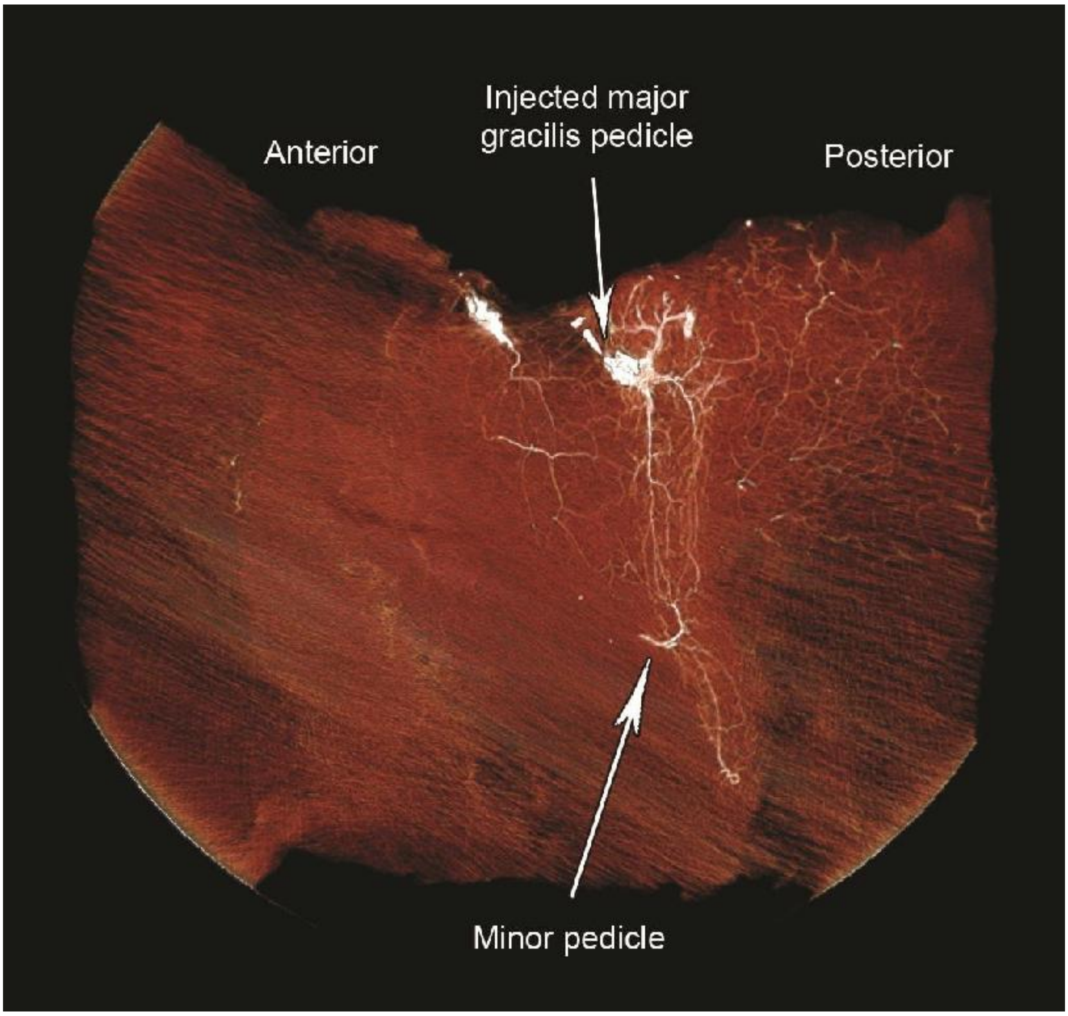

Figure 4.1.4 *Second example of 3D CTA of circumferential thigh skin. Contrast injection of the major gracilis pedicle showed a cutaneous vascular territory that extended more posteriorly than anteriorly.*

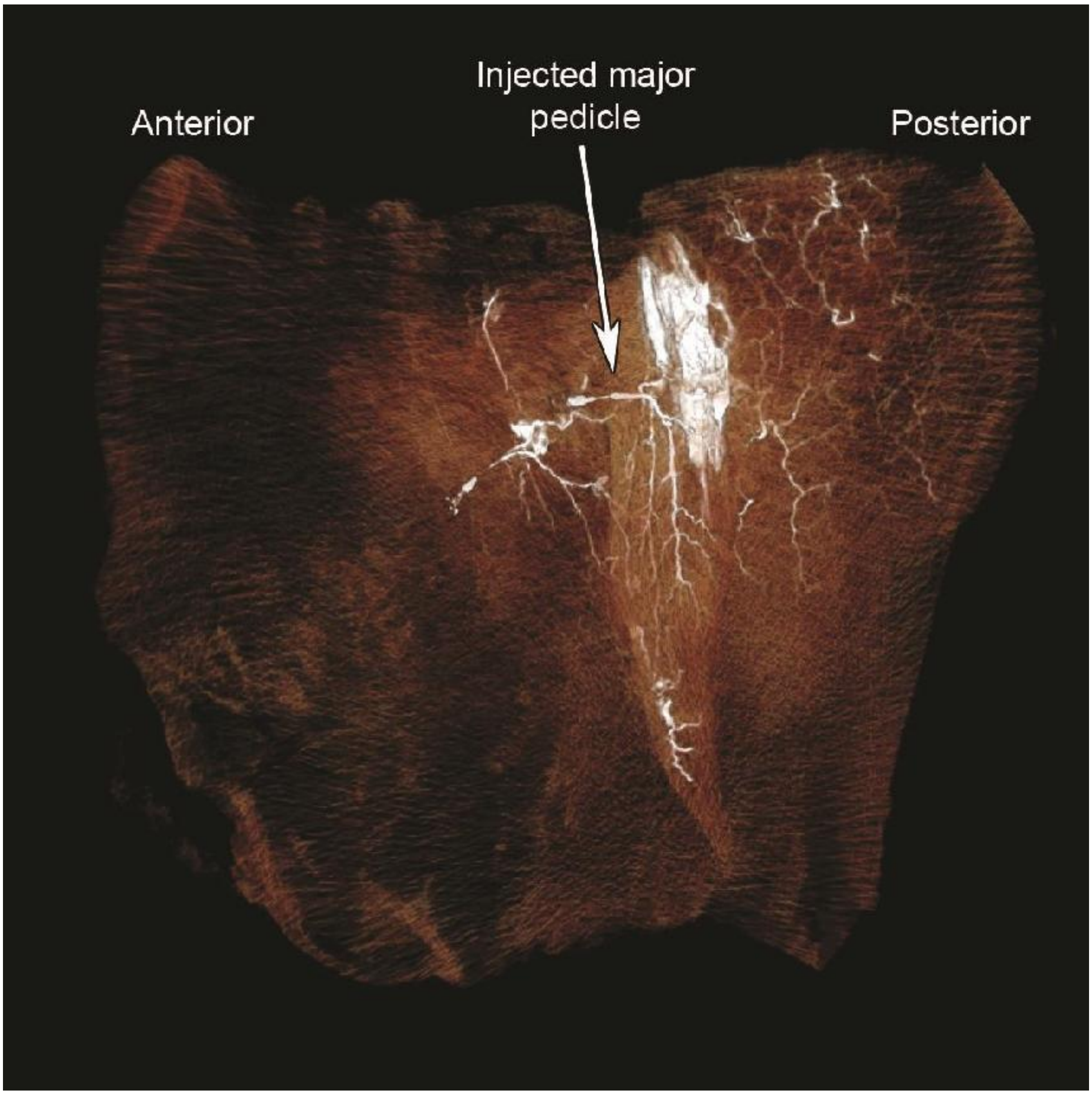

Figure 4.1.5 *Third example of 3D CTA of circumferential thigh skin. Again, contrast injection of the major gracilis pedicle showed a cutaneous vascular territory that extended more posteriorly than anteriorly*.

Presence of contrast was also more concentrated in the superior half of the thigh, and extended inferiorly only in the tissue overlying the distal the gracilis muscle (Figure 4.1.6 and 4.1.7). Contrast perfusion was also frequently found in the vascular territory of the sartorius muscle (Figure 4.1.8).

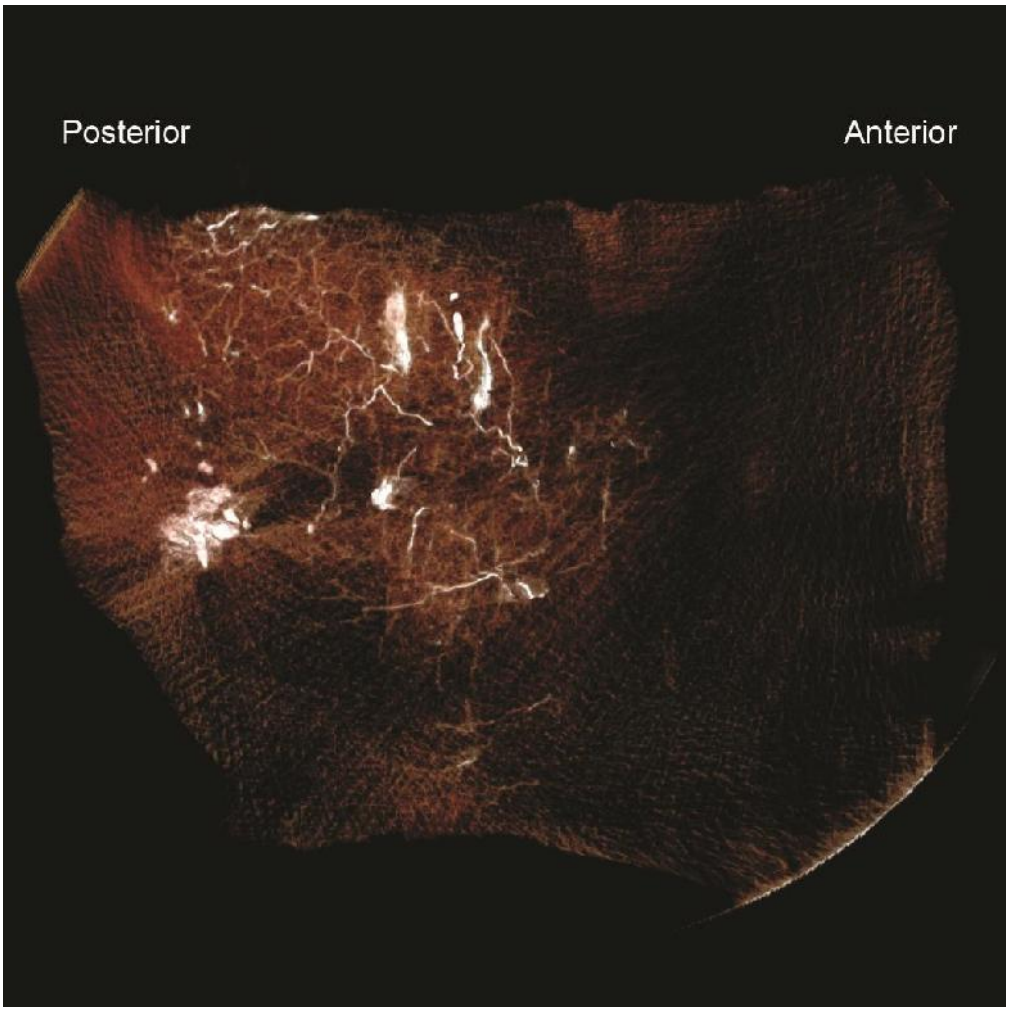

Figure 4.1.6 *3D CTA of circumferential thigh skin, with removal of gracilis muscle. This demonstrates the vascularity of the adipo-cutaneous tissue above the muscle.*

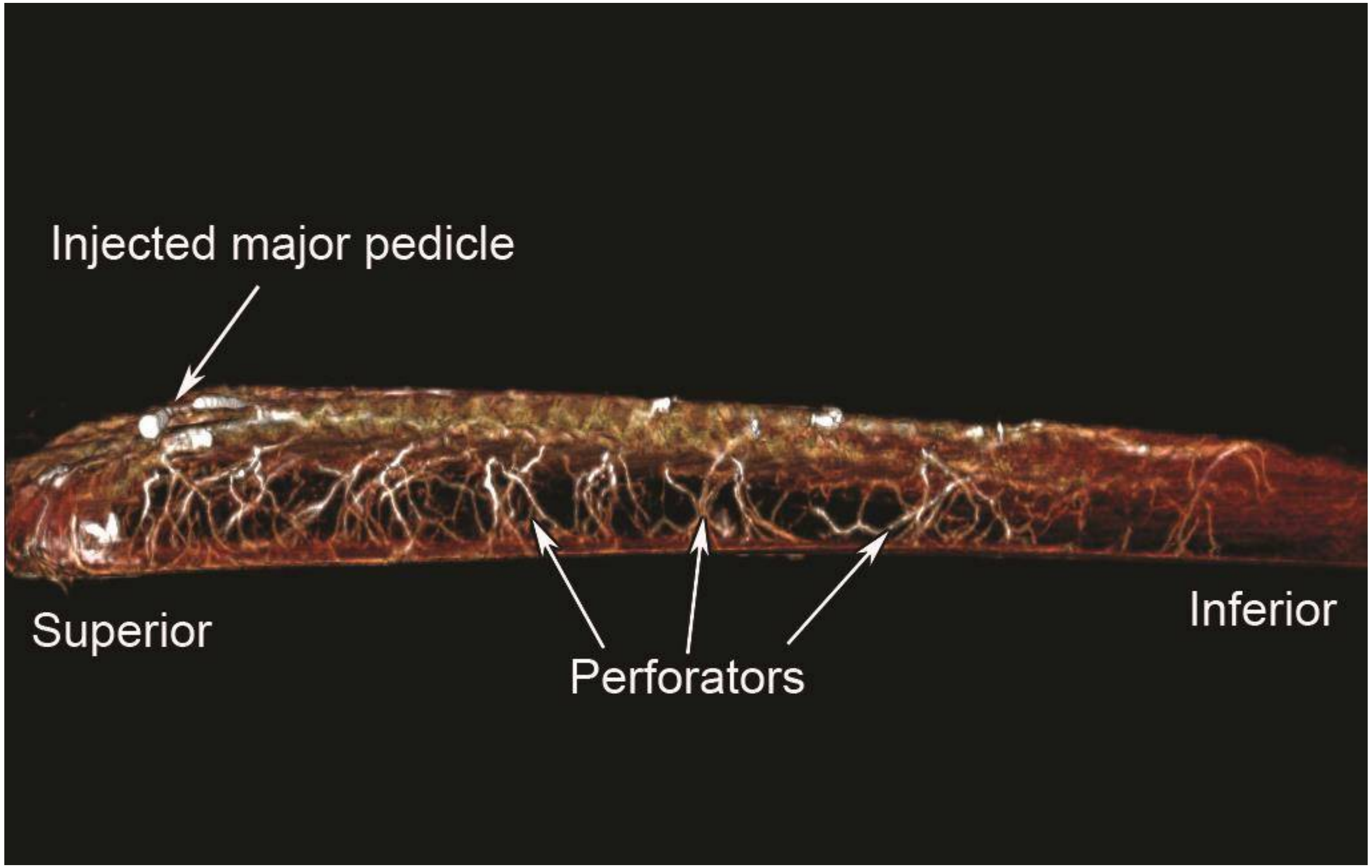

Figure 4.1.7 *Lateral view of 3D CTA of thigh skin, with overlying gracilis muscle. Note the numerous perforators running from the muscle to the dermis, especially in the superior region.*

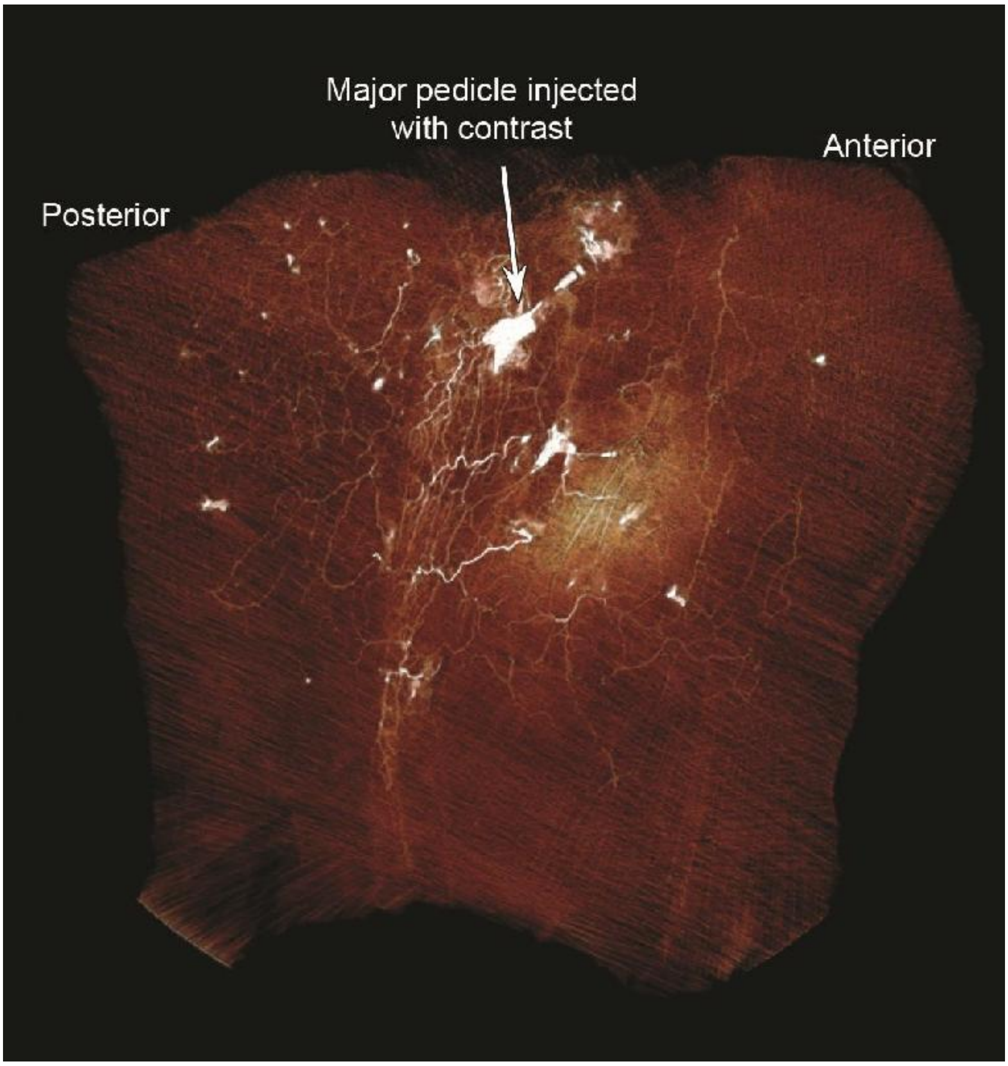

Figure 4.1.8 *3D CTA of circumferential thigh skin, with contrast injection into the major pedicle of the gracilis muscle. Contrast perfusion was sometimes found in the vascular territory of the sartorius muscle.*

Discussion

Our study could be considered as an investigation of the angiosome of the medial circumflex femoral branch providing the pedicle to the gracilis muscle. We have found that in our perfusion studies involving cadaveric tissue, they always underestimate the true extent of perfusion *in vivo*[9-12, 53, 80].

The TMG flap was originally designed to be centered over the major pedicle[71-73]. However, since then, other authors have reported placing the flap more posteriorly[75, 76]. Reasons cited were to minimize visible scarring anteriorly and the possibility of harvesting a greater volume of adipose tissue. Schoeller *et al*. introduced the Siamese flap combining the TMG and infragluteal flaps[81] for extra-large reconstructions. Intra-operatively, they noted that even after the division of the infragluteal pedicle, this extra-large flap was still bleeding at the wound edges. This is not surprising in light of the results of our study, where the cutaneous vascular territory of the major pedicle of the gracilis was found to be concentrated in the supero-posterior region of the thigh. Yousif *et al*. showed that vascularity of the TMG flap is orientated transversely, and branches of perforators travelled more than 5cm beyond the posterior margin of the gracilis muscle[73]. Our 3D CT results which demonstrate that posterior thigh perfusion extends up to a mean of 65% of thigh width. This is advantageous, as not only is the posterior thigh tissue better vascularized than the anterior, but it is also thicker and can give greater flap bulk.

Perfusion was also found to extend downward, in the area overlying the distal gracilis muscle. Peek *et al* demonstrated this too, in their extended gracilis perforator flaps, by maintaining the intramuscular anastomosis between the major and minor pedicles thus recruiting the angiosome of the minor pedicle[77]. These inter-pedicle connections were preserved in all our specimens as whole gracilis muscles were harvested with the flaps. Surgeons can take advantage of the inferior perfusion by adding a vertical component to their extended TMG flaps, either by recruiting the inferior subcutaneous fat (from undermining the skin inferior to the lower incision) or by taking the skin as well, resulting in a modified 'fleur-de-lys' skin paddle. The latter method gives a tri-lobed flap, and this allows harvest of even more volume for the flap. We encourage using a beveling technique when dissecting the edges between the horizontal and vertical limbs (resulting in less of a T-shape and more of a triangle when viewing the underside of the flap. This gives it a larger base compared to the skin paddle side). This aids in avoiding resection of the linking vessels between the horizontal and vertical limbs thus ensuring survival of the flap tips. The tri-lobed TMG flap can also result in improved contouring of the medial thigh. Current medial thighplasty techniques have incorporated a vertical incision for removal of redundant skin[82, 83]. This results in a horizontal pull medially, and allows for both skin and thigh circumference reduction. The downside of this, of course, is a more noticeable scar, whereas the undermining method maintains a transverse scar only. The functional loss of the gracilis muscle would not be different compared to the usual TMG flap, which is minimal.

In the clinical setting, we have classified the different types of extended TMG flaps including our proposed modifications (Table 4.4). Type I is the (E-TMG) with the horizontal skin paddle, but with increased beveling at time of harvest in order to increase bulk, which incorporates a vertical extension of subcutaneous tissue without the overlying skin. And finally type II (vertical component) incorporates both the skin and subcutaneous tissue a vertical elliptical shape, an L-shaped a, or finally a trilobe shape which yields a large volume (Figure 4.1.9). The operating surgeon needs to be aware that with increasing aggressiveness of recruitment of subcutaneous tissue, there may be a concomitant increase in the risk of donor site and flap related complications. There is also a pure vertically orientated skin paddle design but this is used mainly in patients who have extensive horizontal laxity, with minimal vertical laxity, which is very rare. Table 4.5 is an algorithm that outlines our approach to selection of which method of TMG harvest to utilize based on the patient's native breast size, and thigh volume as determined by pinching the vertical skin of the upper thigh. For patients with excessive vertical skin laxity, a horizontal TMG is chosen. Patients who also have excessive horizontal laxity in the upper thigh, a trilobe or L-shaped TMG are selected in order to recruit additional volume and help improve donor site contour.

Table 4.4. Classification of the different types of TMG flaps

	Extended Transverse Myocutanous Gracilis Flap, E-TMG (Type I)	**Vertical Component Myocutaneous Gracilis Flap, VcMG (Type II)**		
		Vertical adipocutaneous	**Transverse + Vertical adipocutaneous extension**	**Trilobed adipocutaneous**
Flap design			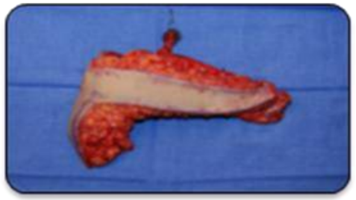	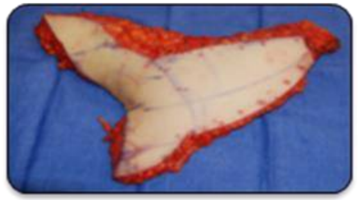
Patient selection	Virtually all patients older than 35 years old - Should be considered the first option	Patients with small breasts and minimal upper thigh laxity, precluding the use of the transverse incision. Patients with moderate/large sized breasts and significant skin redundancy. - would also benefit from circumferential thigh lift	Patients with moderate to large sized breasts and moderate upper thigh laxity - Vertical extension	Large sized breasts and excessive thigh skin redundancy E.g. massive weight loss patients - Benefit from circumferential thigh lift
Advantages	- Moderate flap volume - Inconspicuous scar	- Less risk to lymphatics damage	- Large flap volume - Less risk to lymphatics damage	- Largest flap volume - Contour improvement (circumferential thigh lift)
Disadvantages	- Limited flap volume - Increase undermining	- Conspicuous scar - Small flap volume	- Conspicuous scar - Increased undermining	- Conspicuous scar - Increased undermining - Increased risk of lymphatics disruption - Wound healing complications donor site due to T-shaped incision

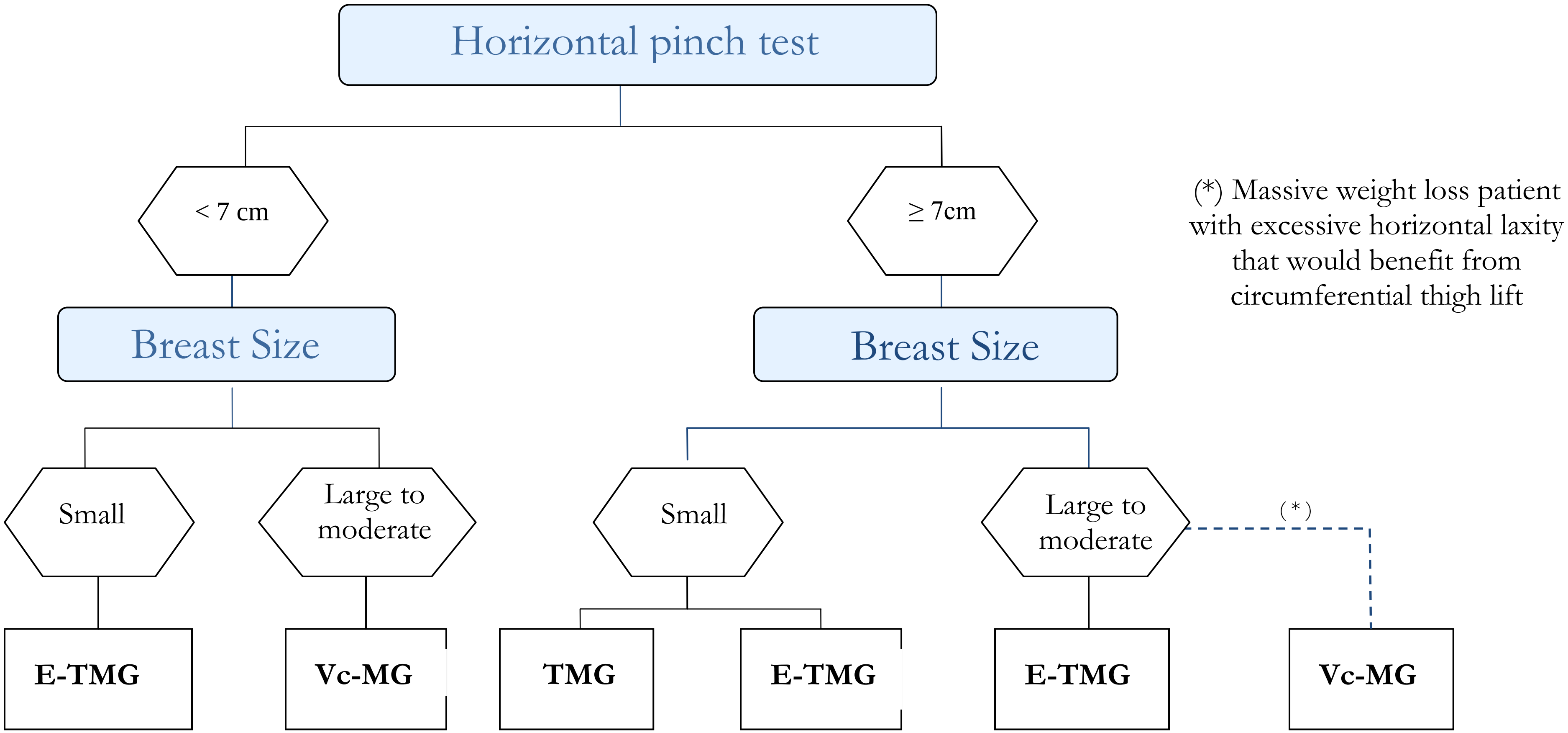

Table 4.5. Algorithm for TMG type based on the patient's native breast size, and thigh volume as determined by pinching the vertical skin of the upper thigh.

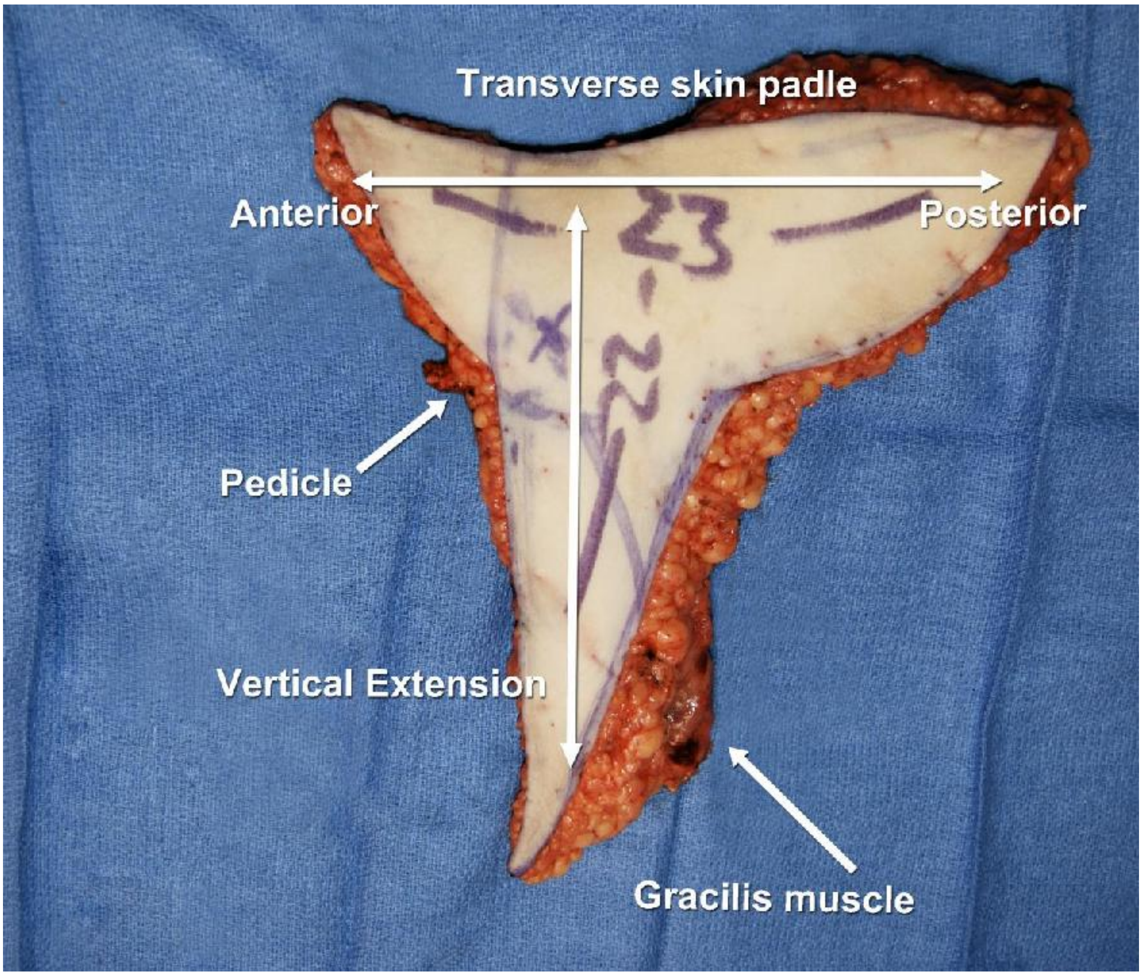

Figure 4.1.9 *Vertical (V) TUG flap after harvest using a trilobe skin paddle design. Note that the majority of the flap volume and sub-cutaneous tissue harvest is located over the gracilis muscle and posteriorly.*

Conclusion

The dimensions of a transverse musculocutaneous gracilis (TMG) flap can be increased, both horizontally (supero-posterior thigh) and vertically. The vertical portion can be harvested either by undermining the skin inferior to the lower transverse skin incision, or by raising vertically-orientated skin paddle extension, to harvest even more tissue from the medial thigh. With these modifications, the TMG flap can achieve greater volume and be applied to larger breast reconstructions.

CHAPTER 5

Discussion

An increased knowledge of vascular anatomy has led to innovations in flap design and use in the clinical arena. The evolution of random-pattern flaps to fasciocutaneous flaps, to myocutaneous flaps, and finally to perforator flaps has followed a relentless progression largely thanks to the pioneering vascular anatomy studies produced by Manchot, Salmon, Cormack, Lamberty, Taylor, Palmer, Morris, Tang and others[1-5, 84]. The information derived from such work has fueled a parallel evolution in flap design and clinical applications. The ultimate goal of reconstruction is to match optimal tissue replacement with minimal donor site expenditure while maintaining function. Perforator flaps meet these goals and are the result of over thirty years of flap design refinement.

Alongside our increasing knowledge of the vascular anatomy of perforator flaps, their clinical use has been pioneered by Koshima[33, 85-91]. The perforator flap era began in 1989 when Koshima and Soeda first described an inferior epigastric artery skin flap with the rectus abdominus muscle for reconstruction of floor of the mouth and groin defects[33]. These authors noted that a large skin flap could survive without muscle, based on a single perforator. Kroll and Rosenfield also suggested that perforator flaps combined the reliable blood supply of myocutaneous flaps without deteriorating donor site morbidity[92]. Numerous other authors and pioneers in the field of perforator flap surgery have also been instrumental in providing us with further clinical experience and expertise in the harvest of perforator flaps. Amongst these authors include; Allen, Blondeel, Kroll, Koshima, Angrigiani, Hallock, Neligan, Morris, Wei and many, many others[34, 92-97].

In essence, any clinically relevant perforator has a potential to be harvested as either a pedicle perforator flap or a free flap, depending on the diameter and length of the source artery and vein. Doppler ultrasonography has been demonstrated to be an acceptable method to map perforators[98-100]. As a result, any skin paddle based on a substantially sized perforator, localized by audible Doppler signal, can be potentially harvested. With the substantial number of available perforators in the body, this approach certainly increases the surgeon's degree of freedom in terms of reconstructive options. However, many questions remain, including if a perforator of a certain size in different locations of the body would be sufficient to support a flap of the same size? For example, clinically, it would seem a that a single perforator perfusing a large ALT flap would not be able to support a DIEP flap of the same size if that same-sized perforator was used.

With over 350 perforators in the body, a myriad of options exist for either traditional or free-style perforator flaps. The only limiting factors are the length and diameter of the source vessels for a free-style free flap, and location of the pivot point perforator relative to the defect for pedicle perforator flaps. To further advance the evolution of perforator flaps, it is essential to understand the vascular anatomy of an individual perforator relative to its vascular territory and flow characteristics. Knowledge of the direction as well as the axiality or orientation of flow within the tissue is also of prime importance when designing perforator flaps, whether pedicle or free.

Although Taylor and Palmer have been instrumental in increasing our knowledge of vascular anatomy via the angiosome concept, this theory is based on the vascular supply of source arteries[4-6]. In the dawning of an era of perforator flaps, the impetus of vascular knowledge has shifted from the source artery to the perforator itself. A further consideration is to determine the dynamic vascularity of perforator flaps, compared to whole body static imaging, which does not provide an accurate description of a single perforator's vascular distribution and flow characteristics.

In order to truly understand and determine a single perforator's vascular territory, this perforator must be cannulated and injected individually. This is clinically relevant as many perforator flap designs are based on a single perforator. Therefore, knowledge of the axiality of blood flow, connections with adjacent perforators, and contribution of the subdermal plexus and fascia are all vital when designing perforator flaps.

In our study, note that most flaps involved perforators which were individually cannulated to assess the individual perforator vascular territories which we have termed a 'perforasome' (arterial) (**Figure 5.1).**

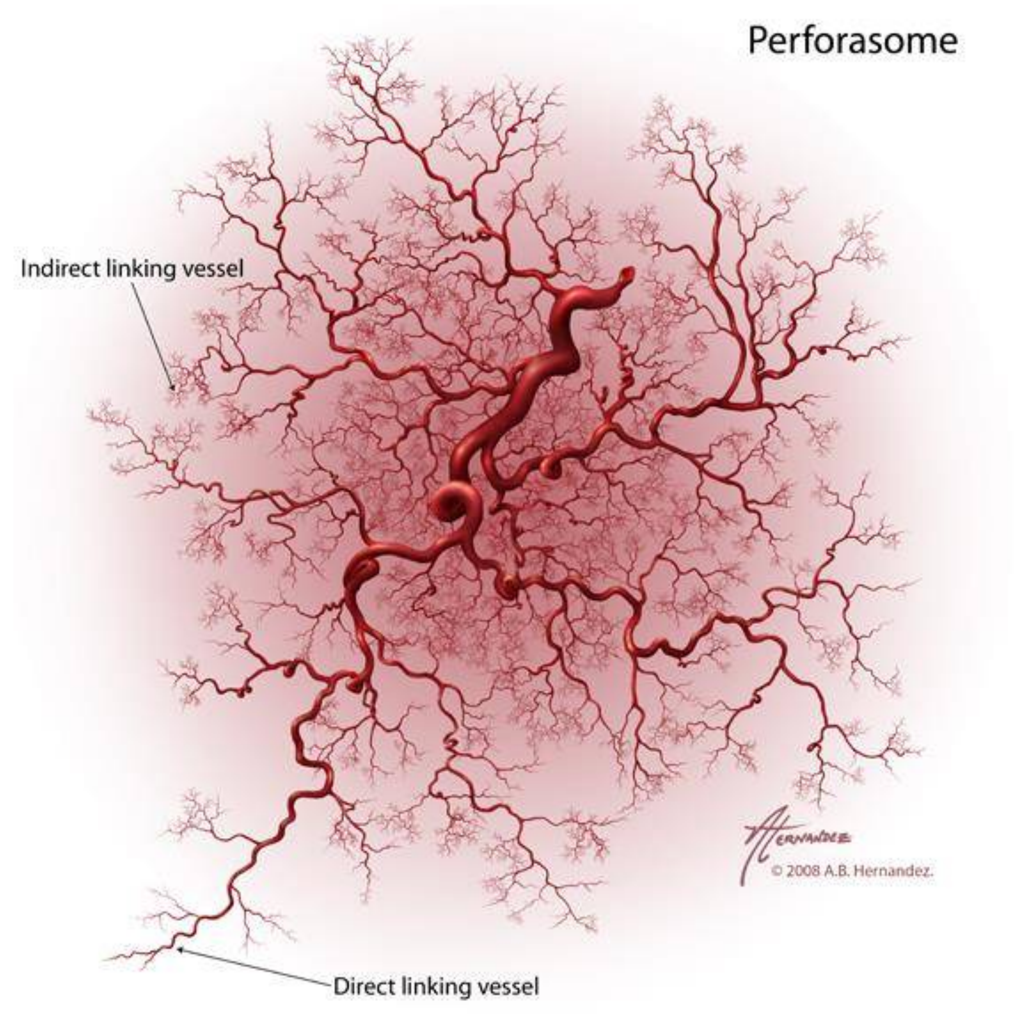

Figure 5.1 *The perforasome is the vascular territory of a single perforator.*

Others had the source vessel injected (e.g. radial and deep inferior epigastric artery) to study orientation of linking vessels between perforators.

The vascular territory of perforators was found to be highly complex and variable. Nevertheless, some common principles have been reproduced throughout our multiple perforator injection studies. When perforators were individually cannulated, the flow was multi-directional as can be seen in Figure 5.2. Each perforator has its own unique vascular arterial territory which we termed a 'perforasome' (arterial).

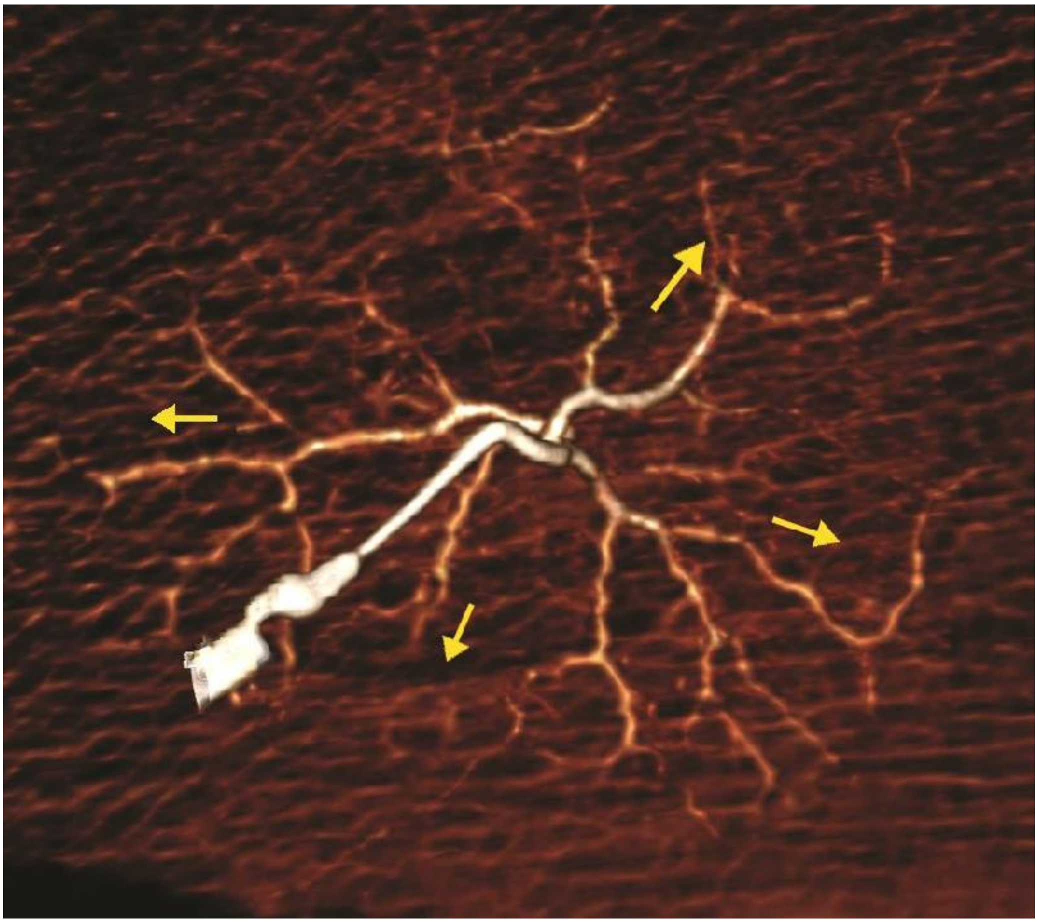

Figure 5.2 *The flow from a perforator is multi-directional. Yellow arrows show direction of flow.*

First principle:

Each perforasome is linked with adjacent perforasomes via two main mechanisms. These include both direct and indirect linking vessels (Figure 5.3).

Direct linking vessels are large vessels which communicate directly from one perforator to the next and permit capture of adjacent perforasomes through an inter-perforator flow mechanism. Large filling pressures or perfusion pressures through a single perforator can allow for large perforator flap harvests such as the extended ALT flap[101]. The linking vessels connect multiple perforasomes to one another **(Figure 5.4).**

Perforasomes are also linked to one another by indirect linking vessels or recurrent flow via the subdermal plexus **(Figures 5.5, 5.6).** These are similar to the choke vessels described by Taylor. In reality, perforators give off oblique and vertical branches to the subdermal plexus, and recurrent flow from the subdermal plexus to adjacent perforator oblique branches allows capture of an adjacent perforasome via this recurrent flow.

These two patterns of flow are protective mechanisms which ensure vascular connections between adjacent perforasomes in the event of a vascular injury. We have also found multiple communicating branches which link the direct and indirect linking vessels themselves **(Figures 5.3, 5.7).** These numerous communicating branches maintain vascular continuity between both the direct and indirect linking vessels in the coronal, sagittal and transverse planes. These communicating branches also confer an additional protective mechanism to ensure vascular flow to the skin in the event of damage to either direct or indirect linking vessels.

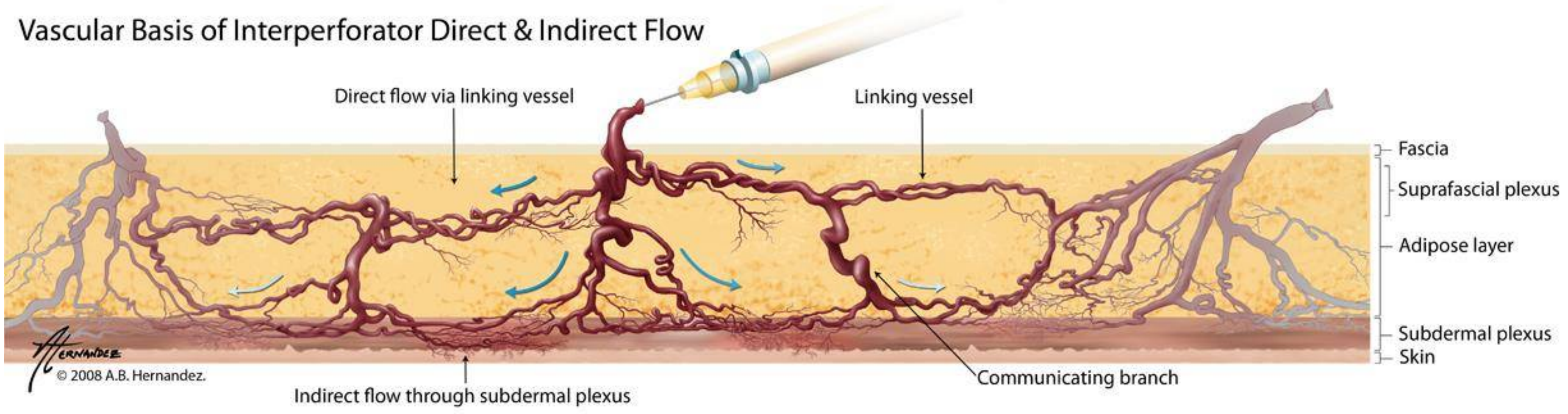

Figure 5.3 *Perforators are connected through two mechanisms- direct flow via linking vessels and indirect flow through the subdermal plexus. Communicating branches connect the direct and indirect linking vessels*.

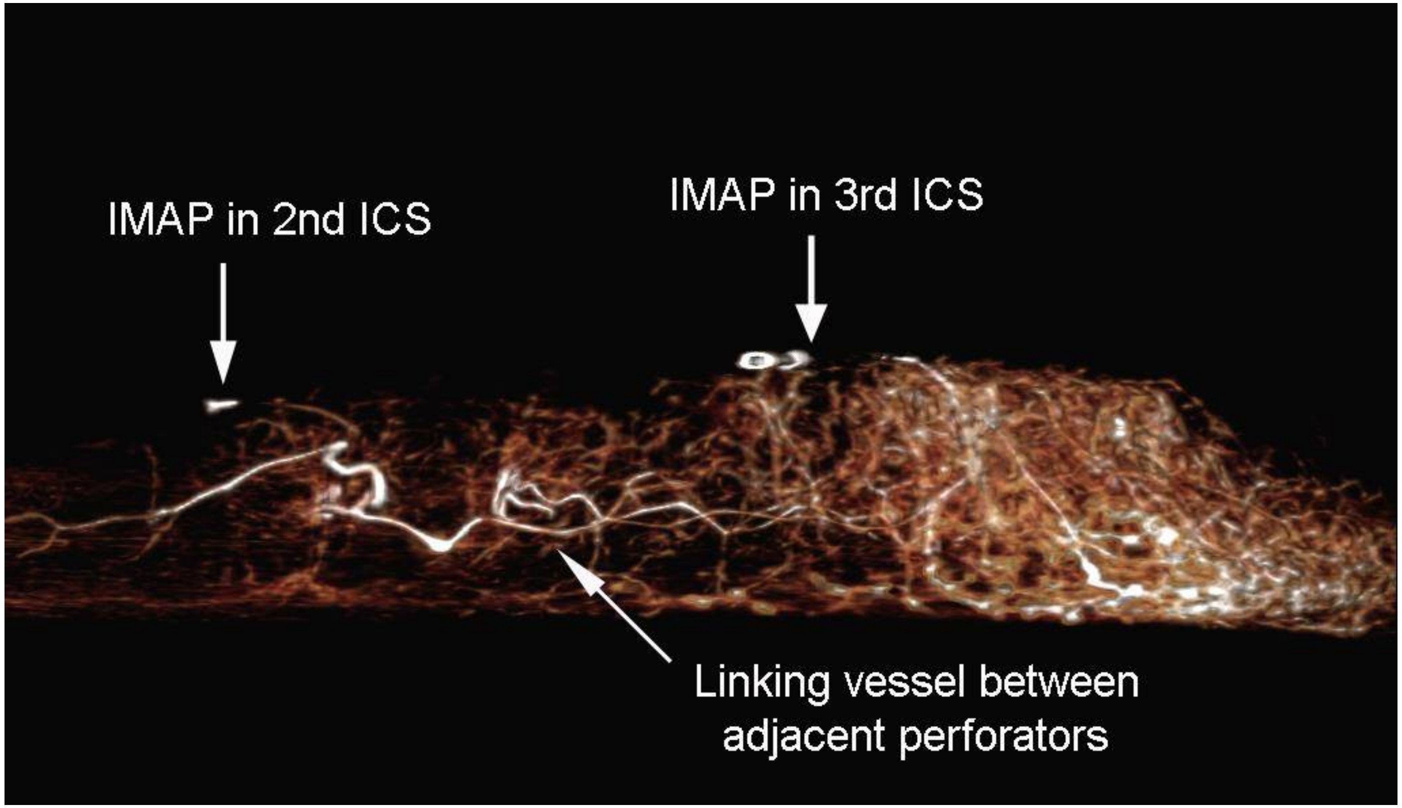

Figure 5.4 *Sagittal view of the chest from the midline. Linking vessels connect the internal mammary artery perforators (IMAP) in the second and third intercostals spaces (ICS).*

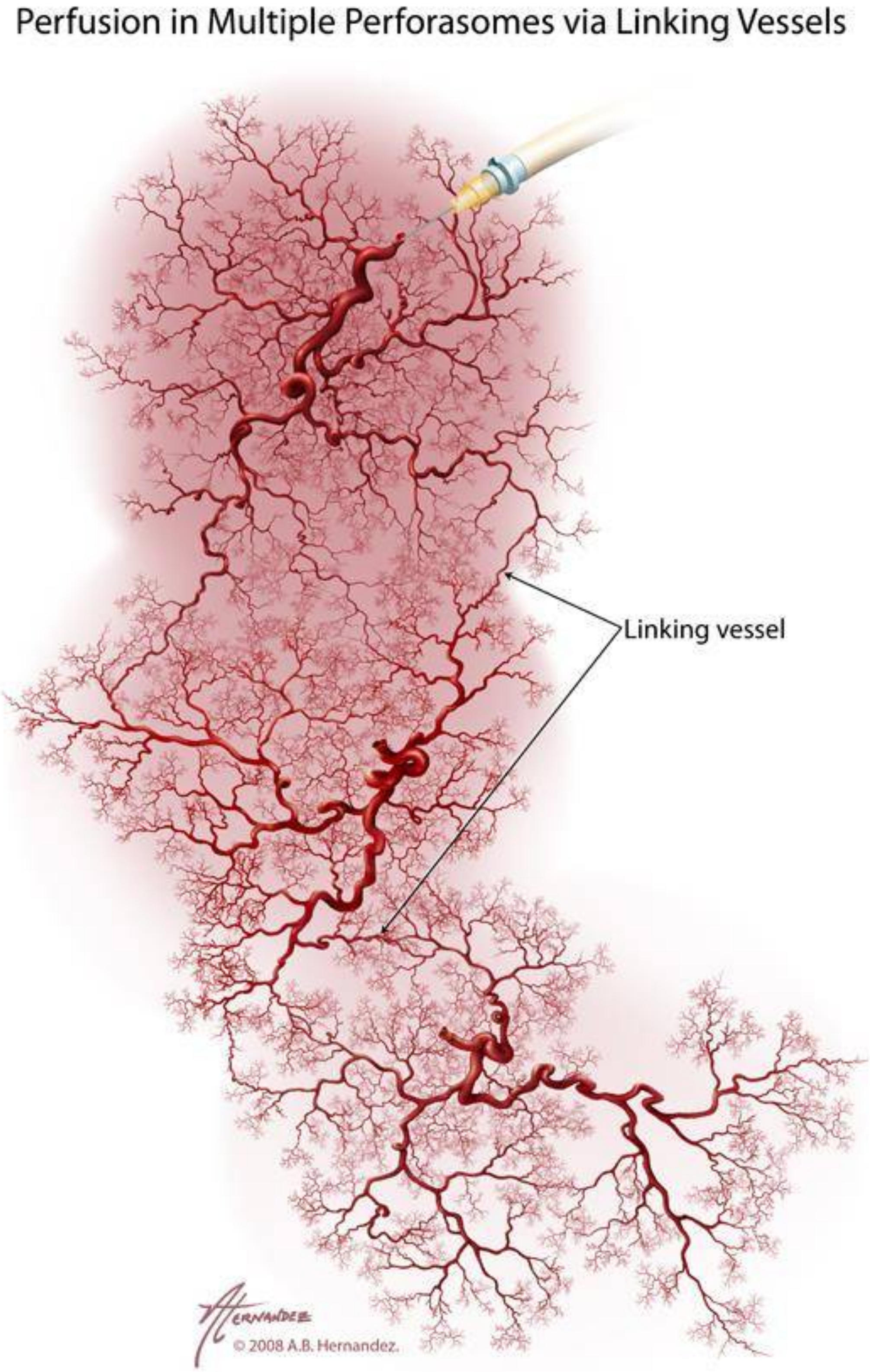

Figure 5.5 *Linking vessels connect multiple perforasomes.*

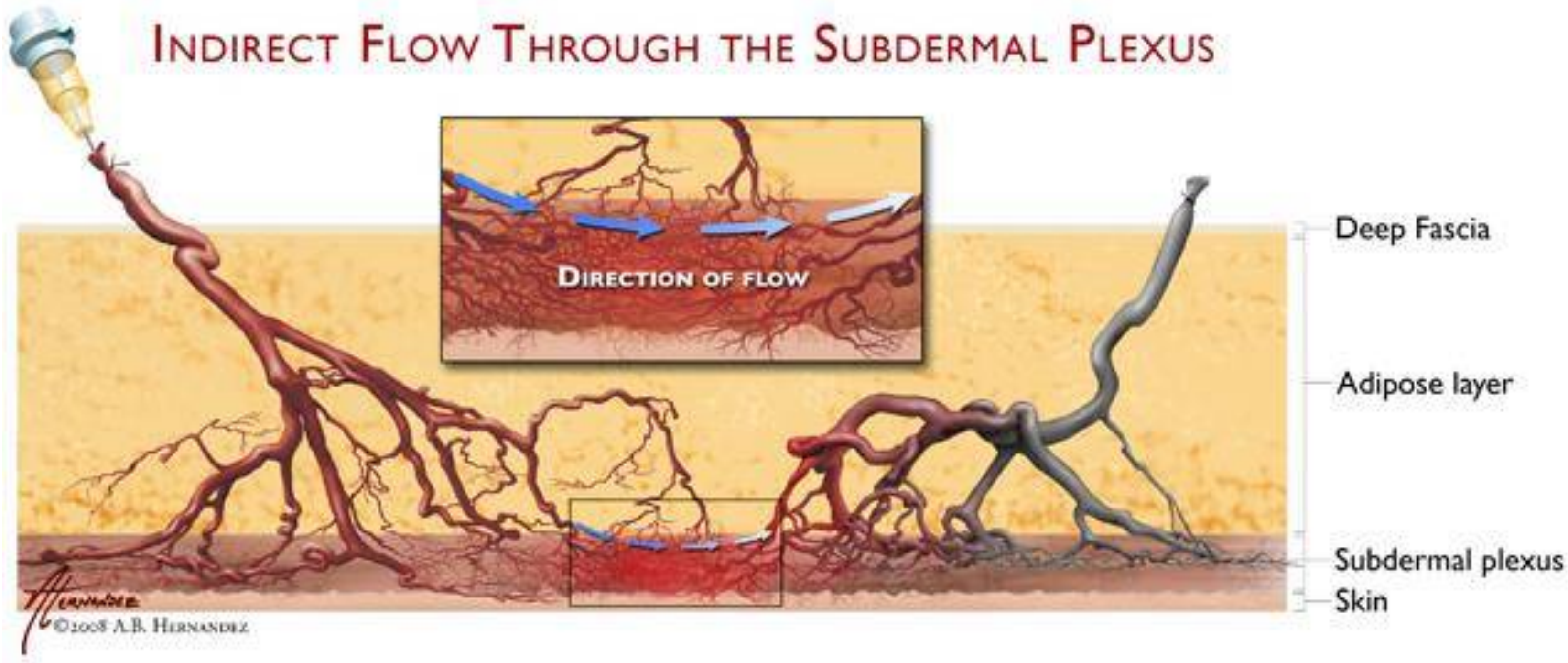

Figure 5.6 *Perforators can also be linked to one another by indirect linking vessels or recurrent flow via the subdermal plexus.*

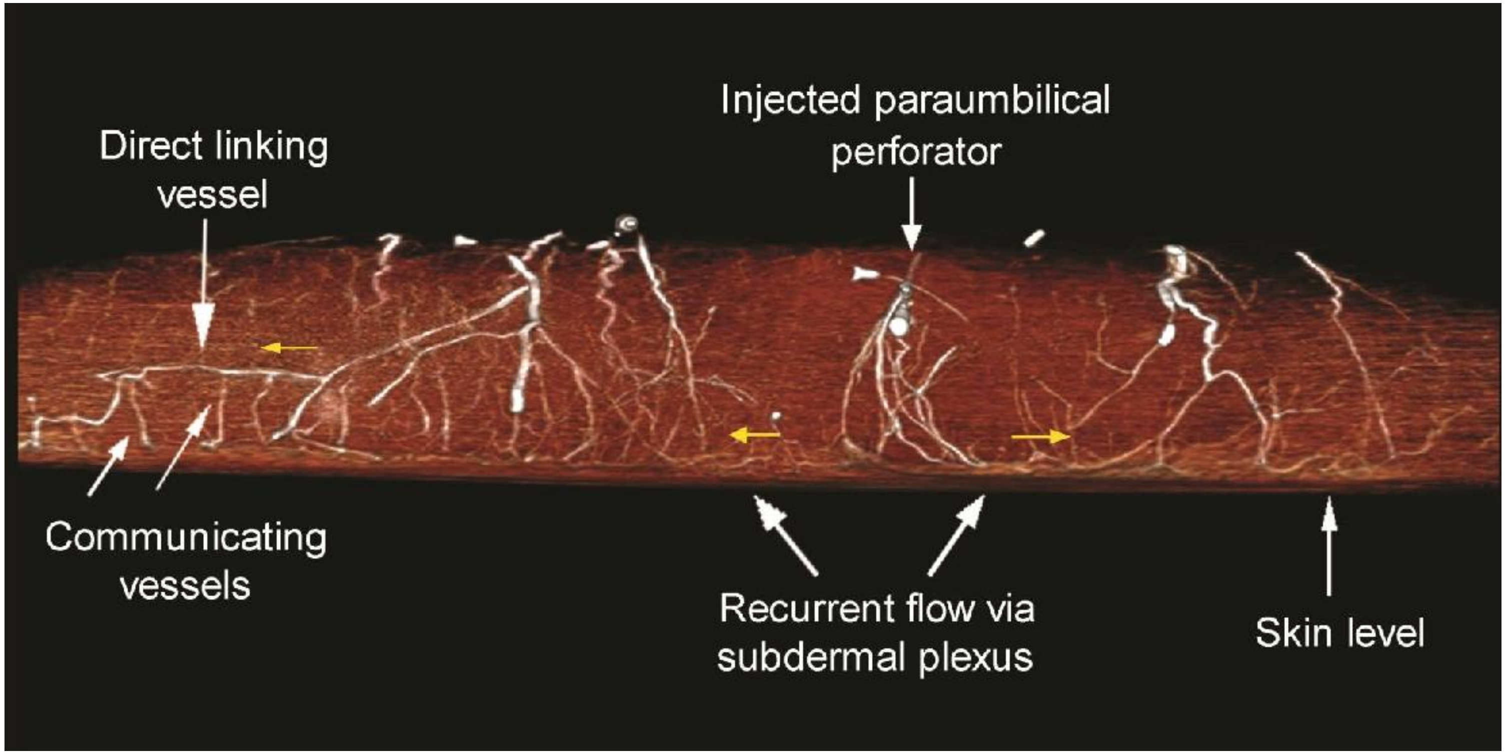

Figure 5.7 *Transverse view of an abdominal flap, where a paraumbilical perforator was injected with contrast. Direct and indirect linking vessels are demonstrated*

Second principle:

Flap design and skin paddle orientation should be based on the direction of the linking vessels which is axial in the extremities and perpendicular to the midline in the trunk.

Extremities:

Vascular axis follows the axiality of the limbs. This is demonstrated in the radial artery perforator **(Figure 5.8)**, ulnar artery perforator, anterior tibial artery perforator **(Figure 5.9)**, peroneal artery perforator **(Figure 5.10)**, and posterior tibial artery perforator flaps. The limbs have source arteries which are most often directed axial to the limb themselves. Each axially directed source artery from either the lower or upper extremity provides multiple sequential perforators along its course. Linking vessels allow perforators from the same source artery to communicate with each other as well as with perforators from adjacent source arteries. In order to do this effectively, linking vessels have an orientation which is predominantly parallel to axis of the limbs **(Figures 5.8-5.10).** Perforator flaps should be designed in parallel to the axis of the linking vessels of the limbs in order to capture the largest and most reliable vascular territory.

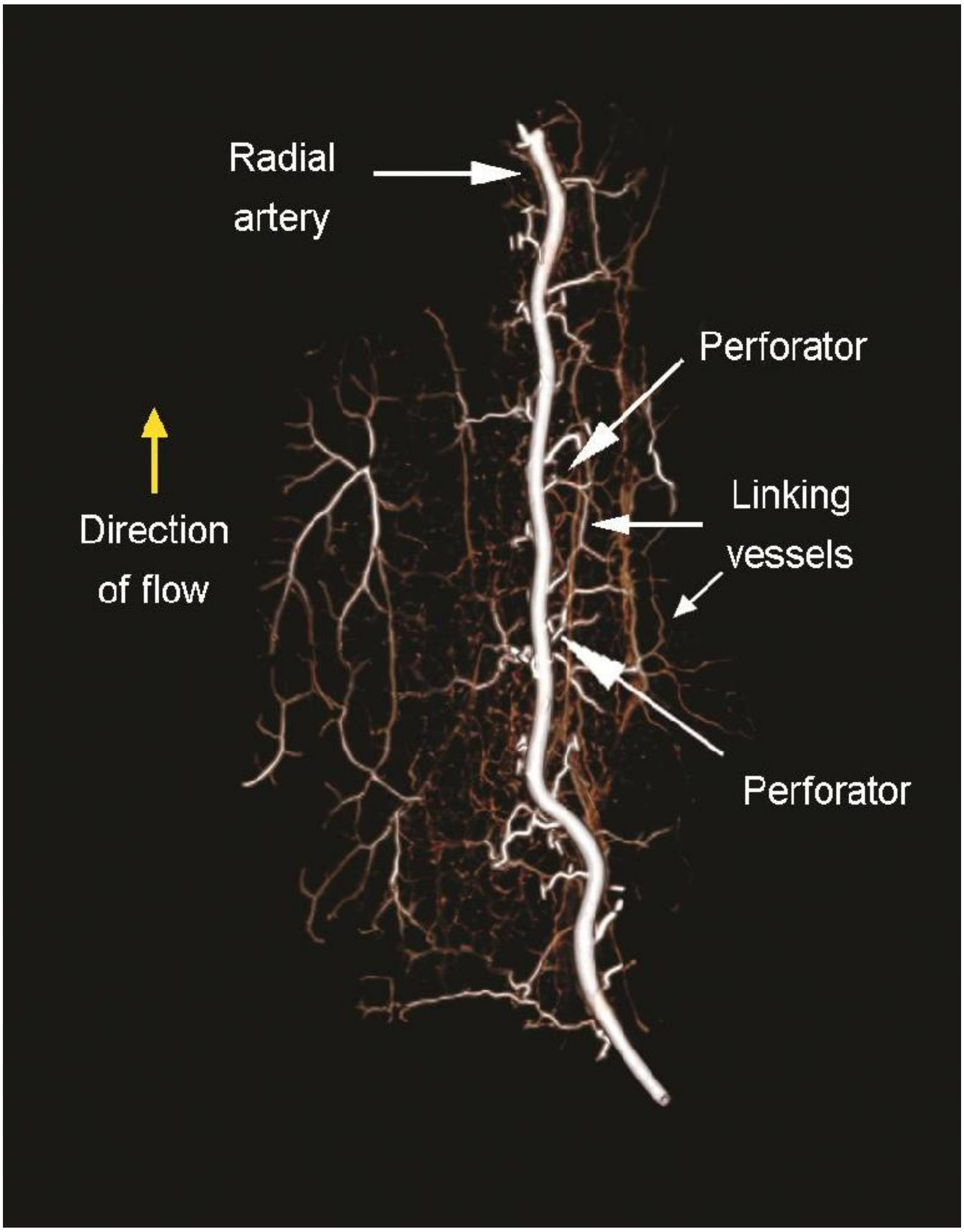

Figure 5.8. *Forearm flap where the radial artery was injected with contrast. Linking vessels follow the axiality of the limb. Yellow arrow shows direction of flow.*

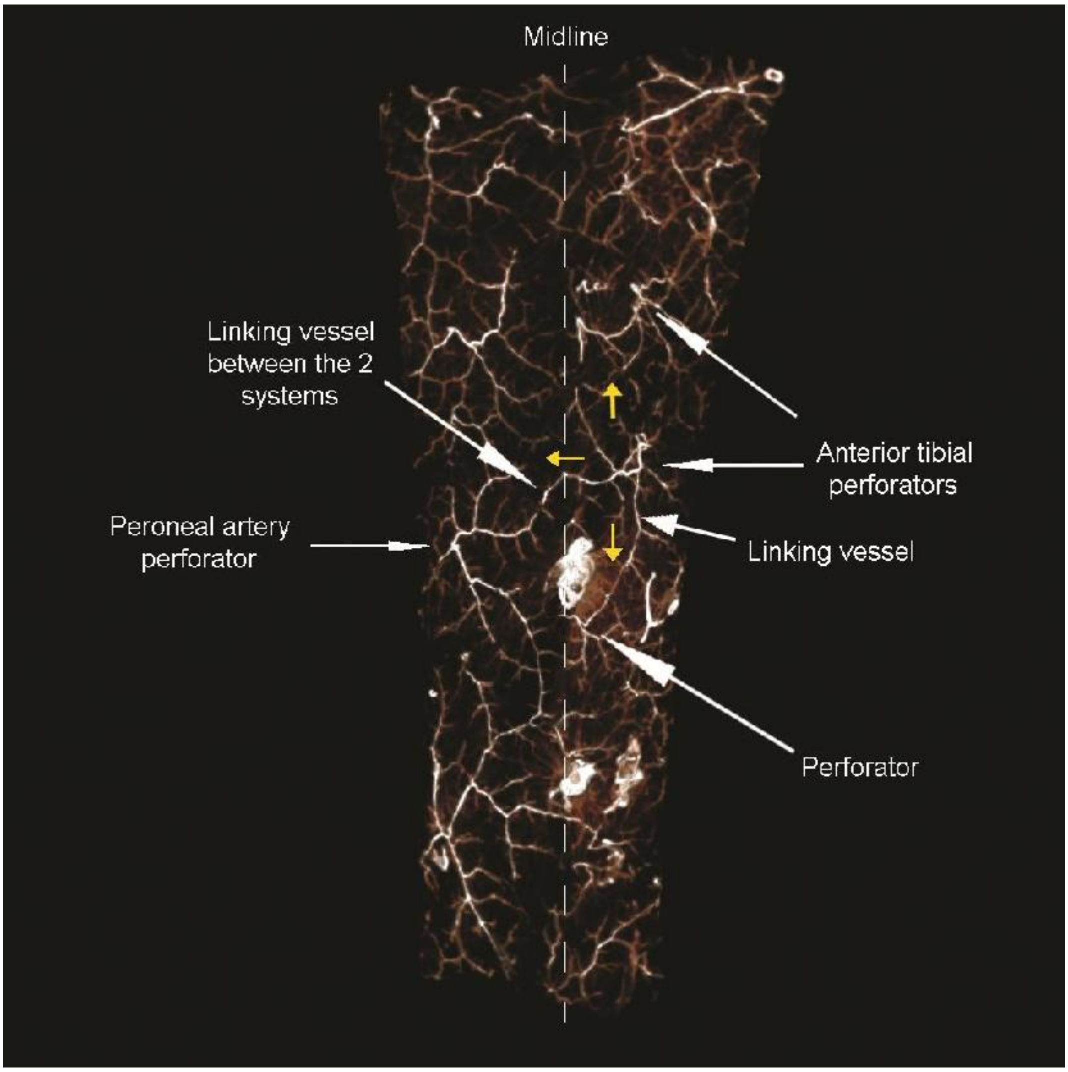

Figure 5.9 *Skin from the anterior lower leg from knee level to ankle level. Anterior tibial artery perforators and peroneal artery perforators have linking vessels that follow the axiality of the limb. There are also linking vessels between the two systems. Yellow arrows show direction of flow.*

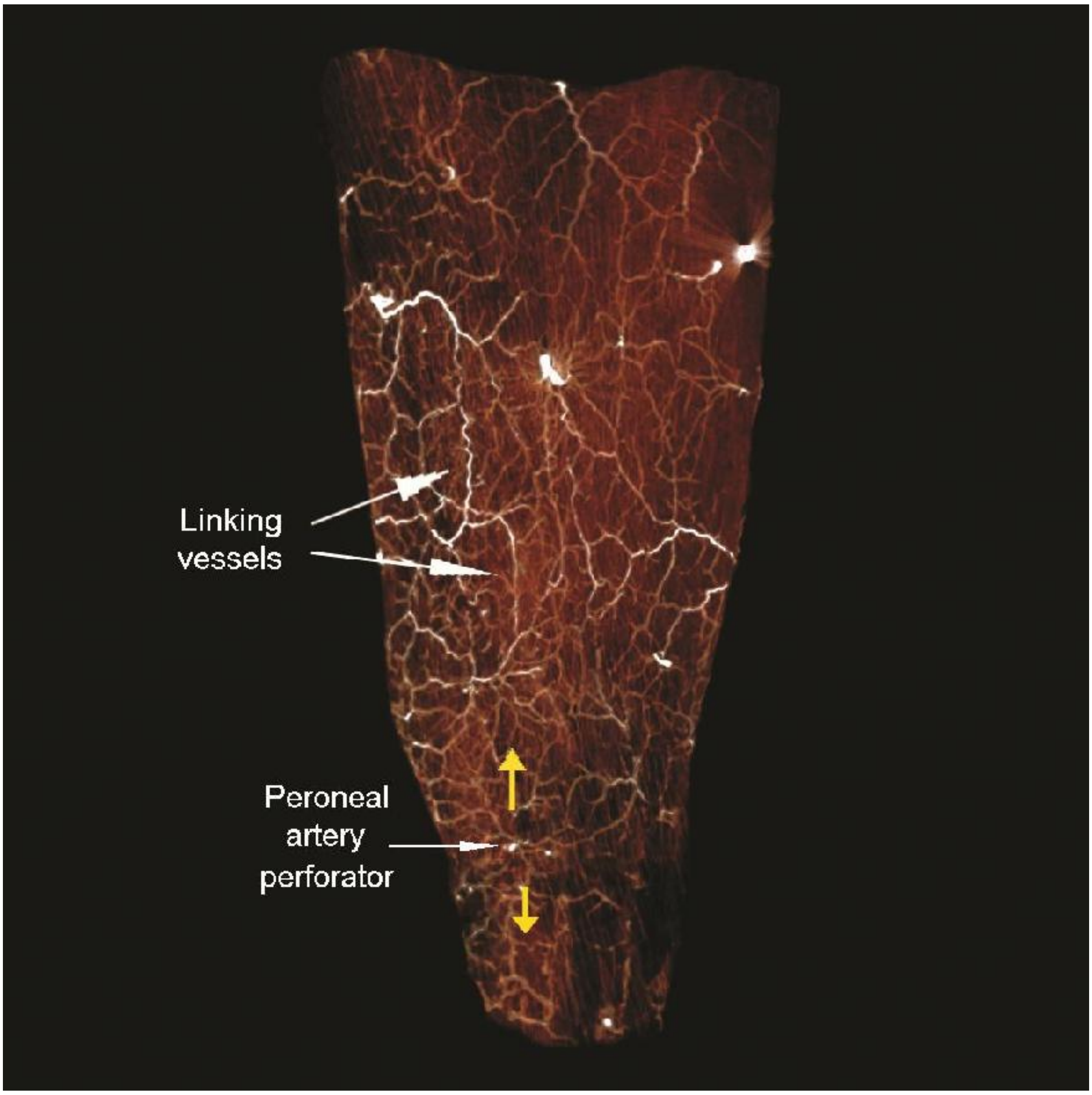

Figure 5.10 *Skin from the posterior lower leg from knee to ankle level. Peroneal artery perforator injected with contrast. Yellow arrows show direction of flow.*

Trunk:

Linking vessels in the trunk are commonly directed perpendicular to the midline and follow an oblique transverse direction, parallel to the cutaneous dermatomes. This is shown in the supra-clavicular artery perforator **(Figure 5.11)**, internal mammary artery perforator **(Figure 5.12),** paraumbilical perforator **(Figure 5.13),** superior epigastric artery perforator **(Figure 5.14),** posterior intercostal artery perforator **(Figure 5.15),** lumbar artery perforator **(Figure 5.16)** and superior gluteal artery perforator **(Figure 5.17).** Again, multiple communicating branches between linking vessels are found in the anterior and posterior trunk. Perforators that are found close to the midline and which follow a vertical row distribution e.g. DIEP and IMAP flaps, usually have contralateral perforators which are also close to the midline. Perforasome flow is multidirectional and crosses the midline in many cases (e.g. DIEP flap), but preferential flow is directed away from the midline towards the lateral trunk borders. In instances where multiple perforators are found along a vertical row and close to the midline bilaterally (e.g. DIEP, IMAP, LAP etc), flow is directed away from the midline in order to provide adequate vascularity to the lateral trunk region which has a less dense perforator population. The anterior and posterior midlines of the trunk are heavily populated by perforators (e.g. IMAP, SEAP, DIEP, PIAP, LAP, SGAP/IGAP) as are the lateral and mid-axial regions (LIAP, TDAP, SCAP etc). Flow is therefore preferentially directed laterally away from the midline or midaxial regions in order to maintain adequate blood supply to less perforator populated adjacent regions.

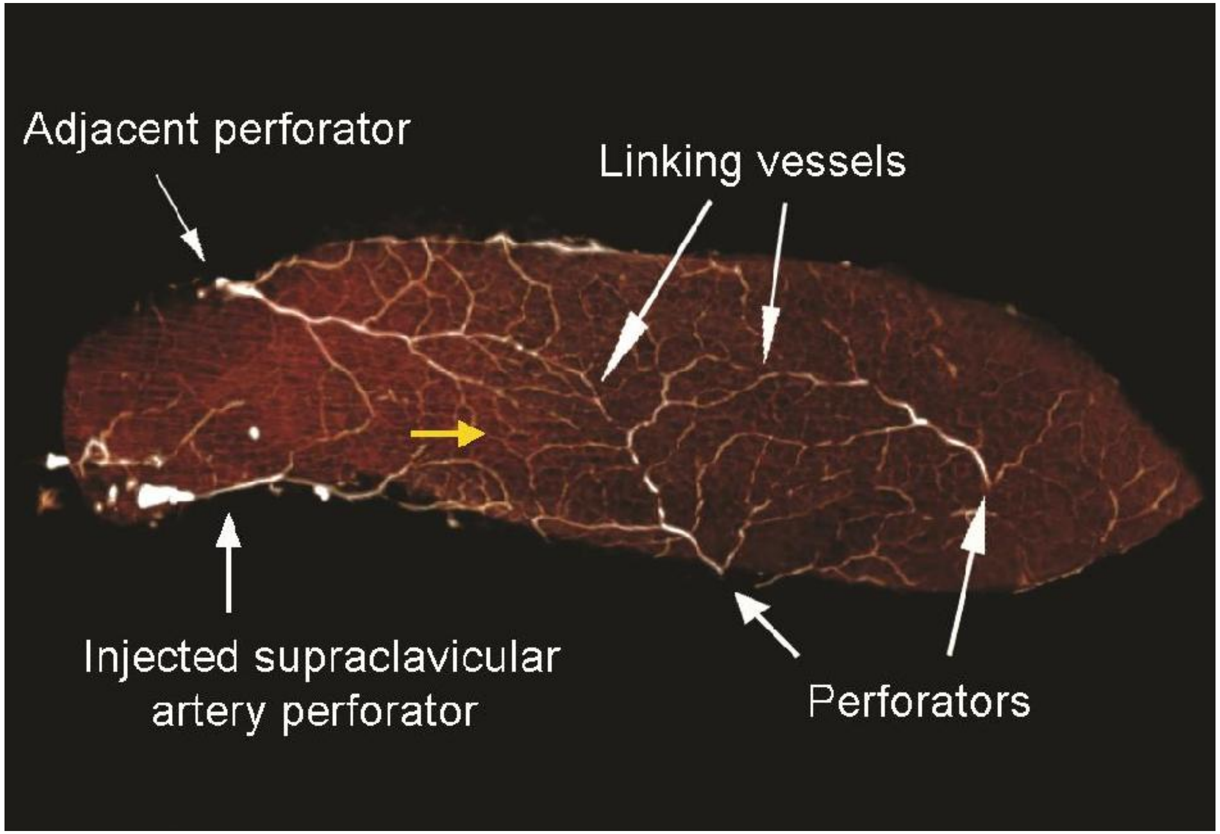

Figure 5.11. *Supraclavicular artery perforator injected with contrast. Yellow arrow shows direction of flow.*

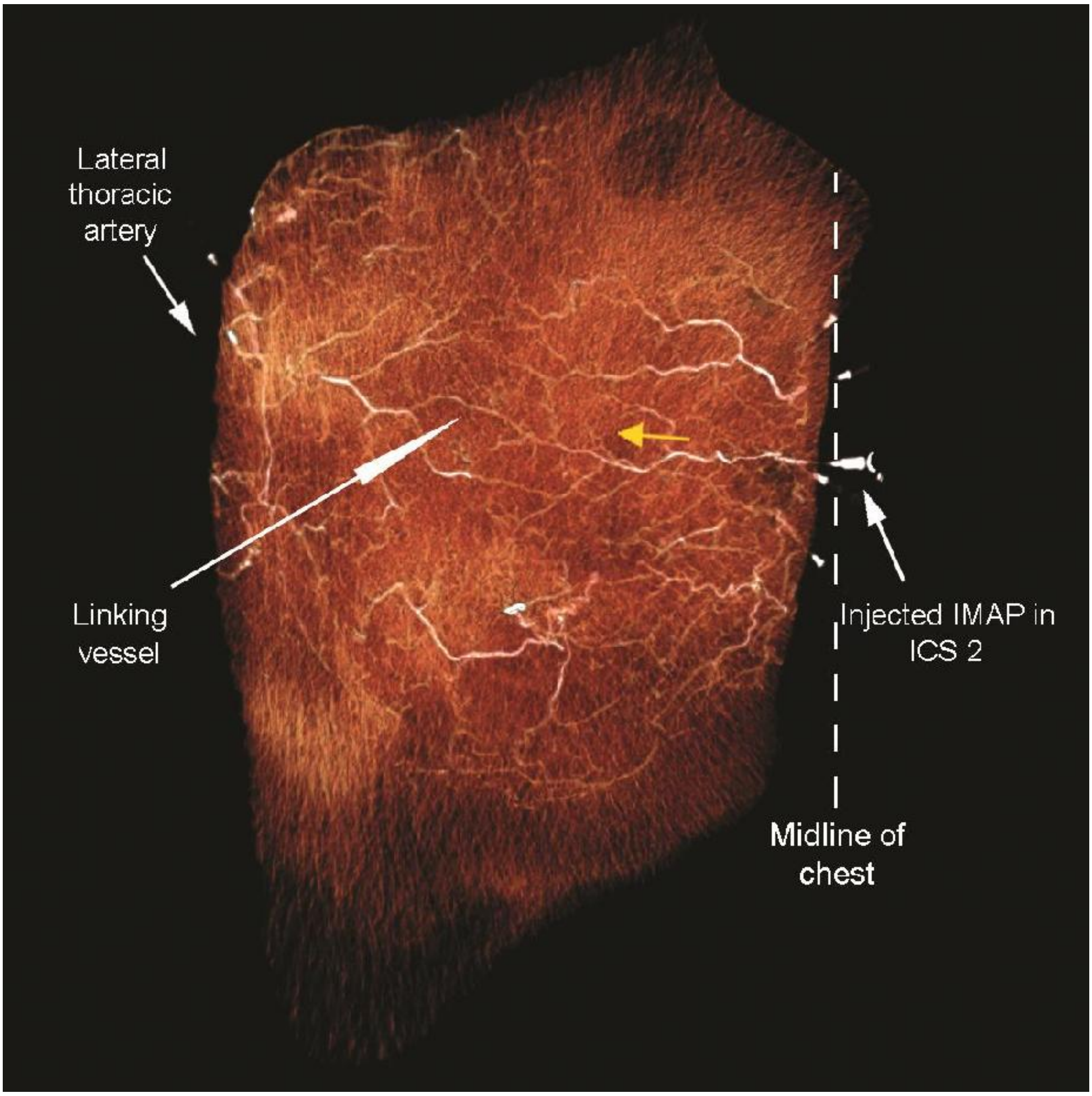

Figure 5.12 *Skin from the anterior trunk (hemichest). Internal mammary artery perforator (IMAP) in second intercostal space (ICS) injected with contrast. Linking vessels are perpendicular to the midline (seen here connecting with the lateral thoracic artery). Yellow arrow shows direction of flow.*

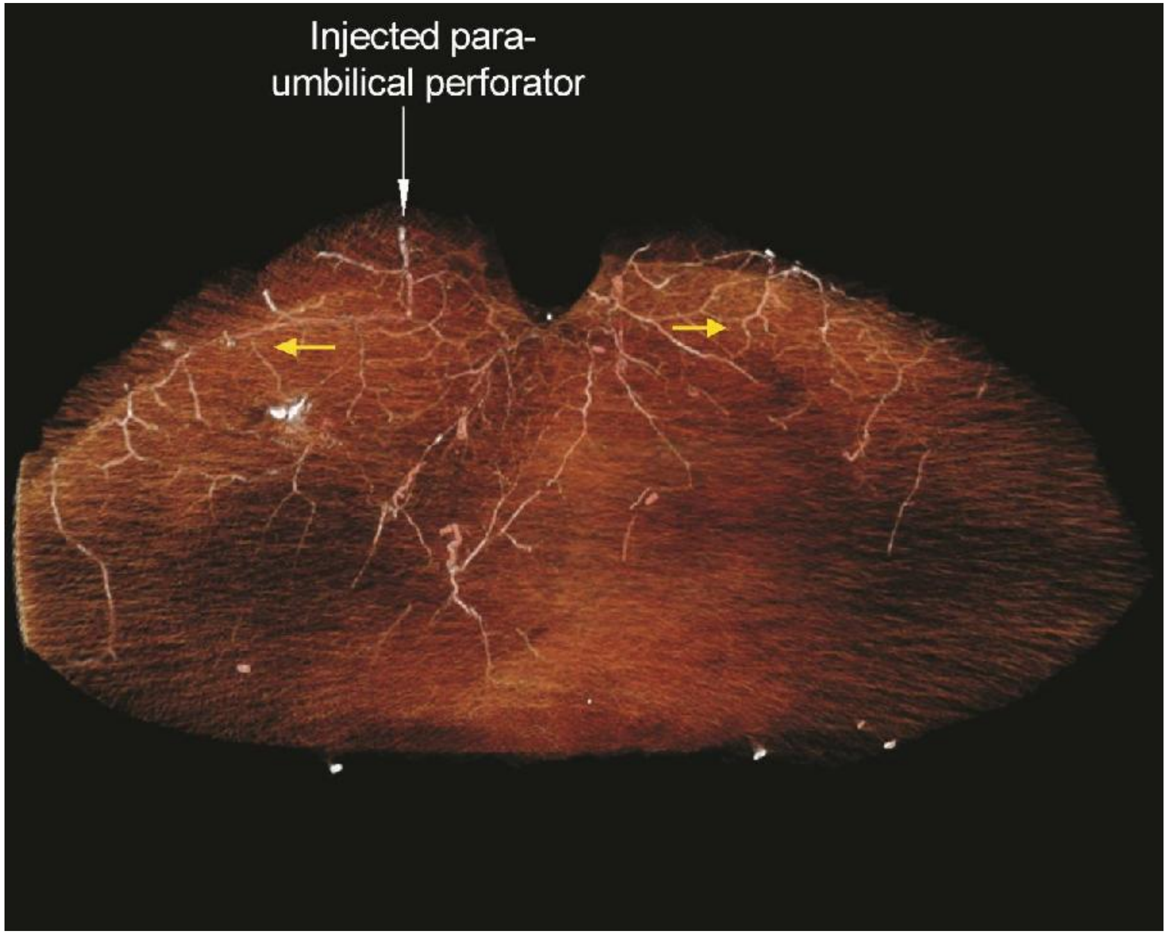

Figure 5.13 *Lower transverse abdominal skin flap. Paraumbilical artery perforator injected with contrast. Linking vessels travel perpendicular to the midline. Yellow arrows show direction of flow.*

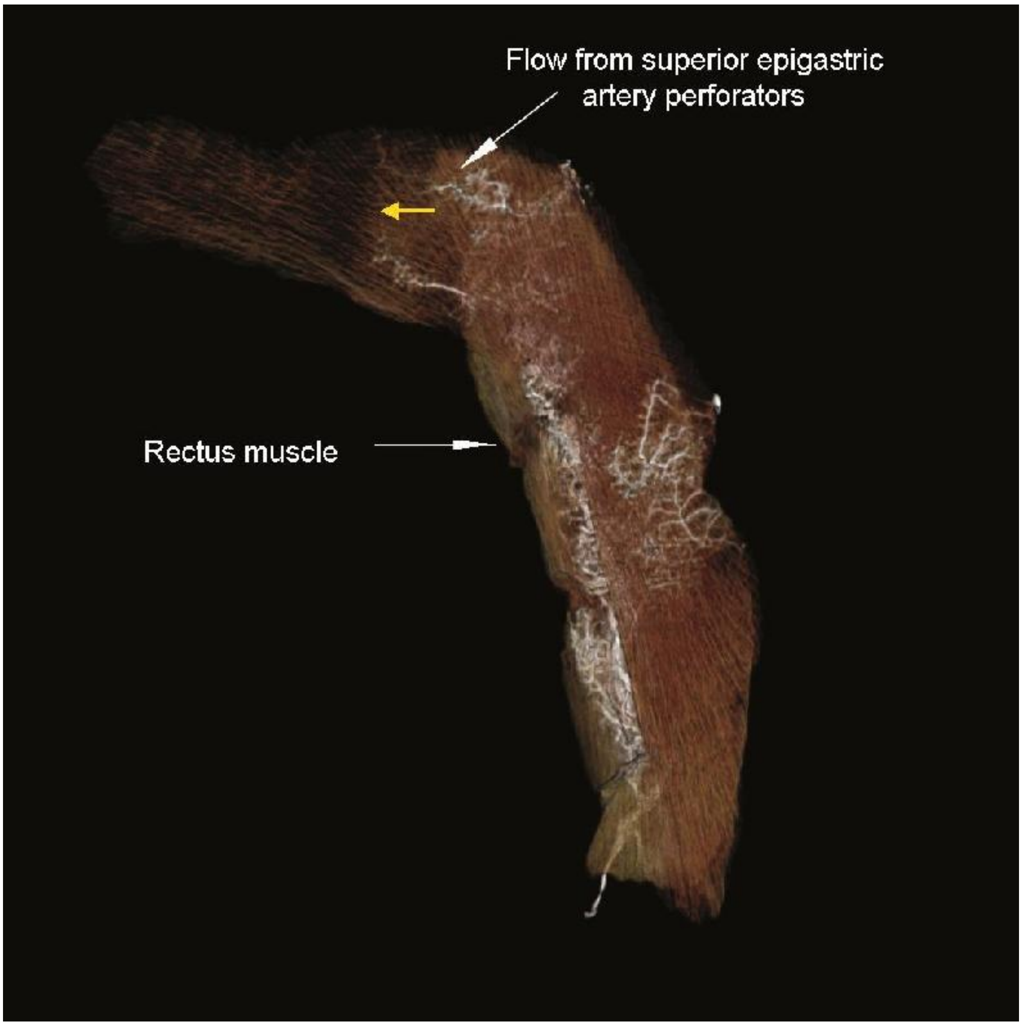

Figure 5.14 *Extended vertical rectus muscle flap, where the superior skin flap is extended to the region below the inframammary fold. The superior epigastric artery perforators were found to have linking vessels perpendicular to the midline. Yellow arrow shows direction of flow.*

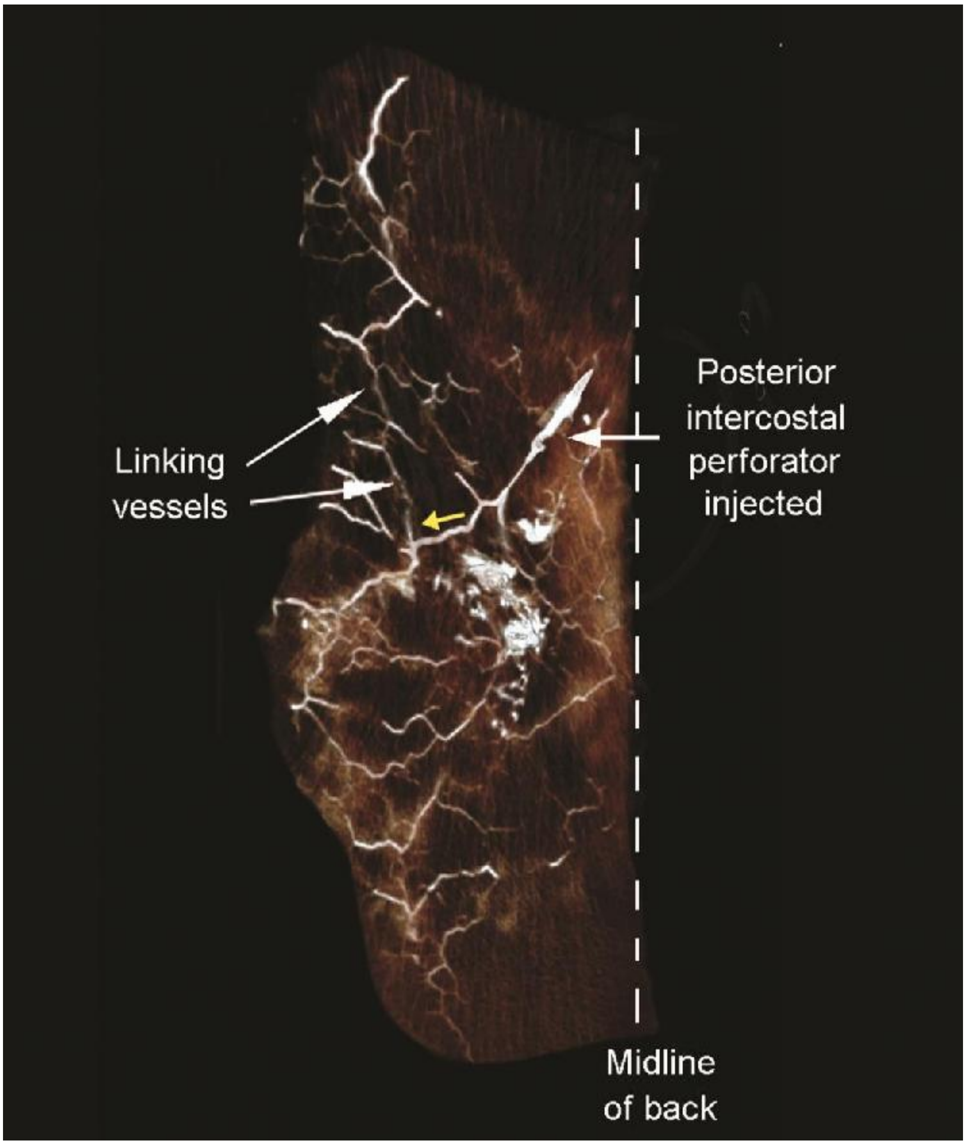

Figure 5.15 *Hemiback flap where a posterior intercostal perforator was injected with contrast. Yellow arrow shows direction of flow.*

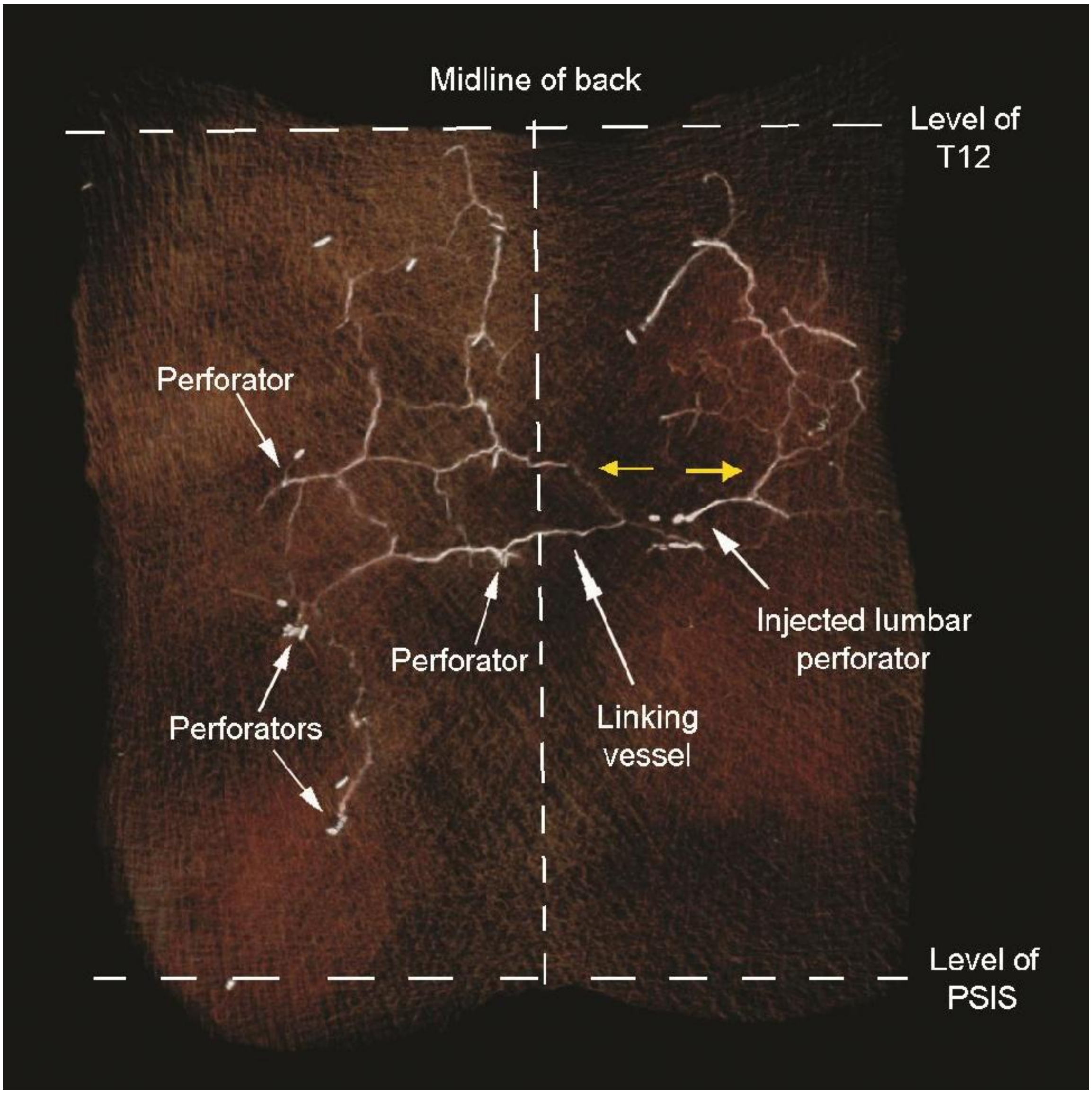

Figure 5.16 *Whole lumbar skin from T12 level to posterior superior iliac spine (PSIS). Lumbar perforator injected with contrast, and was found to perfuse across the midline, as well as ipsilaterally in a transverse direction. Yellow arrows show direction of flow.*

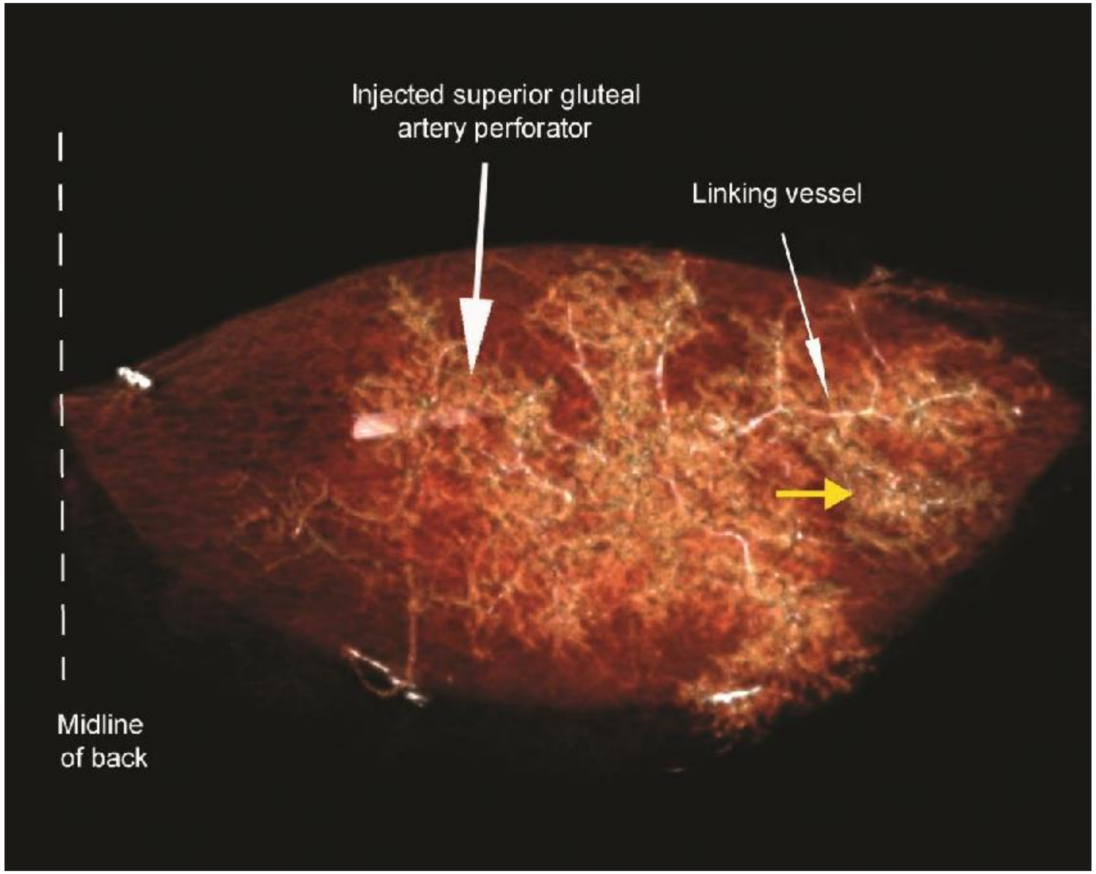

Figure 5.17 *Superior gluteal artery perforator flap. Yellow arrow shows direction of flow.*

Because of the multiple communicating branches between linking vessels, there is a very large variation in pedicle flap design potential. The ultimate flap design depends on the overall vascular territory (perforasome) of the involved perforator. Perforators with a very large perforasome will have a higher degree of freedom in flap design and orientation, e.g. the IMAP flap which has been harvested horizontally, obliquely or vertically [30-34].

Third principle:

Preferential filling of perforasomes occurs within perforators of the same source artery first, followed by perforators of other adjacent source arteries.

An example of this includes the descending branch of the lateral femoral circumflex artery (ALT flap); perforator B will vascularize perforator A and C and will then capture adjacent vascular territory perforasomes such as the anterior medial thigh or superficial femoral artery perforasomes (Figure 5.18). Vascular filling and density is maximized in the periphery of the perforasome within the same source artery. The linking vessels then emanate from this main perforasome to perforasomes of adjacent vascular territories from other source arteries (e.g. antero-medial thigh perforators). Single large perforators originating from a source artery that does not have a series of sequential perforators along its course (e.g. medial circumflex femoral artery) will have less of an axial vascular distribution.

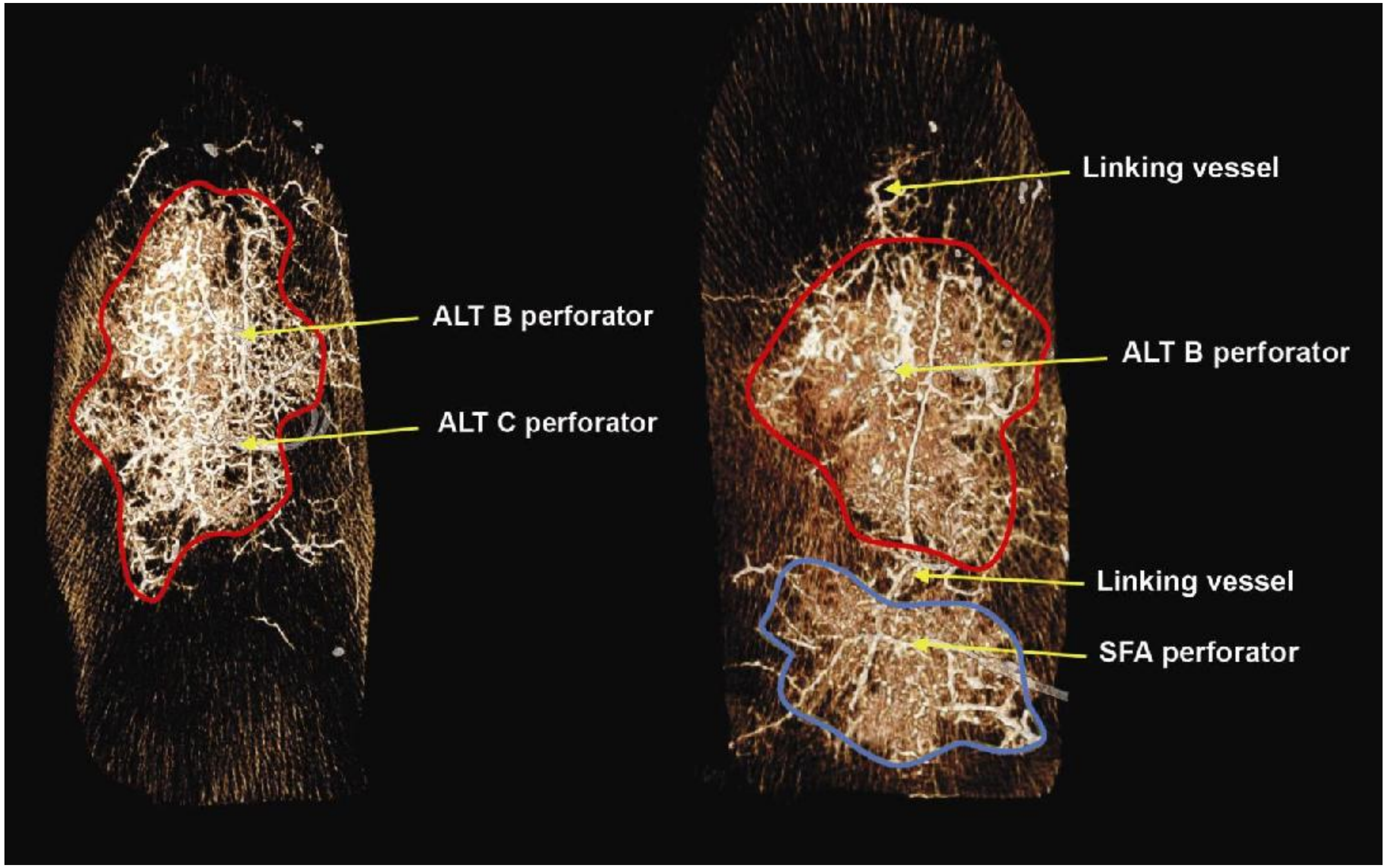

Figure 5.18 *Preferential filling is demonstrated in this anterolateral thigh (ALT) flap as perforator B and C are perfused before linking with the superficial femoral artery (SFA) perforator.*

Fourth principle:

Mass vascularity of a perforator found adjacent to an articulation is directed away from that same articulation (e.g. distally and proximally based radial artery perforator flaps). Whereas perforators found at a midpoint between two articulations (e.g. upper extremity, **Figure 5.19**), or midpoint in the trunk have a multidirectional flow distribution.

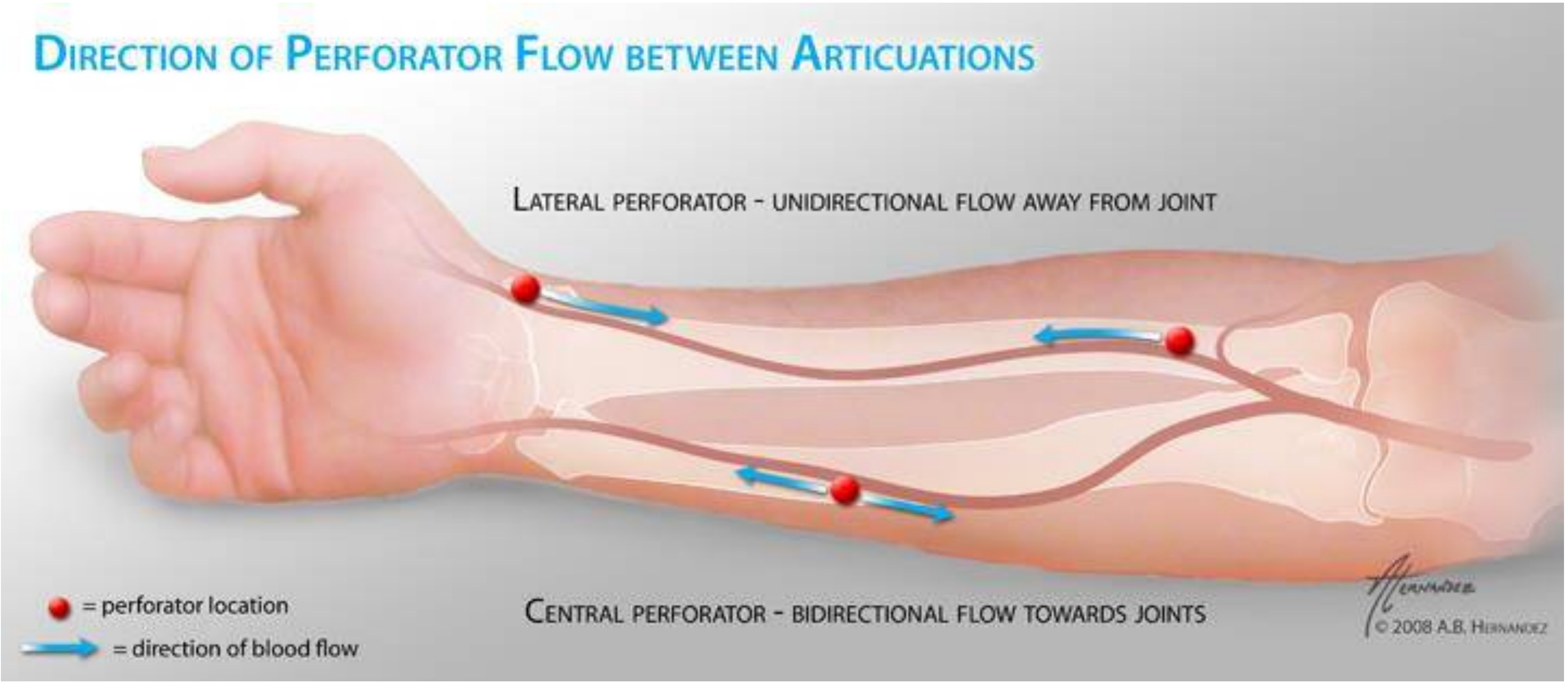

Figure 5.19 *Perforators located near a joint flow away from that joint (unidirectional), whereas perforators found midway between two joints have a bidirectional flow towards both joints.*

These numerous vascular connections confer further protection from ischaemia and vascular injury in cases of trauma. Linking vessels allow communication with adjacent perforasomes and follow a direction which is parallel to the direction of perforator flow. Therefore perforator flap skin paddles should be parallel to the linking vessel orientation whenever possible. These linking vessels make it possible to harvest large perforator flaps based on a single perforator such as the extended ALT flap.[99] When a perforator flap is harvested all muscle and cutaneous branches from the source artery are ligated which results in hyperperfusion of the selected perforator. Increased vascular filling pressures clinically dilate the perforator itself and allow extensive inter-perforator flow via opening and recruitment of additional linking vessels. These linking vessels, both direct and indirect, are subject to higher than normal filling pressures and are able to capture additional adjacent perforator vascular territories (perforasomes).

Perforator flaps designed at a midpoint between two articulations can be designed in multiple fashions because of the multidirectional perforator flow distribution. Dense fibrous septae and ligamentous attachments can be found overlying each major articulation in order to maintain proper skin stability and draping during flexion and extension. Also, each articulation forms a boundary for a different vascular territory proximal and distal to that same articulation. Both these factors might explain why perforators adjacent to an articulation will have flow directed away from it. Midline cross-over of perforator flow was found in almost all instances in the trunk via direct and indirect linking vessels. Indirect flow via the subdermal plexus becomes important when there is a paucity of subcutaneous tissue (less direct linking vessels) and where skin is intimately adherent over bone (e.g. sternum, anterior tibia).

Summary of the 4 principles

1. Each perforasome is linked with adjacent perforasomes via two main mechanisms -direct and indirect linking vessels
2. Flap design and skin paddle orientation should be based on the direction of the linking vessels which is axial in the extremities and perpendicular to the midline in the trunk
3. Preferential filling of perforasomes occurs within perforators of the same source artery first, followed by perforators of other adjacent source arteries
4. Mass vascularity of a perforator found adjacent to an articulation is directed away from that same articulation (e.g. distally and proximally based radial artery perforator flaps). Whereas perforators found at a midpoint between two articulations, or midpoint in the trunk have a multidirectional flow distribution.

CONCLUSION:

Each perforator holds a unique vascular territory (perforasome). Perforator vascular supply is highly complex and follows some common guidelines. Both direct and indirect linking vessels play a critical part in perforator flap perfusion. Every perforator has a potential to become either a pedicle or free perforator flap depending on the size of the source artery. As a result, this allows a myriad of perforator flap designs which can be tailored to better reconstruct defects. The reconstructive surgeon now has more options in replacing like with like. Local flap alternatives become more plentiful and flap design is limited only by the availability of clinically relevant perforators close to the defect for pedicle perforator flaps. Free-style perforator flap options are only limited by the size and length of their respective source artery and vein.

Hyperperfusion of a single perforator can capture multiple adjacent perforasomes. This explains why large perforator flaps can be harvested based on single perforator, e.g. extended ALT flap[102]. Additional adjacent perforasome territories can be captured via direct and indirect linking vessels via hyperperfusion.

This methodology does not pretend to mimic physiological conditions and cannot account for aspects such as vasoconstriction and physiological shunting. Actual vascularity may be quite different in a physiological situation, where nervous, hormonal and local controls of the vessels come into play. This merely gives us a means of comparing two different types of perforators using identical experimental conditions.

As mentioned before, we found that anatomical vascular imaging always underestimates the true clinical vascular perfusion area. This is one of the limitations of our series. This is likely due to the nature of our flaps which are cadaveric and may have small calibre vessels or capillary beds which have collapsed post-mortem, or clotted from vascular stasis. We are also missing physiological factors which control vasoconstriction and dilation such as carbon dioxide, nitrous oxide, vasomotor tone, etc. Furthermore, our method of harvesting the flaps may traumatize the delicate branching system and reduce the area contrast is able to infiltrate, hence upon scanning, perfusion is less then what it really should be. As such, all our studies cannot mimic in-vivo conditions, and can only investigate the architectural structure of the vascular system. This way we compare cadaveric flaps against each other or compare different regions of the body. This is still useful as it gives us a better idea of the perfusion patterns when specific vessels are focused on.

Further works would include improved methods of harvesting and processing flaps to increase the true areas of perfusion. Also if there was a method to keep small calibre blood vessels from clotting post mortem or perhaps an infusion of tPA to open all the vascular beds would be beneficial to increasing our area of contrast infiltration. Our studies did not look at the head and neck region, so this is an area which would be a goldmine of perfusion studies if an interested party were to pursue this. Of course many other flaps from the non-head and neck region have not been investigated, including new flaps such as the profunda artery perforator (PAP) flap and the myriad of hand/ finger flaps. Also other works could include turbo- or super-charged flaps, as well as one versus multiple perforator DIEP flaps. Perhaps the lymphatic system would also be amenable to our method of perfusion studies.

Clearly this is a technique that is tremendously useful in investigating any vessel network as long as meticulous care is taken to harvest tissue without injuring the vessels being studied. Three and four dimension computer tomography can provide not only qualitative data on vascular anatomy, but information on the direction and path of contrast flow through the tissue planes of an injected flap. Three dimensional anatomy is defined as an appraisal of the perforator vasculature in the sagittal, coronal and transverse views whereas four-dimensional anatomy refers to sequential images produced by repeated scanning as contrast flows through the flap, therefore demonstrating contrast flow through time, giving us direction and orientation of flow. This modern method gives us much more information compared to the lead injection, x-ray method which only gives us limited two-dimension data.

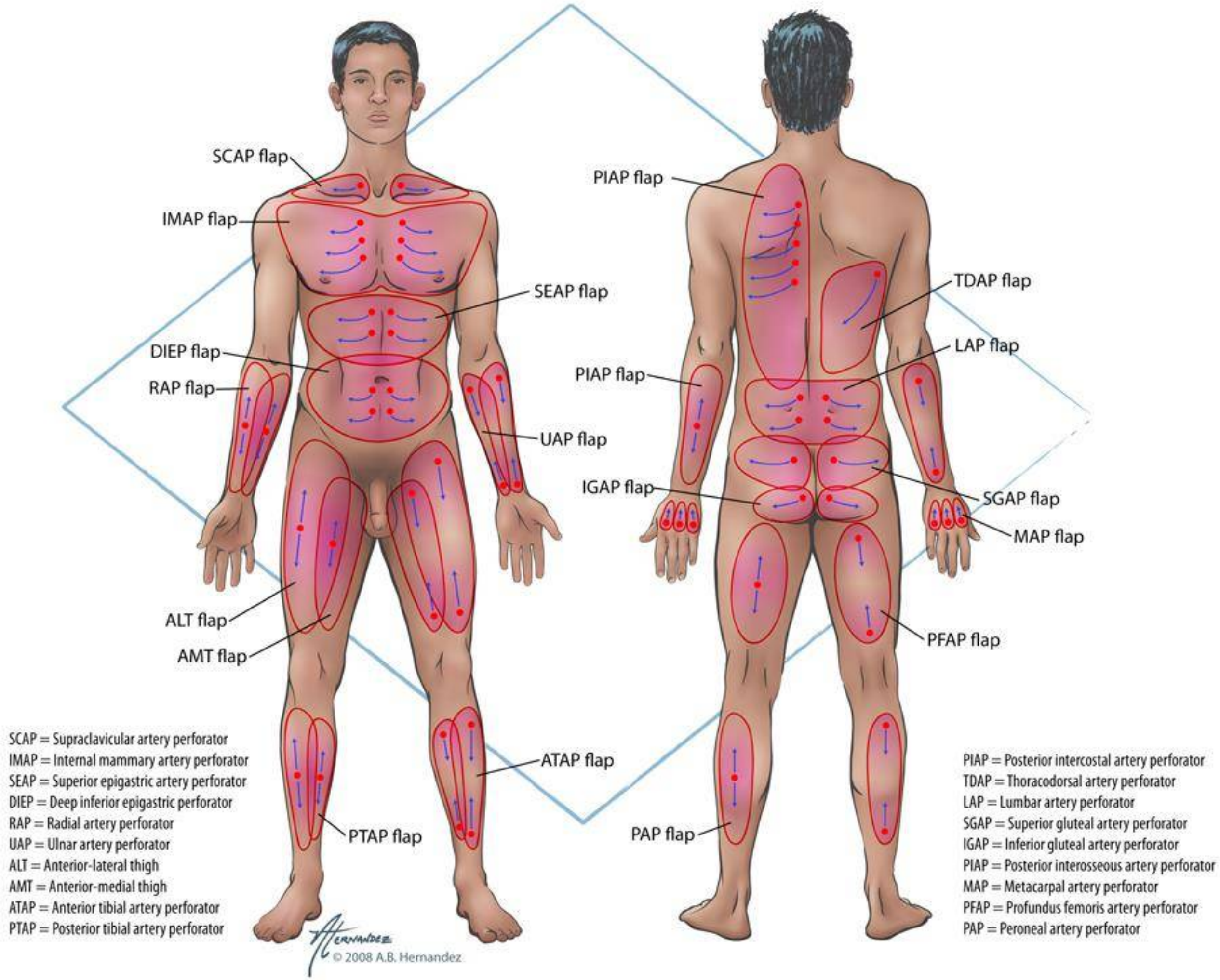

Figure 5.20 *Perforasomes of the body*

References

1. Manchot, C. *The Cutaneous Arteries of the Human Body*. New York: Springer-Verlag, 1983.
2. Morris, S. F., Taylor, G. I. Predicting the survival of experimental skin flaps with a knowledge of the vascular architecture. *Plast Reconstr Surg* 92: 1352-1361, 1993.
3. Salmon, M. *Arteries of the Skin*. London: Churchill Livingstone, 1988.
4. Taylor, G. I., Caddy, C. M., Watterson, P. A., et al. The venous territories (venosomes) of the human body: experimental study and clinical implications. *Plast Reconstr Surg* 86: 185-213, 1990.
5. Taylor, G. I., Palmer, J. H. The vascular territories (angiosomes) of the body: experimental study and clinical applications. *Br J Plast Surg* 40: 113-141, 1987.
6. Taylor, G. I., Palmer, J. H. 'Angiosome theory'. *Br J Plast Surg* 45: 327-328, 1992.
7. McCormack, G. C., Lamberty, B. G. H. *The Arterial Anatomy of Skin Flaps*, 2nd Ed. Ed. Edinburgh: Churchill-Livingstone 1994.
8. McGregor, I. A., Morgan, G. Axial and random pattern flaps. 26: 202. *Br. J. Plast. Surg.* 26: 202, 1973.
9. Saint-Cyr, M., Schaverien, M., Arbique, G., et al. Three- and four-dimensional computed tomographic angiography and venography for the investigation of the vascular anatomy and perfusion of perforator flaps. *Plast Reconstr Surg* 121: 772-780, 2008.
10. Schaverien, M., Saint-Cyr, M., Arbique, G., et al. Arterial and venous anatomies of the deep inferior epigastric perforator and superficial inferior epigastric artery flaps. *Plast Reconstr Surg* 121: 1909-1919, 2008.
11. Schaverien, M., Saint-Cyr, M., Arbique, G., et al. Three- and four-dimensional arterial and venous anatomies of the thoracodorsal artery perforator flap. *Plast Reconstr Surg* 121: 1578-1587, 2008.
12. Schaverien, M., Saint-Cyr, M., Arbique, G., et al. Three- and four-dimensional computed tomographic angiography and venography of the anterolateral thigh perforator flap. *Plast Reconstr Surg* 121: 1685-1696, 2008.
13. Tan, B. K., Ng, R. T., Tay, N. S., et al. Tissue microangiography using a simplified barium sulphate cadaver injection technique. *Ann Acad Med Singapore* 28: 152-154, 1999.
14. Bakamjian, V. Y. A Two-Stage Method for Pharyngoesophageal Reconstruction with a Primary Pectoral Skin Flap. *Plast Reconstr Surg* 36: 173-184, 1965.
15. Krizek, T. J., Robson, M. C. The deltopectoral flap for reconstruction of irradiated cancer of the head and neck. *Surg Gynecol Obstet* 135: 787-789, 1972.
16. Bakamjian, V. Y., Long, M., Rigg, B. Experience with the medially based deltopectoral flap in reconstructive surgery of the head and neck. *Br J Plast Surg* 24: 174-183, 1971.
17. Gilas, T., Sako, K., Razack, M. S., et al. Major head and neck reconstruction using the deltopectoral flap. A 20 year experience. *Am J Surg* 152: 430-434, 1986.
18. Pallua, N., Machens, H. G., Rennekampff, O., et al. The fasciocutaneous supraclavicular artery island flap for releasing postburn mentosternal contractures. *Plast Reconstr Surg* 99: 1878-1884; discussion 1885-1876, 1997.
19. Pallua, N., Magnus Noah, E. The tunneled supraclavicular island flap: an optimized technique for head and neck reconstruction. *Plast Reconstr Surg* 105: 842-851; discussion 852-844, 2000.

20. Yu, P., Roblin, P., Chevray, P. Internal mammary artery perforator (IMAP) flap for tracheostoma reconstruction. *Head Neck* 28: 723-729, 2006.
21. Vesely, M. J., Murray, D. J., Novak, C. B., et al. The internal mammary artery perforator flap: an anatomical study and a case report. *Ann Plast Surg* 58: 156-161, 2007.
22. Neligan, P. C., Gullane, P. J., Vesely, M., et al. The internal mammary artery perforator flap: new variation on an old theme. *Plast Reconstr Surg* 119: 891-893, 2007.
23. Munhoz, A. M., Ishida, L. H., Montag, E., et al. Perforator flap breast reconstruction using internal mammary perforator branches as a recipient site: an anatomical and clinical analysis. *Plast Reconstr Surg* 114: 62-68, 2004.
24. Palmer, J. H., Taylor, G. I. The vascular territories of the anterior chest wall. *Br J Plast Surg* 39: 287-299, 1986.
25. Rosson, G. D., Holton, L. H., Silverman, R. P., et al. Internal mammary perforators: a cadaver study. *J Reconstr Microsurg* 21: 239-242, 2005.
26. Marcus, G. H. Untersuchungen uber die arterielle Blutversorgung der Mamilla. *Archiv fur klinische Chirurgie* 179, 1934.
27. Holmstrom, H. The free abdominoplasty flap and its use in breast reconstruction. An experimental study and clinical case report. *Scand J Plast Reconstr Surg* 13: 423-427, 1979.
28. Hartrampf, C. R., Scheflan, M., Black, P. W. Breast reconstruction with a transverse abdominal island flap. *Plast Reconstr Surg* 69: 216-225, 1982.
29. Boyd, J. B., Taylor, G. I., Corlett, R. The vascular territories of the superior epigastric and the deep inferior epigastric systems. *Plast Reconstr Surg* 73: 1-16, 1984.
30. Miller, L. B., Bostwick, J., 3rd, Hartrampf, C. R., Jr., et al. The superiorly based rectus abdominis flap: predicting and enhancing its blood supply based on an anatomic and clinical study. *Plast Reconstr Surg* 81: 713-724, 1988.
31. Moon, H. K., Taylor, G. I. The vascular anatomy of rectus abdominis musculocutaneous flaps based on the deep superior epigastric system. *Plast Reconstr Surg* 82: 815-832, 1988.
32. Watterson, P. A., Bostwick, J., 3rd, Hester, T. R., Jr., et al. TRAM flap anatomy correlated with a 10-year clinical experience with 556 patients. *Plast Reconstr Surg* 95: 1185-1194, 1995.
33. Koshima, I., Soeda, S. Inferior epigastric artery skin flaps without rectus abdominis muscle. *Br J Plast Surg* 42: 645-648, 1989.
34. Allen, R. J., Treece, P. Deep inferior epigastric perforator flap for breast reconstruction. *Ann Plast Surg* 32: 32-38, 1994.
35. Scheflan, M., Dinner, M. I. The transverse abdominal island flap: Part II. Surgical technique. *Ann Plast Surg* 10: 120-129, 1983.
36. Scheflan, M., Dinner, M. I. The transverse abdominal island flap: part I. Indications, contraindications, results, and complications. *Ann Plast Surg* 10: 24-35, 1983.
37. Holm, C., Mayr, M., Hofter, E., et al. Perfusion zones of the DIEP flap revisited: a clinical study. *Plast Reconstr Surg* 117: 37-43, 2006.
38. Kroll, S. S., Evans, G. R., Reece, G. P., et al. Comparison of resource costs of free and conventional TRAM flap breast reconstruction. *Plast Reconstr Surg* 98: 74-77, 1996.
39. Kroll, S. S., Gherardini, G., Martin, J. E., et al. Fat necrosis in free and pedicled TRAM flaps. *Plast Reconstr Surg* 102: 1502-1507, 1998.

40. Blondeel, P. N., Arnstein, M., Verstraete, K., et al. Venous congestion and blood flow in free transverse rectus abdominis myocutaneous and deep inferior epigastric perforator flaps. *Plast Reconstr Surg* 106: 1295-1299, 2000.
41. Kroll, S. S. Fat necrosis in free transverse rectus abdominis myocutaneous and deep inferior epigastric perforator flaps. *Plast Reconstr Surg* 106: 576-583, 2000.
42. Nahabedian, M. Y., Momen, B., Galdino, G., et al. Breast Reconstruction with the free TRAM or DIEP flap: patient selection, choice of flap, and outcome. *Plast Reconstr Surg* 110: 466-475; discussion 476-467, 2002.
43. Nahabedian, M. Y., Tsangaris, T., Momen, B. Breast reconstruction with the DIEP flap or the muscle-sparing (MS-2) free TRAM flap: is there a difference? *Plast Reconstr Surg* 115: 436-444; discussion 445-436, 2005.
44. Bajaj, A. K., Chevray, P. M., Chang, D. W. Comparison of donor-site complications and functional outcomes in free muscle-sparing TRAM flap and free DIEP flap breast reconstruction. *Plast Reconstr Surg* 117: 737-746; discussion 747-750, 2006.
45. Itoh, Y., Arai, K. The deep inferior epigastric artery free skin flap: anatomic study and clinical application. *Plast Reconstr Surg* 91: 853-863; discussion 864, 1993.
46. Munhoz, A. M., Ishida, L. H., Sturtz, G. P., et al. Importance of lateral row perforator vessels in deep inferior epigastric perforator flap harvesting. *Plast Reconstr Surg* 113: 517-524, 2004.
47. Blondeel, P. N. One hundred free DIEP flap breast reconstructions: a personal experience. *Br J Plast Surg* 52: 104-111, 1999.
48. Nahabedian, M. Y., Dooley, W., Singh, N., et al. Contour abnormalities of the abdomen after breast reconstruction with abdominal flaps: the role of muscle preservation. *Plast Reconstr Surg* 109: 91-101, 2002.
49. Futter, C. M., Webster, M. H., Hagen, S., et al. A retrospective comparison of abdominal muscle strength following breast reconstruction with a free TRAM or DIEP flap. *Br J Plast Surg* 53: 578-583, 2000.
50. Garvey, P. B., Buchel, E. W., Pockaj, B. A., et al. DIEP and pedicled TRAM flaps: a comparison of outcomes. *Plast Reconstr Surg* 117: 1711-1719; discussion 1720-1711, 2006.
51. Heitmann, C., Felmerer, G., Durmus, C., et al. Anatomical features of perforator blood vessels in the deep inferior epigastric perforator flap. *Br J Plast Surg* 53: 205-208, 2000.
52. Wong, C., Saint-Cyr, M., Arbique, G., et al. Three and Four- Dimensional Computer Tomography Angiographic Studies of Commonly Used Abdominal Flaps in Breast Reconstruction. *Plast Reconstr Surg*, Accepted for publication July 2009.
53. Wong, C., Saint-Cyr, M., Arbique, G., et al. Three- and four-dimensional computed tomography angiographic studies of commonly used abdominal flaps in breast reconstruction. *Plast Reconstr Surg* 124: 18-27, 2009.
54. Man, L. X., Selber, J. C., Serletti, J. M. Abdominal Wall Following free TRAM or DIEP Reconstruction: A Meta-Analysis and Critical Review. *Plast Reconstr Surg*, 2009.
55. Saint-Cyr, M., Wong, C., Schaverien, M., et al. Perforasome Theory: Vascular Anatomy and Clinical Implications. *Plast Reconstr Surg* 124: 1529, 2009.
56. Kazanjian, V. H., Converse, J. *The Surgical Treatment of Facial Injuries*. Baltimore: Williams & Wilkins, 1949.
57. Mathes, S. J., Vasconez, L. O. The cervicohumeral flap. *Plast Reconstr Surg* 61: 7-12, 1978.

58. Lamberty, B. G., Cormack, G. C. Misconceptions regarding the cervico-humeral flap. *Br J Plast Surg* 36: 60-63, 1983.
59. Blevins, P. K., Luce, E. A. Limitations of the cervicohumeral flap in head and neck reconstruction. *Plast Reconstr Surg* 66: 220-224, 1980.
60. Pallua, N., Demir, E. Postburn head and neck reconstruction in children with the fasciocutaneous supraclavicular artery island flap. *Ann Plast Surg* 60: 276-282, 2008.
61. Lamberty, B. G. The supra-clavicular axial patterned flap. *Br J Plast Surg* 32: 207-212, 1979.
62. Abe, M., Murakami, G., Abe, S., et al. Supraclavicular artery in Japanese: an anatomical basis for the flap using a pedicle containing a cervical, non-perforating cutaneous branch of the superficial cervical artery. *Okajimas Polia Anat Jpn.* 77: 149-154, 2000.
63. Alkureishi, L. W., Shaw-Dunn, J., Ross, G. L. Effects of thinning the anterolateral thigh flap on the blood supply to the skin. *Br J Plast Surg* 56: 401-408, 2003.
64. Ma, X., Zheng, Y., Xia, W., et al. An anatomical study with clinical application of one branch of the supraclavicular artery. *Clin Anat* 22: 215-220, 2009.
65. Blondeel, P. N., Boeckx, W. D. Refinements in free flap breast reconstruction: the free bilateral deep inferior epigastric perforator flap anastomosed to the internal mammary artery. *Br J Plast Surg* 47: 495-501, 1994.
66. Arnez, Z. M., Khan, U., Pogorelec, D., et al. Breast reconstruction using the free superficial inferior epigastric artery (SIEA) flap. *Br J Plast Surg* 52: 276-279, 1999.
67. Allen, R. J., Tucker, C., Jr. Superior gluteal artery perforator free flap for breast reconstruction. *Plast Reconstr Surg* 95: 1207-1212, 1995.
68. Granzow, J. W., Levine, J. L., Chiu, E. S., et al. Breast reconstruction with gluteal artery perforator flaps. *J Plast Reconstr Aesthet Surg* 59: 614-621, 2006.
69. Paletta, C. E., Bostwick, J., 3rd, Nahai, F. The inferior gluteal free flap in breast reconstruction. *Plast Reconstr Surg* 84: 875-883; discussion 884-875, 1989.
70. de Weerd, L., Elvenes, O. P., Strandenes, E., et al. Autologous breast reconstruction with a free lumbar artery perforator flap. *Br J Plast Surg* 56: 180-183, 2003.
71. Arnez, Z. M., Pogorelec, D., Planinsek, F., et al. Breast reconstruction by the free transverse gracilis (TUG) flap. *Br J Plast Surg* 57: 20-26, 2004.
72. Wechselberger, G., Schoeller, T. The transverse myocutaneous gracilis free flap: a valuable tissue source in autologous breast reconstruction. *Plast Reconstr Surg* 114: 69-73, 2004.
73. Yousif, N. J., Matloub, H. S., Kolachalam, R., et al. The transverse gracilis musculocutaneous flap. *Ann Plast Surg* 29: 482-490, 1992.
74. Schoeller, T., Wechselberger, G. Breast reconstruction by the free transverse gracilis (TUG) flap. *Br J Plast Surg* 57: 481-482, 2004.
75. Schoeller, T., Huemer, G. M., Wechselberger, G. The transverse musculocutaneous gracilis flap for breast reconstruction: guidelines for flap and patient selection. *Plast Reconstr Surg* 122: 29-38, 2008.
76. Fattah, A., Figus, A., Mathur, B., et al. The transverse myocutaneous gracilis flap: technical refinements. *J Plast Reconstr Aesthet Surg*, 2009.
77. Peek, A., Muller, M., Ackermann, G., et al. The free gracilis perforator flap: anatomical study and clinical refinements of a new perforator flap. *Plast Reconstr Surg* 123: 578-588, 2009.

78. Vega, S. J., Sandeen, S., Bossert, R., et al. Gracilis Myocutaneous Free Flap in Autologous Breast Reconstruction. *Plast Reconstr Surg* 124: 1400-1409, 2009.
79. Fansa, H., Schirmer, S., Warnecke, I. C., et al. The transverse myocutaneous gracilis muscle flap: a fast and reliable method for breast reconstruction. *Plast Reconstr Surg* 122: 1326-1333, 2008.
80. Wong, C., Saint-Cyr, M., Rasko, Y., et al. Three- and four-dimensional arterial and venous perforasomes of the internal mammary artery perforator flap. *Plast Reconstr Surg* 124: 1759-1769, 2009.
81. Schoeller, T., Huemer, G. M., Kolehmainen, M., et al. A new "Siamese" flap for breast reconstruction: the combined infragluteal-transverse myocutaneous gracilis muscle flap. *Plast Reconstr Surg* 115: 1110-1117, 2005.
82. Kenkel, J. M., Eaves, F. F., 3rd. Medial thigh lift. *Plast Reconstr Surg* 122: 621-622, 2008.
83. Mathes, D. W., Kenkel, J. M. Current concepts in medial thighplasty. *Clin Plast Surg* 35: 151-163, 2008.
84. Cormack, G. C., Lamberty, B. G. Fasciocutaneous vessels. Their distribution on the trunk and limbs, and their clinical application in tissue transfer. *Anat Clin* 6: 121-131, 1984.
85. Koshima, I., Moriguchi, T., Fukuda, H., et al. Free, thinned, paraumbilical perforator-based flaps. *J Reconstr Microsurg* 7: 313-316, 1991.
86. Koshima, I., Soeda, S. Free posterior tibial perforator-based flaps. *Ann Plast Surg* 26: 284-288, 1991.
87. Koshima, I., Moriguchi, T., Soeda, S., et al. The gluteal perforator-based flap for repair of sacral pressure sores. *Plast Reconstr Surg* 91: 678-683, 1993.
88. Koshima, I., Moriguchi, T., Etoh, H., et al. The radial artery perforator-based adipofascial flap for dorsal hand coverage. *Ann Plast Surg* 35: 474-479, 1995.
89. Koshima, I., Urushibara, K., Inagawa, K., et al. Free medial plantar perforator flaps for the resurfacing of finger and foot defects. *Plast Reconstr Surg* 107: 1753-1758, 2001.
90. Koshima, I., Nanba, Y., Tsutsui, T., et al. Superficial circumflex iliac artery perforator flap for reconstruction of limb defects. *Plast Reconstr Surg* 113: 233-240, 2004.
91. Koshima, I., Narushima, M., Mihara, M., et al. New thoracodorsal artery perforator (TAPcp) flap with capillary perforators for reconstruction of upper limb. *J Plast Reconstr Aesthet Surg*, 2008.
92. Kroll, S. S., Rosenfield, L. Perforator-based flaps for low posterior midline defects. *Plast Reconstr Surg* 81: 561-566, 1988.
93. Angrigiani, C., Grilli, D., Siebert, J. Latissimus dorsi musculocutaneous flap without muscle. *Plast Reconstr Surg* 96: 1608-1614, 1995.
94. Wei, F. C., Jain, V., Suominen, S., et al. Confusion among perforator flaps: what is a true perforator flap? *Plast Reconstr Surg* 107: 874-876, 2001.
95. Hallock, G. G. Direct and indirect perforator flaps: the history and the controversy. *Plast Reconstr Surg* 111: 855-865; quiz 866, 2003.
96. Wei, F. C., Celik, N. Perforator flap entity. *Clin Plast Surg* 30: 325-329, 2003.
97. Blondeel, P. N., Morris, S. F., Hallock, G. G., et al. (Eds.). *Perforator Flaps: Anatomy, Technique and Clinical Applications*. St. Loius: Quality Medical Publishing, Inc., 2006.
98. Blondeel, P. N., Beyens, G., Verhaeghe, R., et al. Doppler flowmetry in the planning of perforator flaps. *Br J Plast Surg* 51: 202-209, 1998.

99. Khan, U. D., Miller, J. G. Reliability of handheld Doppler in planning local perforator-based flaps for extremities. *Aesthetic Plast Surg* 31: 521-525, 2007.
100. Yu, P., Youssef, A. Efficacy of the handheld Doppler in preoperative identification of the cutaneous perforators in the anterolateral thigh flap. *Plast Reconstr Surg* 118: 928-933; discussion 934-925, 2006.
101. Mosahebi, A., Disa, J. J., Pusic, A. L., et al. The use of the extended anterolateral thigh flap for reconstruction of massive oncologic defects. *Plast Reconstr Surg* 122: 492-496, 2008.
102. Saint-Cyr, M., Schaverien, M., Wong, C., et al. The extended anterolateral thigh flap: anatomical basis and clinical experience. *Plast Reconstr Surg* 123: 1245-1255, 2009.

Acknowledgements

Many thanks to Alexandra B. Hernandez for the medical illustrations featured in these studies.

Three- and Four-Dimensional Arterial and Venous Perforasomes of the Internal Mammary Artery Perforator Flap

Corrine Wong, M.R.C.S.
Michel Saint-Cyr, M.D.
Yvonne Rasko, M.D.
Ali Mojallal, M.D.
Steven Bailey, M.D.
Simon Myers, Ph.D., F.R.C.S.
Rod J. Rohrich, M.D.

Dallas, Texas; and London, United Kingdom

Background: The internal mammary artery perforator flap has been used in head and neck reconstruction. Although anatomical and perfusion studies with ink have been performed previously, the authors now use three- and four-dimensional computed tomographic angiography to precisely visualize vascular anatomy of individual perforators (perforasomes) and the axiality of perfusion.
Methods: Eleven hemichest adipocutaneous flaps were dissected from cadavers. Measurements were recorded, such as the distance of each internal mammary artery perforator from the sternal edge, diameter of vessels, and number and location of internal mammary artery perforators per hemichest. Single internal mammary artery perforator injections with Isovue contrast were carried out, and the flaps were subjected to dynamic computed tomographic scanning. Static computed tomographic scanning was also undertaken using a barium-gelatin mixture. Images were viewed using both General Electric and TeraRecon systems, allowing the appreciation of vascular territory (three-dimensional), and analysis of perfusion flow (four-dimensional).
Results: Each hemichest flap had one to three internal mammary artery perforators, most commonly in intercostal spaces 1, 2, and 3. Twenty-six internal mammary artery perforators were dissected, and 19 perforator arteries and six perforator veins were injected with contrast. The internal mammary artery perforator in the second intercostal space had the largest mean diameter and a large vascular territory. Linking vessels, both direct and indirect, communicate between perforators and can enlarge perforasomes. Linking vessels were also found between internal mammary artery perforators and the lateral thoracic artery.
Conclusions: Three- and four-dimensional computed tomographic angiography allows detailed analysis of vascular anatomy. Important information such as internal mammary artery perforator flap dimensions, linking vessels, and axiality of perfusion is elucidated, thus contributing to a better understanding of perforator flaps. (*Plast. Reconstr. Surg.* 124: 1759, 2009.)

Although free tissue transfer methods have been added to techniques available for head and neck reconstruction, local or regional flaps are still widely used, as there is good tissue match in terms of color, texture, and thick-

From the Department of Plastic Surgery, University of Texas Southwestern Medical Center, and Queen Mary University of London.
Received for publication February 9, 2009; accepted June 16, 2009.
Presented at the Annual Scientific Meeting of the American Society for Reconstructive Microsurgery, in Maui, Hawaii, January 10 through 13, 2009.

DOI: 10.1097/PRS.0b013e3181bf815f

Disclosure: *The authors have no financial interest in this research project or in any of the techniques or equipment used in this study.*

Supplemental digital content is available for this article. Direct URL citations appear in the printed text; simply type the URL address into any Web browser to access this content. Clickable links to the material are provided in the HTML text of this article on the *Journal*'s Web site (www.PRSJournal.com).

ness. Such options include the deltopectoral, pectoralis major, trapezius, and latissimus dorsi flaps. The deltopectoral flap was once the workhorse for head and neck reconstruction,[1,2] although its use was limited by a high rate of flap necrosis,[3,4] the need for skin grafting of the donor site, and the dog-ear created by its pedicle. The pectoralis major flap tends to be bulky and can result in a poor cosmetic outcome for both donor and recipient sites.

Since the description of the perforator flap concept by Koshima, new types of perforator flaps have been described for neck reconstruction, including the supraclavicular flap[5,6] and the internal mammary artery perforator flap. The internal mammary artery perforator flap has been reported in the reconstruction of the tracheostoma[7] and anterior neck.[8,9] It replaces the deltopectoral flap in its indications and avoids the disadvantages of this flap.

Previous anatomical studies of the internal mammary artery perforators have reported the number, location, and sizes of the internal mammary artery perforators.[8,10–12] Ink injection studies have been carried out either on the internal mammary artery[11] or on the perforators themselves.[8] This reflects the cutaneous territory of the perforators but is not able to demonstrate the charac-

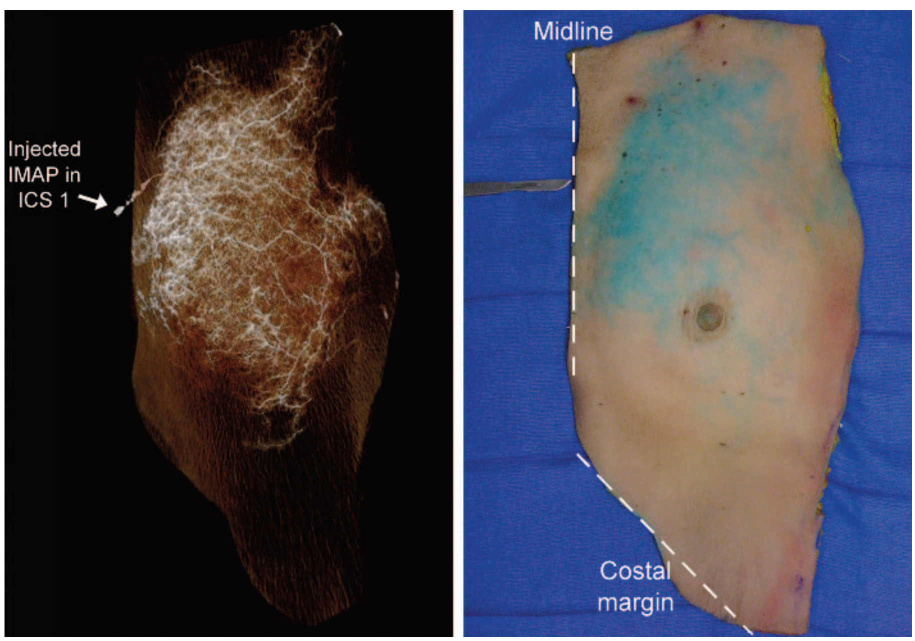

Fig. 1. An adipocutaneous flap of the chest is delineated by the inferior border of the clavicle, the midline of the chest, the costal margin, and the midaxillary line. Both images show the same flap, where the internal mammary artery perforator (*IMAP*) in intercostal space (*ICS*) 1 is injected with contrast in a three-dimensional computed tomographic scan (*left*) and methylene blue dye in the photograph (*right*). The scalpel shows the level of the internal mammary artery perforator injected.

Table 1. Internal Mammary Artery Perforators Identified: Recorded Intercostal Space and Distance from the Sternal Edge

	Cadaver											
	1		2		3		4		5		6	
	L	R	L	R	L	R	L	R	L	R	L	R
ICS (mm from the sternal edge)	1 (7)*	1 (0)	1 (10) 2 (0) 3 (37)	2 (0)* 3 (26)* 4 (0)	2 (5)* 6 (25) 7 (0)	2 (10)* 6 (0)*	N/A	1 (15)* 3 (55)* 5 (12)	2 (9.3)* 3 (0)*	1 (0) 3 (32)	1 (6.7)* 2 (5.2)* 3 (0)	1 (0)* 2 (0)* 3 (0)

L, left (hemichest); R, right (hemichest); ICS, intercostal space.
*Communicates with the lateral thoracic artery.

Table 2. Characteristics of Internal Mammary Artery Perforators and Their Vascular Territories According to Location

	Intercostal Space				
Characteristic	1	2	3	6	7
No. of perforators injected	6	6	5	1	1
Mean horizontal length of vascular territory (mm)	183	198	164	229*	163
Mean vertical length of vascular territory (mm)	221	271	219	288*	172
Mean diameter of perforator (mm)	1.5	1.83	1.47	1.3	0.8
Mean distance from the sternal edge (mm)	5.5	4.2	21	0	0

*The lateral thoracic artery forms a "bridge" between the territory of the perforators, thus enlarging the vascular territory of the internal mammary artery perforator in intercostal space 6.

Table 3. Vascular Territories of Internal Mammary Artery Perforators According to Their Intercostal Level

Extent	No.	Level of Clavicle	Level of Xiphisternum	NAC	Lateral Mammary Fold	Lateral Thoracic Communication*
ICS 1	6	6/6	2/6	5/6	6/6	3/6
ICS 2	6	4/6	4/6	6/6	6/6	5/6
ICS 3	5	2/5	3/5	5/5	4/5	3/5
ICS 6	1	0/1	1/1	1/1	1/1	1/1
ICS 7	1	0/1	1/1	1/1	0/1	0/1

NAC, nipple-areola complex; ICS, intercostal space.
*Communicates with the lateral thoracic artery.

teristics of the vessels within the tissue or the communication either between adjacent perforators or between an internal mammary artery perforator and another artery such as the lateral thoracic artery.

Although Yu et al.[7] and Vesely et al.[8] speculated that there existed communications between the perforators in differing intercostal spaces, this had never been proven previously. In this study, we used three- and four-dimensional computed tomographic angiography methods to precisely visualize the arterial and venous vascular anatomy of each perforator and the axiality of their perfusion.

MATERIALS AND METHODS

Eleven hemichest adipocutaneous flaps were harvested from fresh adult cadavers acquired through the Willed Body Program at the University of Texas Southwestern Medical Center. One cadaver was male, and the rest were female. The margins of the adipocutaneous flap were the inferior border of the clavicle, the midline of the chest, the costal margin, and the midaxillary line (Fig. 1). Specimen dissection was performed under loupe magnification on a plane superficial to the thin pectoral fascia. We recorded the distance of each internal mammary artery perforator from the sternal edge and the number of perforators per hemichest, and measured their external diameters. The perforator arteries/veins were cannulated individually with a 24-gauge catheter. Injection of a dilute methylene blue solution through the investigated perforator artery or vein

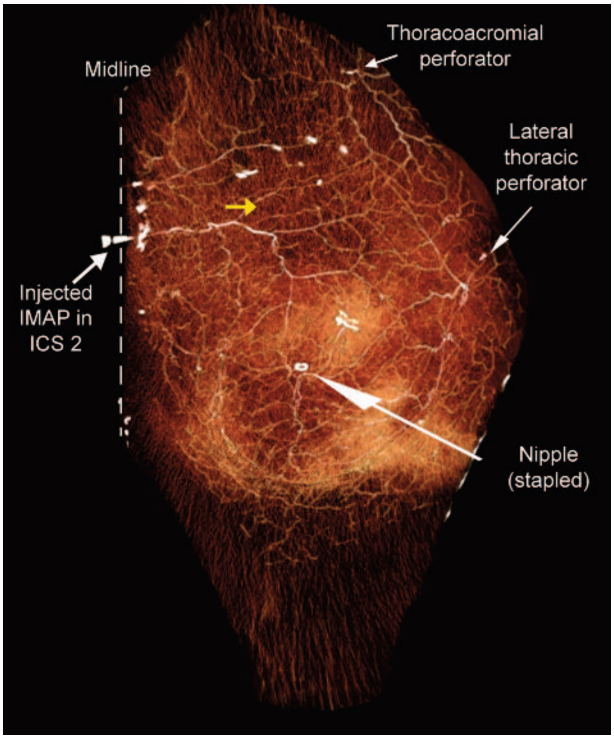

Fig. 2. Three-dimensional computed tomographic scan of a flap where the internal mammary artery perforator (*IMAP*) in intercostal space (*ICS*) 2 was injected with contrast. The vascular territory is found to encompass the nipple (stapled) and extends to the levels of the xiphisternum, clavicle, and lateral mammary fold. Linking vessels are shown to communicate with perforators of the thoracoacromial and lateral thoracic artery. The *yellow arrow* shows the direction of flow.

enabled all vascular leaks to be sealed, through either bipolar diathermy or suture ligation.

Dynamic (Four-Dimensional) Computed Tomographic Scanning

Dynamic or four-dimensional computed tomographic scanning refers to sequential images produced by repeated scanning as contrast flows through the flap. This results in a video of simulated flap perfusion. Single internal mammary artery perforator artery or vein injections were carried out with Isovue contrast (Bracco Diagnostics, Princeton, N.J.) using a Harvard precision pump (PHD 2000; Harvard Apparatus, Inc., Holliston, Mass.) running at 0.5 ml/minute and the flap was subjected to dynamic computed tomographic scanning using a GE Lightspeed 16-slice scanner (General Electric, Milwaukee, Wis.) set to perform 0.625-mm slices using a 0.5-second rotation time. Each scan was set to 80 kVp and the current ran at 300 mA. Scans were repeated at 0.125-ml increments (every 15 seconds) for the first 1 ml and then at 0.5-ml increments (every 60 seconds) for the next 2 to 3 ml, thus giving us progressive computed tomographic images over time.

Flaps were washed out with normal saline in between scans for different perforators in the same flap. This was to remove any residual Isovue contrast before injection of a different vessel.

Static (Three-Dimensional) Computed Tomographic Scanning

The barium-gelatin mixture was prepared by warming 100 ml of normal saline to 40°C and adding 3 g of gelatin while stirring continuously. This was followed by slowly adding in 40 g of barium sulfate.[13] This solution was then injected into the investigated perforator artery/vein using the Harvard precision pump running at 1 ml/minute until the vascular tree was saturated (previously repaired leaks would start to leak and had to be recauterized). The flaps were then frozen for at least 24 hours before computed tomographic scanning. Static computed tomographic scanning was performed with barium-gelatin solution for

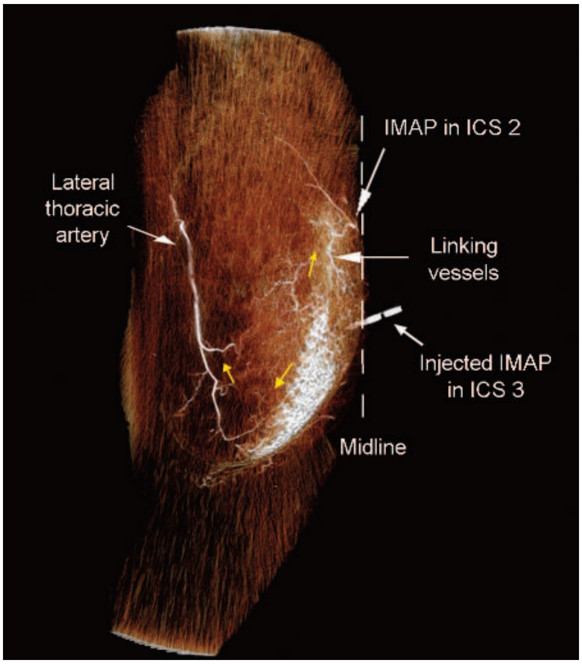

Fig. 3. Three-dimensional computed tomographic scan of a flap where the internal mammary artery perforator (*IMAP*) in intercostal space (*ICS*) 3 was injected with contrast. Linking vessels are found between adjacent internal mammary artery perforators, located proximal to the pedicle of the flap. The *yellow arrows* show the direction of flow.

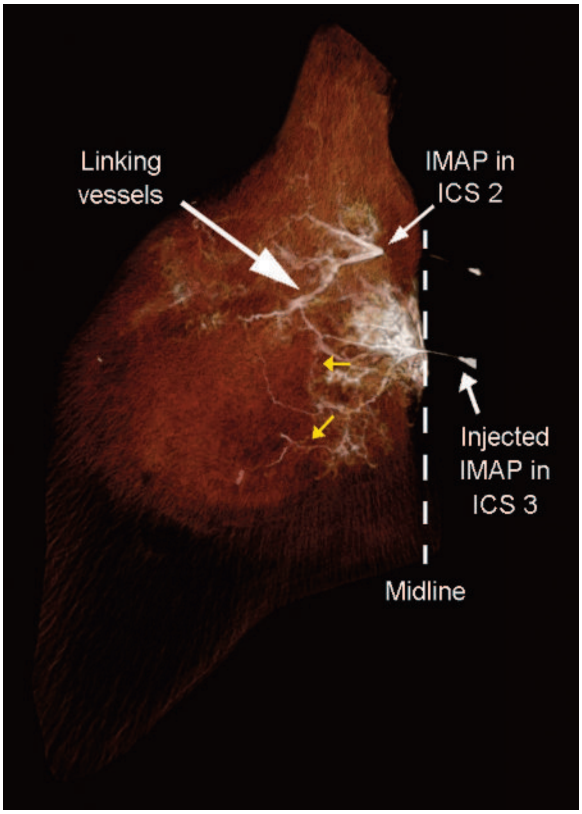

Fig. 4. Three-dimensional computed tomographic scan of a flap where the internal mammary artery perforator (*IMAP*) in intercostal space (*ICS*) 3 was injected with contrast. Linking vessels are found between adjacent internal mammary artery perforators, located distal to the pedicle of the flap. The *yellow arrows* show the direction of flow.

the last injection for all the flaps, as this could not be washed out but gave the best quality images.

Three- and four-dimensional images were viewed using the TeraRecon Aquarius workstation version 3.2.2.1 (TeraRecon, Inc., San Mateo, Calif.). The volume-rendering function allowed us to produce clear and accurate images of the simulated flaps.

RESULTS

Eleven hemichest flaps were raised from six fresh cadavers. One hemichest was unused for this study, as there was an implanted cardiac device placed in the subcutaneous tissue close to the midline in the second and third rib area. We were unable to elevate the pectoral fascia whole with the flaps, as the thin fascia was found to be quite adherent to the underlying muscle. As such, all our flaps were dissected in a suprafascial plane.

Each hemichest flap had one to three internal mammary artery perforators, most commonly in intercostal spaces 1, 2, and 3. We found that the number of perforators but not necessarily their locations tended to be symmetrical (e.g., in cadaver 2 there were three perforators on both sides, but on the left side, the perforators were in intercostal spaces 1, 2, and 3, whereas on the right side, the perforators were located in intercostal spaces 2, 3, and 4). A total of 26 internal mammary artery perforators were dissected, and 19 of the perforator arteries and six perforator veins were injected with contrast for analysis of vascular territory (Table 1).

The mean perforator diameter for internal mammary artery perforators was 1.50 mm (range, 1.0 to 2.2 mm) in intercostal space 1, 1.83 mm (range, 1.3 to 2.4 mm) in intercostal space 2, and 1.47 mm (range, 1.3 to 1.7 mm) in intercostal space 3. The mean horizontal and vertical dimensions of the vascular territory are listed in Table 2.

Perforator Arteries (Arterial Perforasomes)

Injection of single internal mammary perforators demonstrated large vascular territories (Table 3). Internal mammary artery perforators in intercostal space 1 perfused to the level of the clavicle and lateral mammary fold in all cases and to the level of the xiphisternum one-third of the time. Internal mammary artery perforators in intercostal space 2 had a territory reaching the clavicle and xiphisternum in four of six cases and the lateral mammary fold in all cases (Fig. 2). Internal mammary artery perforators in intercostal space 3 reached the clavicle in only 40 percent, the xiphi-

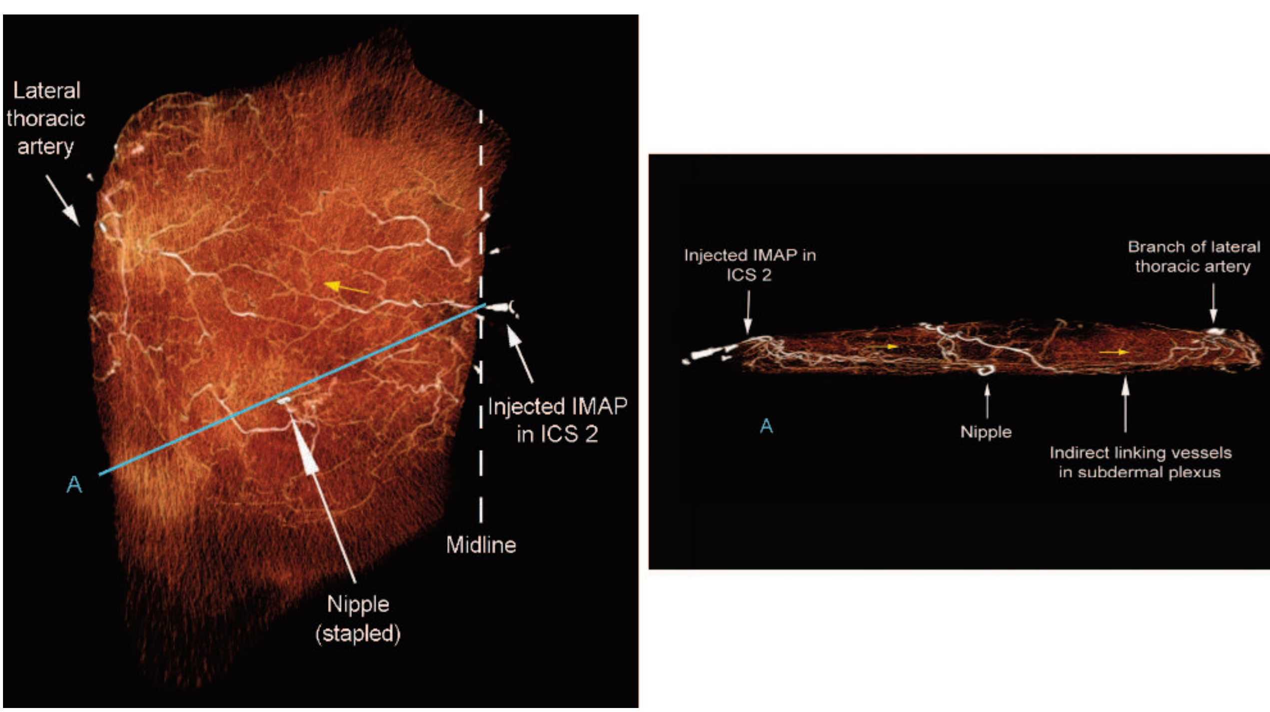

Fig. 5. Three-dimensional computed tomographic scan of a flap where the internal mammary artery perforator (*IMAP*) in intercostal space (*ICS*) 2 was injected with contrast. (*Left*) Anteroposterior view of flap. (*Right*) Oblique-transverse view of flap, corresponding to line A. Indirect linking vessels between the internal mammary artery perforator and the lateral thoracic artery are found at the subdermal level. The *yellow arrows* show the direction of flow.

sternum in 60 percent, and the lateral mammary fold in 80 percent of cases. The internal mammary artery perforator in intercostal space 6 was found to perfuse a large territory, as the lateral thoracic artery acted as a "bridge" between its territory and that of the internal mammary artery perforator in intercostal space 2, thus giving it an even larger territory than any other internal mammary artery perforator (Fig. 8 and Table 2). It did not reach the level of the clavicle but did extend to the level of the xiphisternum and the lateral mammary fold. The internal mammary artery perforator in intercostal space 7 had a territory reaching the xiphisternum but not to the lateral mammary fold or clavicle.

In our series, almost all of the internal mammary artery perforators injected (18 of 19) perfused the nipple-areola complex, including those in intercostal spaces 6 and 7. The one internal mammary artery perforator that did not perfuse the nipple-areola complex originated from intercostal space 1.

Linking Vessels

The phenomenon of linking vessels between adjacent internal mammary artery perforator(s) and linking vessels between the internal mammary artery perforator(s) and the lateral thoracic artery could explain why a single perforator can vascularize an adipocutaneous flap that is extensive in both its superoinferior and mediolateral dimensions. The linking vessels between adjacent internal mammary artery perforators can be proximal (Fig. 3) or distal (Fig. 4) to the pedicle of the flap. We have also found linking vessels between internal mammary artery perforators and branches of the lateral thoracic artery (Figs. 3, 7, and 8). These communicating vessels were located at the subdermal level (indirect linking vessels) (Fig. 5), or midway between the dermis and the pectoral fascia (Fig. 6) (direct linking vessels).

Relationship with the Lateral Thoracic Artery

Internal mammary artery perforators were found to communicate with the lateral thoracic artery in 12 of our flaps. Linking vessels between the internal mammary artery perforators and the lateral thoracic artery are located at and around the nipple-areola complex (Fig. 7). These were also found to be at two levels, the subdermal level (Fig. 5) and midway between the dermis and the

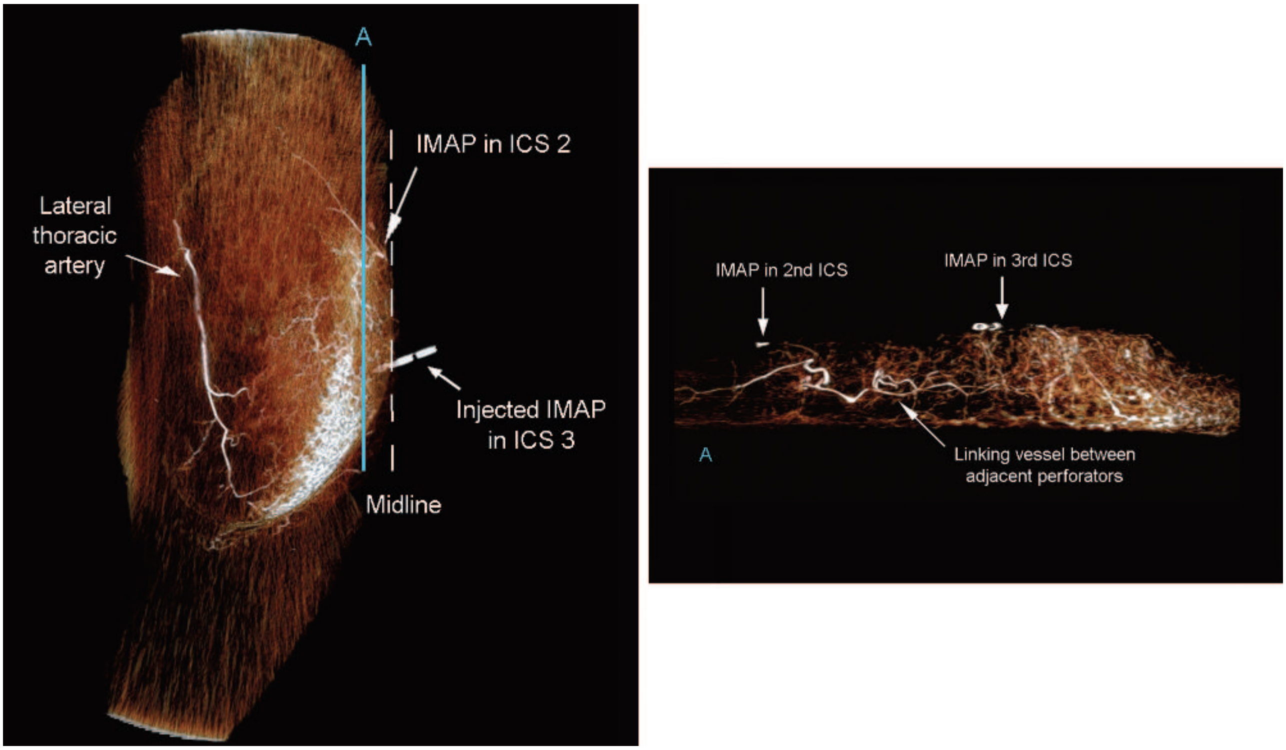

Fig. 6. Three-dimensional computed tomographic scan of a flap where the internal mammary artery perforator (*IMAP*) in intercostal space (*ICS*) 3 was injected with contrast. (*Left*) Anteroposterior view of flap. (*Right*) Sagittal view of flap, corresponding to line A. Direct linking vessels between adjacent perforators (internal mammary artery perforators in intercostal spaces 2 and 3) are located midway between the dermis and the pectoral fascia.

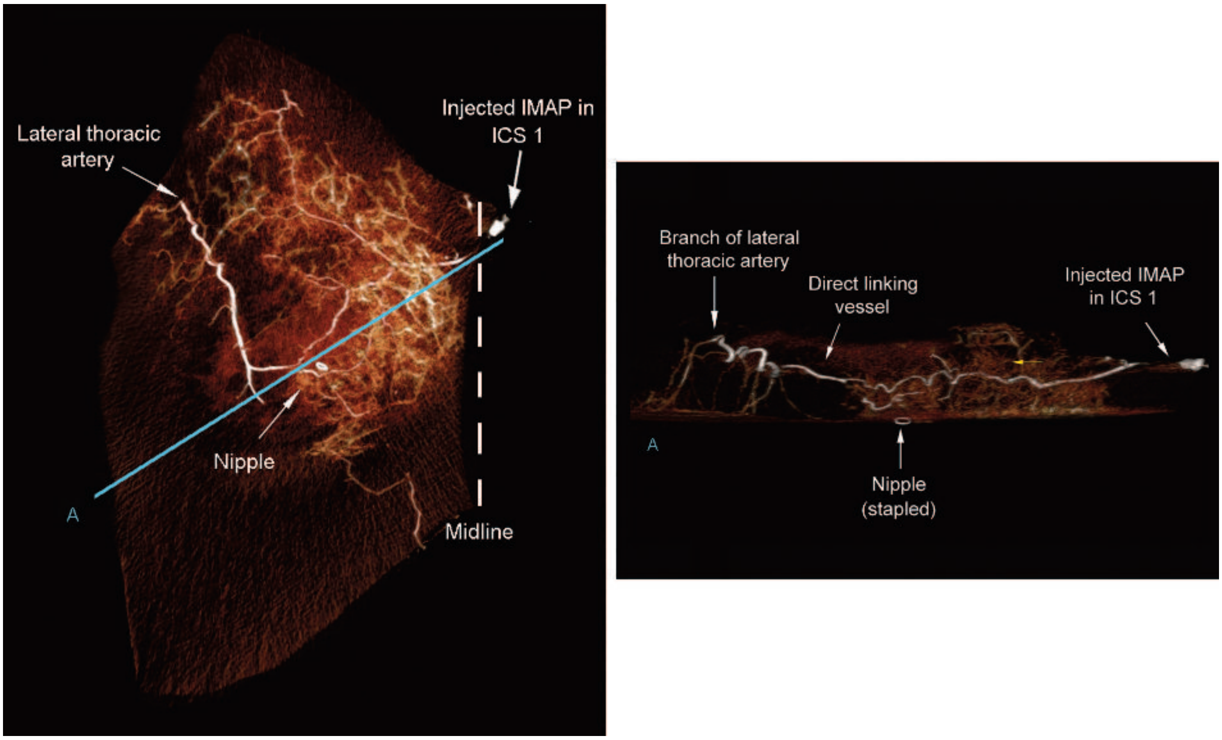

Fig. 7. Three-dimensional computed tomographic scan of a flap where the internal mammary artery perforator (*IMAP*) in intercostal space (*ICS*) 1 was injected with contrast. (*Left*) Anteroposterior view of flap. Linking vessels between the internal mammary artery perforators and the lateral thoracic artery are located around the nipple (stapled). (*Right*) Oblique-transverse view of flap, corresponding to line A. Direct linking vessels between the internal mammary artery perforator and the lateral thoracic artery are found midway between the dermis and the pectoral fascia. The *yellow arrow* shows direction of flow.

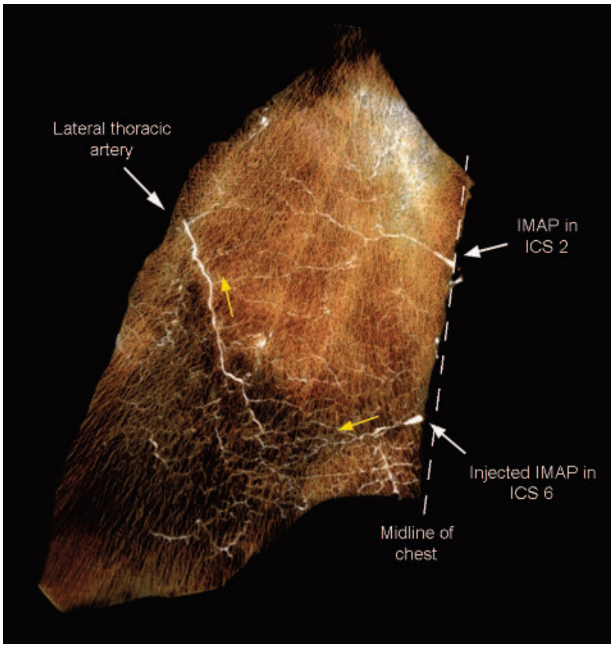

Fig. 8. Three-dimensional computed tomographic scan of a flap where the internal mammary artery perforator (*IMAP*) in intercostal space (*ICS*) 6 was injected with contrast. The lateral thoracic artery was found to "bridge" the vascular territories of the internal mammary artery perforators in intercostal spaces 6 and 2, thus further enlarging both perforasomes.

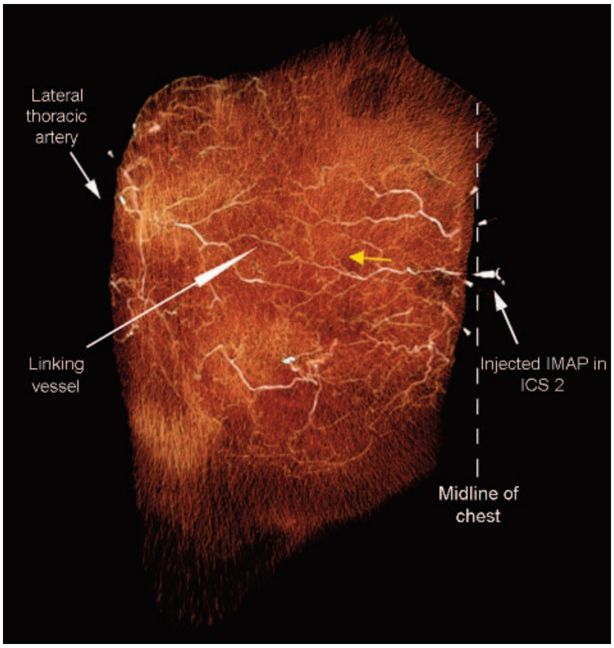

Fig. 9. Three-dimensional computed tomographic scan of a flap where the internal mammary artery perforator (*IMAP*) (artery) in intercostal space (*ICS*) 2 was injected with contrast. The *yellow arrow* shows the direction of flow.

pectoral fascia (Fig. 7). In a few cases, the lateral thoracic artery was found to bridge the vascular territories of the internal mammary artery perforators (Fig. 8), thus enlarging the vascular territory of each internal mammary artery perforator even more.

Perforator Veins (Venous Perforasomes)

Six perforator veins in our series were injected. When a perforator vein was injected, the vascular territory it encompassed was similar to that of its accompanying perforator artery but can be larger than the artery's territory (Figs. 9 and 10). Also, the perforator veins were found to communicate with the lateral thoracic vein in all six cases. The venous system was found to be mostly at the subdermal level (Fig. 10).

Axiality of Flow

When the superior internal mammary artery perforators were injected (intercostal spaces 1 and 2), the linking vessels were found to be orientated in a transverse fashion (Fig. 9). However, when the inferior internal mammary artery perforators (intercostal spaces 3 to 7) were injected, the orientation of the linking vessels took a more inferolateral orientation (Fig. 8). From the four-dimensional computed tomographic angiography scan obtained, we elucidated that the axiality of blood flow of the internal mammary artery perforator flap was lateral if an internal mammary artery perforator in intercostal space 1 or 2 was used and inferolateral if an internal mammary artery perforator in intercostal space 3 and below was used. (See **Video, Supplemental Digital Content 1,** which displays how the injection of an internal mammary artery perforator in intercostal space 2 shows flow traveling in a transverse direction, ***http://links.lww.com/PRS/A108***. **Video, Supplemental Digital Content 2,** displays how the injection of an internal mammary artery perforator in intercostal space 3 shows flow traveling in an inferolateral direction, ***http://links.lww.com/PRS/A109***.)

DISCUSSION

Three- and four dimensional computed tomographic angiography is a technology recently applied to the study of flap microvascularity.[14–17] This enables clear visualization of the entire vascular tree in a three-dimensional manner (e.g., the lateral view demonstrates branching patterns of ves-

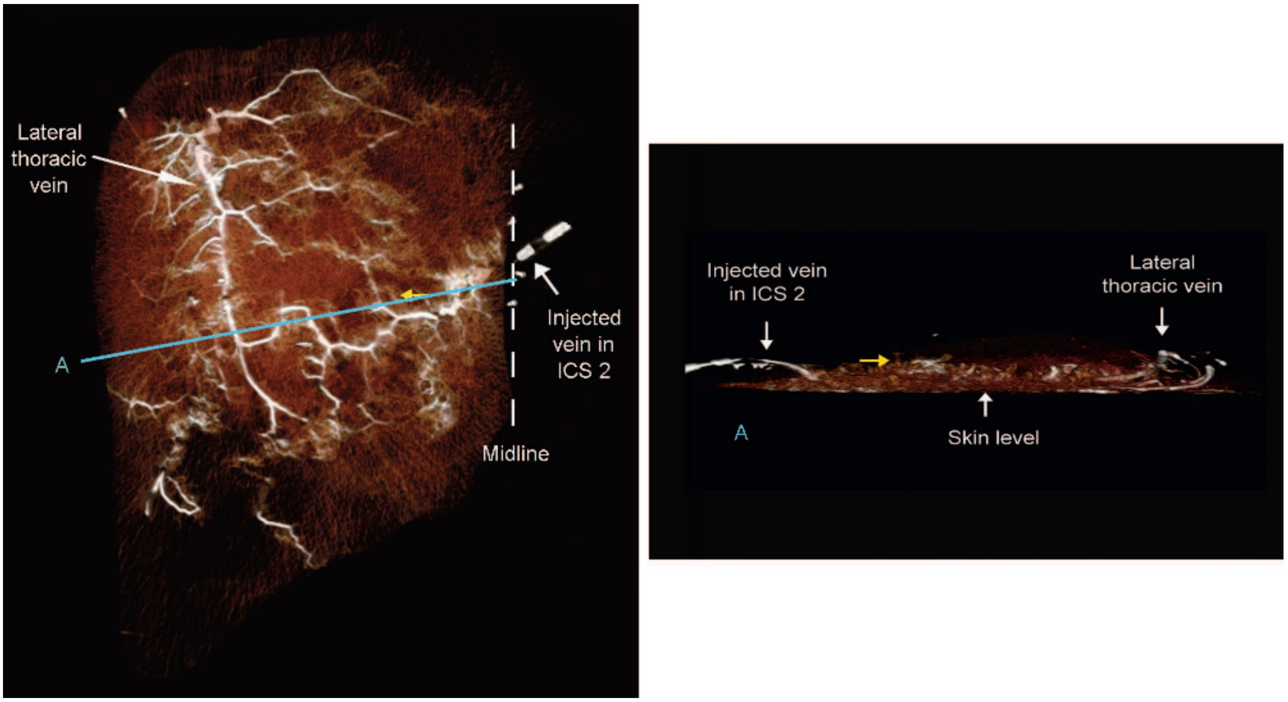

Fig. 10. Three-dimensional computed tomographic scan of the same flap where the corresponding vein in intercostal space (*ICS*) 2 was injected with contrast. (*Left*) Anteroposterior view of the flap. The venous vascular territory was found to be similar to that of the accompanying perforator artery but may be larger than the artery's territory. Communication with the lateral thoracic vein was found in all six cases. (*Right*) Transverse view of the flap, corresponding to line A. The venous system is found to be mostly at the subdermal level. The *yellow arrow* shows the direction of flow.

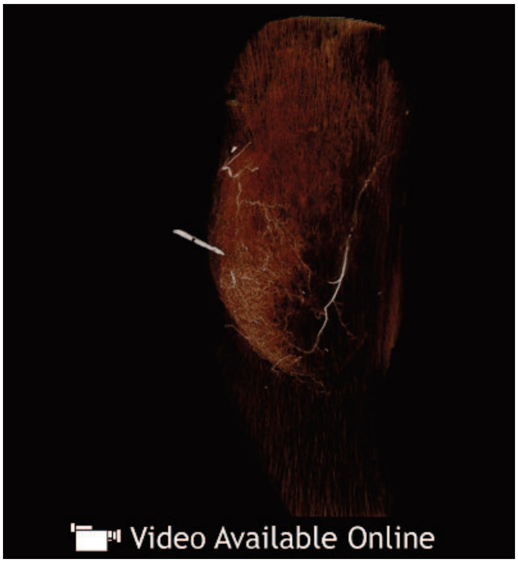

Videos. Video 1, Supplemental Digital Content 1, displays how the injection of an internal mammary artery perforator in intercostal space 2 shows flow traveling in a transverse direction, ***http://links.lww.com/PRS/A108***. Video 2, Supplemental Digital Content 2, displays how the injection of an internal mammary artery perforator in intercostal space 3 shows flow traveling in an inferolateral direction, ***http://links.lww.com/PRS/A109***.

sels) (Figs. 5 through 7 and 10). This allows us to analyze the direct relationship of these vessels with respect to different levels of the skin, specifically, the dermis. The four-dimensional aspect demonstrates the dynamic study of flow in the vascular territory. This shows us which part of the flap is perfused first and which part of the skin receives the greatest blood flow.

The internal mammary artery perforator flap has demonstrated reliability, versatility, freedom of arc of rotation (Fig. 11), neck coverage with skin of similar texture and pigmentation with sensory innervation, and a primary closure of the donor site.[7–9] Strategies to increase its arc of rotation have included division of the fibers of the pectoralis major cephalad to the pedicle[7] and excision of a portion of the costal cartilage of the second rib.[8] Bilateral internal mammary artery perforator flaps can be used to reconstruct a large central defect of the neck,[8] and preexpansion can also be used to maximize internal mammary artery perforator flap size and coverage surface.[18]

This study focuses on the arterial and venous vascular territories of single perforators (which we have termed arterial and venous perforasomes) coming off the internal mammary artery, which

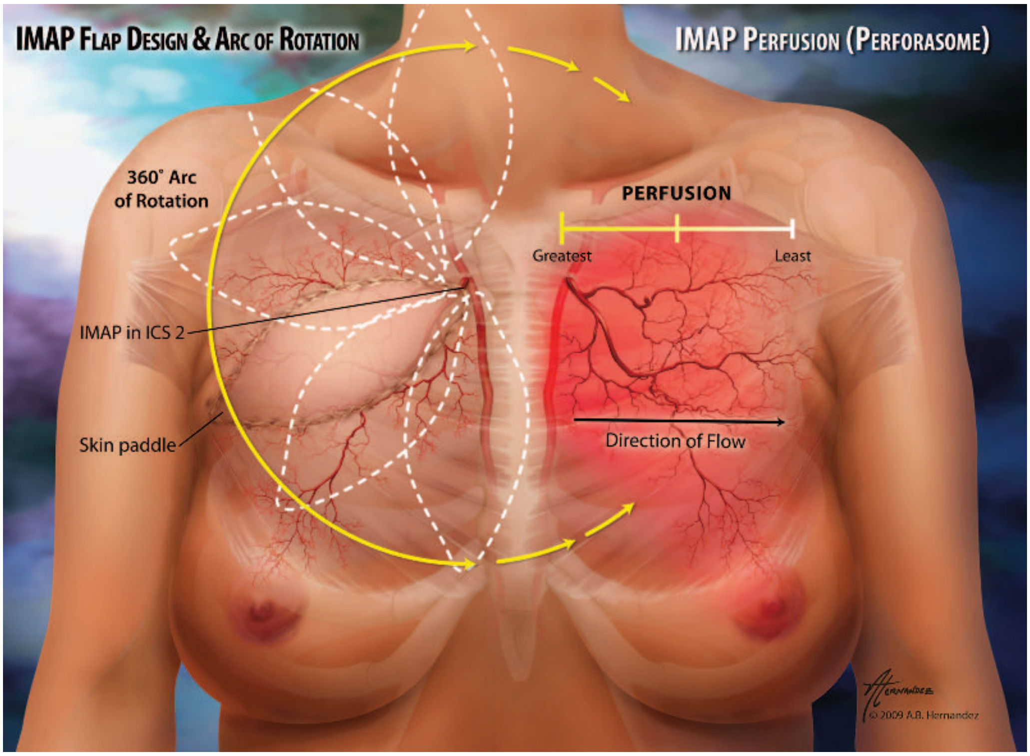

Fig. 11. (*Left*) Arc of rotation of an internal mammary artery perforator (*IMAP*) flap–based perforator in intercostal space (*ICS*) 2. (*Right*) The perforasome of the internal mammary artery perforator is in intercostal space 2.

constitutes the medial vascular supply of the anterior chest/breast (Fig. 12). Marcus[18] and Palmer and Taylor[11] found that the internal mammary artery was dominant over the lateral thoracic artery with regard to vascularity of the breast in 68 to 74 percent of their cases. The largest and most frequently found internal mammary artery perforator has been reported to be in the second or third intercostal space.[11,12]

The phenomenon of linking vessels between adjacent perforators/arteries is an important finding. This explains how perfusion extends to the vascular territory of nearby perforators, and how perfusion is maintained all the way to the distal periphery of the flap. In effect, one perforator can increase its own vascular territory by "sharing" the territory of another perforator, and vice versa, if the flap were to be based on the other perforator. This also demonstrates collateral flow in the pectoral region and thus the ability to minimize devastating effects of ischemic insult.

The lateral thoracic artery was prominent in many of our flaps. Linking vessels between the lateral thoracic artery and the internal mammary artery perforators allows it to serve as a bridge in the lateral thoracic area.

The level at which these linking vessels were found (subdermal and between the dermis and fascia) indicates that an internal mammary artery perforator flap can be raised on a level superficial to the pectoral fascia safely. As the venous system was also found to be at a superficial level, problems with flap congestion will likely be minimized if elevation of the flap occurs at this recommended level. Thinning of the flap should not go beyond halfway through the thickness of the flap. Based on the axiality of perfusion of the internal mammary artery per-

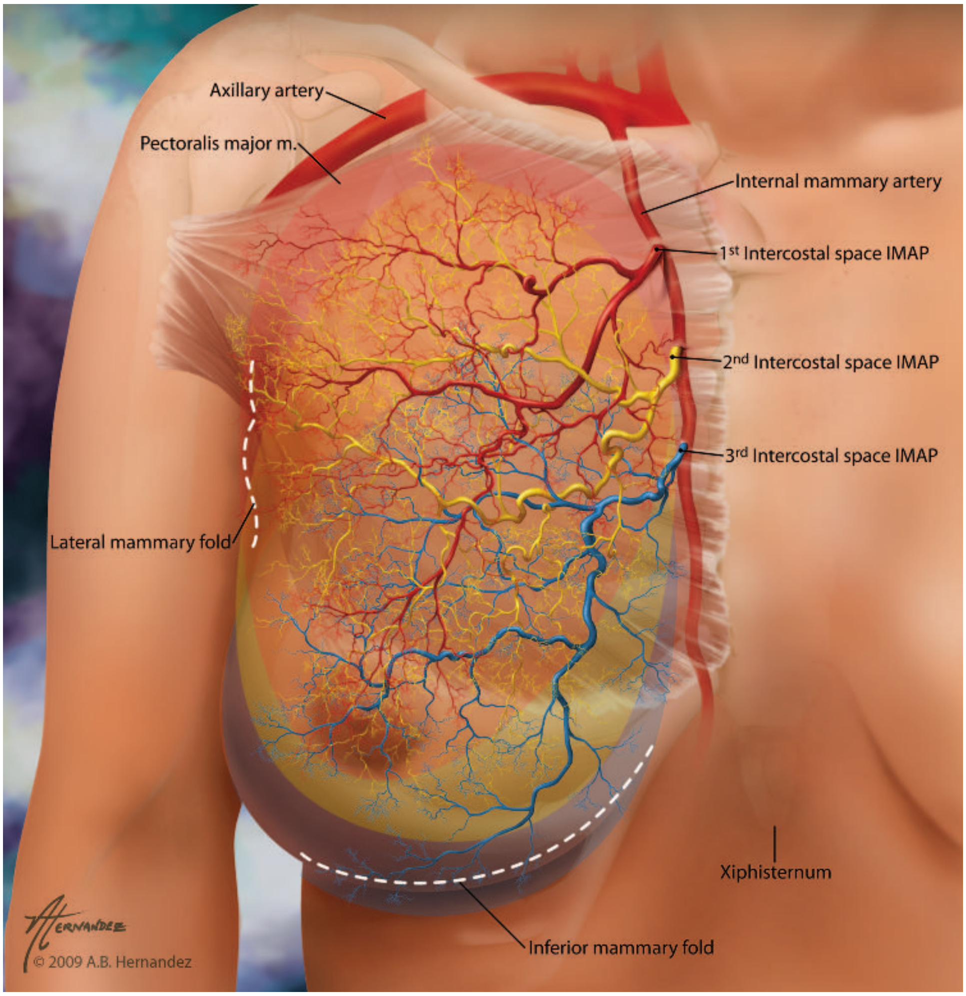

Fig. 12. Vascular territories/perforasomes of the internal mammary artery perforators in the first, second, and third intercostal spaces. *IMAP*, internal mammary artery perforator.

forators, the orientation of the flap should preferentially be transverse if based on internal mammary artery perforators in intercostal spaces 1 and 2, and lateral or inferolateral if based on intercostal space 3 and below.

CONCLUSIONS

With three- and four-dimensional computed tomographic angiographic techniques, we have elucidated the arterial and venous perforasomes of the internal mammary artery perforators with respect to their intercostal spaces, the level of their linking vessels, and the relationship between the internal mammary artery perforator and the lateral thoracic artery. We have demonstrated the dimensions of the internal mammary artery perforator flap and recommended the safe level of flap dissection/thinning and orientation of skin paddle. This contributes to our knowledge of the internal mammary artery perforator flap, which remains an important option in reconstruction of the head and neck region.

Michel Saint-Cyr, M.D.
Department of Plastic Surgery
University of Texas Southwestern Medical Center
1801 Inwood Road
Dallas, Texas 75390-9132
michel.saint-cyr@utsouthwestern.edu

REFERENCES

1. Bakamjian VY. A two-stage method for pharyngoesophageal reconstruction with a primary pectoral skin flap. *Plast Reconstr Surg.* 1965;36:173–184.
2. Krizek TJ, Robson MC. The deltopectoral flap for reconstruction of irradiated cancer of the head and neck. *Surg Gynecol Obstet.* 1972;135:787–789.
3. Bakamjian VY, Long M, Rigg B. Experience with the medially based deltopectoral flap in reconstructive surgery of the head and neck. *Br J Plast Surg.* 1971;24:174–183.
4. Gilas T, Sako K, Razack MS, Bakamjian VY, Shedd DP, Calamel PM. Major head and neck reconstruction using the deltopectoral flap: A 20 year experience. *Am J Surg.* 1986;152:430–434.
5. Pallua N, Machens HG, Rennekampff O, Becker M, Berger A. The fasciocutaneous supraclavicular artery island flap for releasing postburn mentosternal contractures. *Plast Reconstr Surg.* 1997;99:1878–1884; discussion 1885–1876.
6. Pallua N, Magnus Noah E. The tunneled supraclavicular island flap: An optimized technique for head and neck reconstruction. *Plast Reconstr Surg.* 2000;105:842–851; discussion 852–844.
7. Yu P, Roblin P, Chevray P. Internal mammary artery perforator (IMAP) flap for tracheostoma reconstruction. *Head Neck* 2006;28:723–729.
8. Vesely MJ, Murray DJ, Novak CB, Gullane PJ, Neligan PC. The internal mammary artery perforator flap: An anatomical study and a case report. *Ann Plast Surg.* 2007;58:156–161.
9. Neligan PC, Gullane PJ, Vesely M, Murray D. The internal mammary artery perforator flap: New variation on an old theme. *Plast Reconstr Surg.* 2007;119:891–893.
10. Munhoz AM, Ishida LH, Montag E, et al. Perforator flap breast reconstruction using internal mammary perforator branches as a recipient site: An anatomical and clinical analysis. *Plast Reconstr Surg.* 2004;114:62–68.
11. Palmer JH, Taylor GI. The vascular territories of the anterior chest wall. *Br J Plast Surg.* 1986;39:287–299.
12. Rosson GD, Holton LH, Silverman RP, Singh NK, Nahabedian NY. Internal mammary perforators: A cadaver study. *J Reconstr Microsurg.* 2005;21:239–242.
13. Tan BK, Ng RT, Tay NS, Tan BS. Tissue microangiography using a simplified barium sulphate cadaver injection technique. *Ann Acad Med Singapore* 1999;28:152–154.
14. Saint-Cyr M, Schaverien M, Arbique G, Hatef D, Brown SA, Rohrich RJ. Three- and four-dimensional computed tomographic angiography and venography for the investigation of the vascular anatomy and perfusion of perforator flaps. *Plast Reconstr Surg.* 2008;121:772–780.
15. Schaverien M, Saint-Cyr M, Arbique G, Brown SA, Rohrich RJ. Three- and four-dimensional arterial and venous anatomies of the thoracodorsal artery perforator flap. *Plast Reconstr Surg.* 2008;121:1578–1587.
16. Schaverien M, Saint-Cyr M, Arbique G, Hatef D, Brown SA, Rohrich RJ. Three- and four-dimensional computed tomographic angiography and venography of the anterolateral thigh perforator flap. *Plast Reconstr Surg.* 2008;121:1685–1696.
17. Saint-Cyr M, Schaverien M, Rohrich RJ. Preexpanded second intercostal space internal mammary artery pedicle perforator flap: Case report and anatomical study. *Plast Reconstr Surg.* 2009;123:1659–1664.
18. Marcus GH. Untersuchungen uber die arterielle Blutversorgung der Mamilla. *Arch Klin Chir.* 1934;179:361–369.

Three- and Four-Dimensional Computed Tomography Angiographic Studies of Commonly Used Abdominal Flaps in Breast Reconstruction

Corrine Wong, M.R.C.S.
Michel Saint-Cyr, M.D.
Gary Arbique, Ph.D.
Stephen Becker, M.D.
Spencer Brown, Ph.D.
Simon Myers, Ph.D., F.R.C.S. (Plast.)
Rod J. Rohrich, M.D.

Dallas, Texas

Background: The innovative technique of three- and four-dimensional computed tomographic angiography allows us to analyze the areas of perfusion in commonly used free abdominal flaps in breast reconstruction, such as pedicled transverse rectus abdominis musculocutaneous (TRAM) flaps, full TRAMs, muscle-sparing TRAMs, and deep inferior epigastric perforator (DIEP) flaps. The authors compared the vascular territories in these flaps.
Methods: A total of 11 lower abdominal flaps were obtained from nine cadavers and two abdominoplasty procedures. The authors simulated the perfusion of seven pedicled TRAMs, eight full TRAMs, eight muscle-sparing TRAMs, 14 DIEPs, and six superficial inferior epigastric artery flaps. For each simulated flap, the named artery/perforator was injected with Omnipaque contrast using a Harvard precision pump at 0.5 ml/minute, and the flap was subjected to dynamic computed tomographic scanning using a GE Lightspeed 16-slice scanner. Scans were repeated at 0.125-ml increments (every 15 seconds) for the first 1 ml, then at 0.5-ml increments (every 60 seconds) for the next 2 to 3 ml, thus giving progressive computed tomographic images over time. Images were viewed using both General Electrics and TeraRecon systems, allowing analysis of branching patterns and perfusion flow as well as measurements of vascular territory.
Conclusions: This study shows that there are definitive differences in vascular territory based on flap type. The sequences of images also allow us to reappraise the classic Hartrampf zones of perfusion. (*Plast. Reconstr. Surg.* 124: 18, 2009.)

Utilization of abdominal tissue for autologous breast reconstruction has been long and widely practiced. It is an ideal source, as most patients who develop breast cancer are at an age when they also have excessive abdominal fat and skin. Autologous breast reconstruction has many advantages over implant reconstruction, including reduced risks of infection, capsular contracture, and a more natural and aesthetically pleasing breast.

Holstrom first described the free transverse rectus abdominis myocutaneous (TRAM) flap in 1979 for breast reconstruction.[1] In 1982, Hartrampf et al. popularized the pedicled TRAM flap, based on the superior epigastric artery.[2] This, however, has been shown to be the secondary blood supply to the tissue of the anterior abdominal

From the Department of Plastic Surgery, University of Texas Southwestern Medical Center.
Received for publication April 16, 2008; accepted September 12, 2008.
Presented at the 2008 Summer Scientific Meeting of the British Association of Plastic, Reconstructive, and Aesthetic Surgeons, in Liverpool, England, June of 2008.

DOI: 10.1097/PRS.0b013e3181aa0db8

Disclosure: *None of the authors has any financial relationships, interests, or commercial associations to disclose in relation to the content of this article.*

Supplemental digital content is available for this article. Direct URL citations appear in the printed text; simply type the URL address into any web browser to access this content. Clickable links to the material are provided in the HTML text of this article on the *Journal*'s Web site (www.PRSJournal.com).

wall.[2–7] Currently, the inferior rather than the superior epigastric pedicle plays the dominant role in abdominal tissue transfer in autologous breast reconstruction.

From the free TRAM flap, attempts to minimize donor-site morbidity (e.g., abdominal bulge, herniae) led to the development of muscle-sparing TRAM flap and deep inferior epigastric perforator (DIEP) flaps. Koshima and Soeda described the inferior epigastric artery skin flap for reconstruction of the floor of the mouth and groin defects,[8] but it was Allen and Treece who first used the DIEP flap for breast reconstruction,[9] which has now become common practice in some plastic surgery centers.

The perfusion of the transverse abdominal flap was studied by Scheflan and Dinner,[10,11] but became better known after Hartrampf et al. published their work on the TRAM flap.[2] The Hartrampf zones of perfusion (I to IV) are familiar to most plastic surgeons (Fig. 1). The classic Hartrampf zones II and III, however, were demonstrated by Holm et al. to be reversed[12] using fluorescent perfusion techniques (Fig. 2). This gave significant weight to the suggestion that blood flow from the pedicle travels to the ipsilateral side before crossing the midline.

In this study, we compared the vascular territories of the pedicled TRAM, full-width TRAM, muscle-sparing TRAM, DIEP (medial or lateral row perforator), and superficial inferior epigastric artery (SIEA) flaps utilizing three- and four-dimensional computed tomographic angiography. The sequential images also allow us to reappraise the four zones of vascularity.

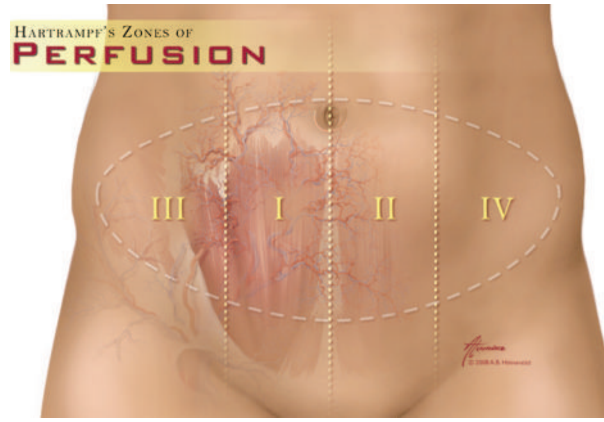

Fig. 1. Hartrampf's zones of perfusion.

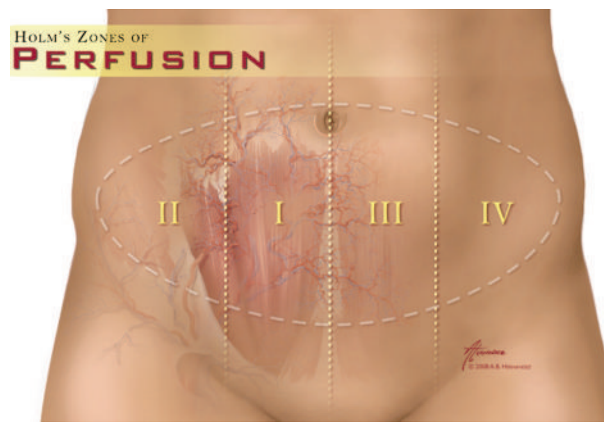

Fig. 2. Holm's zones of perfusion.

MATERIALS AND METHODS

Nine transverse abdominal flaps were harvested from fresh adult cadavers acquired through the Willed Body Program at the University of Texas Southwestern Medical Center, and two specimens were harvested from abdominoplasty procedures after informed consent.

The margins of all the skin paddles were the anterior superior iliac spines, the suprapubic crease, and 2 cm superior to the umbilicus. Four cadaveric abdominal flaps were studied with respect to two pedicled TRAMs, two full-width TRAMs, two muscle-sparing TRAMs, and two DIEP flaps each. One of these also had a SIEA flap studied. Five other cadaver flaps were used to study SIEA flaps. The abdominoplasty specimens were cannulated and irrigated with heparinized saline before the perfusion studies. With these tissues, six single-perforator DIEP flaps were simulated as the three medial row perforators and three lateral row perforators were cannulated. In total, 43 flap perfusions were simulated with computed tomographic angiography.

Specimen dissection was performed under loupe magnification. Each cadaveric flap was accompanied by full-width and full-length bilateral rectus muscle. Injection of a dilute methylene blue solution through the artery according to the type of flap studied enabled all vascular leaks to be sealed, either through bipolar diathermy or by suture ligation.

First, while studying the perfusion of the pedicled TRAM, the superior epigastric artery was cannulated and injected with contrast medium and subjected to dynamic computed tomographic scanning. The process was repeated with cannulation of the deep inferior epigastric artery for a full-width TRAM. For a muscle-sparing TRAM, either the lateral or medial row perforators were perfused. The simulation of a DIEP flap was performed by injecting a single perforator (either lateral or medial dominant row perforator). For a

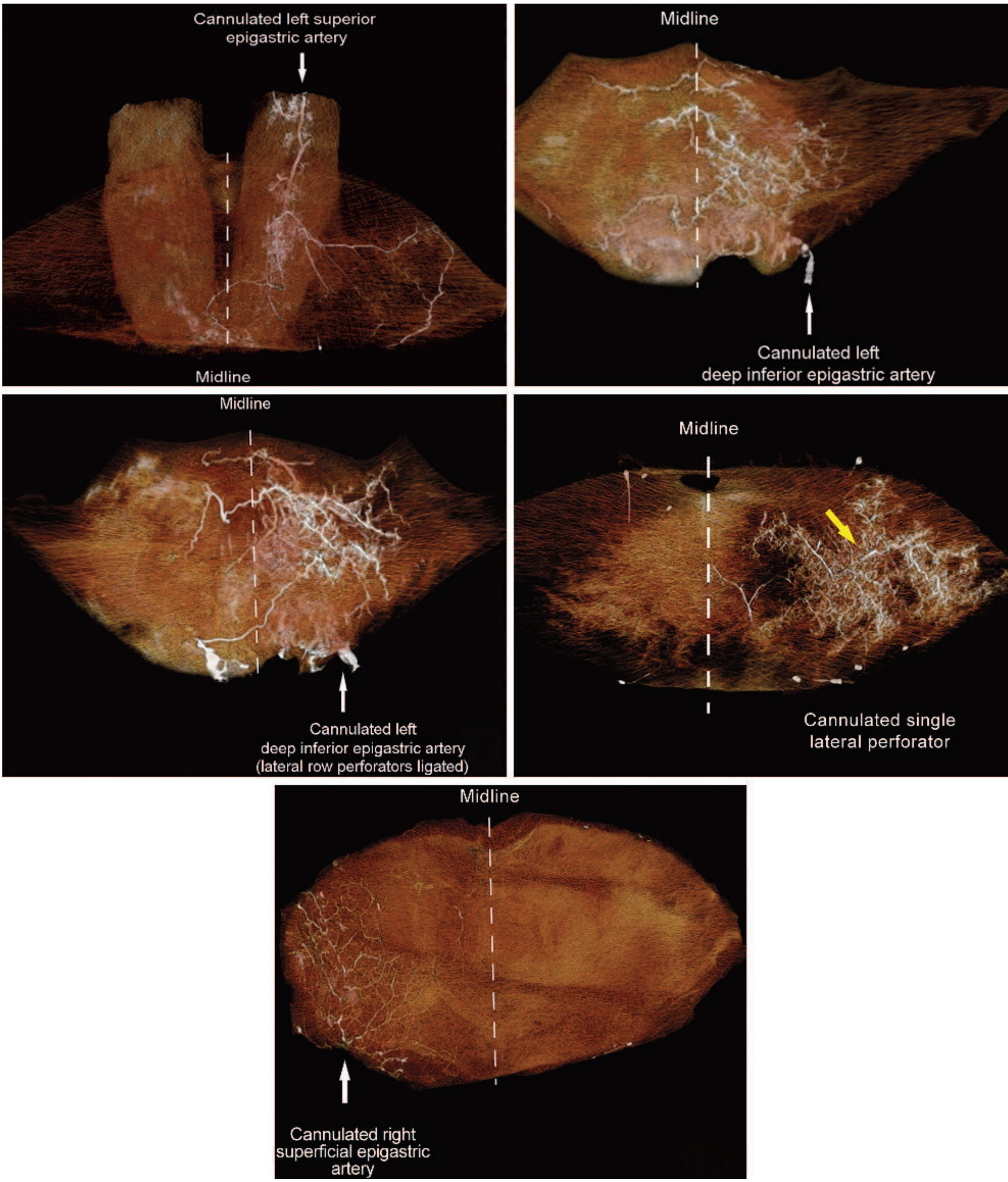

Fig. 3. (*Above, left*) Pedicled TRAM flap. Left superior epigastric artery injected with contrast. (*Above, right*) Full-width TRAM flap. Left deep inferior epigastric artery injected with contrast. (*Center, left*) Muscle-sparing TRAM flap (medial row perforators perfused). Left deep inferior epigastric artery injected with contrast after ligation of the lateral row perforators. (*Center, right*) DIEP flap (medial perforator– based). Single medial row perforator injected with contrast. (*Below*) SIEA flap. Right superficial inferior epigastric artery injected with contrast.

SIEA flap, the superficial epigastric artery was injected.

In between the sets of perfusion studies, the flap was irrigated with saline to remove remnant contrast medium. Previous experimental studies have shown that multiple washouts did not affect the diameter or vascular territories of the vessels within the flap.[13,14]

Dynamic Computed Tomographic Imaging

Iodinated contrast medium (Omnipaque; iohexol; 300 mg/ml; Amersham, Princeton, N.J.) was heated to 37°C to reduce the viscosity and improve vascular filling and placed in a syringe loaded into a Harvard precision infusion pump (PHD 2000; Harvard Apparatus, Inc., Holliston, Mass.). Adequate filling of the vascular territory was achieved with 3 to 4 ml of contrast at a rate of injection of 0.5 ml/minute to gain a detailed appreciation of the development of the microvascularity over time. Helical scans were performed using a GE Lightspeed 16-slice scanner (General Electric, Milwaukee, Wis.) set to perform 0.625-mm slices using a 0.5-second rotation time. Each scan was set to 80 kVp and current ran at 300 mA. Scans were repeated at 0.125-ml fill increments (every 15 seconds) for the first 1 ml of the contrast injection to reveal the pattern of early filling and then at 0.5-ml fill increments (every 60 seconds) for the last 3 ml.

Three- and four-dimensional images were viewed using the TeraRecon Aquarius workstation (version 3.2.2.1; TeraRecon Inc., San Mateo, Calif.). The volume rendering function allowed us to produce clear and accurate images of the simulated pedicled TRAM (Fig. 3, *above, left*), full-width TRAM (Fig. 3, *above, right*), muscle-sparing TRAM (Fig. 3, *center, left*), DIEP (Fig. 3, *center, right*), and SIEA (Fig. 3, *below*) flaps. Areas of the skin paddles and vascular territories of the flaps were measured using the General Electrics Medical Systems Advantage workstation (Aw 4.1_06.3).

RESULTS

Three-Dimensional Computed Tomographic Angiography

The perfusion of a total of 43 flaps was simulated. The area of the vascular territory of each individual flap in square millimeters and as a percentage of the corresponding skin paddle is tabulated in Table 1. The mean areas of the different types of flaps are summarized in Table 2.

The pedicled TRAM flap is found to have the smallest vascular territory, with a mean area of 32.6 ± 13.1 percent of the skin paddle perfused.

Table 1. Vascular Territory According to Flap Type

	Specimen 1*	Specimen 2*	Specimen 3*	Specimen 4*	Specimen 5*	Specimen 6*	Specimen 7*	Specimen 8*	Specimen 9*	Specimen 10 (Left)†	Specimen 10 (Right)†	Specimen 11†
Areas of skin paddle (mm^2)	34591.4	69071.1	43766.1	34632.1	62578.8	43689.6	46352.5	50969.4	68457.2	44877.5		64408.8
Pedicled TRAM (mm^2)/% of skin paddle	6904.1/20.0	17753.4/25.7	23087.1/52.8	10486.6/30.3	n/a	n/a	n/a	n/a	n/a	n/a	n/a	n/a
	n/a	22133.3/32.0	20929.8/47.8	6733.3/19.4	n/a	n/a	n/a	n/a	n/a	n/a	n/a	n/a
Full width TRAM (mm^2)/% of skin paddle	12448.5/36.0	23863.3/34.5	27324.8/62.4	18672.0/53.9	n/a	n/a	n/a	n/a	n/a	n/a	n/a	n/a
	14448.5/41.8	24763.4/35.9	25629.8/58.6	22088.7/63.8	n/a	n/a	n/a	n/a	n/a	n/a	n/a	n/a
Lateral muscle-sparing TRAM (mm^2)/% of skin paddle	11542.6/33.4	28958.6/41.9	19687.1/45.0	18174.7/52.5	n/a	n/a	n/a	n/a	n/a	n/a	n/a	n/a
Medial muscle-sparing TRAM (mm^2)/% of skin paddle	14648.4/42.3	29408.5/42.6	19388.5/44.3	18523.3/53.5	n/a	n/a	n/a	n/a	n/a	n/a	n/a	n/a
Lateral perforator DIEP (mm^2)/% of skin paddle	11377.3/32.9	25894.2/37.5	12585.6/28.8	10785.9/31.1	n/a	n/a	n/a	n/a	n/a	16069.6/35.8	14864.4/33.1	20248.3/31.4
Medial perforator DIEP (mm^2)/% of skin paddle	11619.4/33.6	23307.3/33.7	25426.5/58.0	15395.9/44.5	n/a	n/a	n/a	n/a	n/a	27311.4/60.9	17434.1/38.8	27281.4/42.4
SIEA (mm^2)/% of skin paddle	n/a	18049.1/26.1	n/a	n/a	15451.1/24.7	15997.1/36.6	18782.4/40.5	16616.9/32.6	26998.2/39.4	n/a	n/a	n/a

n/a, not applicable.
*Cadaver specimen.
†Abdominoplasty specimen.

Table 2. Summary of Vascular Territory According to Flap Type

	Pedicled TRAM	Full-Width TRAM	Muscle-Sparing TRAM (Lateral Row)	Muscle-Sparing TRAM (Medial Row)	DIEP (Lateral Perforator)	DIEP (Medial Perforator)	SIEA
No. of flaps	7	8	4	4	7	7	6
Percentage of paddle	20	36	33.4	42.3	32.9	33.6	26.1
	25.7	41.8	41.9	42.6	37.5	33.7	24.7
	32.0	34.5	52.5	53.5	31.1	44.5	36.6
	30.3	35.9	45.0	44.3	35.8	60.9	40.5
	19.4	53.9			33.1	38.8	32.6
	52.8	63.8			31.4	42.4	39.4
	47.8	62.4			28.8	58.0	
		58.6					
Average percentage of paddle (SD)	32.6 (13.1)	48.4 (12.6)	43.2 (7.9)	45.7 (5.3)	32.9 (2.9)	44.6 (11.0)	33.3 (6.7)

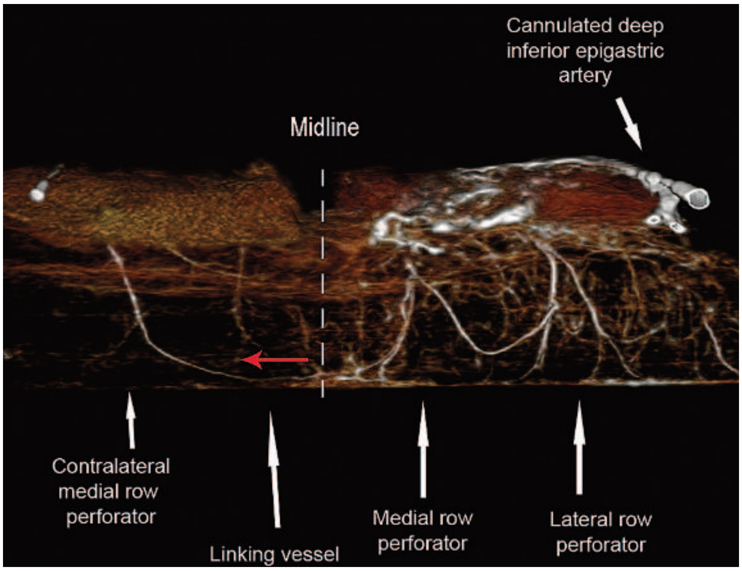

Fig. 4. Lateral view of muscle-sparing TRAM flap. Linking vessels among perforator complexes are shown, crossing the midline. Note direction of flow (*red arrow*).

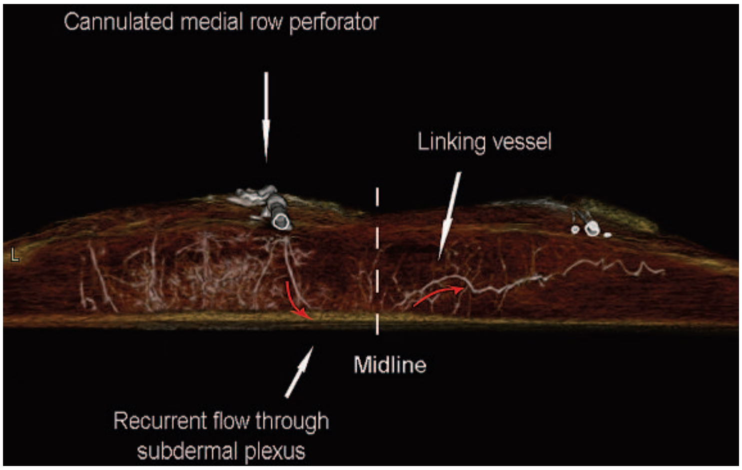

Fig. 5. Lateral view of DIEP flap. Linking vessels among perforator complexes are shown, crossing the midline. Note direction of flow (*red arrows*).

Two-sample difference of means of pedicled TRAM versus full-width TRAM gave a p value of less than 0.03.

The full-width TRAM had a mean area of 48.4 ± 12.6 percent skin paddle perfused, which is comparable to the medial row–perfused muscle-sparing TRAM, which had a mean area of 45.7 ± 5.3 percent skin paddle perfusion ($p < 0.70$). The lateral row–perfused muscle-sparing TRAM had a reduced area, with a mean of 43.2 ± 7.9 percent ($p < 0.47$ when compared with full-width TRAM).

The DIEP flap that utilizes the medial row perforator has a wider area of perfusion, with a mean area of 44.6 ± 11.0 percent ($p < 0.55$, medial DIEP versus full TRAM) compared with one that is perfused by a lateral row perforator, with a mean area of 32.9. ± 2.9 percent ($p < 0.007$ lateral DIEP versus full TRAM, $p < 0.02$ lateral DIEP versus medial DIEP).

The SIEA flap has a mean area perfused of 33.3 ± 6.7 percent, which is comparable to a lateral perforator DIEP flap ($p < 0.94$). Not only do they have vascular territory of similar size, they also have a tendency to stay in one hemi-abdomen. Vascular flow among zones of perfusion (I to IV) can be explained by the linking vessels that communicate among the perforators (Figs. 4 and 5) as well as recurrent flow via the subdermal plexus (Figs. 6 and 7).

Four-Dimensional Computed Tomographic Angiography

In full-width TRAM flaps (i.e., both medial and lateral row perforators still present), we found that

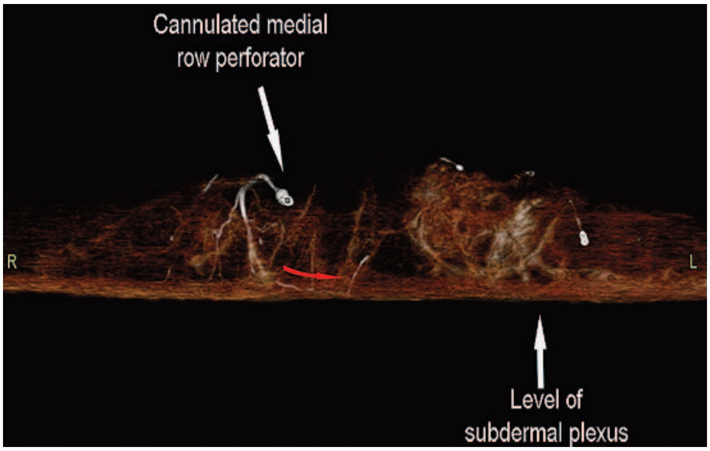

Fig. 6. Contrast (0.25 ml) injected into a perforator of a DIEP flap. Note direction of flow (*red arrow*).

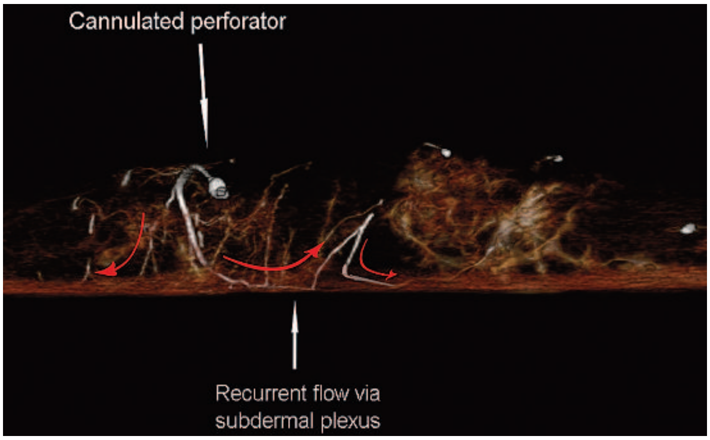

Fig. 7. Contrast (0.4 ml) injected into the same perforator of the DIEP flap. Linking vessels demonstrate recurrent flow from the subdermal plexus to the deeper tissues before flowing superficially and away from the primary perforator (*red arrows*).

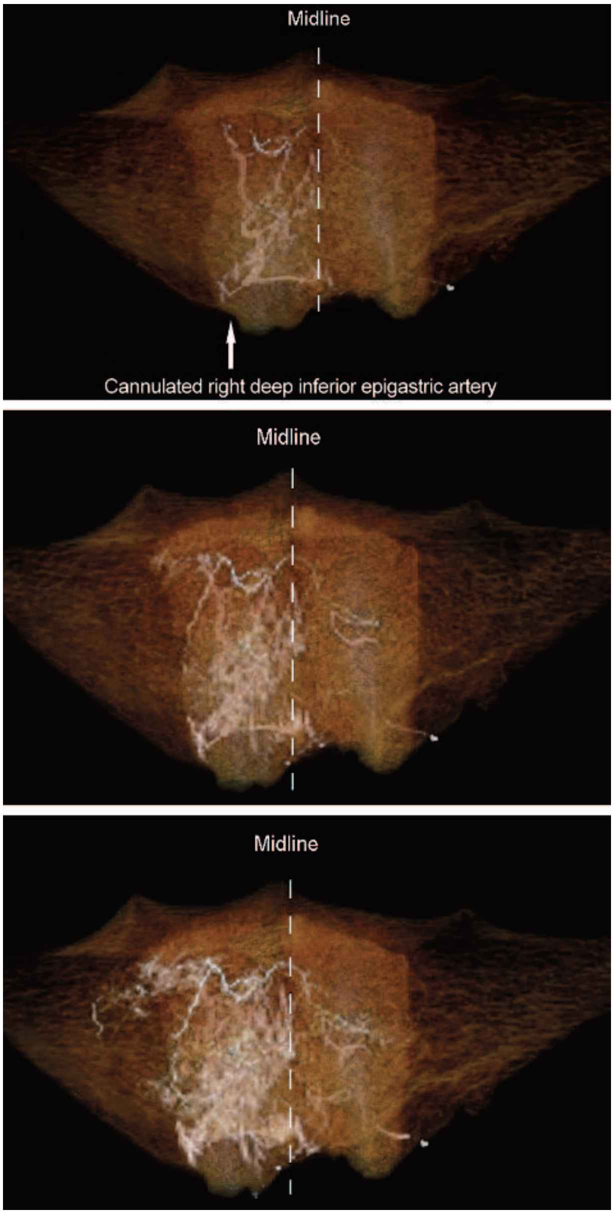

Fig. 8. Perfusion of right deep inferior epigastric artery (in full-width TRAM flap). (*Above*) At initial stage, only zone I is perfused. (*Center*) At middle stage, zones I and II are perfused, demonstrating a dominant medial row perforator. (*Below*) At late stage, zones I, II, and III are perfused.

vascular perfusion from zone I to II (contralateral medial zone) or zone III (ipsilateral lateral zone) depends on perforator dominance. If the medial row perforator is dominant, then zone I perfuses to zone II earlier and more intensely than zone III (Fig. 8) (Video 1; see **Video, Supplemental Digital Content 1,** which demonstrates perfusion of the right deep inferior epigastric artery in a full-width TRAM flap; a dominant medial row perforator is demonstrated, as perfusion extends from zone I to

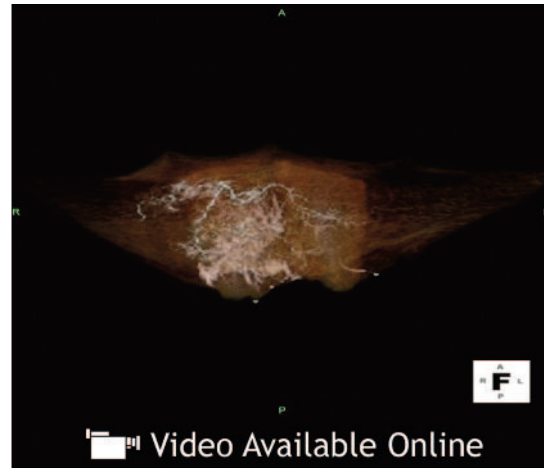

Video 1. Perfusion of right deep inferior epigastric artery (in full-width TRAM flap). At late stage, zones I, II, and III are perfused (***http://links.lww.com/A1275***).

II and then finally to zone III; ***http://links.lww.com/A1275***).

If the lateral row perforator is dominant, then zone III is perfused before and more so than zone II (Fig. 9). See **Video, Supplemental Digital Content 2,** which demonstrates perfusion of left deep inferior epigastric artery (in full-width TRAM flap). A dominant lateral row perforator is demonstrated, as perfusion extends from zone I to zone III, and then finally to zone II; ***http://links.lww.com/A1276***. Needless to say, in muscle-sparing TRAM and DIEP flaps, the perfusion depends on whether the perforators are medial or lateral row.

DISCUSSION

We have found that perfusion studies involving cadaveric tissue underestimate the extent of vascular territory in vivo. Even so, this study gives us an idea of how the lower abdominal flaps perfuse with respect to the named artery/perforator investigated.

The superior epigastric artery has been acknowledged to be the secondary blood supply to the tissue of the anterior abdominal wall.[2–7] Although no microsurgery is necessary, it has been suggested that the pedicled TRAM has a rate of partial necrosis approaching 25 percent and fat necrosis rate of up to 27 percent.[15,16] Comparatively, TRAM, muscle-sparing TRAM, and DIEP flaps that utilize the deep inferior epigastric artery have failure rates quoted to be 1 to 4 percent and fat necrosis rates of 4 to 16 percent.[17–22] This is supported by the fact that the caliber of the superior epigastric artery is considerably smaller than that of the deep inferior epigastric artery and

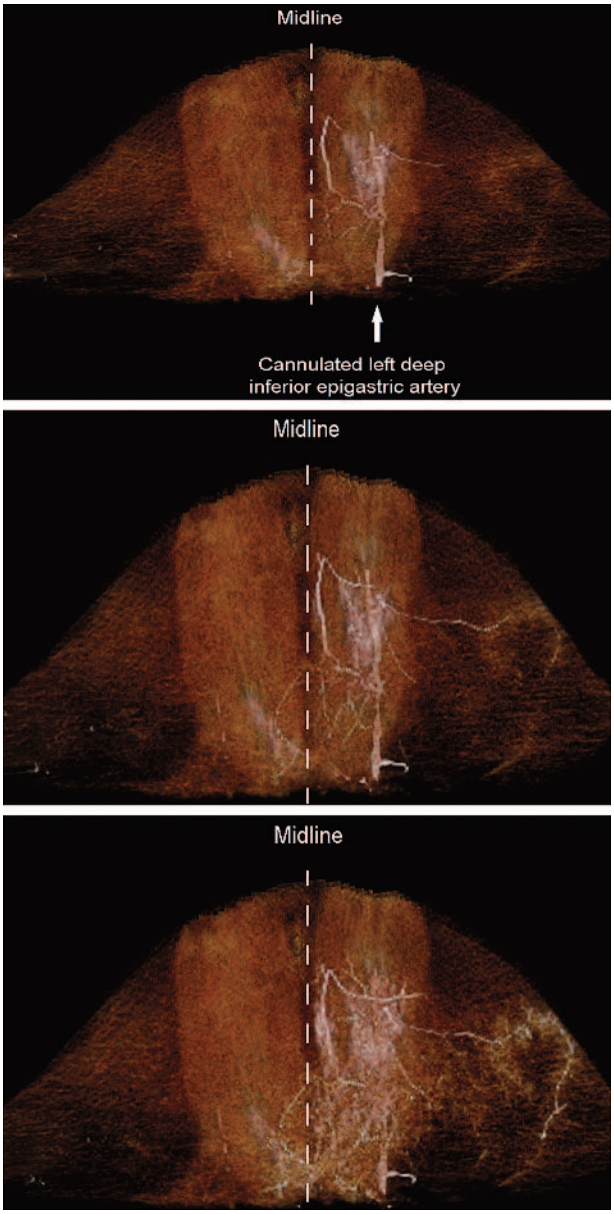

Fig. 9. Perfusion of left deep inferior epigastric artery (in full-width TRAM flap). (*Above*) At initial stage, only zone I is perfused. (*Center*) At middle stage, zones I and III are perfused, demonstrating a dominant lateral row perforator. (*Below*) At late stage, zones I, II, and III are perfused.

by our findings of the vascular territory of a pedicled TRAM being about 60 percent of the territory of a full-width TRAM flap.

The full-width TRAM flap, muscle-sparing medial row TRAM flap, muscle-sparing lateral row TRAM flap, and medial perforator–based DIEP flap were shown to have comparable areas of perfusion (48, 46, 43, and 45 percent, respectively). Therefore, we recommend the use of a muscle-sparing TRAM flap or medial perforator–based DIEP flap, as opposed to the full-width TRAM, to reduce the risk of donor-site morbidity.

The DIEP flap based on a medial perforator has a perfusion area of 44.6 percent and is reduced to 32.9 percent if based on a lateral perforator, which is a smaller area compared with both types of TRAM flaps. In his 2000 study, Kroll implied that DIEP flaps have a less robust blood supply than free TRAM flaps,[21] as he found higher rates of partial flap loss and fat necrosis in the former compared with the latter. For TRAM flaps, the partial failure rate was 2.2 percent and the fat necrosis rate was 12.9 percent. For DIEP flaps, in selected patients, the partial failure rate was 8.7 percent and the fat necrosis rate was 17.4 percent. Whether the DIEP flaps were based on lateral or medial row perforators was not specified, so the author's conclusion would concur with our results if most of the DIEP flaps were based on lateral row perforators. The DIEP flaps harvested in this study were all based on a single perforator from either the medial or lateral branch. We realize that the DIEP flap's vascular territory could be potentially increased if two or more perforators were also selected.

We found that the vascular territory of a DIEP flap based on a lateral row perforator was similar to that of the SIEA flap, in that the vascular territories tend to reside in one hemi-abdomen. Studies have been performed which advocate the use of the lateral branch of the deep inferior epigastric artery in DIEP flap harvesting. It is more frequently dominant and tends to run a more rectilinear course, allowing for easier dissection.[23,24] We recommend using the medial row perforators, however, if these are clinically dominant and if a larger flap (encroaching zones III and IV) is needed. Blondeel noted in a clinical series that all flaps with compromised vascularization of zone IV in the study were perfused by lateral row perforators and, therefore, advised that the use of medial row perforators is imperative if zone IV is required.[24] Therefore, if a large breast reconstruction is required, then we recommend harvesting a medial row–based perforator DIEP flap, or a muscle-sparing TRAM flap, to secure a larger area of perfusion across the midline. If a small volume breast is to be reconstructed, for which only a hemi-abdominal flap is required, then a lateral row perforator DIEP flap or SIEA flap can be considered when available.

Holm et al. performed perfusion studies that demonstrated that Hartrampf zones II and III should be reversed[12] (Fig. 2). They stated that Hartrampf's concept was erroneous and that "perfusion of the vascular territories across the midline was always delayed and less intensive than in the territories on the ipsilateral side." This elegant study was well carried out, but its bold statement does not always hold true. With four-dimensional computed tomographic angiography, we found that perfusion from zone I can spread either to (Hartrampf) zone II or zone III, depending on perforator dominance. In Holm et al.'s study, only two of 15 flaps utilized just the medial row perforators, and eight used only lateral row perforators (the rest had both medial and lateral row perforators). Itoh and Arai's anatomical study showed that the lateral branch of the deep inferior epigastric artery is more frequently dominant compared with the medial branch[22]; therefore, Holm et al.'s results are not surprising.

Our studies show that if the medial row perforator is dominant, zone II is perfused before zone III (Fig. 8; see **Video, Supplemental Digital Content 1, *http://links.lww.com/A1275***) and if the lateral row perforator is dominant, zone III is perfused before zone II (Fig. 9; see **Video, Supplemental Digital Content 2, *http://links.lww.com/A1276***). This demonstrates that both Hartrampf's and Holm's concepts are correct and that no rule is absolute. We acknowledge that our samples are small, and a study on a larger scale is needed to achieve better statistical significance.

Clinical Applications

Numerous authors have reported excellent clinical results with all flaps described in this vascular perfusion study. Cadaver injection perfusion studies will underestimate the true clinical flap territory; therefore, a larger area of perfusion can be expected and is commonly seen in vivo for all flaps investigated in the present study. When reconstructing a large breast that requires zones I, II, and III, consideration should be given to harvesting flaps that will provide adequate perfusion across the midline such as the full TRAM, muscle-sparing TRAM, and medial perforator–based DIEP flaps. The lateral row perforator DIEP flaps in our study crossed the midline in certain cases but were based solely on a single perforator and therefore underestimate the consistent perfusion across the midline seen in vivo. Although we have found perfusion differences in both lateral and medial perforator DIEP flaps, perforator selection of a DIEP flap should be based on the largest perforator size and dominance regardless of its lateral or medial row origin. When available, the SIEA flap results in minimal donor-site morbidity and remain an excellent choice for breast reconstructions requiring hemi-abdominal tissue only.

CONCLUSIONS

Vascular territories of commonly used abdominal flaps for breast reconstruction in increasing size are the pedicled TRAM flap, lateral row perforator DIEP flap, SIEA flap, lateral row muscle-sparing TRAM flap, medial row perforator DIEP flap, medial row muscle-sparing TRAM flap, and full-width TRAM flap (Fig. 10). The last four flaps have comparable areas of perfusion; therefore, we recommend using a muscle-sparing TRAM flap or medial perforator DIEP flap to decrease risk of

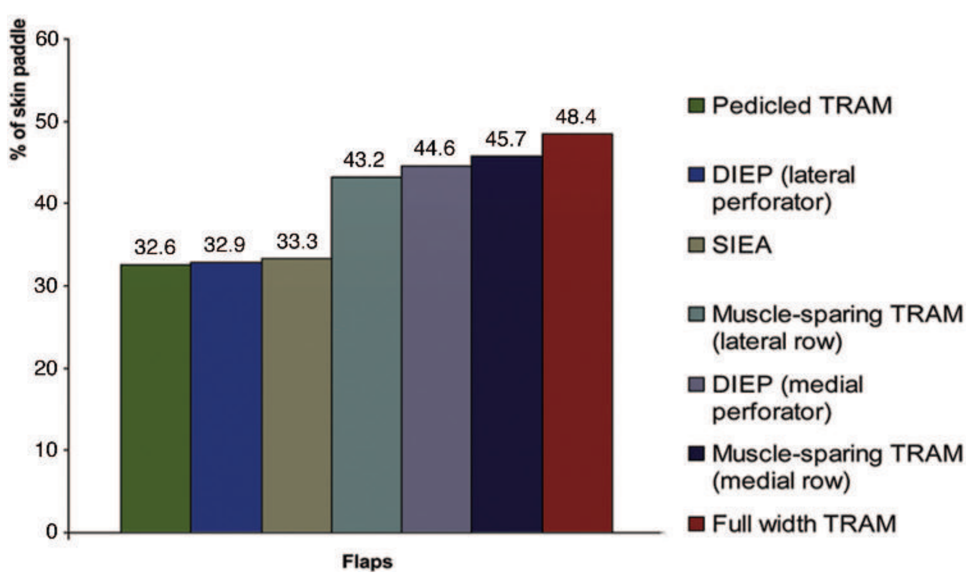

Fig. 10. Histogram of vascular territory according to flap type.

donor-site morbidity. The extension of perfusion from zone I to zone II or III will depend on perforator dominance.

Michel Saint-Cyr, M.D.
Department of Plastic Surgery
University of Texas Southwestern Medical Center
1801 Inwood Road
Dallas, Texas 75390-9132
michel.saint-cyr@utsouthwestern.edu

ACKNOWLEDGMENTS

The authors thank the University of Texas Southwestern Medical Center Willed Body Program. The authors are also very grateful for the artwork provided by Alexandra Hernandez from Gory Details Inc.

REFERENCES

1. Holstrom H. The free abdominoplasty flap and its use in breast reconstruction: An experimental study and clinical case report. *Scand J Plast Reconstr Surg.* 1979;13:423–427.
2. Hartrampf CR, Scheflan M, Black PW. Breast reconstruction with transverse abdominal island flap. *Plast Reconstr Surg.* 1982;69:216–225.
3. Boyd JB, Taylor GI, Corlett R. The vascular territories of the superior epigastric and the deep inferior epigastric systems. *Plast Reconstr Surg.* 1984;73:1.
4. Moon HK, Taylor GI. The vascular anatomy of rectus abdominis musculocutaneous flaps based on the deep superior epigastric system. *Plast Reconstr Surg.* 1988;82:815.
5. Miller LB, Bostwick J III, Hartrampf CR Jr, et al. The superiorly based rectus abdominis flap: Predicting and enhancing its blood supply based on an anatomic and clinical study. *Plast Reconstr Surg.* 1988;81:713.
6. Taylor GI, Minabe T. The angiosomes of the mammals and other vertebrates. *Plast Reconstr Surg.* 1992;89:181.
7. Watterson PA, Bostwick J III, Hester TR Jr, et al. TRAM flap anatomy correlated with a 10-year clinical experience with 556 patients. *Plast Reconstr Surg.* 1995;95:1185.
8. Koshima I, Soeda S. Inferior epigastric artery skin flap without rectus abdominis muscle. *Br J Plast Surg.* 1989;42:645.
9. Allen RJ, Treece P. Deep inferior epigastric perforator flap for breast reconstruction. *Ann Plast Surg.* 1994;32:32–38.
10. Scheflan M, Dinner MI. The transverse abdominal island flap: Part I. Indication, contraindications, results, and complications. *Ann Plast Surg.* 1983;10:24.
11. Scheflan M, Dinner MI. The transverse abdominal island flap: Part II. Surgical technique. *Ann Plast Surg.* 1983;10:120.
12. Holm C, Mayr M, Hofter E, Ninkovic M. Perfusion zones of the DIEP flap revisited: A clinical study. *Plast Reconstr Surg.* 2006;117:37–43.
13. Saint-Cyr M, Schaverien M, Arbique G, et al. Three- and four-dimensional computed tomographic angiography and venography for the investigation of the vascular anatomy and perfusion of perforator flaps. *Plast Reconstr Surg.* 2008;121:772–780.
14. Schaverien M, Saint-Cyr M, Arbique G, et al. Three- and four-dimensional computed tomographic angiography and venography of the anterolateral thigh perforator flap. *Plast Reconstr Surg.* 2008;121:1685–1696.
15. Kroll SS, Evans G, Reece R, et al. Comparison of resource costs of free and conventional TRAM flap breast reconstruction. *Plast Reconstr Surg.* 1996;98:74–77.
16. Kroll SS, Cherardini G, Martin JE, et al. Fat necrosis in free and pedicled TRAM flaps. *Plast Reconstr Surg.* 1998;102:1502.
17. Blondeel PN, Arnstein M, Verstraete K, et al. Venous congestion and blood flow in free transverse rectus abdominis myocutaneous and deep inferior epigastric perforator flaps. *Plast Reconstr Surg.* 2000;106:1295.
18. Nahabedian MY, Momen B, Galdino G, Manson PN. Breast reconstruction with the free TRAM or DIEP flap: Patient selection, choice of flap, and outcome. *Plast Reconstr Surg.* 2002;110:466.
19. Nahabedian MY, Tsangaris T, Momen B. Breast reconstruction with the DIEP flap or the muscle-sparing (MS-2) free TRAM flap: is there a difference? *Plast Reconstr Surg.* 2005;115:436–444.
20. Bajaj AK, Chevray PM, Chang DW. Comparison of donor-site complications and functional outcomes in free muscle-sparing TRAM flap and free DIEP flap breast reconstruction. *Plast Reconstr Surg.* 2006;117:737–746.
21. Kroll SS. Fat necrosis in free transverse rectus abdominis myocutaneous and deep inferior epigastric perforator flaps. *Plast Reconstr Surg.* 2000;106:576–583.
22. Itoh Y, Arai K. The deep inferior epigastric artery free skin flap: Anatomic study and clinical application. *Plast Reconstr Surg.* 1993;91:5.
23. Munhoz AM, Ishida LH, Sturtz GP, et al. Importance of lateral row perforator vessels in deep inferior epigastric perforator flap harvesting. *Plast Reconstr Surg.* 2004;113:517–524.
24. Blondeel PN. One hundred free DIEP flap breast reconstructions: A personal experience. *Br J Plast Surg.* 1999;52:104–111.

Perforasomes of the DIEP Flap: Vascular Anatomy of the Lateral versus Medial Row Perforators and Clinical Implications

Corrine Wong, M.R.C.S.
Michel Saint-Cyr, M.D.
Ali Mojallal, M.D.
Tim Schaub, M.D.
Steven H. Bailey, M.D.
Simon Myers, Ph.D., F.R.C.S.
Spencer Brown, Ph.D.
Rod J. Rohrich, M.D.

Dallas, Texas

Background: Regarding the perfusion of a deep inferior epigastric perforator (DIEP) flap, the classic Hartrampf zones II and III were demonstrated by Holm et al. to be reversed using fluorescent perfusion techniques, implying that blood flow from the pedicle travels to the ipsilateral side before crossing the midline. The authors' hypothesis is that the zones of perfusion and the vascular anatomy differ greatly between lateral row and medial row perforators.
Methods: Three-dimensional and four-dimensional computed tomographic angiography was utilized to reappraise the zones of vascularity. Thirty-six DIEP flaps were simulated for this study (14 lateral row perforators versus 22 medial row perforators). Individual perforators were injected with contrast and each flap was subjected to dynamic computed tomography scanning. Images were viewed using TeraRecon software, allowing analysis of branching patterns and perfusion flow.
Results: The mean vascular territory for a medial perforator DIEP flap injected with contrast was 296 cm^2, compared with 196 cm^2 for a lateral perforator DIEP flap. Zone II perfusion was greater in a medial perforator compared with a lateral perforator. Zone III had greater perfusion in a lateral perforator compared with a medial perforator. The authors found that medial perforators conform to the Hartrampf zones of perfusion and lateral perforators follow the Holm theory of perfusion (zones II and III should be reversed for lateral perforator DIEP flaps). Injection of a lateral row–based perforator flap gave a vascular territory that rarely crossed the midline.
Conclusion: Medial and lateral row perforators offer distinct and stereotypical zones of perfusion that have a significant effect on flap design and harvesting. (*Plast. Reconstr. Surg.* 125: 772, 2010.)

The deep inferior epigastric artery perforator (DIEP) flap has held and continues to hold an important role in free autologous tissue breast reconstruction. It provides autologous tissue for breast reconstruction without sacrificing the underlying rectus muscle, with minimal risks of bulge or hernia formation.[1,2] The literature is replete with comparison of different DIEP series comparing flap results, fat necrosis, and clinical outcomes.[2–6] One of the major problems is that not all DIEP flaps are alike, and a proper classification system based on zones of perfusion is required to make a meaningful comparison between different flaps.

The perfusion of the transverse abdominal flap was studied by Scheflan and Dinner[7,8] but became better known after Hartrampf published his work on the transverse rectus abdominis musculocutaneous (TRAM) flap.[9] Since then, other authors have given us detailed anatomical studies

From the Department of Plastic Surgery, University of Texas Southwestern Medical Center.
Received for publication July 5, 2009; accepted September 21, 2009.
Presented at the Plastic Surgery Research Council 54th Annual Meeting, in Pittsburgh, Pennsylvania, May 28 through 30, 2009, and given the Shenaq International Research Award. Presented as an Outstanding Paper at the American Society for Reconstructive Microsurgery Annual Scientific Meeting in Boca Raton, Florida, January 9 through 12, 2010.

DOI: 10.1097/PRS.0b013e3181cb63e0

Disclosure: *The authors have no financial interests in this research project or in any of the techniques or equipment used in this study.*

of the deep inferior epigastric arterial system.[10–12] In 2006, the classic Hartrampf zones II and III were demonstrated by Holm et al. to be reversed[13] using fluorescent perfusion techniques. This gave significant weight to the suggestion that blood flow from the pedicle travels to the ipsilateral side before crossing the midline.

We hypothesize that the zones of perfusion of the DIEP flap differ greatly based on whether a lateral row perforator or a medial row perforator is selected. Increased knowledge of the lateral and medial row perforator vascular anatomy may have a significant effect on flap design and in turn help decrease flap-related complications. This hypothesis will be tested using three- and four-dimensional computed tomographic angiography, which has been previously utilized in other vascular anatomical studies.[14–17]

PATIENTS AND METHODS

A total of 36 DIEP flaps were simulated for this study. These flaps were harvested from fresh cadavers from the University of Texas Willed Body Program. A total of 14 single lateral row perforators versus 22 medial row perforators were injected with contrast to determine the vascular territory in the zones of perfusion. All dissections were performed under loupe magnification, and a 23-gauge catheter was used to cannulate all selected perforators (see Fig. 4). Dilute methylene blue dye was used to inject each perforator to identify vascular leakage points, which were subsequently ligated with bipolar cautery or with silk suture. The single most dominant perforator was selected in all cases. The dominant perforator was determined to be the largest perforator in the DIEP flap by direct examination of the external diameter of perforators upon dissection of the rectus muscle. Flaps were then submitted to static and dynamic computed tomography scan imaging.

Dynamic (Four-Dimensional) Computed Tomography Scanning

Dynamic or four-dimensional computed tomography scanning refers to sequential images produced by repeated scanning as contrast flows through the flap over time. This results in a video of simulated flap perfusion. Single DIEP perforator injections were carried out with iodinated contrast medium (Isovue; Bracco Diagnostics, Princeton, N.J.) using a Harvard precision pump (PHD 2000; Harvard Apparatus, Inc., Holliston, Mass.) running at 0.5 ml/minute, and the flap was subjected to dynamic computed tomography scanning using a GE Lightspeed 16-slice scanner (General Electric, Milwaukee, Wis.) set to perform 0.625-mm slices using a 0.5-second rotation time. Each scan was set to 80 kVp, and current ran at 300 mA. Scans were repeated at 0.125-ml increments (every 15 seconds) for the first 1 ml, then at 0.5-ml increments (every 60 seconds) for the next 2 to 3 ml, thus giving us progressive computed tomography images over time. We found a total volume of 3 to 4 ml of contrast was sufficient for each flap injection.

Supplemental digital content is available for this article. Direct URL citations appear in the printed text; simply type the URL address into any Web browser to access this content. Clickable links to the material are provided in the HTML text of this article on the *Journal*'s Web site (www.PRSJournal.com).

Static (Three-Dimensional) Computed Tomography Scanning

The barium-gelatin mixture was prepared by warming 100 ml of normal saline to 40°C, and adding 3 g of gelatin while stirring continuously. This was followed by slowly adding in 40 g of barium sulfate.[18] This solution was then injected into the investigated perforator using the Harvard precision pump running at 1 ml/minute until the vascular tree was saturated (previously repaired leaks will start to leak and have to be recauterized). The flaps were then frozen for at least 24 hours before computed tomography scanning.

Three- and four-dimensional images were viewed using the TeraRecon Aquarius workstation (version 3.2.2.1; TeraRecon Inc., San Mateo, Calif.). The volume rendering function allowed us to produce clear and accurate images of the simulated flaps.

The mean vascular territory of the medial perforator was compared with that of the lateral perforator using the t test. The mean percentage of zones II and III perfusion between medial and lateral perforators was compared using the Kruskal-Wallis test.

RESULTS

The results of our study are summarized in Table 1. All of our simulated DIEP flaps were based on single perforators.

Table 1. Medial versus Lateral Perforators of a DIEP Flap: Comparison of Areas of Perfusion

Perforator Injected	*n*	Mean Vascular Territory (cm²)	Mean Area of Zone II Perfused (cm²)	Mean % of Zone II Perfused	Mean Area of Zone III Perfused (cm²)	Mean % of Zone III Perfused
Medial	22	296.4*	93.1	65.8†	122.3	43.9†
Lateral	14	195.6	5.2	4.8	95.3	85.2

*$p < 0.008$ using t test.
†$p < 0.01$ using Kruskal-Wallis test.

Medial Row Perforators

Twenty-two medial perforator DIEP flaps were used in this study. The mean vascular territory for a medial perforator DIEP flap injected with contrast was 296 cm² ($p < 0.008$ when compared with vascular territory of lateral perforator). The branches of the medial row perforator were seen to be directed both laterally and medially, and crossed the midline in all cases. The vascular territories of these flaps were more centralized compared with those perfused by a lateral perforator. Large-diameter linking vessels were found to connect perforators within the same medial row (Fig. 1). The injected medial perforators connected with contralateral medial row perforators (across the midline) through the indirect linking vessels via the subdermal plexus (Figs. 2 and 3). Moon and Taylor also noted that crossover of the midline is predominantly in the subdermal plexus.[11] Medial row and lateral row perforators within the same hemi-abdomen were connected via both direct and indirect linking vessels (Fig. 3).

Lateral Row Perforators

Fourteen lateral perforator DIEP flaps were analyzed. The mean vascular territory of a DIEP flap when a lateral row perforator was injected was 196 cm². Perfusion was found to be more lateralized, and very few of these flaps crossed the midline (three of 14). Contrast injected into a lateral perforator tended to stay in one hemi-abdomen (Fig. 4). Again, large-diameter linking vessels were found to connect perforators within the same lateral row perforators, and both direct and indirect linking vessels were found to communicate between perforators of the same hemi-abdomen (Fig. 5). We found that for both lateral and medial perforators, indirect linking vessels (through the subdermal plexus) outnumber direct linking vessels, which implies that perfusion occurs mostly at the superficial level of the skin.

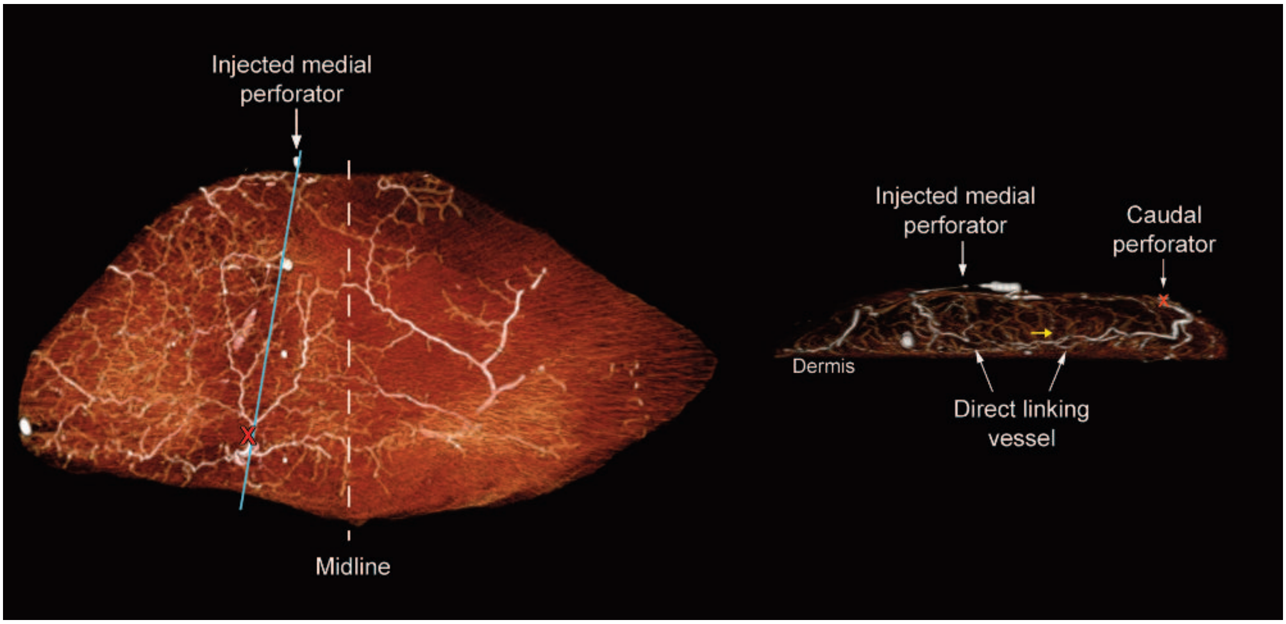

Fig. 1. Three-dimensional computed tomography angiogram of a medial perforator DIEP flap. (*Left*) Anteroposterior view. (*Right*) Sagittal view of flap, corresponding to *blue* line in the anteroposterior view. Direct linking vessels connect perforators within the same medial row. X marks a perforator caudal to the injected medial one. The *yellow arrow* shows the direction of flow.

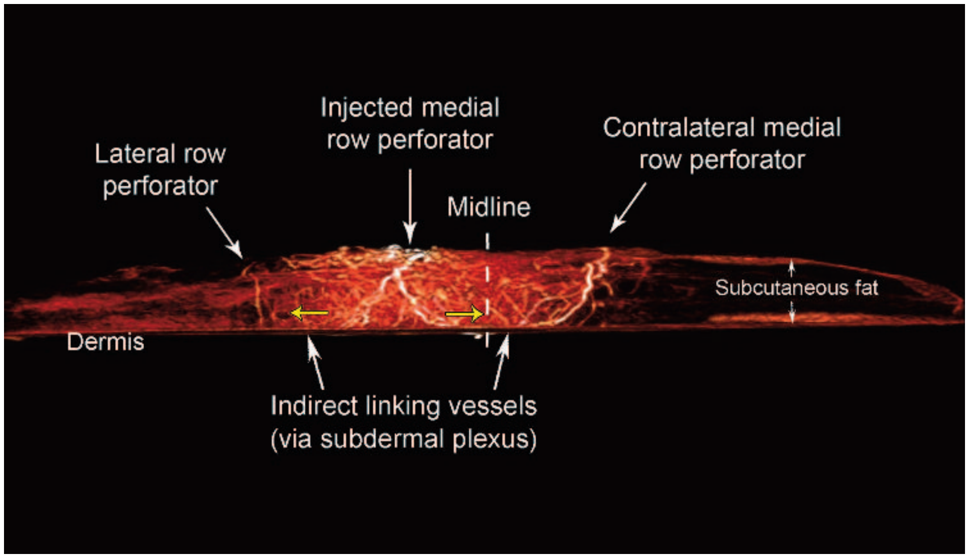

Fig. 2. Three-dimensional computed tomography angiogram of a medial perforator DIEP flap, transverse view. The injected medial perforator was connected to the contralateral medial row perforator through indirect linking vessels via the subdermal plexus. The *yellow arrows* show the direction of flow.

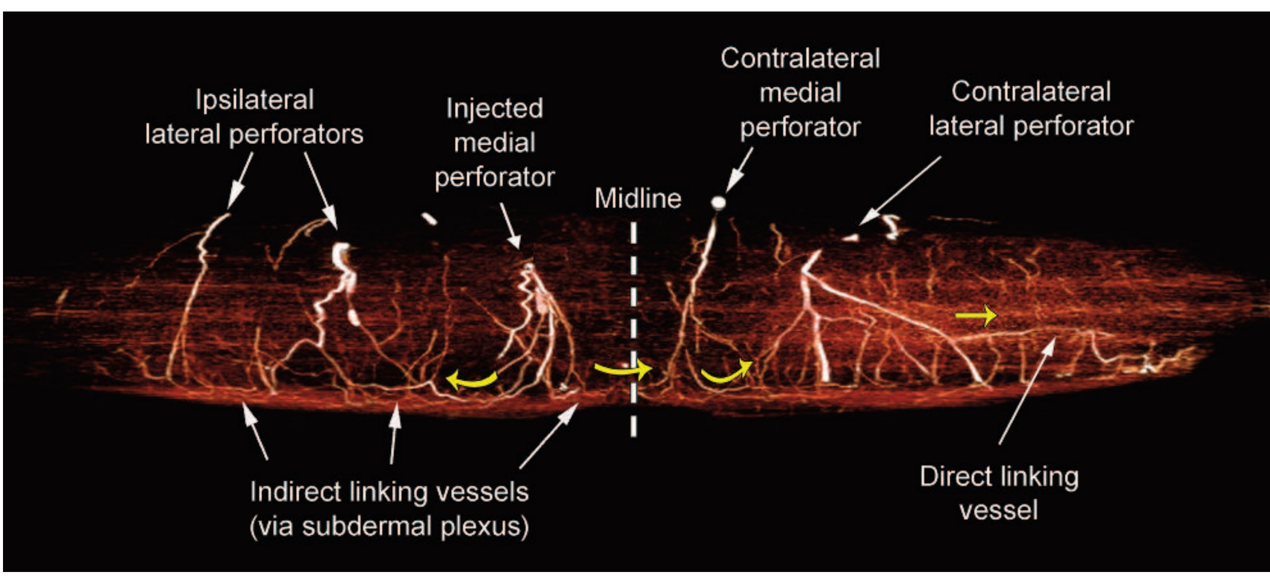

Fig. 3. Three-dimensional computed tomography angiogram of a medial perforator DIEP flap, transverse view. Medial row and lateral row perforators within the same hemi-abdomen were connected via both direct and indirect linking vessels. Contrast traveled across the midline via indirect linking vessels via the subdermal plexus. The *yellow arrows* show the direction of flow.

Zones of Perfusion

In a medial perforator DIEP flap, the mean percentage of Hartrampf zone II perfused was 65.8 percent, compared with 4.8 percent for a lateral perforator DIEP flap. For Hartrampf zone III, a medial perforator injection had only 43.9 percent, compared with 85.2 percent for a lateral perforator ($p < 0.01$) (Fig. 6). Five medial perforator flaps had vascular territories encroaching zone IV, whereas none of the lateral perforator flaps did.

In our four-dimensional computed tomography investigations, we found that flow of contrast for a medial perforator DIEP traveled earlier to Har-

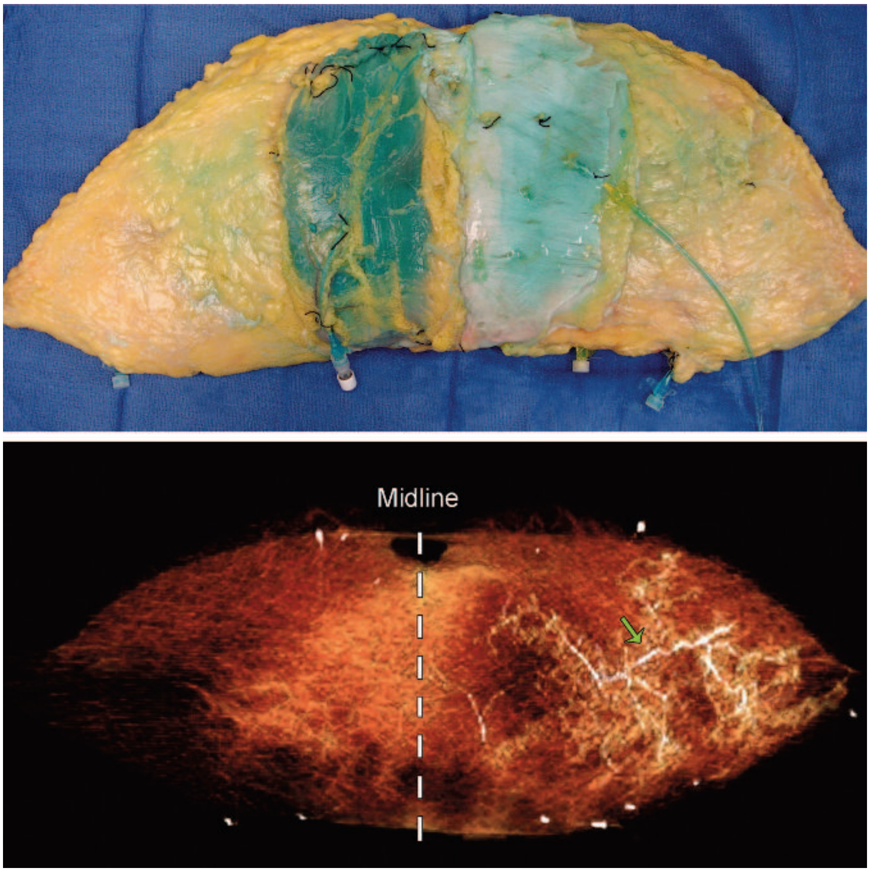

Fig. 4. (*Above*) In this cadaveric DIEP flap, the lateral perforator on the right side is cannulated and attached to tubing. The left rectus muscle is still intact, whereas the right had been removed. (*Below*) Three-dimensional computed tomography angiogram of a lateral perforator DIEP flap, anteroposterior view. The *arrow* shows the location of the lateral row perforator injected with contrast. Perfusion tends to stay in one hemi-abdomen.

trampf zone II and had a greater area of vascularity compared with Hartrampf zone III (Fig. 7). (See **Video, Supplemental Digital Content 1,** which demonstrates the infusion of contrast agent over time in a single medial row DIEP flap perforator, ***http://links.lww.com/PRS/A149.*** Note the large linking vessels that communicate with other medial row and lateral row perforators. The flow of contrast for a medial perforator travels earlier to Hartrampf zone II and has a greater area of vascularity compared with Hartrampf III.) The lateral perforator DIEP flaps had earlier and greater contrast flow into Hartrampf zone III compared with Hartrampf zone II (Fig. 8). (See **Video, Supplemental Digital Content 2,** which shows that in contrast to the medial row perforator, the lateral row DIEP flap perforator has earlier and greater contrast flow into Hartrampf zone III compared with Hartrampf zone II, ***http://links.lww.com/PRS/A150***).

DISCUSSION

This methodology does not pretend to mimic physiological conditions and cannot account for aspects such as vasoconstriction and physiological shunting. Actual vascularity may be quite different in a physiological situation, where nervous, hormonal, and local controls of the vessels come into play. This merely gives us a means of comparing two different types of perforators using identical experimental conditions.

We found that anatomical vascular imaging always underestimates the true clinical vascular perfusion area (many surgeons will attest to harvesting lateral perforator DIEP flaps that were larger than a hemi-abdomen without complications). Therefore, larger vascular territories can be anticipated in a clinical arena. Medial and lateral row perforators offer distinct and stereotypical zones of perfusion that have a significant impact on flap de-

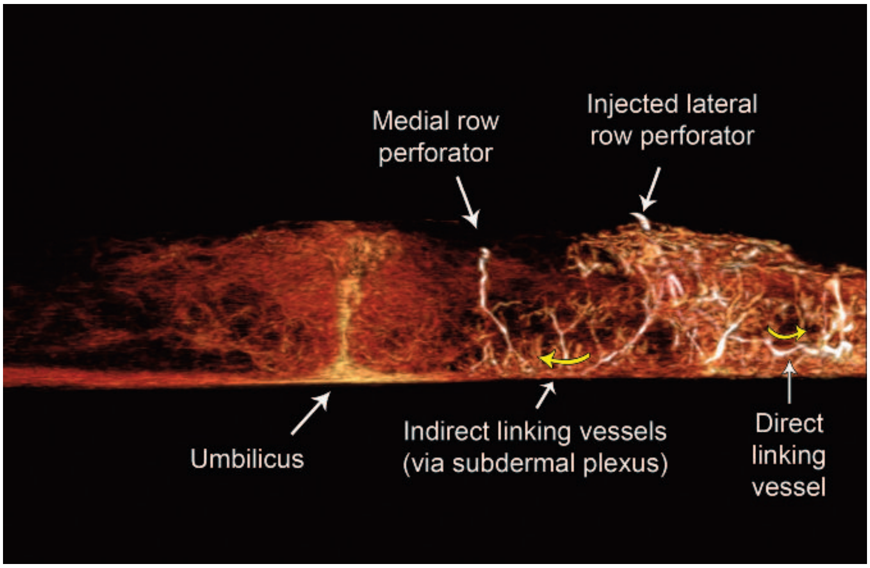

Fig. 5. Three-dimensional computed tomography angiogram of a lateral perforator DIEP flap, transverse view. Both direct and indirect linking vessels were found to communicate between perforators of the same hemi-abdomen. Contrast rarely crossed the midline. The *yellow arrows* show the direction of flow.

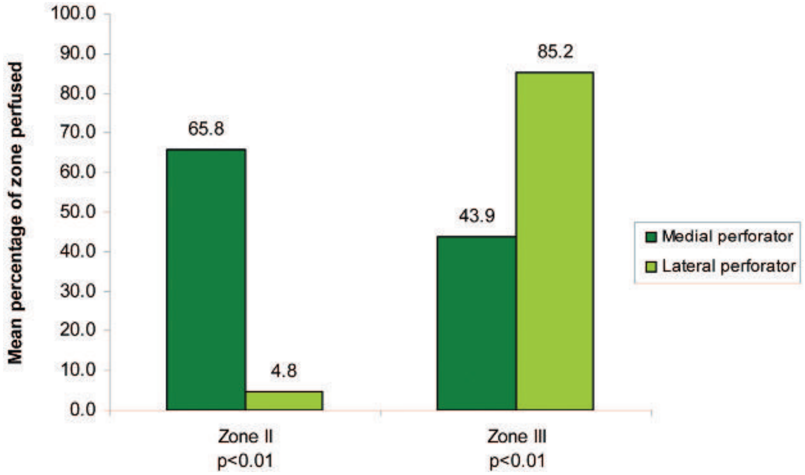

Fig. 6. Graphical comparison of zone II and III perfusion according to perforator (medial versus lateral).

sign and harvesting. When considering a lateral row–based perforator flap, vascularity was found to rarely cross the midline in our anatomical cadaver computed tomography studies. We propose that this was due to a higher number of communicating vessels needed to cross the midline, compared with a flap based on a medial perforator (Fig. 9).

When planning a large breast reconstruction, a medial row perforator or a combination of medial and lateral perforators (muscle-sparing TRAM or TRAM flap) should be considered. If a single medial row perforator is selected, the vascular territory is larger and more centralized compared with a lateral row perforator-based flap. Therefore, both tips of the flap are subjected to a higher risk of ischemia (Fig. 10). We routinely discard the distal third or half of Hartrampf zone III and half or all of zone IV when selecting a medial row single-perforator DIEP flap.

Studies have been to done to advocate the use of the lateral row perforators in DIEP flap harvesting. The lateral branch is frequently wider and tends to run a more rectilinear course, allowing for easier and speedier dissection.[19,20] Lateral row

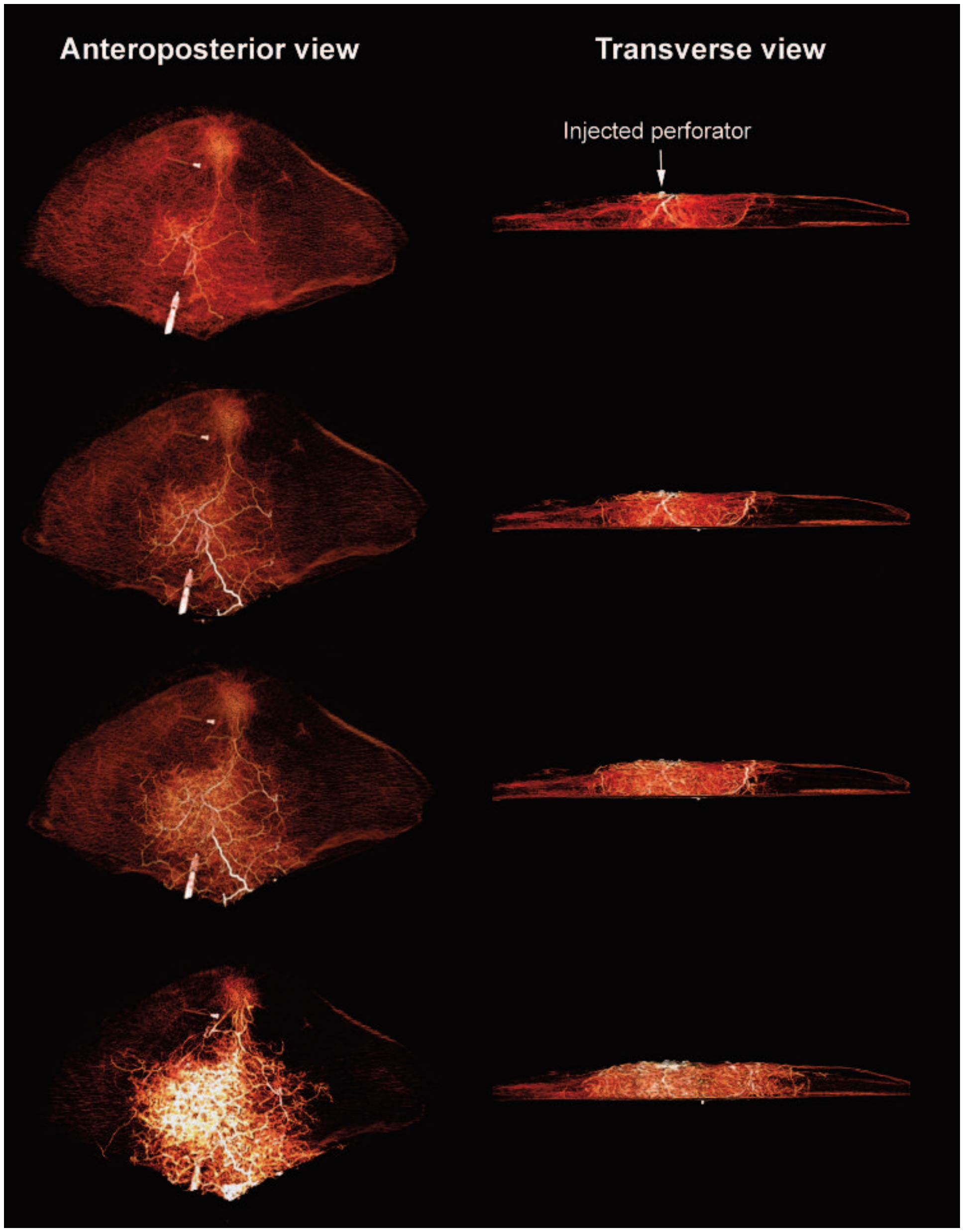

Fig. 7. Four-dimensional computed tomography angiograms demonstrating perfusion of a medial perforator DIEP flap. (*Left*) Anteroposterior views. (*Right*) Transverse views. Flow of contrast traveled earlier to zone II and had a greater area of vascularity compared with zone III.

perforators used in a hemi-abdominal flap have more of a central position and have less risk of partial flap necrosis of the most distal ipsilateral tip of the flap. Therefore, hemi-abdominal flaps tend to be safely harvested based on a single lateral row perforator (Fig. 11), and this can be used in small to medium breast reconstructions. It is also very useful for bilateral breast reconstruction. In a previous study, we found that the free TEAM flap, which has both medial and lateral perforators, had the largest vascular territory among the commonly used abdominal flaps for breast reconstruction, and perfused Hartrampf zones I, II, and III.[17]

Reappraisal of the Zones of Perfusion

Holm et al. performed perfusion studies which demonstrated that Hartrampf zones II and III should be reversed.[13] They stated that Hartrampf's concept was erroneous and that "perfusion of the vascular territories across the midline was always delayed and less intensive than in the territories on the ipsilateral side." This elegant study was well carried

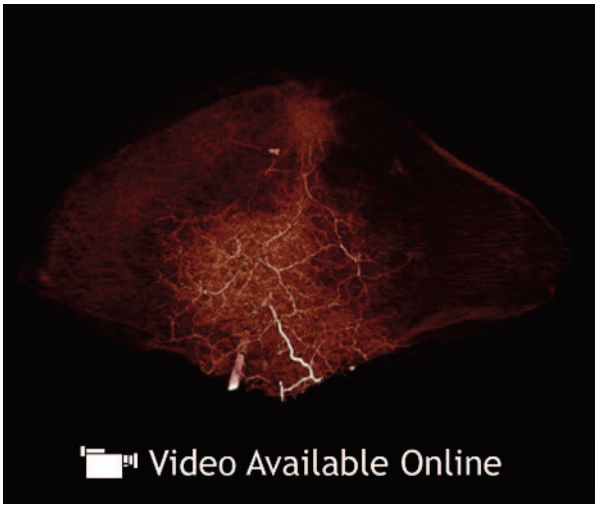

Video 1. Supplemental Digital Content 1 demonstrates the infusion of contrast agent over time in a single medial row DIEP flap perforator, ***http://links.lww.com/PRS/A149***. Large linking vessels communicate with other medial row and lateral row perforators. The flow of contrast for a medial perforator travels earlier to Hartrampf zone II and has a greater area of vascularity compared to Hartrampf III.

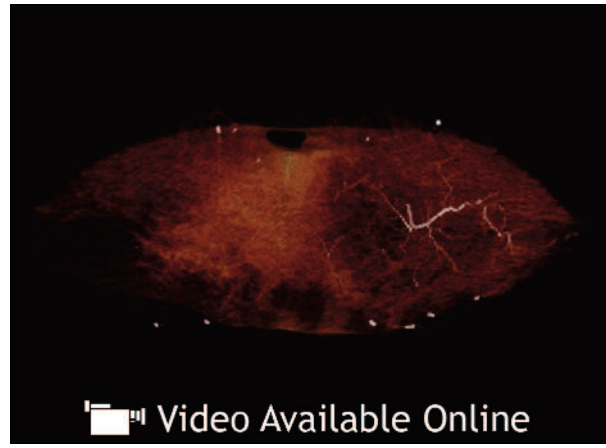

Video 2. Supplemental Digital Content 2 shows that in contrast to the medial row perforator, the lateral row DIEP flap perforator has earlier and greater contrast flow into Hartrampf zone III compared to Hartrampf zone II, ***http://links.lww.com/PRS/A150.***

out, but its bold statement does not always hold true. In Holm et al.'s study, only two of 15 flaps utilized just the medial row perforators, and eight used only lateral row perforators (the rest had both medial and lateral row perforators).

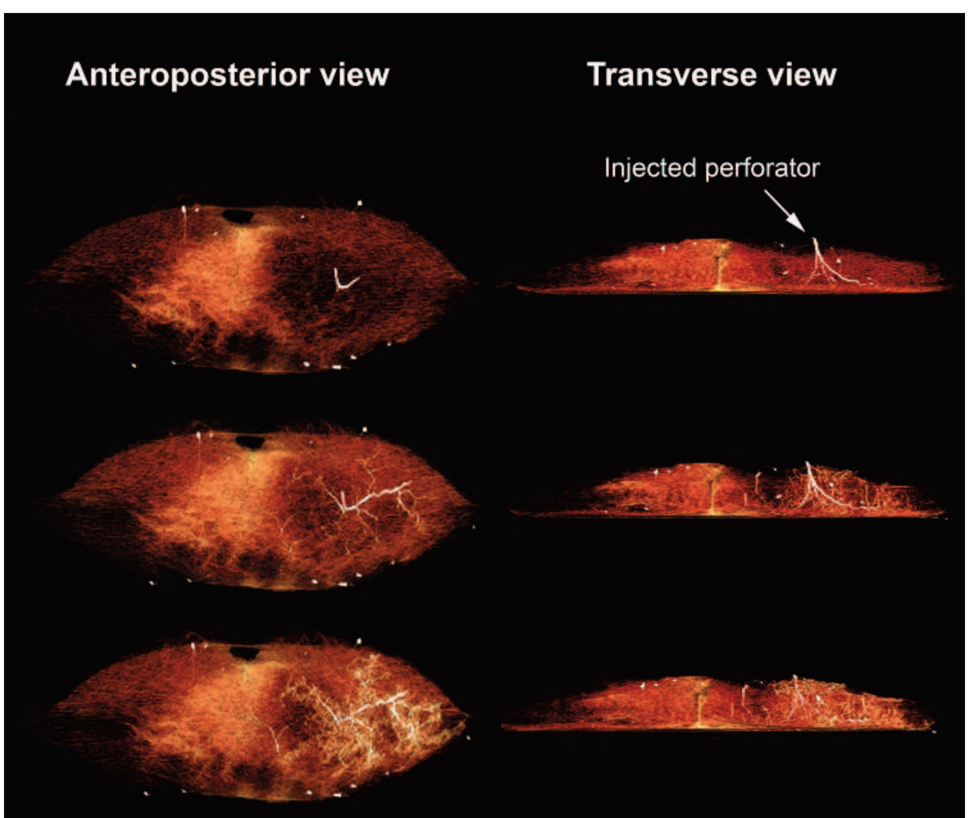

Fig. 8. Four-dimensional computed tomography angiograms demonstrating perfusion of a lateral perforator DIEP flap. (*Left*) Anteroposterior views. (*Right*) Transverse views. There was earlier and greater contrast flow into zone III compared with zone II.

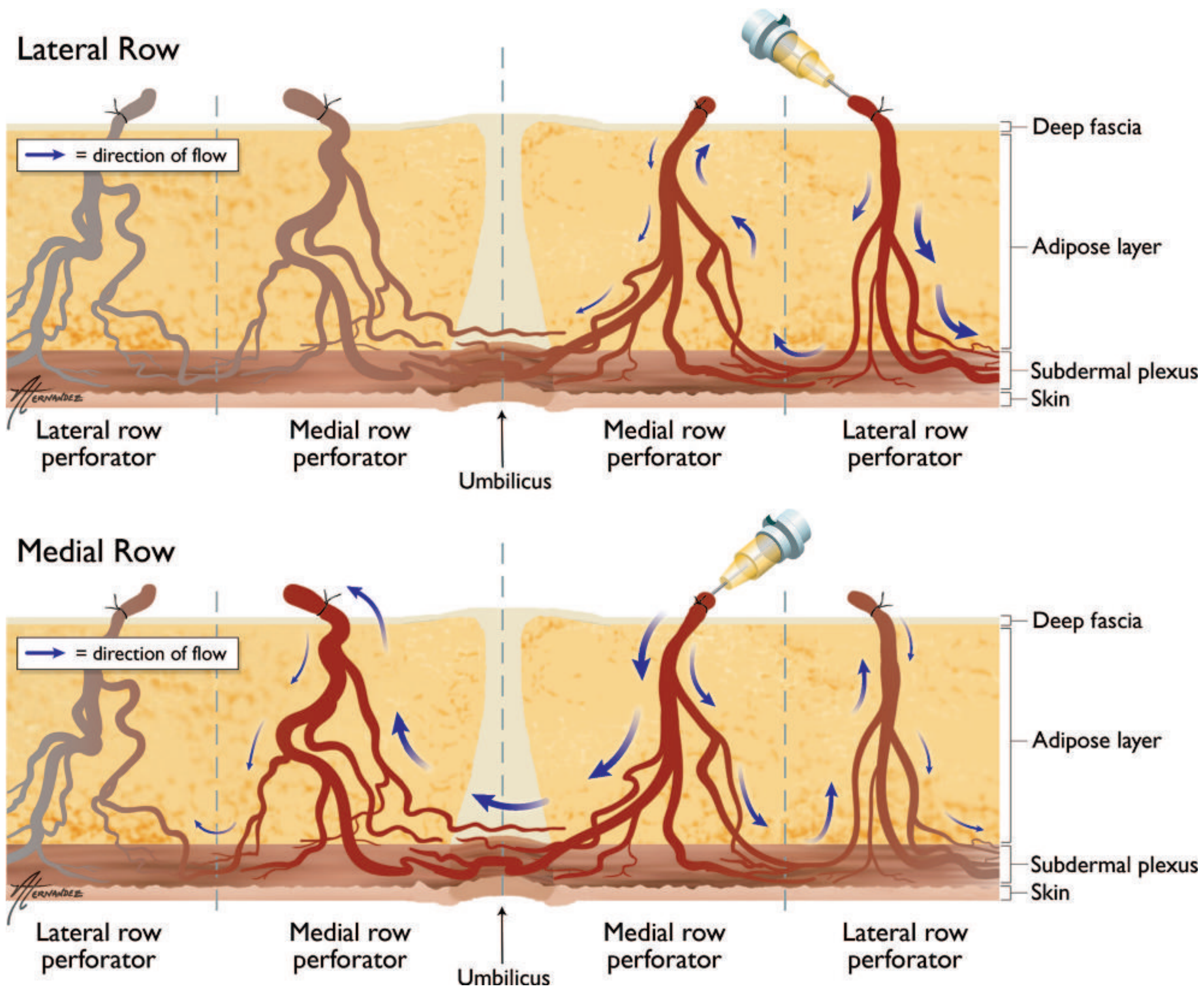

Fig. 9. Illustrations of contrast flow in a DIEP flap. (*Above*) Lateral row perforator is injected. At least two sets of linking vessels need to be crossed to reach the midline. (*Below*) Medial row perforator is injected. Fewer linking vessels are required to cross the midline, thus contrast flows into zone II more easily, hence a more centralized perfusion. Also, at least two sets of linking vessels are needed to be crossed to reach zone III.

Based on our three- and four-dimensional computed tomographic angiography studies, contrast flow from a medial perforator perfused Hartrampf zone II earlier and more so than Hartrampf zone III. The resultant area of vascularity of Hartrampf zone II is greater than in Hartrampf zone III. Therefore, flaps based on a single medial row perforator are shown to be more centralized and follow Hartrampf's classification of perfusion zones, with zone II being the contralateral medial region of a transverse abdominal flap. Zone III is ipsilateral to zone I, and zone IV is ipsilateral to zone II (Fig. 12).

In contrast, perfusion for a lateral perforator DIEP is more lateralized. Contrast traveled to Hartrampf zone III earlier and had a greater area of vascularity compared with Hartrampf zone II. Therefore, this perfusion pattern follows Holm's classification, and zones II and III should be in reverse order (Fig. 13). Holm's zone II corresponds to the area ipsilateral to zone I, and Holm's zone III should now be the contralateral medial region, in the same hemi-abdomen with zone IV.

Still, regardless of perforator location, the largest perforator should always be selected during a flap harvest. The DIEP flap has allowed a significant decrease in donor-site morbidity and can provide an aesthetic breast reconstruction that is comparable to all other abdominal donor-site flaps. Thorough knowledge of the vascular anatomy of medial or lateral-based perforators is crucial for safe flap design and harvesting, and can

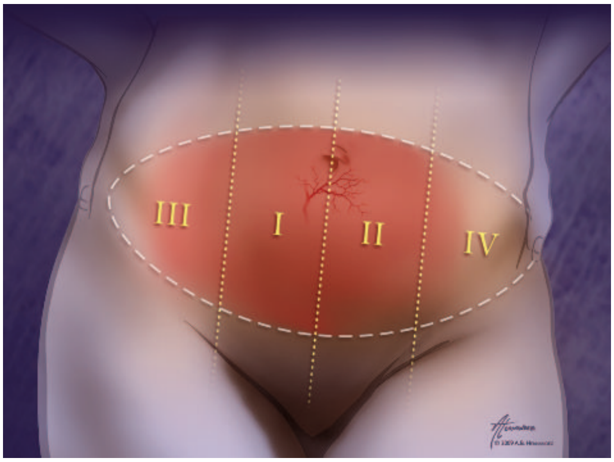

Fig. 10. Illustration of a medial perforator DIEP flap, in which perfusion is more centralized and has a bigger vascular territory. These are useful for large breast reconstructions.

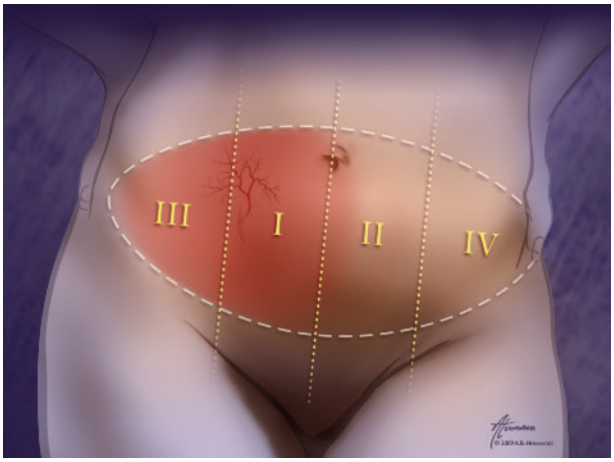

Fig. 11. Illustration of a lateral perforator DIEP flap, in which perfusion is more lateralized. These are useful for small to moderate-sized and bilateral breast reconstructions.

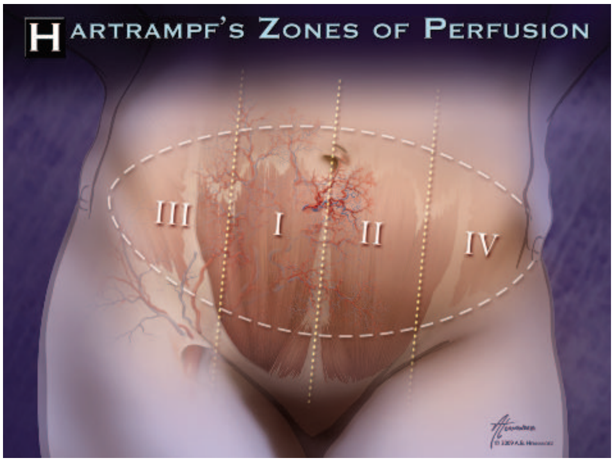

Fig. 12. Medial perforator DIEP flaps follow Hartrampf zones of perfusion. Zone II is on the contralateral hemi-abdomen.

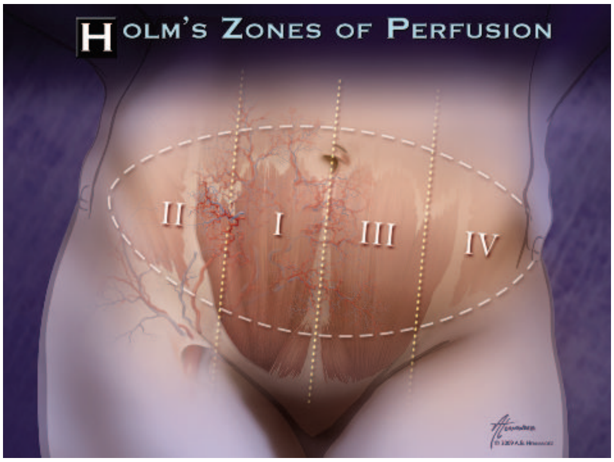

Fig. 13. Lateral perforator DIEP flaps follow Holm's zones of perfusion. Zone II is on the ipsilateral hemi-abdomen.

help minimize the risks of postoperative fat necrosis and partial flap necrosis. In a recent meta-analysis, the risk of fat necrosis in DIEP flaps was reported to be twice that of TRAM flaps.[21] This is likely due to improper knowledge of the vascular anatomy of lateral versus medial row-based perforators. Both of these perforator types will have distinct vascular territories, and this should be respected during DIEP flap harvesting to avoid such complications.

Our study demonstrates that the perfusion characteristics of a medial row perforator differ significantly from those of a lateral row-based perforator. Therefore, each perforator has its own distinct vascular territory, which has been termed a "perforasome."[22] This may also explain why there are significant differences in the literature regarding fat necrosis and DIEP flap complications. Numerous series mention their complications by combining both lateral and medial row-based perforator DIEP flaps. Therefore, if a meaningful comparison is to be made, medial row perforator DIEP flaps need to be compared with medial row perforator DIEP flaps and likewise with lateral row perforator DIEP flaps. We acknowledge that a limitation of this study is the focus on only single-perforator DIEP flaps, as we were investigating the vascular territory of single perforators. Clinically, although some DIEP flaps are based on two or more perforators, many DIEP flaps are based on single perforators, so we believe the findings from this study are still valid.

CONCLUSIONS

DIEP flaps based on medial row perforators will have a different vascular territory compared with those based on lateral perforators. Increased knowledge of the vascular anatomy and zones of perfusion of both these perforator types will likely help decrease flap-related complications, such as fat necrosis and partial flap loss. This, in general, will yield better patient outcome and decreased morbidity in the reconstructive process.

Michel Saint-Cyr, M.D.
Department of Plastic Surgery
University of Texas Southwestern Medical Center
1801 Inwood Road
Dallas, Texas 75290-9132
michel.saintcyr@utsouthwestern.edu

ACKNOWLEDGMENTS

The authors thank the staff at the University of Texas Southwestern Willed Body Program for their help with this study. They are also indebted to Alexandra Hernandez of Gory Details for invaluable assistance in preparing the images for this article.

REFERENCES

1. Nahabedian MY, Dooley W, Singh N, et al. Contour abnormalities of the abdomen after breast reconstruction with abdominal flaps: The role of muscle preservation. *Plast Reconstr Surg.* 2002;109:91–101.
2. Nahabedian MY, Momen B, Galdino G, et al. Breast reconstruction with the free TRAM or DIEP flap: Patient selection, choice of flap, and outcome. *Plast Reconstr Surg.* 2002;110:466–475; discussion 476–477.
3. Futter CM, Webster MH, Hagen S, et al. A retrospective comparison of abdominal muscle strength following breast reconstruction with a free TRAM or DIEP flap. *Br J Plast Surg.* 2000;53:578–583.
4. Kroll SS. Fat necrosis in free transverse rectus abdominis myocutaneous and deep inferior epigastric perforator flaps. *Plast Reconstr Surg.* 2000;106:576–583.
5. Bajaj AK, Chevray PM, Chang DW. Comparison of donor-site complications and functional outcomes in free muscle-sparing TRAM flap and free DIEP flap breast reconstruction. *Plast Reconstr Surg.* 2006;117:737–746; discussion 747–750.
6. Garvey PB, Buchel EW, Pockaj BA, et al. DIEP and pedicled TRAM flaps: A comparison of outcomes. *Plast Reconstr Surg.* 2006;117:1711–1719; discussion 1720–1721.
7. Scheflan M, Dinner MI. The transverse abdominal island flap: Part II. Surgical technique. *Ann Plast Surg.* 1983;10:120–129.
8. Scheflan M, Dinner MI. The transverse abdominal island flap: Part I. Indications, contraindications, results, and complications. *Ann Plast Surg.* 1983;10:24–35.
9. Hartrampf CR, Scheflan M, Black PW. Breast reconstruction with a transverse abdominal island flap. *Plast Reconstr Surg.* 1982;69:216–225.
10. Boyd JB, Taylor GI, Corlett R. The vascular territories of the superior epigastric and the deep inferior epigastric systems. *Plast Reconstr Surg.* 1984;73:1–16.
11. Moon HK, Taylor GI. The vascular anatomy of rectus abdominis musculocutaneous flaps based on the deep superior epigastric system. *Plast Reconstr Surg.* 1988;82:815–832.
12. Heitmann C, Felmerer G, Durmus C, et al. Anatomical features of perforator blood vessels in the deep inferior epigastric perforator flap. *Br J Plast Surg.* 2000;53:205–208.
13. Holm C, Mayr M, Hofter E, et al. Perfusion zones of the DIEP flap revisited: A clinical study. *Plast Reconstr Surg.* 2006;117:37–43.
14. Saint-Cyr M, Schaverien M, Arbique G, et al. Three- and four-dimensional computed tomographic angiography and venography for the investigation of the vascular anatomy and perfusion of perforator flaps. *Plast Reconstr Surg.* 2008;121:772–780.
15. Schaverien M, Saint-Cyr M, Arbique G, et al. Three- and four-dimensional arterial and venous anatomies of the thoracodorsal artery perforator flap. *Plast Reconstr Surg.* 2008;121:1578–1587.
16. Schaverien M, Saint-Cyr M, Arbique G, et al. Three- and four-dimensional computed tomographic angiography and venography of the anterolateral thigh perforator flap. *Plast Reconstr Surg.* 2008;121:1685–1696.
17. Wong C, Saint-Cyr M, Arbique G, et al. Three and four-dimensional computed tomographic angiography studies of commonly used abdominal flaps in breast reconstruction. *Plast Reconstr Surg.* 2009;124:18–27.
18. Tan BK, Ng RT, Tay NS, et al. Tissue microangiography using a simplified barium sulphate cadaver injection technique. *Ann Acad Med Singapore* 1999;28:152–154.
19. Itoh Y, Arai K. The deep inferior epigastric artery free skin flap: Anatomic study and clinical application. *Plast Reconstr Surg.* 1993;91:853–863; discussion 864.
20. Munhoz AM, Ishida LH, Sturtz GP, et al. Importance of lateral row perforator vessels in deep inferior epigastric perforator flap harvesting. *Plast Reconstr Surg.* 2004;113:517–524.
21. Man LX, Selber JC, Serletti JM. Abdominal wall following free TRAM or DIEP reconstruction: A meta-analysis and critical review. *Plast Reconstr Surg.* 2009;124:752–764.
22. Saint-Cyr M, Wong C, Schaverien M, et al. The perforasome theory: Vascular anatomy and clinical implications. *Plast Reconstr Surg.* 2009;124:1529–1544.

Three- and Four-Dimensional Computed Tomographic Angiography Studies of the Supraclavicular Artery Island Flap

Jennifer W. H. Chan, M.D.
Corrine Wong, M.R.C.S.
Kenneth Ward, M.D.
Michel Saint-Cyr, M.D.
Ernest S. Chiu, M.D.

New Orleans, La.; and Dallas, Texas

Background: The supraclavicular artery island flap is a useful regional option in head and neck reconstruction. Previous studies have recorded pedicle length, caliber, and ink injection studies of the supraclavicular artery. This study presents a three- and four-dimensional appraisal of the vascular anatomy and perfusion of the supraclavicular artery island flap using a novel computed tomographic technique.

Methods: Ten supraclavicular artery island flaps were harvested from fresh cadavers. Each flap was injected with contrast media and subjected to dynamic computed tomographic scanning using a GE Lightspeed 16-slice scanner. Static computed tomographic scanning was also undertaken using a barium-gelatin mixture. Images were viewed using both General Electric and TeraRecon systems, allowing the appreciation of vascular territory (three-dimensional) and analysis of perfusion flow (four-dimensional).

Results: The entire skin paddle was perfused in the majority (nine of 10) of flaps. One of the flaps was perfused only 50 percent. In this case, the pedicle artery was found to be much smaller than the other flap pedicles. Direct linking vessels and recurrent flow by means of the subdermal plexus were found to convey the flow of contrast between adjacent perforators. This explains how perfusion extends to adjacent perforators by means of interperforator flow, and how perfusion is maintained all the way to the distal periphery of the flap.

Conclusions: Using this imaging technique, the authors elucidated the vascular anatomy of the supraclavicular artery island flap. This study confirms previous clinical findings that the supraclavicular artery island flap is a reliable option and gives surgeons new information for future flap refinement. (*Plast. Reconstr. Surg.* 125: 525, 2010.)

Oropharyngeal oncologic resection often results in complex wounds requiring the use of local, regional, or free tissue transfer to return form and function. Microvascular free tissue transfer revolutionized reconstructive surgery in the head and neck by providing more flap options to reliably replace tissue defects with minimal donor-site morbidity. However, they require technical expertise and increased operative time. Local flaps often are not of adequate size and regional flaps are bulky and associated with increased donor-site morbidity.

From the Division of Plastic and Reconstructive Surgery, Tulane Health Sciences Center; Department of Plastic and Reconstructive Surgery, University of Texas Southwestern Medical Center; and Children's Hospital, New Orleans.
Received for publication April 21, 2009; accepted August 11, 2009.

DOI: 10.1097/PRS.0b013e3181c82e37

In 1903, Toldt, an anatomist, first illustrated and named the vessel arteria cervicalis superficialis. It originates from the thyrocervical trunk, exiting between the trapezius and sternocleidomas-

Disclosure: *The authors have no financial interests in this research project or in any of the techniques or equipment used in this study.*

Supplemental digital content is available for this article. Direct URL citations appear in the printed text; simply type the URL address into any Web browser to access this content. Clickable links to the material are provided in the HTML text of this article on the *Journal*'s Web site (www.PRSJournal.com).

toid muscle. In 1949, the first clinical application of a flap from the shoulder ("charretera" or acromial flap) was performed by Kazanjian and Converse.[1] The word *charretera*, in Spanish, means the shoulder area where honors are bestowed on military personnel. In 1979, the first anatomical studies were performed by Mathes and Vasconez who described the vascular territory and clinical applications of head and neck reconstruction.[2] The flap was renamed the cervicohumeral flap. In 1983, Lamberty and Cormack named a vessel cephalad to the clavicular insertion of the trapezius muscle the supraclavicular artery.[3] This flap the flap has been controversial because of the reported incidence of distal flap necrosis.[4] Beginning in the 1990s, Pallua et al. "rediscovered" this flap and popularized its use by performing detailed anatomical studies examining the vascularity of what is known today as the supraclavicular island flap.[5–7] Although the supraclavicular artery island flap has been shown to be a versatile regional flap for head and neck reconstruction, its vascular anatomy is still poorly understood. In this study, the vascular anatomy of this flap is examined using computed tomographic angiography which, to date, has not been performed.

MATERIALS AND METHODS

Ten supraclavicular flaps were harvested from fresh adult cadavers acquired through the Willed Body Program at the University of Texas Southwestern Medical Center. The adipocutaneous paddle was incised over the proximal half of the lateral upper arm (overlying the deltoid muscle) and shoulder joint, with the proximal portion of the flap extending to the area superior to the lateral third of the clavicle. The supraclavicular artery, which perfuses the flap, was dissected out in the proximal portion of the flap. It was usually found to be superior to the lateral third of the clavicle.

Specimen dissection was performed under loupe magnification. Injection of a dilute methylene blue solution through the supraclavicular artery enabled all vascular leaks to be sealed, through either bipolar diathermy or suture ligation.

Three-Dimensional and Four-Dimensional Computed Tomographic Imaging

Iodinated contrast medium, 300 mg/ml iohexol (Omnipaque; Amersham, Princeton, N.J.), was heated to 37°C to reduce the viscosity and improve vascular filling. This was injected into the supraclavicular artery. Adequate filling of the vascular territory was achieved with approximately 1.5 to 2 ml of contrast at a rate of injection of 0.5 ml/minute to gain a detailed appreciation of the development of the microvascularity over time. Helical scans were performed using a GE Lightspeed 16-slice scanner (General Electric, Milwaukee, Wis.) set to perform 0.625-mm slices using a 0.5-second rotation time. Each scan was set to 80 kVp and the current ran at 300 mA.

Static Computed Tomographic Scanning

The barium-gelatin mixture was prepared by warming 100 ml of normal saline to 40°C and adding 3 g of gelatin while stirring continuously. This was followed by slowly adding 40 g of barium sulfate. This solution was then injected into the investigated perforator artery/vein using the Harvard precision pump running at 1 ml/minute until the vascular tree was saturated (previously repaired leaks will start to leak and have to be recauterized). The flaps were then frozen for at least 24 hours before computed tomographic scanning.

Three- and four-dimensional images were viewed using the TeraRecon Aquarius workstation, version 3.2.2.1 (TeraRecon, Inc., San Mateo, Calif.). The volume-rendering function allowed us to produce clear and accurate images of the simulated flaps.

RESULTS

The supraclavicular artery island flaps were found to have a mean length of 24.2 cm and a mean width of 8.7 cm. The mean area measured was 152.8 cm^2. The mean diameter of the supraclavicular artery was 1.33 mm. It was found 3.6 ± 0.8 cm above the clavicle and 8.6 ± 0.3 cm from the sternoclavicular junction. The supraclavicular artery was found to perfuse the whole skin paddle in nine flaps (Figs. 1 and 2). One of the flaps was perfused only 50 percent (Fig. 3). In this case, the pedicle artery was found to be much smaller than the other flap pedicles (0.7 mm).

Direct linking vessels and recurrent flow via the subdermal plexus were found to convey the flow of contrast between adjacent perforators (Figs. 4 through 6). This allows the capture of adjacent areas through an inter-perforator flow mechanism. This explains how perfusion is maintained all the way to the distal periphery of the flap.

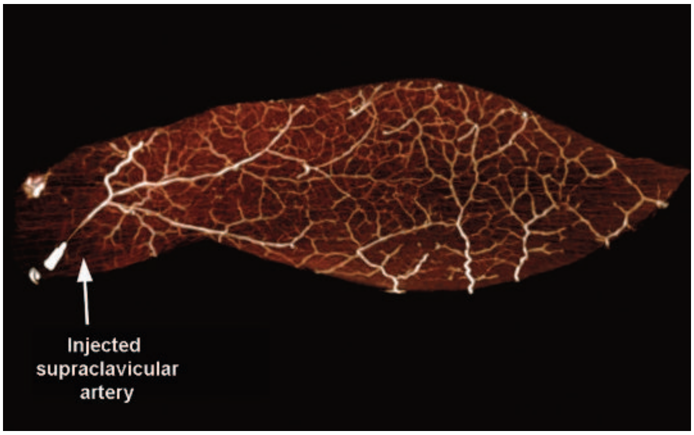

Fig. 1. Three-dimensional computed tomographic angiogram of a supraclavicular flap (anteroposterior view). The flap was infused almost 100 percent.

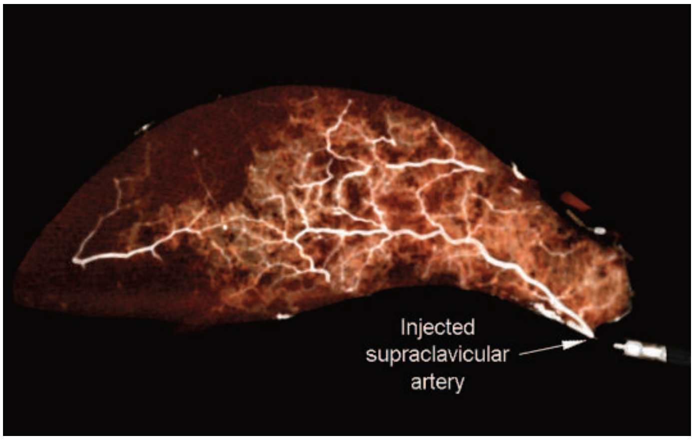

Fig. 2. Three-dimensional computed tomographic angiogram of a supraclavicular flap (anteroposterior view). The flap was infused almost 100 percent.

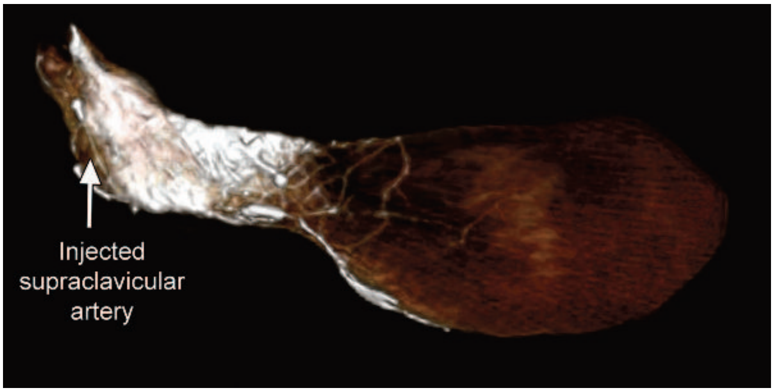

Fig. 3. Three-dimensional computed tomographic angiogram of a supraclavicular flap (anteroposterior view). This flap was perfused only 50 percent on contrast injection.

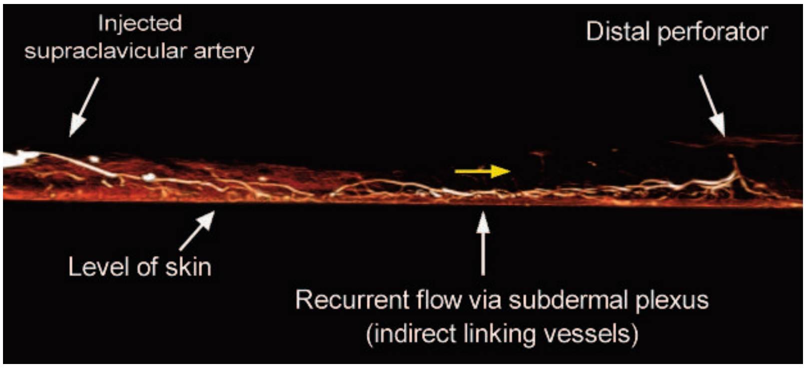

Fig. 4. Lateral view of supraclavicular flap. Communication between adjacent perforators demonstrated by means of recurrent flow through the subdermal plexus. *Yellow arrow* shows the direction of flow.

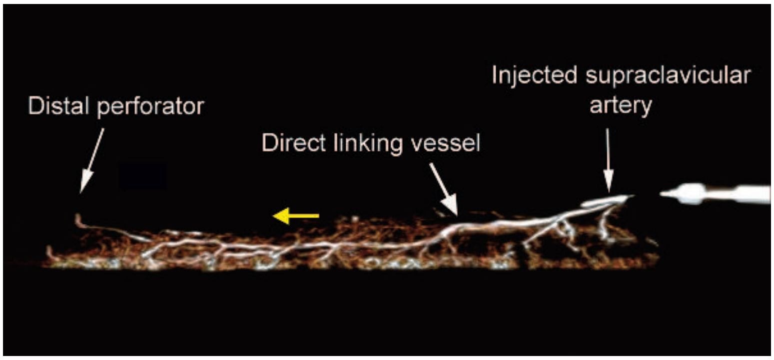

Fig. 5. Lateral view of supraclavicular flap demonstrating direct linking vessels between perforators. *Yellow arrow* shows the direction of flow.

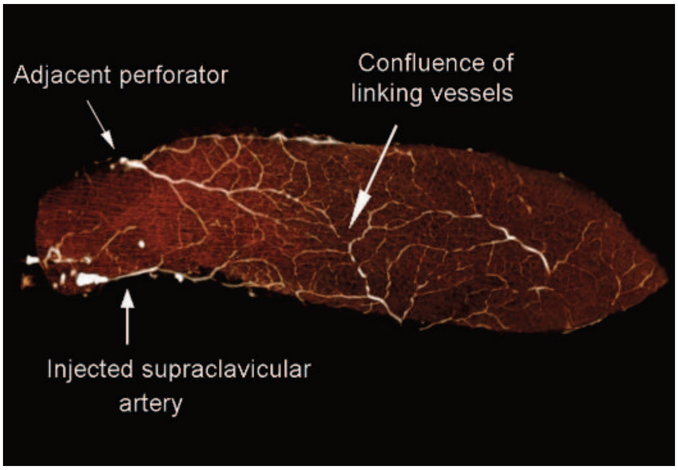

Fig. 6. Linking vessels are found to communicate between adjacent perforators.

Perfusion follows the axiality of linking vessels, and these linking vessels follow the axiality of the limb. This is demonstrated in four dimensions. (See **Videos**, **Supplemental Digital Content 1,** which demonstrates four-dimensional computed tomographic angiography of flap 1, ***http://links.lww.com/PRS/A126***, and **Supplemental Digital Content 2,** which demonstrates four-dimensional computed tomographic angiography of flap 3, ***http://links.lww.com/PRS/A127***).

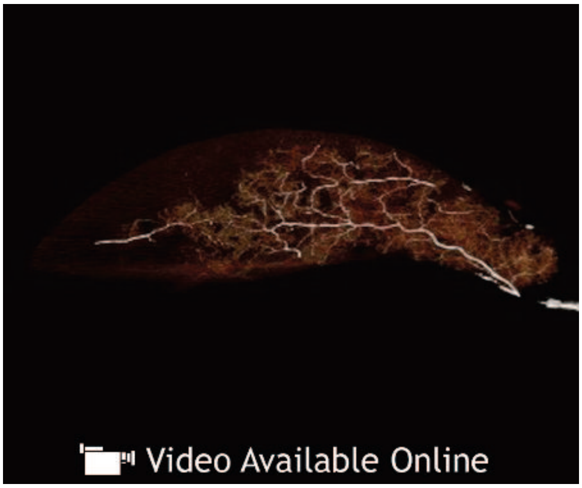

Videos. Supplemental Digital Content 1 demonstrates four-dimensional computed tomographic angiography of flap 1, ***http://links.lww.com/PRS/A126***. Supplemental Digital Content 2 demonstrates four-dimensional computed tomographic angiography of flap 3, ***http://links.lww.com/PRS/A127***.

We have found that perfusion studies involving cadaveric tissue underestimate the extent of vascular territory in vivo. Therefore, clinically, the flap could possibly be extended to beyond the margins of the deltoid muscle in most cases.

DISCUSSION

The supraclavicular artery is a branch of the transverse cervical artery. Less frequently, the supraclavicular artery may arise from the suprascapular artery, which may be smaller. The arterial vessel averages 1.0 to 1.5 mm in diameter and is constantly joined by one or two major concomitant veins. Lamberty[8] found this vessel constantly in 30 fresh cadavers examined as the superficial branch of the superficial transverse cervical artery, later named the supraclavicular artery.

An elegant anatomical dissection study was performed by Abe et al.[9] They showed that the supraclavicular artery mean diameter varied from 1.1 to 1.5 mm, and that the pedicle length ranged from 1 to 7 cm and was present 80 percent of the time ($n = 55$). Two-thirds of the vessels were found not to have crossed the clavicle. The venous drainage is usually through the accompanying transverse cervical vein.

Pallua and Magnus Noah[6] studied the supraclavicular artery in 19 cadavers. In all specimens, they found the supraclavicular artery to arise 3 to 4 cm from the origin of the transverse cervical artery. Examination of the skin landmarks revealed that the artery exited 3.0 ± 0.7 cm above the clavicle at a distance of 8.2 ± 1.7 cm from the sternoclavicular joint and approximately 2.1 ± 0.9 cm dorsal to the sternocleidomastoid muscle. The mean diameter of the artery was 0.15 ± 0.034 cm. They used India ink to demonstrate which skin region was supplied by the supraclavicular artery. In all cases, the vascular territory extended from the supraclavicular region to the shoulder cap. They noted that the distal part of the angiosome was on the ventral surface of the deltoid muscle. The area of this angiosome ranged from 10 × 22 cm to 16 × 30 cm.

Three- and four-dimensional computed tomographic angiography has been used to investigate the anatomy and perfusion of various other flaps in the axial, coronal, and sagittal views in cadaveric flaps.[10–12] No studies to date have evaluated the vascular anatomy of this flap using computed tomographic angiography. Our results show that with an adequately sized supraclavicular artery, the entire flap is based on its flow. We have also shown that the distal part of the flap is dependent on interperforator flow from direct linking vessels and recurrent flow through the subdermal plexus.

The phenomenon of recurrent flow through the subdermal plexus was first noted by Moon and Taylor in the transverse abdominal adipocutaneous paddle perfused by the deep superior epigastric artery,[13] and was seen by Alkureishi et al. in their study of the arterial anatomy of the anterolateral thigh flap in specimens following diaphanization.[14] The study published recently by Schaverien et al. on the anterolateral thigh perforator flap is the first study in which it has been demonstrated dynamically, and it appears to be an important mechanism of flap perfusion.[12] This supports the perforasome theory, where the perforasome is defined as the vascular territory of a single perforator, and perfusion of a flap is conveyed through these methods of interperforator communications.[15]

A weakness of this study is the use of cadaveric flaps. We know from prior cadaveric perfusion studies that the vascular territory is most likely underestimated. However, the dynamic three-dimensional imaging method used in this study more closely models in vivo effects than has been achievable previously. The margins of the flap could likely be extended to beyond that of the deltoid muscle. The four-dimensional computed tomographic angiograms demonstrating the injection of the supraclavicular artery (see **Video 1, Supplemental Digital Content 1,** ***http://links.lww.com/PRS/A126***, and **Video 2, Supplemental Digital Content 2,** ***http://links.lww.com/PRS/A127***) showed the direction of flow as away from the trunk (proximal to distal), highlighted by the orientation of the larger vessels. The density of the capillaries filled with contrast was interpreted as areas of optimal perfusion, and were more frequently found in the proximal regions of the flaps.

Recently, Ma et al.[16] investigated a pectorally extended supraclavicular flap. Microangiograms of their flap showed that there were extensive anastomoses with perforators of the thoracoacromial artery and the second and third perforators of the internal thoracic arteries. Their vascular territory flap extended from a width of 18 cm and a length of 20 cm.

One of the senior authors (E.S.C.) has recently published his clinical experience with this flap.[17] He frequently will obtain a computed tomographic angiogram of the head and neck to evaluate the supraclavicular artery. Figures 7 and 8 are examples from a 25-year-old medical student who underwent contrast bolus–enhanced computed tomographic angiography of the head and neck. Helical scans were performed using a 64-slice Toshiba Aquilion scanner (Toshiba America, Tustin, Calif.) at 0.5-mm acquisitions. Two- and three-dimensional images were viewed using a Vitrea workstation with software version 4.1.0.0 (Vital Images, Inc., Minnetonka, Minn.). The thyrocervical trunk is seen branching off of the subclavian artery. The supraclavicular artery is clearly seen branching off of the thyrocervical trunk. The diameter of the supraclavicular artery is 1.3 mm.

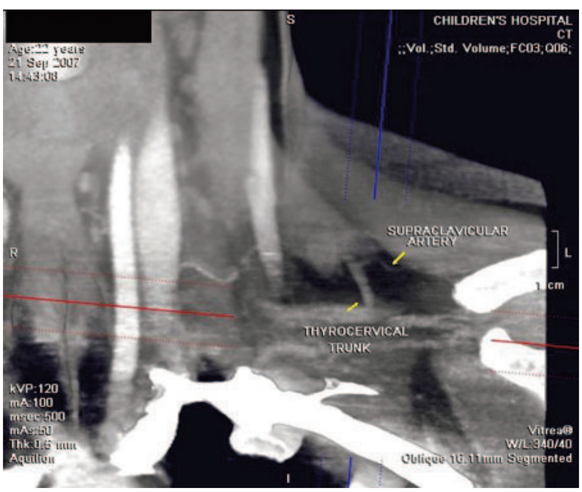

Fig. 7. Computed tomographic angiogram of a patient, demonstrating the supraclavicular artery branching from the thyrocervical trunk.

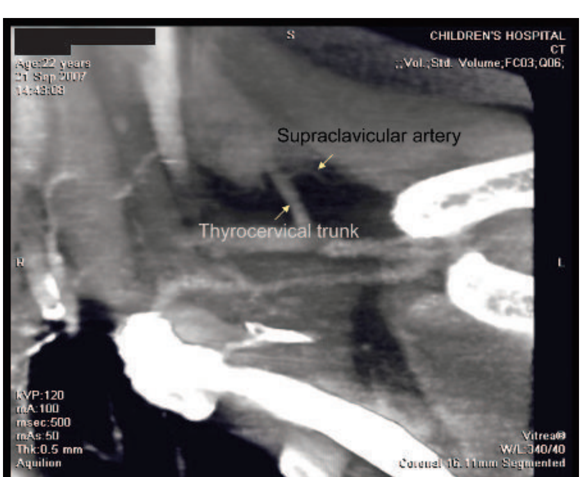

Fig. 8. The diameter of the supraclavicular artery is 1.3 mm (see Video 2, Supplemental Digital Content 2, ***http://links.lww.com/PRS/A127***).

The supraclavicular artery island flap has been used successfully for difficult facial reconstruction cases, providing acceptable results without using microsurgical techniques. Its utility has been demonstrated in reconstructing a variety of head and neck oncologic defects that normally require traditional regional or free flaps to repair surgical wounds. In our study, we were able to provide a better understanding of the vascularization of this flap.

Michel Saint-Cyr, M.D.
Department of Plastic Surgery
University of Texas Southwestern Medical Center
1801 Inwood Road
Dallas, Texas 75290-9132
michel.saintcyr@utsouthwestern.edu

REFERENCES

1. Kazanjian VH, Converse J. *The Surgical Treatment of Facial Injuries.* Baltimore, Md.: Williams & Wilkins; 1949.
2. Mathes SJ, Vasconez LO. The cervico-humeral flap. *Plast Reconstr Surg.* 1978;61:7–12.
3. Lamberty BG, Cormack GC. Misconceptions regarding the cervico-humeral flap. *Br J Plast Surg.* 1983;36:60–63.
4. Blevins PK, Luce EA. Limitations of the cervicohumeral flap in head and neck reconstruction. *Plast Reconstr Surg.* 1980;66:220–224.
5. Pallua N, Machens HG, Rennekampff O, Becker M, Berger A. The fasciocutaneous supraclavicular artery island flap for releasing postburn mentosternal contractures. *Plast Reconstr Surg.* 1997;99:1878–1884.
6. Pallua N, Magnus Noah E. The tunneled supraclavicular island flap: An optimized technique for head and neck reconstruction. *Plast Reconstr Surg.* 2000;105:842–851.
7. Pallua N, Demir E. Postburn head and neck reconstruction in children with the fasciocutaneous supraclavicular artery island flap. *Ann Plast Surg.* 2008;60:276–282.
8. Lamberty BGH. The supraclavicular axial patterned flap. *Br J Plast Surg.* 1979;32:207–212.
9. Abe M, Murakami G, Abe S, Sakakura I, Yajima I. Supraclavicular artery in Japanese: An anatomical basis for the flap using a pedicle containing a cervical, non-perforating cutaneous branch of the superficial cervical artery. *Okajimas Folia Anat Jpn.* 2000;77:149–154.
10. Saint-Cyr M, Schaverien M, Arbique G, Hatef D, Brown SA, Rohrich RJ. Three- and four-dimensional computed tomographic angiography and venography for the investigation of

the vascular anatomy and perfusion of perforator flaps. *Plast Reconstr Surg.* 2008;121:772–780.
11. Schaverien M, Saint-Cyr M, Arbique G, Brown SA, Rohrich RJ. Three-and four-dimensional arterial and venous anatomies of the thoracodorsal artery perforator flap. *Plast Reconstr Surg.* 2008;121:1578–1587.
12. Schaverien M, Saint-Cyr M, Arbique G, Hatef D, Brown SA, Rohrich RJ. Three- and four-dimensional computed tomographic angiography and venography of the anterolateral thigh perforator flap. *Plast Reconstr Surg.* 2008;121:1685–1696.
13. Moon HK, Taylor GI. The vascular anatomy of rectus abdominis musculocutaneous flaps based on the deep superior epigastric system. *Plast Reconstr Surg.* 1988;82:815–832.
14. Alkureishi LW, Shaw-Dunn J, Ross GL. Effects of thinning the anterolateral thigh flap on the blood supply to the skin. *Br J Plast Surg.* 2003;56:401–408.
15. Saint-Cyr M, Wong C, Schaverien M, Mojallal A, Rohrich RJ. The perforasome theory: Vascular anatomy and clinical implications. *Plast Reconstr Surg.* 2009;124:1529–1544.
16. Ma X, Zheng Y, Xia W, et al. An anatomical study with clinical application of one branch of the supraclavicular artery. *Clin Anat.* 2009;22:215–220.
17. Chiu ES, Liu PH, Friedlander PL. Supraclavicular artery island flap for head and neck oncologic reconstruction: Indications, complications, and outcomes. *Plast Reconstr Surg.* 2009;124:115–123.

Instructions for Authors: *Update*

Registering Clinical Trials

Beginning in July of 2007, *PRS* has required all articles reporting results of clinical trials to be registered in a public trials registry that is in conformity with the International Committee of Medical Journal Editors (ICMJE). All clinical trials, regardless of when they were completed, and secondary analyses of original clinical trials must be registered before submission of a manuscript based on the trial. Phase I trials designed to study pharmacokinetics or major toxicity are exempt.

Manuscripts reporting on clinical trials (as defined above) should indicate that the trial is registered and include the registry information on a separate page, immediately following the authors' financial disclosure information. Required registry information includes trial registry name, registration identification number, and the URL for the registry.

Trials should be registered in one of the following trial registries:

- http://www.clinicaltrials.gov/ (Clinical Trials)
- http://actr.org.au (Australian Clinical Trials Registry)
- http://isrctn.org (ISRCTN Register)
- http://www.trialregister.nl/trialreg/index.asp (Netherlands Trial Register)
- http://www.umin.ac.jp/ctr (UMIN Clinical Trials Registry)

More information on registering clinical trials can be found in the following article: Rohrich, R. J., and Longaker, M. T. Registering clinical trials in *Plastic and Reconstructive Surgery. Plast. Reconstr. Surg.* 119: 1097, 2007.

The Extended Transverse Musculocutaneous Gracilis Flap

Vascular Anatomy and Clinical Implications

Corrine Wong, MRCS, Ali Mojallal, MD, Steven H. Bailey, MD, Andrew Trussler, MD, and Michel Saint-Cyr, MD

Background: The transverse musculocutaneous gracilis (TMG) flap has been used in autologous breast reconstruction, but disadvantages include a small flap volume; therefore, it is only used in small-to-moderate breast reconstructions. We investigated the vascular territory of this flap and the possibility of extending its dimensions.
Methods: Ten circumferential thigh adipocutaneous flaps attached to the gracilis muscle were harvested from adult cadavers. The following parameters were recorded: diameter and length of pedicles, distance of pedicles from pubis, and number and locations of cutaneous perforators. The major pedicles were injected with contrast and subjected to 3-dimensional computed tomography scanning. Images were viewed using both General Electrics and TeraRecon systems, and the vascular territories were measured. Flaps were then incised to include only tissue that was perfused with contrast, and measured for weight and volume.
Results: The major pedicle had a mean length of 6.7 cm, diameter of 2.2 mm, and distance from pubis of 8.6 cm. There was a mean of 4.3 cutaneous perforators associated with this flap. Three-dimensional images from contrast injection of the major pedicle showed a cutaneous vascular territory that extended more posteriorly than anteriorly, and had a vertical component. Tissue perfused with contrast had a mean weight of 573 g and volume of 617 mL. Two clinical cases were included to show applications of the extended TMG flap.
Conclusion: The dimensions of a TMG flap can be increased horizontally (superoposterior thigh) as well as vertically. The vertical portion can be harvested either by undermining the skin inferior to the lower transverse skin incision or by raising a trilobed skin paddle to harvest even more tissue from the medial thigh.

Key Words: extended transverse upper gracilis flap, angiosome

(*Ann Plast Surg* 2011;67: 170–177)

There are currently multiple options for breast reconstruction. Possible autologous tissue transfers include latissimus dorsi, transverse rectus abdominis myocutaneous,[1] deep inferior epigastric perforator,[2,3] superficial inferior epigastric artery,[4] superior gluteal artery perforator,[5,6] inferior gluteal artery perforator,[6,7] and lumbar artery perforator flaps.[8] The transverse musculocutaneous gracilis (TMG) flap has gained popularity, especially in Europe, because of its many advantages.[9,10] These include a reliable vascular anatomy, a faster and simpler dissection compared with other flaps, no need for patient repositioning, minimal donor function loss, and since the transverse orientation of the flap was described,[11] a discrete scar that also helps to lift the medial thigh.

However, 1 major disadvantage is the lower flap volume compared with abdominal- and gluteal-based flaps. Therefore, the TMG flap has traditionally only been used to reconstruct small-to-moderate-sized breasts. Modifications to increase this have included harvesting the flap from a more posterior location using the bulkier posterior thigh tissue.[12–14] In addition, Fattah et al have also taken to undermining the skin and using the superficial fat of the thigh distal to the inferior border of the transverse skin paddle. Peek et al described the vertically orientated extended gracilis perforator flap (which precludes the gracilis muscle), which is made possible by preserving the intramuscular connection between the major and minor pedicles, thus recruiting the neighboring angiosome of the minor pedicle.[15] Vega et al have included a vertical portion to form an L-shaped flap in their bid for a larger gracilis flap.[16] The heaviest flaps have been reported to be 420 to 576 g.[14,17] Volumes of 180 to 550 mL have been recorded by Schoeller et al.[13] The largest skin paddles were 30 × 10 cm.[13,17] Even with these maneuvers, sur-

TABLE 1. Measurements of the Major and Minor Pedicles of the Gracilis Muscle

	Major Pedicle (SD, Range)	Minor Pedicle (SD, Range)
Distance from pubis/cm	8.57 (0.76, 7.6–9.8)	23.32 (1.11, 21.8–26.0)
Mean length of pedicle/cm	6.69 (0.48, 6.0–7.4)	4.09 (0.78, 2.8–5.3)
Mean arterial diameter/mm	2.24 (0.32, 1.8–2.8)	1.55 (0.33, 0.9–1.9)
Mean venous diameter/mm	2.33 (0.29, 2.0–2.8)	1.83 (0.11, 1.7–2.0)

SD indicates standard deviation.

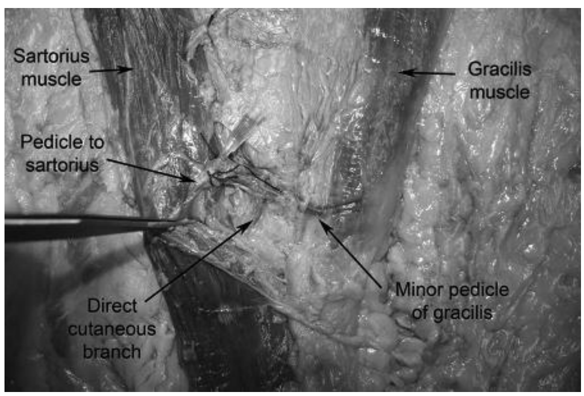

FIGURE 1. Photograph of cadaveric anterior thigh tissue, including sartorius and gracilis muscles. The minor pedicle of the gracilis was found to have a common arterial input with a large pedicle of the sartorius in all cases.

Received March 25, 2010, and accepted for publication, after revision, July 21, 2010.
From the Department of Plastic Surgery, UT Southwestern Medical Center, Dallas, TX.
Presented at the 2010 Annual Meeting of American Society of Reconstructive Microsurgery; January 6–9, 2010; Boca Raton, FL.
Reprints: Michel Saint-Cyr, MD, Department of Plastic Surgery, University of Texas Southwestern Medical Center, 1801 Inwood Rd, Dallas, TX 75390. E-mail: michel.saint-cyr@utsouthwestern.edu.

ISSN: 0148-7043/11/6702-0170
DOI: 10.1097/SAP.0b013e3181f32319

geons still occasionally have to resort to “doubling up” bilateral TMG flaps for one breast to make up sufficient volume.[13,14]

Our study uses 3-dimensional (3D) computed tomography (CT) angiography, barium-gelatin solution, and anatomic dissection to ascertain the vascular territory of the major pedicle of the gracilis muscle. This will help in deciding whether extension beyond the traditional margins of the TMG flap is possible, thereby increasing its volume.

METHODS AND MATERIALS

Ten circumferential thigh adipocutaneous flaps attached to the gracilis muscle were harvested from fresh adult cadavers acquired through the Willed Body Program at the University of Texas Southwestern Medical Center. An incision was made in the midlateral thigh, and the flap was harvested from lateral to medial (for both anterior and posterior). The margins of the adipocutaneous flap were the midlateral thigh, groin crease, gluteal crease, and superior patella. Specimen dissection was performed under loupe magnification. The minor pedicle of the gracilis was ligated. The following parameters were recorded during dissection: diameter of major and minor vascular pedicles, length of pedicles, distance of pedicles from pubis, and number and locations of cutaneous perforators. Thigh width was defined as the length between the midlateral and midmedial lines of each thigh.

TABLE 2. Perforators Dissected

Flap	No. Perforators	MC	SC
1	8	4	4
2	3	3	0
3	4	4	0
4	3	1	2
5	3	2	1
6	4	3	1
7	6	4	2
8	3	3	0
9	5	3	2
10	4	3	1
Total	43	30	13

MC indicates musculocutaneous; SC, septocutaneous.

3D CT Scanning

The major pedicles were cannulated and injected with a dilute methylene blue solution to enable all vascular leaks to be sealed, either through bipolar diathermy or suture ligation. After we were satisfied with the repair of leaks, the major pedicle was then injected with contrast and subjected to 3D CT scanning.

A barium-gelatin mixture was prepared by warming 100 mL of normal saline to 40°C, and adding 3 g of gelatin while stirring continuously. This is followed by slowly adding in 40 g of barium sulfate.[18] This solution is then injected into the major pedicle using a Harvard precision pump running at 1 mL/min until the vascular tree is saturated (previously repaired leaks will start to leak and have to be recauterized). The flaps are then frozen for at least 24 hours before CT scanning.

Three-dimensional images were viewed using the TeraRecon Aquarius workstation (TeraRecon Inc, version 3.2.2.1). The volume rendering function allowed us to produce clear and accurate images of the simulated flaps. This software also allowed us to perform measurements such as length and area of the images produced. Comparison of vascularity extension from midmedial thigh anteri-

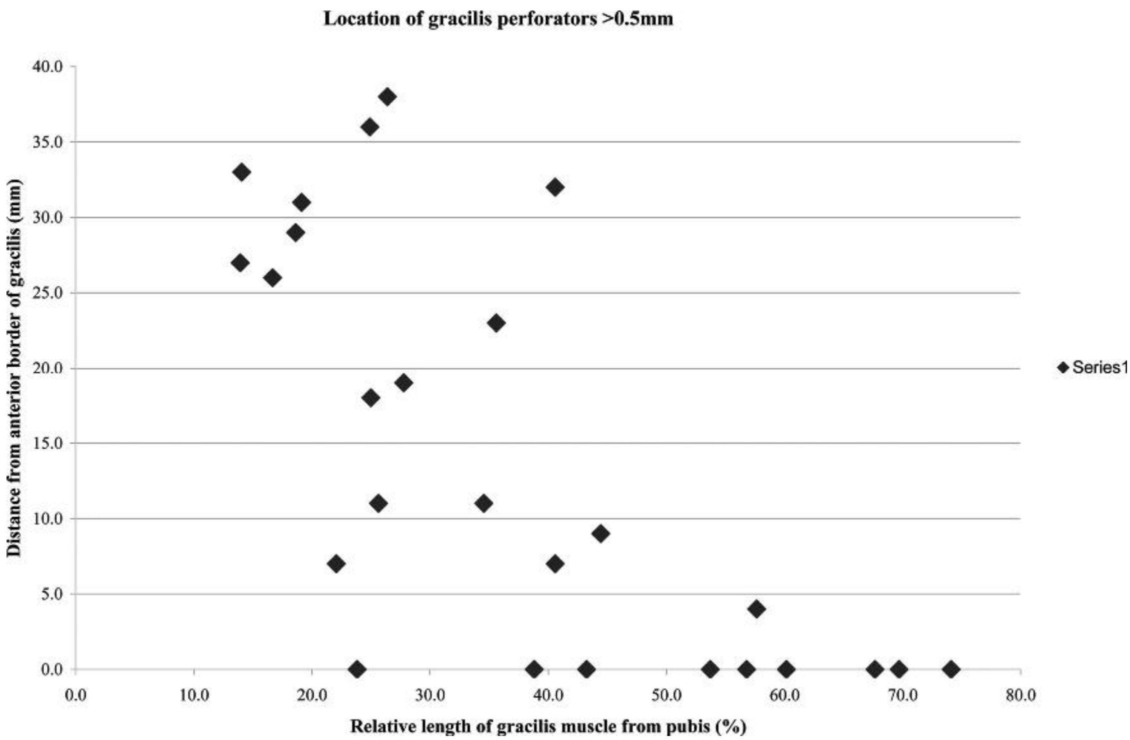

FIGURE 2. Location of gracilis perforators that are 0.5 mm or larger (n = 26). X-axis refers to distance from pubis, as a relative length of the gracilis. Y-axis refers to the distance from the anterior border of the gracilis muscle (perforators located at 0 are septocutaneous).

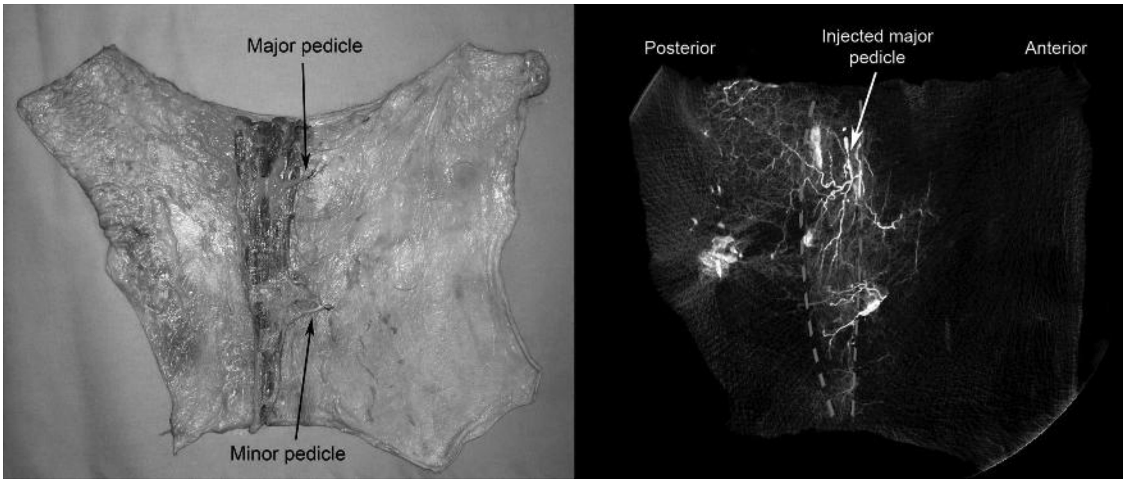

FIGURE 3. Left, Photograph of cadaveric circumferential thigh tissue, including the gracilis muscle. The margins of the flap are the midlateral thigh, groin crease, gluteal crease, and superior patella. Right, 3D CTA image of the flap. The red dotted lines depict the margins of the gracilis muscle. Contrast injection of the major gracilis pedicle showed a cutaneous vascular territory that extended more posteriorly than anteriorly.

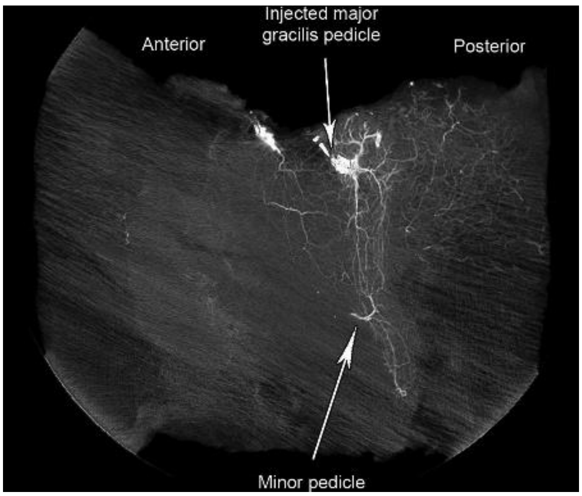

FIGURE 4. Second example of a 3D CTA of the circumferential thigh skin. Contrast injection of the major gracilis pedicle showed a cutaneous vascular territory that extended more posteriorly than anteriorly.

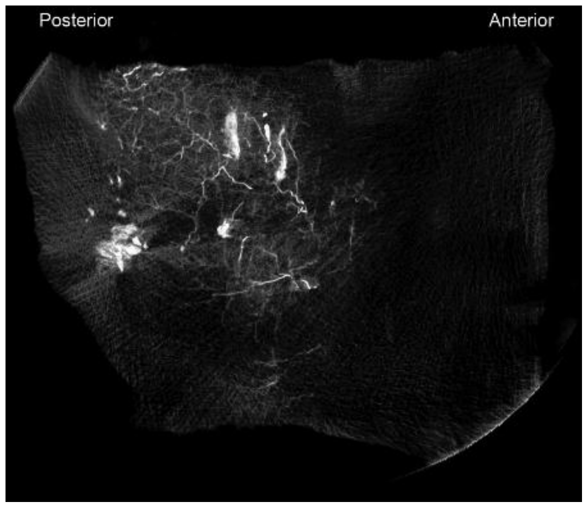

FIGURE 5. Three-dimensional CTA of the circumferential thigh skin, with removal of gracilis muscle. This demonstrates the vascularity of the adipocutaneous tissue above the muscle.

orly and posteriorly was calculated using the paired student *t* test on Microsoft Excel.

Weight and Volume

After CT scanning, the flaps were incised to include only tissue that was perfused with contrast. This was done initially by viewing the images and measuring the extent of the vascular territory from the major pedicle, and then while making incisions, looking out for the white barium-gelatin contrast still in the tissue vasculature (contrast is solidified after freezing). This "perfused" tissue is then measured for weight and volume.

RESULTS

The mean muscle length was 35.4 cm. The mean muscle widths at the major and minor pedicles were 5.4 and 2.7 cm, respectively. The recorded measurements of the major and minor pedicles are summarized in Table 1. The minor pedicle of the gracilis was found to have a common arterial input with a large pedicle of the sartorius in all cases (Fig. 1).

A total of 43 perforators were dissected, with median of 4 cutaneous perforators per flap, range 3 to 8 (Table 2). The mean external diameter of the perforators was 0.61 mm. Locations of the perforators that are 0.5 mm or larger are mapped out in Figure 2 (n = 26). The majority of the musculocutaneous perforators 0.5 mm or larger was found at 14% to 45% of the relative length of the gracilis muscle (0 is origin of muscle from pubic tubercle) and 7 to 38 mm from the anterior border of the gracilis. The septocutaneous perforators were found anterior to the gracilis muscle (0 on the y-axis of Fig. 2) and were located 24% to 74% of the relative length of the gracilis muscle.

Tissue perfused with contrast had a mean weight of 573 g (range: 313–812 g) and volume of 617 mL (range: 330–850 mL).

TABLE 3. Extent of Cutaneous Perfusion Based on Injection of Contrast Into Major Gracilis Pedicle

Flap	Thigh Width*/mm	Extent of Perfusion† on Posterior Thigh/mm	Extent of Perfusion† on Anterior Thigh/mm	Posterior Perfusion as Percentage of Thigh Width‡	Anterior Perfusion as Percentage of Thigh Width‡
1	267	167	88	62.8	33.2
2	215	157	147	72.9	68.2
3	198	124	60	62.6	30.5
4	193	96	53	49.9	27.3
5	215	205	96	95.3	44.7
6	272	166	100	61.0	36.8
7	301	131	103	43.5	34.4
8	287	173	111	60.3	38.7
9	218	158	82	72.5	37.5
10	248	170	78	68.6	31.2
Mean	241.4	154.8	91.8	64.9	38.2
SD (range)	39 (193–301)	30 (96–173)	27 (53–147)	14.1 (43.5–95.3)	11.6 (27.3–68.2)

*Thigh width was defined as the length between the midlateral and midmedial lines of each thigh.
†Transversely, medial to lateral direction.
‡$P < 0.05$, using the paired student t test.
SD indicates standard deviation.

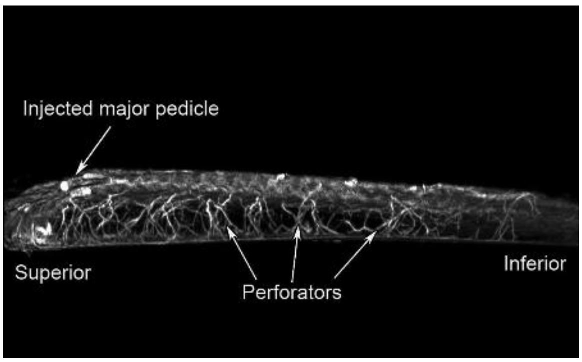

FIGURE 6. Lateral view of a 3D CTA of the thigh skin, with overlying gracilis muscle. Note the numerous perforators running from the muscle to the dermis, especially in the superior region.

3D CT Angiography (CTA)

Three-dimensional images from contrast injection of the major gracilis pedicle showed a cutaneous vascular territory that extended more posteriorly than anteriorly (Figs. 3–5). The extent of cutaneous perfusion on the posterior thigh was found to be a mean of 65% of the thigh width. Maximum was 95% of posterior thigh width. In comparison, contrast perfusion in the anterior thigh was found to extend to merely 38% of the thigh width, $P < 0.05$ (Table 3).

Presence of contrast was also more concentrated in the superior half of the thigh, and extended inferiorly only in the tissue overlying the distal the gracilis muscle (Figs. 5, 6). Contrast perfusion was also frequently found in the vascular territory of the sartorius muscle (Fig. 7).

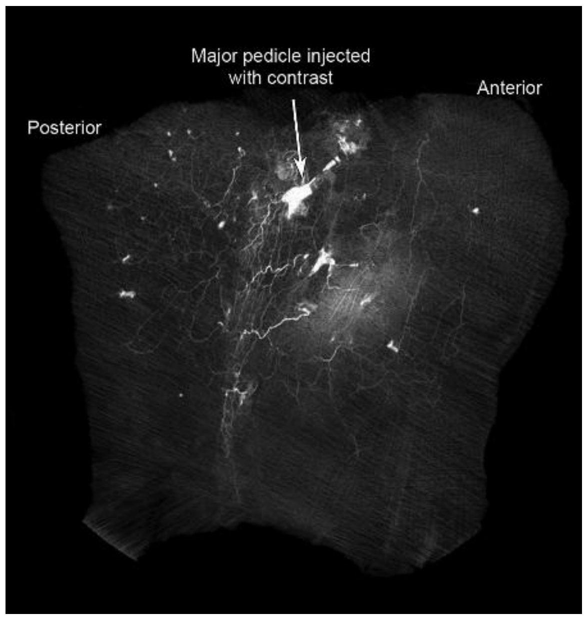

FIGURE 7. Three-dimensional CTA of circumferential thigh skin, with contrast injection into the major pedicle of the gracilis muscle. Contrast perfusion was sometimes found in the vascular territory of the sartorius muscle.

CLINICAL EXAMPLES

Case 1

A 41-year-old patient presented with bilateral severe capsular contractures of previously reconstructed breasts with latissimus dorsi flaps and implants after mastectomies for breast cancer (Fig. 8). The patient's abdomen was not suitable as a flap donor site; therefore, bilateral extended TMG flaps were performed after removal of both breast implants and capsulectomies. The larger extended TMG flap had a transverse skin paddle measuring 38 × 10 cm, with the distance between the posterior border of the gracilis muscle and the posterior tip of the flap measuring 20 cm. Both great saphenous veins were preserved during flap harvests. The superior incision of the skin paddles were continued along the infragluteal creases. We undermined the distal thigh skin beyond the inferior skin incisions to recruit further subcutaneous tissue to increase the bulk of the flap[14] (Fig. 9). The gracilis pedicles were dissected all

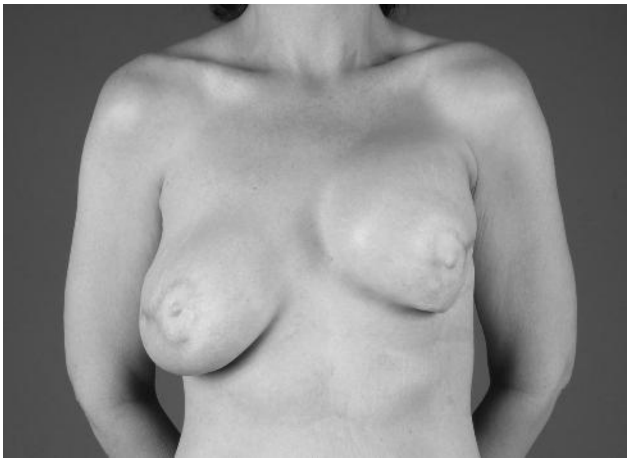

FIGURE 8. Preoperative photograph of patient with severe bilateral breast capsular contractures.

FIGURE 10. The flap was turned 180 degrees onto itself to form a "teardrop" shaped breast mound. Immediate nipple reconstruction can also be performed on-table.

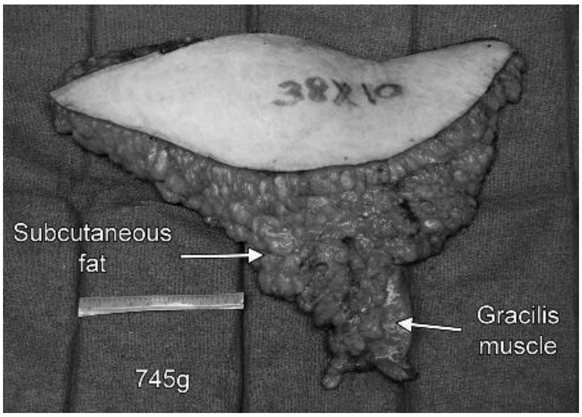

FIGURE 9. TMG flap after ligation of the pedicle. Extension of the flap can be in the horizontal direction (lower buttock region) and in the vertical direction (subcutaneous tissue overlying gracilis muscle).

FIGURE 11. Side view of reconstructed left breast with extended TMG flap immediately postoperatively.

the way up to its origin from the femoral artery, and measured 7 cm in length in both cases. The external diameters of the arteries were 1.7 to 1.8 mm, and the veins were 2.0 to 2.5 mm. Both flap pedicles were anastomosed to the contralateral internal mammary arteries and veins. The smaller flap weighed 585 g, and the larger was 745 g. Each flap was turned 180 degrees onto itself to form a "teardrop," and shaped to become a breast mound (Fig. 10). Nipple reconstruction was also performed on-table both times (Fig. 11). The patient's length of stay was 3 days postoperatively. She suffered no complications, and both flaps as well as both donor sites all healed well (Figs. 12, 13).

Case 2

A 48-year-old patient presented with right-sided breast cancer and required prophylactic mastectomy for her left breast (Fig. 14). A bilateral skin-sparing mastectomy and immediate reconstruction with extended TMG flaps were planned. To harvest further tissue from the medial thigh, trilobed TMG flaps were raised (Figs. 15, 16), with beveling of the edges between the horizontal and vertical limbs. The posterior tips of the flaps did not extend past the posterior thigh midline. The harvested flaps weighed 560 g for the right side, and 760 g for the left. The larger flap measured 35 cm horizontally and

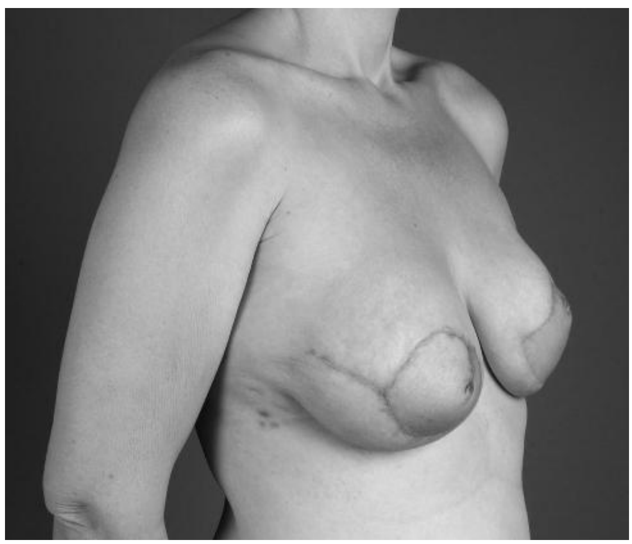

FIGURE 12. Postoperative photograph of patient with extended TMG flaps for bilateral breast reconstruction.

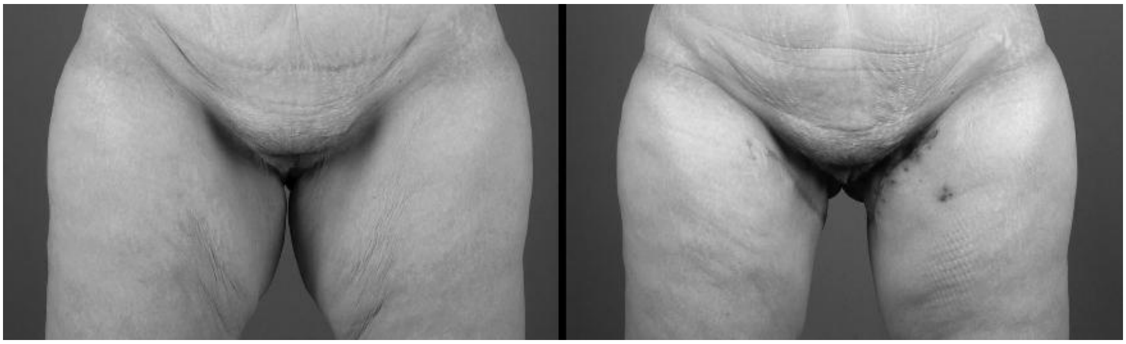

FIGURE 13. Left, Preoperative photograph of the donor sites. Right, Postoperative photograph, demonstrating that the donor sites on the inner thighs do not result in any contour deformity, and can even help to confer a better silhouette.

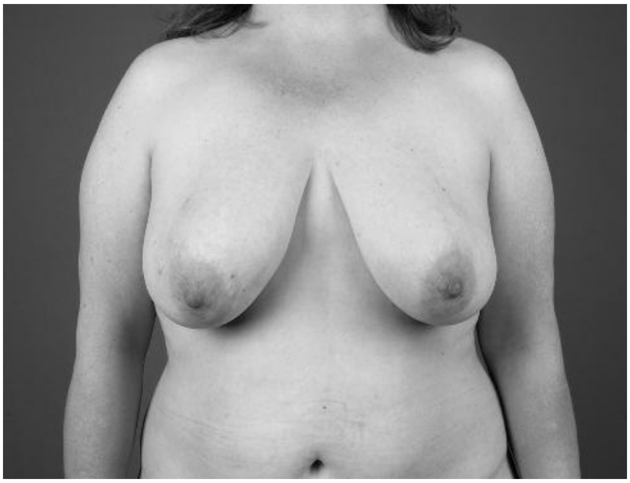

FIGURE 14. Preoperative photograph of patient in Case 2.

FIGURE 15. Trilobed TMG flap marked out on the medial thigh.

18 cm vertically. The vertical and posterior limbs were sutured together side-by-side. The anterior limb was placed under the flap to form the deep section of the breast mound, thus providing medial fullness and better projection. The flaps were deepithelialized except for the nipple-areolar area and inset beneath the skin-sparing mastectomy flaps. Her length of stay in hospital was 5 days. One week

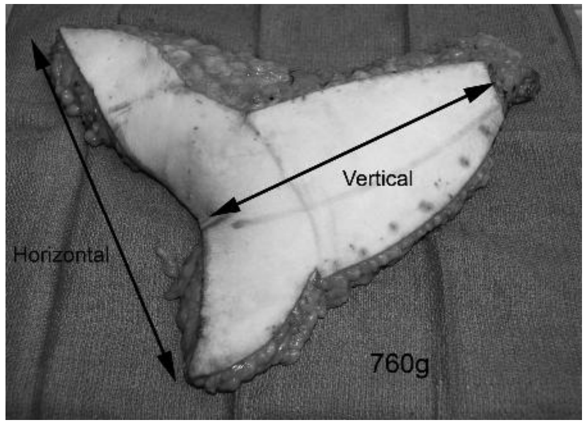

FIGURE 16. Trilobed TMG flap laid out flat.

later, she presented for follow-up with a 80-mL seroma in her right breast, which was aspirated, and she had no further problems with the flaps or donor sites (Figs. 17, 18).

DISCUSSION

Our study could be considered as an investigation of the angiosome of the medial circumflex femoral branch providing the pedicle to the gracilis muscle. We have found that in our perfusion studies involving cadaveric tissue, they always underestimate the true extent of perfusion in vivo.[19–24]

The TMG flap was originally designed to be centered over the major pedicle.[9–11] However, since then, other authors have reported placing the flap more posteriorly.[13,14] Reasons cited were to minimize visible scarring anteriorly and the possibility of harvesting a greater volume of adipose tissue. Schoeller et al introduced the Siamese flap combining the TMG and infragluteal flaps[25] for extra-large reconstructions. Intraoperatively, they noted that even after the division of the infragluteal pedicle, this extra-large flap was still bleeding at the wound edges, which was not surprising in light of the results of our study, in which the cutaneous vascular territory of the major pedicle of the gracilis was found to be concentrated in the superoposterior region of the thigh. A study of Yousif et al showed that vascularity of the TMG flap is orientated transversely, and branches of perforators traveled more than 5 cm beyond the posterior margin of the gracilis muscle.[11] The results of 3D CT demonstrate that posterior thigh perfusion extends up to a mean of 65% of thigh width. This is advantageous, as not only is the posterior thigh tissue better vascularized than the anterior, but it is also thicker and can give greater flap bulk. However, although we have had success-

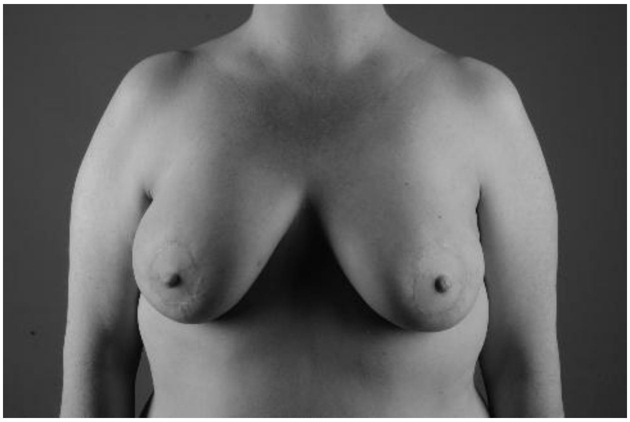

FIGURE 17. Postoperative photograph of patient after bilateral breast reconstruction with trilobed TMG flaps.

FIGURE 18. Close-up of donor sites on medial thighs, showing healed T-shaped scars.

ful TMG flaps extending past the posterior thigh midline, we have ceased to routinely use tissue past this level (as in Case 2). This was due to some cases of fat necrosis, which occurred in the area harvested past the thigh midline.

Perfusion was also found to extend downward, in the area overlying the distal gracilis muscle. In the study, Peek et al demonstrated this too, in their extended gracilis perforator flaps, by maintaining the intramuscular anastomosis between the major and minor pedicles, thus recruiting the angiosome of the minor pedicle.[15] These interpedicle connections were preserved in all our specimens as whole gracilis muscles were harvested with the flaps. We took advantage of the inferior perfusion by adding a vertical component to our extended TMG flaps, either by recruiting the inferior subcutaneous fat (from undermining the skin inferior to the lower incision) or by taking the skin as well, resulting in a modified "fleur-de-lys" skin paddle (Figs. 15, 16). For the former method, harvesting the medial thigh fat is limited more by closure than by vascularity. Removing excessive tissue may not only reduce padding and potentially cause a contour deformity but also increase the likelihood of skin flap ischemia (from excessive thinning) that causes necrosis and poor wound healing.

The latter method gives a trilobed flap, and this allows harvest of even more volume for the flap. We encourage using a beveling technique when dissecting the edges between the horizontal and vertical limbs (resulting in less of a T-shape and more of a triangle when viewing the underside of the flap). This is done to avoid resection of the linking vessels between the horizontal and vertical limbs, thus ensuring survival of the flap tips. The trilobed TMG flap can also result in improved contouring of the medial thigh. Recent medial thighplasty techniques have incorporated a vertical incision for removal of redundant skin.[26,27] This results in a horizontal pull medially, and allows for both skin and thigh circumference reduction. The downside of this, of course, is a more noticeable scar, whereas the undermining method maintains a transverse scar only. The functional loss of the gracilis muscle would not be different compared with the usual TMG flap, which is minimal.

CONCLUSIONS

The dimensions of a TMG flap can be increased, both horizontally (superoposterior thigh) and vertically. The vertical portion can be harvested either by undermining the skin inferior to the lower transverse skin incision or by raising a trilobed skin paddle to harvest even more tissue from the medial thigh. With these modifications, the TMG flap can achieve greater volume and be applied to larger breast reconstructions.

REFERENCES

1. Hartrampf CR, Scheflan M, Black PW. Breast reconstruction with a transverse abdominal island flap. *Plast Reconstr Surg*. 1982;69:216–225.
2. Allen RJ, Treece P. Deep inferior epigastric perforator flap for breast reconstruction. *Ann Plast Surg*. 1994;32:32–38.
3. Blondeel PN, Boeckx WD. Refinements in free flap breast reconstruction: the free bilateral deep inferior epigastric perforator flap anastomosed to the internal mammary artery. *Br J Plast Surg*. 1994;47:495–501.
4. Arnez ZM, Khan U, Pogorelec D, et al. Breast reconstruction using the free superficial inferior epigastric artery (SIEA) flap. *Br J Plast Surg*. 1999;52:276–279.
5. Allen RJ, Tucker C Jr. Superior gluteal artery perforator free flap for breast reconstruction. *Plast Reconstr Surg*. 1995;95:1207–1212.
6. Granzow JW, Levine JL, Chiu ES, et al. Breast reconstruction with gluteal artery perforator flaps. *J Plast Reconstr Aesthet Surg*. 2006;59:614–621.
7. Paletta CE, Bostwick J III, Nahai F. The inferior gluteal free flap in breast reconstruction. *Plast Reconstr Surg*. 1989;84:875–883; discussion 884–875.
8. de Weerd L, Elvenes OP, Strandenes E, et al. Autologous breast reconstruction with a free lumbar artery perforator flap. *Br J Plast Surg*. 2003;56:180–183.
9. Arnez ZM, Pogorelec D, Planinsek F, et al. Breast reconstruction by the free transverse gracilis (TUG) flap. *Br J Plast Surg*. 2004;57:20–26.
10. Wechselberger G, Schoeller T. The transverse myocutaneous gracilis free flap: a valuable tissue source in autologous breast reconstruction. *Plast Reconstr Surg*. 2004;114:69–73.
11. Yousif NJ, Matloub HS, Kolachalam R, et al. The transverse gracilis musculocutaneous flap. *Ann Plast Surg*. 1992;29:482–490.
12. Schoeller T, Wechselberger G. Breast reconstruction by the free transverse gracilis (TUG) flap. *Br J Plast Surg*. 2004;57:481–482.
13. Schoeller T, Huemer GM, Wechselberger G. The transverse musculocutaneous gracilis flap for breast reconstruction: guidelines for flap and patient selection. *Plast Reconstr Surg*. 2008;122:29–38.
14. Fattah A, Figus A, Mathur B, et al. The transverse myocutaneous gracilis flap: technical refinements. *J Plast Reconstr Aesthet Surg*. 2010;63:305–313.

15. Peek A, Muller M, Ackermann G, et al. The free gracilis perforator flap: anatomical study and clinical refinements of a new perforator flap. *Plast Reconstr Surg*. 2009;123:578–588.
16. Vega SJ, Sandeen S, Bossert R, et al. Gracilis myocutaneous free flap in autologous breast reconstruction. *Plast Reconstr Surg*. 2009;124:1400–1409.
17. Fansa H, Schirmer S, Warnecke IC, et al. The transverse myocutaneous gracilis muscle flap: a fast and reliable method for breast reconstruction. *Plast Reconstr Surg*. 2008;122:1326–1333.
18. Tan BK, Ng RT, Tay NS, et al. Tissue micro angiography using a simplified barium sulphate cadaver injection technique. *Ann Acad Med Singapore*. 1999;28:152–154.
19. Saint-Cyr M, Schaverien M, Arbique G, et al. Three- and four-dimensional computed tomographic angiography and venography for the investigation of the vascular anatomy and perfusion of perforator flaps. *Plast Reconstr Surg*. 2008; 121:772–780.
20. Schaverien M, Saint-Cyr M, Arbique G, et al. Arterial and venous anatomies of the deep inferior epigastric perforator and superficial inferior epigastric artery flaps. *Plast Reconstr Surg*. 2008;121:1909–1919.
21. Schaverien M, Saint-Cyr M, Arbique G, et al. Three- and four-dimensional arterial and venous anatomies of the thoracodorsal artery perforator flap. *Plast Reconstr Surg*. 2008;121:1578–1587.
22. Schaverien M, Saint-Cyr M, Arbique G, et al. Three- and four-dimensional computed tomographic angiography and venography of the anterolateral thigh perforator flap. *Plast Reconstr Surg*. 2008;121:1685–1696.
23. Wong C, Saint-Cyr M, Arbique G, et al. Three- and four-dimensional computed tomography angiographic studies of commonly used abdominal flaps in breast reconstruction. *Plast Reconstr Surg*. 2009;124: 18–27.
24. Wong C, Saint-Cyr M, Rasko Y, et al. Three- and four-dimensional arterial and venous perforasomes of the internal mammary artery perforator flap. *Plast Reconstr Surg*. 2009;124:1759–1769.
25. Schoeller T, Huemer GM, Kolehmainen M, et al. A new "Siamese" flap for breast reconstruction: the combined infragluteal-transverse myocutaneous gracilis muscle flap. *Plast Reconstr Surg*. 2005;115:1110–1117.
26. Kenkel JM, Eaves FF III. Medial thigh lift. *Plast Reconstr Surg*. 2008;122: 621–622.
27. Mathes DW, Kenkel JM. Current concepts in medial thighplasty. *Clin Plast Surg*. 2008;35:151–163.

The Perforasome Theory: Vascular Anatomy and Clinical Implications

Michel Saint-Cyr, M.D.
Corrine Wong, M.R.C.S.
Mark Schaverien, M.R.C.S.
Ali Mojallal, M.D.
Rod J. Rohrich, M.D.

Dallas, Texas

Background: A clear understanding of the vascular anatomy of an individual perforator relative to its vascular territory and flow characteristics is essential for both flap design and harvest. The authors investigated the three-dimensional and four-dimensional arterial vascular territory of a single perforator, termed a "perforasome," in major clinically relevant areas of the body.

Methods: A vascular anatomy study was performed using 40 fresh cadavers. A total of 217 flaps and arterial perforasomes were studied. Dissection of all perforators was performed under loupe magnification. Perforator flaps on the anterior trunk, posterior trunk, and extremities were studied. Flaps underwent both static (three-dimensional) and dynamic (four-dimensional) computed tomographic angiography to better assess vascular anatomy, flow characteristics, and the contribution of both the subdermal plexus and fascia to flap perfusion.

Results: The perfusion and vascular territory of perforators is highly complex and variable. Each perforasome is linked with adjacent perforasomes by means of two main mechanisms that include both direct and indirect linking vessels. Vascular axis follows the axiality of linking vessels. Mass vascularity of a perforator found adjacent to an articulation is directed away from that same articulation, whereas perforators found at a midpoint between two articulations, or midpoint in the trunk, have a multidirectional flow distribution.

Conclusions: Each perforator holds a unique vascular territory (perforasome). Perforator vascular supply is highly complex and follows some common guidelines. Direct and indirect linking vessels play a critical part in perforator flap perfusion, and every clinically significant perforator has the potential to become either a pedicle or free perforator flap. (*Plast. Reconstr. Surg.* 124: 1529, 2009.)

Increased knowledge of vascular anatomy has inevitably led to innovations in flap design and use in the clinical arena. The evolution of random-pattern flaps to fasciocutaneous flaps to myocutaneous flaps and finally to the perforator flaps has followed a linear progression, largely because of the pioneering vascular anatomy studies produced by Manchot, Salmon, Cormack, Lamberty, Taylor, Palmer, Morris, Tang, and others.[1–8] The information derived from such work has fueled an evolution in flap design and clinical applications. The ultimate goal of reconstruction is to match optimal tissue replacement with minimal donor-site expenditure while maintaining function. Perforator flaps meet these goals and are the result of over 30 years of evolution in flap refinements and design.

In conjunction with our increased knowledge of vascular anatomy of perforator flaps, their clinical use has been pioneered by the works of Koshima et al.[9–16] The perforator flap era began in 1989, when Koshima and Soeda first described an inferior epigastric artery skin flap with the rectus

From the Department of Plastic Surgery, University of Texas Southwestern Medical Center.
Received for publication January 9, 2009; accepted May 4, 2009.

DOI: 10.1097/PRS.0b013e3181b98a6c

Disclosure: *The authors have no financial interests in this research project or in any of the techniques or equipment used in this study.*

Supplemental digital content is available for this article. Direct URL citations appear in the printed text; simply type the URL address into any web browser to access this content. Clickable links to the material are provided in the HTML text of this article on the *Journal*'s Web site (www.PRSJournal.com).

abdominis muscle for reconstruction of floor-of-mouth and groin defects.[9] These authors noted that a large skin flap could survive without muscle, based on a single perforator. Kroll and Rosenfield also suggested that perforator flaps combined the reliable blood supply of myocutaneous flaps without deteriorating donor-site morbidity.[17] Numerous other authors and pioneers in the field of perforator flap surgery have also been instrumental in providing us with further clinical experience and expertise in the harvest of perforator flaps. Among these authors are Allen, Blondeel, Kroll, Koshima, Angrigiani, Hallock, Neligan, Morris, Wei, and many others.[17–23]

In essence, any clinically relevant perforator has the potential to be harvested as either a pedicle perforator flap or a free flap, depending on the diameter and length of the source artery and vein. With over 350 perforators in the body, a myriad of options exist for either traditional or free-style perforator flaps. The only limiting factors are the length and diameter of the source vessels for a free-style free flap, and the location of the pivot point perforator relative to the defect for pedicle perforator flaps. To further advance the evolution of perforator flaps, it is essential to understand the vascular anatomy of an individual perforator relative to its vascular territory and flow characteristics. Knowledge of the direction and the axiality of flow within the tissue is also of prime importance when designing perforator flaps, whether pedicled or free.

Although Taylor and Palmer have been instrumental in increasing our knowledge of vascular anatomy by means of the angiosome concept, this theory is based on the vascular supply of source arteries.[3,5,24] In the dawning of an era of perforator flaps, the impetus of vascular knowledge has shifted from the source artery to the perforator itself. A further consideration is to determine the dynamic vascularity of perforator flaps compared with whole body static imaging, which does not provide an accurate description of a single perforator's vascular distribution and flow characteristics.

To truly understand and determine a single perforator's vascular territory, this perforator must be cannulated and injected individually. This is clinically relevant, as many perforator flap designs are based on a single perforator. Therefore, knowledge of the axiality of blood flow, connections with adjacent perforators, and contribution of the subdermal plexus and fascia are all vital when designing perforator flaps.

This study represents the accumulation of 3 years of research on the vascular anatomy of perforator flaps,[25–28] and over 200 flaps were studied in combination with static and dynamic computed tomographic angiography imaging. Note that most flaps involved perforators that were individually cannulated to assess the individual perforator vascular territories, which we have termed a "perforasome" (arterial) (Fig. 1). Others had the source vessel injected (e.g., radial and deep inferior epigastric artery) to study orientation of linking vessels between perforators. The goals of this study are to report arterial perforasomes in the body to better guide perforator flap design in clinical use.

MATERIALS AND METHODS

A vascular anatomy study was performed using 40 fresh cadavers acquired through the Willed Body Program at the University of Texas Southwestern Medical Center. A total of 217 flap perforasomes were studied. All of these were fresh cadaveric specimens, and dissection of all perforators was performed under loupe magnification.

Injection of a dilute methylene blue solution through all perforators enabled identification of the latter and also allowed identification of any leaking in the periphery of the flap or undersur-

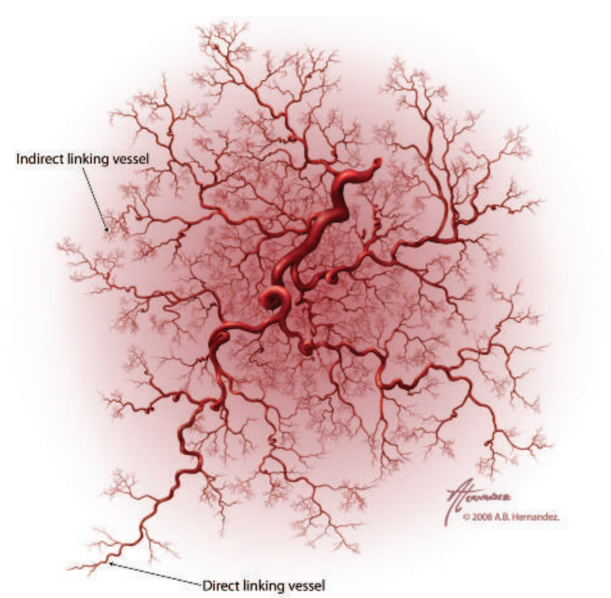

Fig. 1. Perforators have a distinct arterial and venous vascular territory. This image depicts the vascular arterial anatomy of a perforasome. Note the dense vascular network centered around the perforator that decreases progressively toward the periphery. Large linking vessels branch peripherally in multiple directions away from the perforator origin.

face of the flap. Perforator flaps on the anterior trunk studied were the internal mammary artery perforator flap, the superior epigastric artery perforator flap, the deep inferior epigastric artery perforator flap, and supraclavicular artery perforator flap. Posterior trunk flaps included the thoracodorsal artery perforator flap, the posterior intercostal artery perforator flap, the lumbar artery perforator flap, and the superior gluteal artery perforator and inferior gluteal artery perforator flaps.

For the upper extremity, we studied the ulnar artery perforator flap, the radial artery perforator flap, and the posterior interosseous perforator and the Quaba flaps (dorsal metacarpal artery perforator flap). In the lower extremities, we studied the anterolateral thigh flap, the anteromedial thigh flap, the anterior tibial artery perforator flap, the peroneal artery perforator flap, and the posterior tibial artery perforator flap.

All surgical landmarks relevant to the flap design were marked, and each perforator flap was dissected based on the largest perforator originating from its own main source pedicle. After flap dissection, the perforator was cannulated using a 24-gauge butterfly catheter (0.7 mm in diameter) (BD Insyte; Becton-Dickinson SA, Madrid, Spain). Methylene blue solution was infiltrated into the flap to identify vascular leaks, which were then either coagulated using bipolar cautery or ligated using silk sutures. The use of surgical clips was avoided to prevent computed tomographic angiography artifact.

Flap Harvesting Technique

Skin flaps on the trunk, such as internal mammary artery perforator, posterior intercostal artery perforator, and superior and inferior gluteal artery perforator flaps, were harvested from midline to midaxillary line. The abdominal flaps and lumbar flaps encompassed the midline to determine perforator cross-over through the midline.

For upper and lower extremities, skin incisions were made opposite the source artery of interest (e.g., on the ulnar side of the forearm if radial artery perforators were studied). Borders of flaps were the most distal and proximal articulations.

For the anterior trunk, a total of 26 internal mammary artery perforator flaps were injected. Flaps were harvested by dissecting the complete anterior chest wall skin from the midline to the midaxial line laterally and from the supraclavicular region superiorly to the costal chondral margin inferiorly.

A total of 73 abdominal flaps were injected for the study of deep inferior epigastric artery perforators ($n = 60$) and superior epigastric artery perforators ($n = 13$). Analysis of the superior epigastric artery perforator flap was performed by harvesting skin along the superior epigastrium, and evaluation of the deep inferior epigastric artery perforators was performed by harvesting the totality of the abdominal skin flap with cannulation of individual perforators from the lateral and medial row.

For the posterior trunk, complete hemiback flaps were harvested to analyze the vascular anatomy of the thoracodorsal artery flap[19] and posterior dorsal intercostal artery perforator flap.[11] The whole lumbar skin (no incision through the midline) was harvested from the level of T12 to the level of the iliac crest to study the lumbar artery perforators.[4] The lateral intercostal artery perforator flaps[6] were analyzed using the same technique. For the gluteal region, eight elliptical skin flaps were harvested from the midline to the iliac crest. Perforators of the superior and inferior gluteal arteries were injected and examined.

We examined the anterior thigh by harvesting the skin with midaxial incisions, laterally and medially. The limits of the skin flap were the groin crease superiorly and the suprapatellar region inferiorly. For the perforators of the posterior tibial artery, anterior tibial artery, and peroneal artery, circumferential skin was dissected from the leg, with the incision performed directly 180 degrees opposite the major source artery to maximize skin territory.

Dynamic Computed Tomographic Scan Protocol: Four-Dimensional Computed Tomographic Angiography

Four-dimensional computed tomographic angiography is similar to three-dimensional computed tomographic angiography but with the added fourth element of time. Flaps are scanned with contrast medium injected simultaneously during a predetermined time interval to appreciate the characteristics and distribution of vascular perfusion. In contrast, three-dimensional computed tomographic angiography involves scanning flaps that have already been preinjected and results in a static image only.

Before scanning, each flap was set in individual custom-designed Styrofoam trays to maintain their shape and orientation (as the flap is scanned at 30 degrees from vertical). The flaps were also placed skin downward to avoid pressure on the pedicle and to minimize the risk of increased resistance during vascular imaging and perfusion. Iodinated contrast (Isovue; Bracco Diagnostics, Inc., Princeton, N.J.) was heated to 37°C (to reduce viscosity and improve vascular filling) before the syringe was filled. The volumes of contrast medium required for flap imaging range from 2 to 5 ml, depending on flap size.

Single vessel/perforator injections were carried out with a Harvard precision pump (PHD 2000; Harvard Apparatus, Inc., Holliston, Mass.) running at 0.5 ml/minute, and the flaps were subjected to dynamic computed tomographic scanning using a GE Lightspeed 16-slice scanner (General Electric, Milwaukee, Wis.) set to perform 0.625-mm slices using a 0.5-second rotation time. Each scan was set to 80 kVp and the current ran at 300 mA. Scans were repeated at 0.125-ml increments (every 15 seconds) for the first 1 ml, and then at 0.5-ml increments (every 60 seconds) for the next 2 to 4 ml, thus giving us progressive computed tomographic images over time.[25–28]

Static Computed Tomographic Scan Protocol: Three-Dimensional Computed Tomographic Angiography

The barium-gelatin mixture was prepared by warming 100 ml of normal saline to 40°C and adding 3 g of gelatin while stirring continuously. This was followed by slowly adding 40 g of barium sulfate.[29] This solution was then injected into the investigated perforator artery using the Harvard precision pump running at 1 ml/minute until the vascular tree was saturated (previously repaired leaks would start to leak and had to be recauterized or ligated). The flaps were then frozen for at least 24 hours before computed tomographic scanning.

Three- and four-dimensional images were viewed using the TeraRecon Aquarius workstation (version 3.2.2.1; TeraRecon Inc., San Mateo, Calif.). The volume-rendering function allowed us to produce clear and accurate images of the simulated flaps. Manipulation of static three-dimensional images from different angles enabled us to clearly visualize branching patterns of perforators and the characteristics of their linking vessels. The dynamic images demonstrated the axiality or preferential direction of flow.

RESULTS

The perfusion and vascular territory of perforators is highly complex and variable. Nevertheless, some common principles have been reproduced throughout our multiple perforator injection studies. When perforators are cannulated individually, the flow is multidirectional, as can be seen in Figure 2. Each perforator has its own unique vascular arterial territory, which we termed a perforasome (arterial).

First Principle

Each perforasome is linked with adjacent perforasomes by means of two main mechanisms that include both direct and indirect linking vessels (Fig. 3).

Direct linking vessels are large vessels that communicate directly from one perforator to the next and permit capture of adjacent perforasomes through an interperforator flow mechanism. Large filling pressures or perfusion pressures through a single perforator can allow for large perforator flap harvests, such as the extended anterolateral thigh flap.[30,31] The linking vessels connect multiple perforasomes to one another (Fig. 4). See **Video**, **Supplemental Digital Content 1,** which shows a dynamic computed tomographic angiography scan (anteroposterior view), demonstrating perfusion from the anterolateral thigh flap perforator to the anteromedial thigh perforator by means of large direct linking vessels, ***http://links.lww.com/PRS/A97***. Both direct and indirect linking vessels allow vascular connection between adjacent perforators.

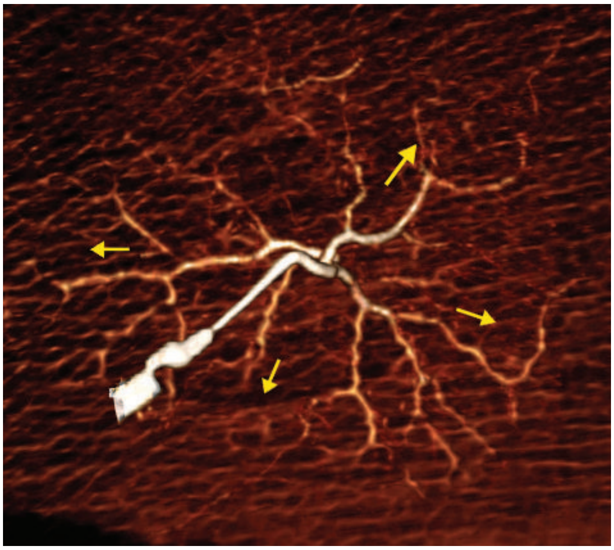

Fig. 2. Static computed tomographic angiography scan of an arterial perforasome demonstrating multidirectional flow. Multiple direct linking vessels can be seen branching away from the cannulated perforator. *Yellow arrows* show direction of flow.

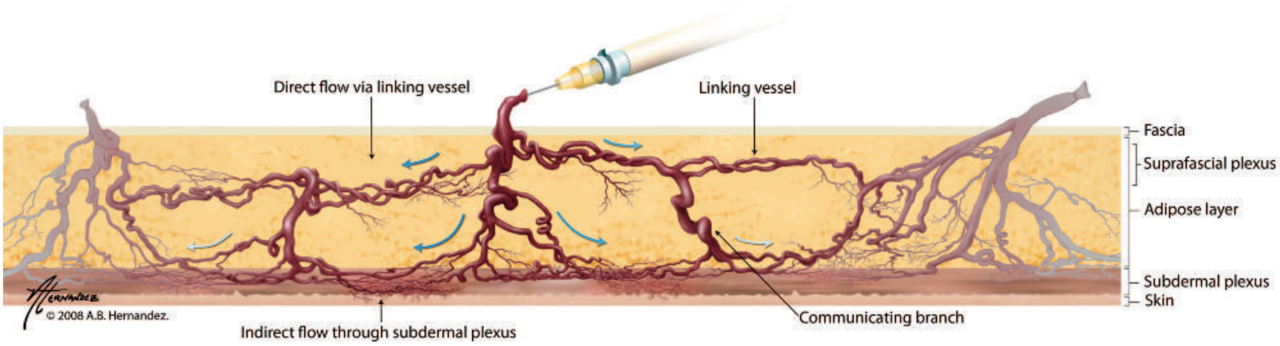

Fig. 3. Interperforator flow occurs by means of direct and indirect linking vessels. Direct linking vessels communicate directly with an adjacent perforator to maintain perfusion, and travel within the suprafascial and adipose tissue layers. Indirect linking vessels communicate with adjacent perforators by means of recurrent flow through the subdermal plexus. Communicating branches between direct and indirect linking vessels are also seen and help maintain vascular perfusion in case of injury.

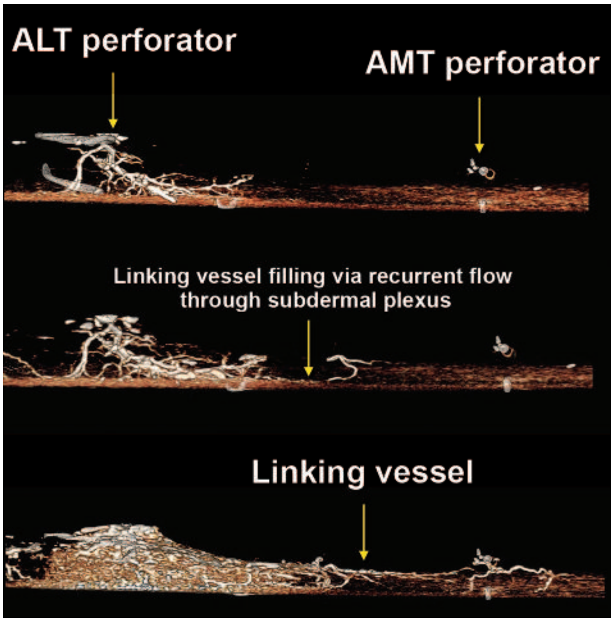

Fig. 4. Dynamic computed tomographic angiography scan (lateral view) showing the linking vessel between the anterolateral thigh perforator (*ALT*) and the anteromedial thigh perforator (*AMT*). Note recurrent flow from the subdermal plexus into a communicating branch that connects with a large direct linking vessel. Flow through communicating branches is bidirectional; therefore, if a vascular injury occurs to either direct or indirect (subdermal plexus) linking vessels, perfusion is still maintained.

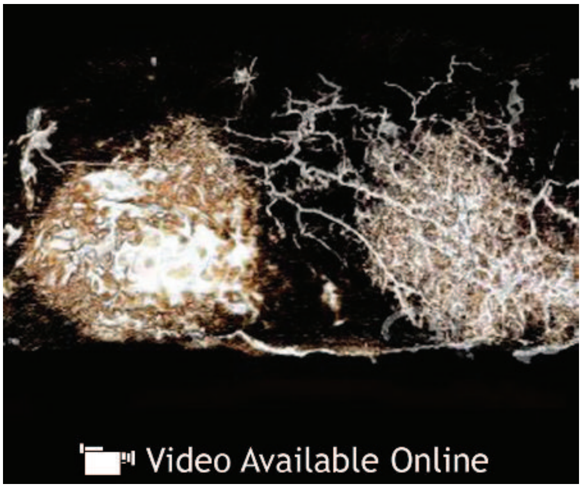

Videos 1 through 4. In Supplemental Digital Content 1 through 4, dynamic computed tomography angiography demonstrates perfusion from the anterolateral thigh flap perforator to the anteromedial thigh perforator and reverse perfusion after cannulation of the anteromedial thigh perforator. Both direct and indirect linking vessels allow vascular connection between adjacent perforators, and the videos show the bidirectional flow that is possible via the communicating branches of these vessels, ***http://links.lww.com/PRS/A97***, ***http://links.lww.com/PRS/A98***, ***http://links.lww.com/PRS/A99***, and ***http://links.lww.com/PRS/A100***.

Supplemental Digital Content 2 shows the same dynamic computed tomographic angiography scan (anteroposterior view) demonstrating reverse perfusion from the anteromedial thigh perforator toward the anterolateral thigh perforator after cannulation of the anteromedial thigh perforator, ***http://links.lww.com/PRS/A98***. This dynamic computed tomographic angiography scan demonstrates the bidirectional flow potential of the direct and indirect linking vessels. **Supplemental Digital Content 3** shows a dynamic computed tomographic angiography scan (lateral view) demonstrating flow by means of direct and indirect linking vessels from the anterolateral thigh flap perforator to the anteromedial thigh flap perforator, ***http://links.lww.com/PRS/A99***. Note flow through the communicating branch that links the indirect linking vessel with the direct linking vessel. **Supplemental Digital Content 4** shows a dy-

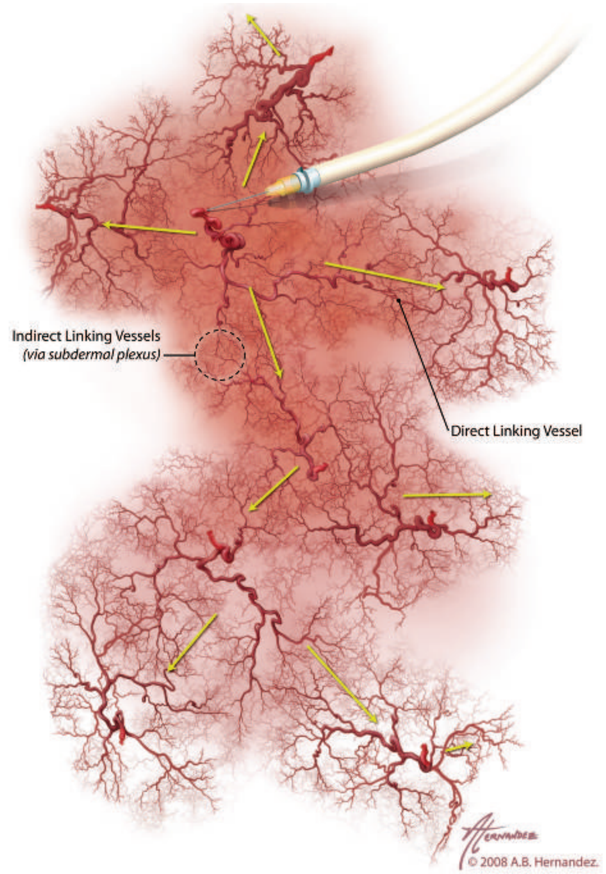

Fig. 5. Interperforator flow occurs from the selected main perforator to multiple adjacent perforators by means of direct linking vessels and indirect linking vessels (recurrent flow from subdermal plexus). High perfusion pressures through the main perforator opens multiple direct and indirect linking vessels and allows perfusion of multiple other perforasomes. In this way, large flaps such as the anterolateral thigh flap can be harvested based on a single perforator.

namic computed tomographic angiography scan (lateral view) demonstrating flow through direct and indirect linking vessels from the anteromedial thigh perforator to the anterolateral thigh perforator, ***http://links.lww.com/PRS/A100***. This dynamic computed tomographic angiography scan demonstrates the bidirectional flow that is possible through the direct and indirect linking vessels. Note also that flow through the communicating branches, which link both direct and indirect linking vessels, can have bidirectional flow as well.

Perforasomes are also linked to one another by indirect linking vessels or recurrent flow through the subdermal plexus (Figs. 5 and 6). These are similar to the choke vessels described by Taylor. In reality, perforators give off oblique and vertical branches to the subdermal plexus, and recurrent flow from the subdermal plexus to adjacent perforator oblique branches allows capture of an adjacent perforasome by means of this recurrent flow.

These two patterns of flow are protective mechanisms that ensure vascular connections between adjacent perforasomes in the event of a vascular injury. We have also found multiple communicating branches that link the direct and indirect linking vessels themselves (Figs. 3 and 7). These numerous communicating branches maintain vascular continuity between both the direct and indirect linking vessels in the coronal, sagittal, and transverse planes. These communicating branches also confer an additional protective mechanism to ensure vascular flow to the skin in the event of damage to either direct or indirect linking vessels.

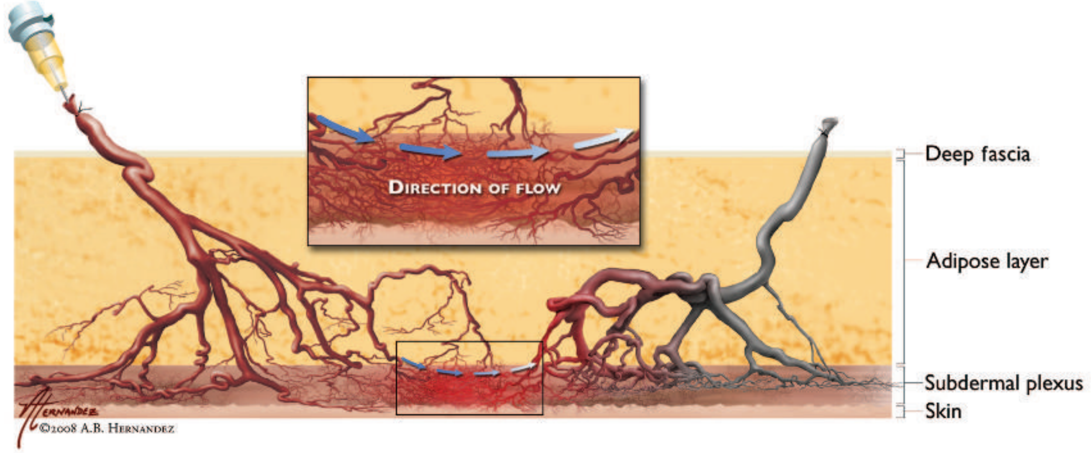

Fig. 6. Lateral view of an indirect linking vessel that maintains perfusion from one perforator to the next by means of recurrent flow from the subdermal plexus.

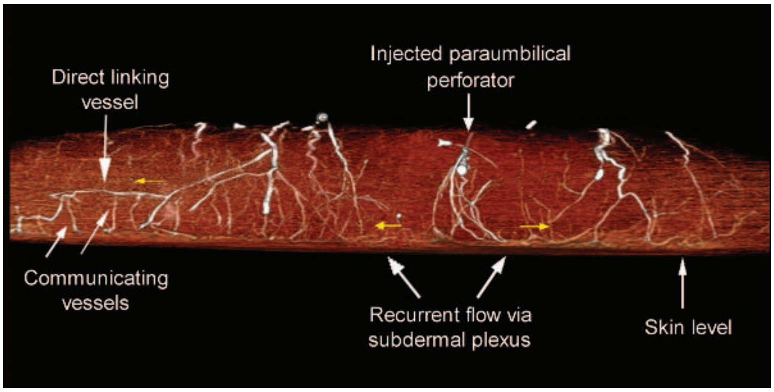

Fig. 7. Transverse view of an abdominal flap, where a paraumbilical perforator was injected with contrast to determine its perforasome. Direct and indirect (recurrent flow through the subdermal plexus) linking vessels are demonstrated. Communicating branches connect the direct and indirect linking vessels. *Yellow arrows* show direction of flow.

Video 5. Supplemental Digital Content 5 shows a dynamic computed tomographic angiography scan (anteroposterior view) after injection of contrast into a thoracodorsal artery perforator, ***http://links.lww.com/PRS/A101*** .

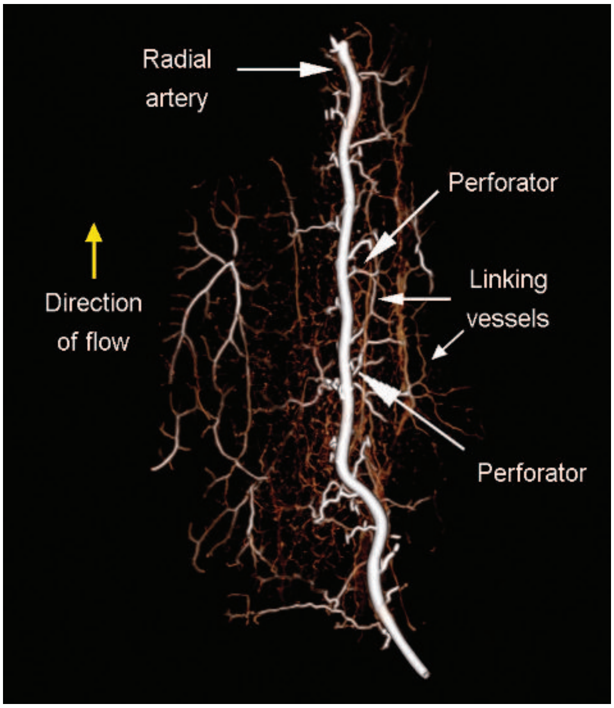

Fig. 8. Computed tomographic angiography scan (anteroposterior view) showing a radial forearm flap in which the radial artery was injected with contrast. Note multiple perforators branching out radial and ulnar from the radial artery. Large direct linking vessels can be seen coursing parallel to the axiality of the limb, allowing perfusion between perforators. *Yellow arrow* shows direction of flow.

Second Principle

Flap design and skin paddle orientation should be based on the direction of the linking vessels, which is axial in the extremities and perpendicular to the midline in the trunk. Orientation of the linking vessels corresponds to the orientation of maximal blood flow, and flap axis should ideally be designed to respect this. Linking vessels in the extremities follow the axiality of the involved limb, whereas axiality of the posterior trunk and chest usually follow the axiality of muscle fibers and ribs (e.g., the thoracodorsal artery perforator flap and the internal mammary artery perforator flap) and are perpendicular to the midline. See **Video, Supplemental Digital Content 5,** which shows a dynamic computed tomographic angiography scan (anteroposterior view) after injection of contrast into a thoracodorsal artery perforator, ***http://links.lww.com/PRS/A101***. The vascular territory of the thoracodorsal artery

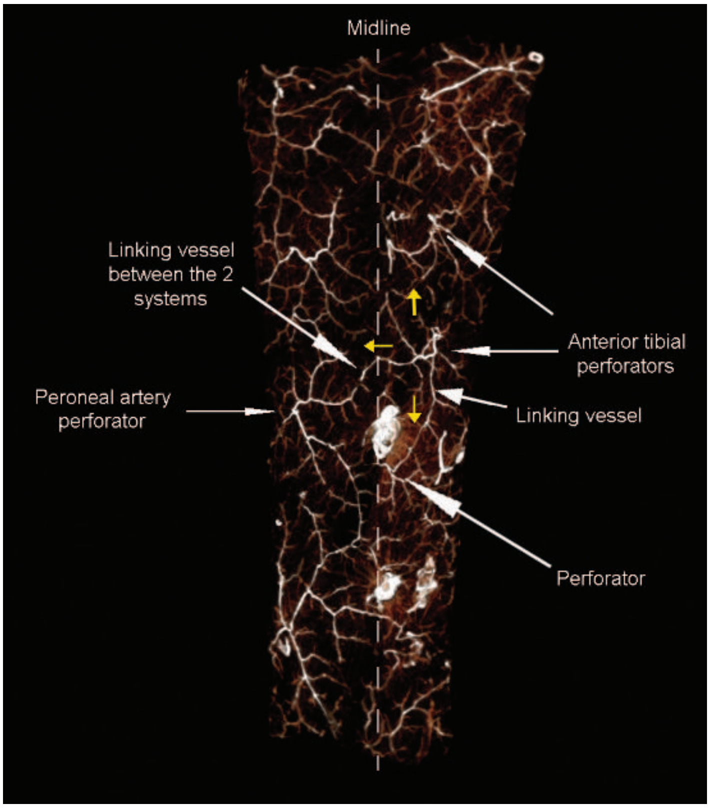

Fig. 9. Computed tomographic angiography scan (anteroposterior view) showing the anterior leg from the knee level to the ankle level. Perforators from both the anterior tibial artery and the peroneal artery have respective direct linking vessels that follow the axiality of the limb and allow interperforator flow. There are also linking vessels that can be seen crossing the midline and that maintain communication between the posteroanterior and anterior tibial artery perforators. *Yellow arrows* show direction of flow.

perforator (perforasome) is demonstrated and large linking vessels are seen coursing parallel to the latissimus dorsi muscle fibers. The axis of flow of the thoracodorsal artery perforator close to the midline follows the orientation of the latissimus dorsi muscle fibers.

The vascular axis follows the axiality of linking vessels, and these linking vessels follow the axiality of the limb for the upper and lower extremities. This is demonstrated in radial artery perforator (Fig. 8), ulnar artery perforator, anterior tibial artery perforator (Fig. 9), peroneal artery perforator (Fig. 10), and posterior tibial artery perforator flaps. The limbs have source arteries that are most often directed axial to the limb themselves. Each axially directed source artery from either the lower or upper extremity provides multiple sequential perforators along its course. Linking vessels allow perforators from the same source artery to communicate with each other and with perforators from adjacent source arteries. To do this effectively, linking vessels have an orientation that is predominantly parallel to the axis of the limbs (Figs. 8 through 10). Perforator flaps should be designed in parallel to the axis of the linking vessels of the limbs to capture the largest and most reliable vascular territory.

Linking vessels in the trunk are commonly directed perpendicular to the midline and follow an oblique transverse direction, parallel to the cutaneous dermatomes. This is shown in the supraclavicular artery perforator (Fig. 11), internal mammary artery perforator (Fig. 12), paraumbilical perforator (Fig. 13), superior epigastric artery perforator (Fig. 14), posterior intercostal artery perforator (Fig. 15), lumbar artery perforator (Fig. 16), and superior gluteal artery perforator (Fig. 17). Again, multiple communicating branches

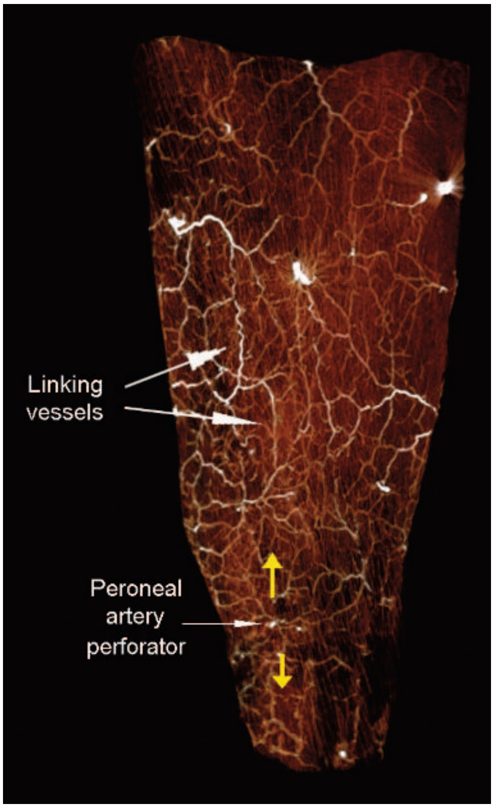

Fig. 10. Computed tomographic angiography scan (anteroposterior view) showing the skin from the posterior leg from the knee level to the ankle level. The peroneal artery perforator was injected with contrast. Note direction of large linking vessels that follows the axiality of the limb. *Yellow arrows* show direction of flow.

between linking vessels are found in the anterior and posterior trunk. Perforators that are found close to the midline and that follow a vertical row distribution (e.g., deep inferior epigastric artery perforator and internal mammary artery perforator flaps) usually have contralateral perforators that are also close to the midline. Perforasome flow is multidirectional and crosses the midline in many cases (e.g., deep inferior epigastric artery perforator flap), but preferential flow is directed away from the midline toward the lateral trunk borders. In instances where multiple perforators are found along a vertical row and close to the midline bilaterally (e.g., deep inferior epigastric artery perforator, internal mammary artery perforator, and lumbar artery perforator), flow is directed away from the midline to provide adequate vascularity to the lateral trunk region, which has a less dense perforator population. The anterior and posterior midlines of the trunk are heavily populated in perforators (e.g., internal mammary artery perforator, superior epigastric artery perforator, deep inferior epigastric artery perforator, posterior intercostal artery perforator, lumbar artery perforator, and superior gluteal artery perforator/inferior gluteal artery perforator), as are the lateral and midaxial regions (e.g., lumbar intercostal artery perforator, thoracodorsal artery perforator, and supraclavicular artery perforator). Flow is therefore preferentially directed laterally away from the midline or midaxial regions to maintain adequate blood supply to adjacent regions populated with fewer perforators.

Because of the multiple communicating branches between linking vessels, there is a very large variation in pedicle flap design potential. The ultimate flap design depends on the overall vascular territory (perforasome) of the involved perforator. Perforators with a very large perforasome will have a higher degree of freedom in flap design and orientation (e.g., the internal mammary artery perforator flap that has been harvested horizontally, obliquely, or vertically).[32–36]

Third Principle

Preferential filling of perforasomes occurs within perforators of the same source artery first, followed by perforators of other adjacent source arteries. An example of this includes the descending branch of the lateral femoral circumflex artery (anterolateral thigh flap); perforator B will vascularize perforators A and C and will then capture adjacent vascular territory perforasomes such as the anterior medial thigh or superficial femoral artery perforasomes (Fig. 18). Vascular filling and density are maximized in the periphery of the perforasome within the same source artery. The linking vessels then emanate from this main perforasome to perforasomes of adjacent vascular territories from other source arteries (e.g., anteromedial thigh perforators). Single large perforators originating from a source artery that does not have a series of sequential perforators along its course (e.g., medial circumflex femoral artery) will have less of an axial vascular distribution.

Fourth Principle

Mass vascularity of a perforator found adjacent to an articulation is directed away from that same articulation (e.g., distally and proximally based radial artery perforator flaps) (Fig. 19),

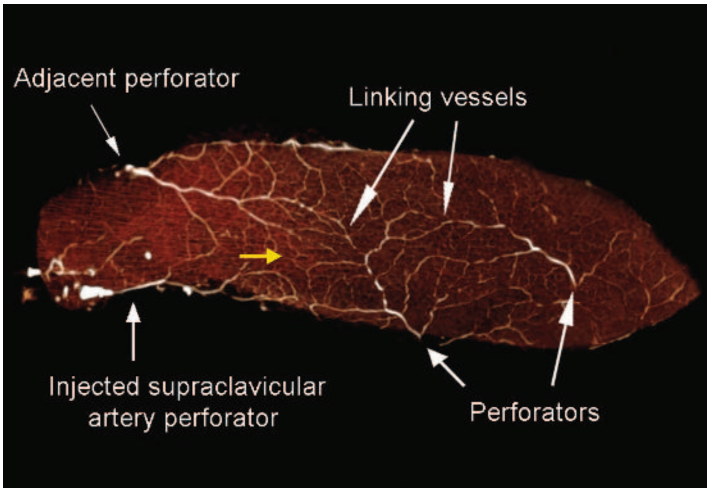

Fig. 11. Computed tomographic angiography scan (anteroposterior view) showing the supraclavicular skin. A supraclavicular artery perforator was injected with contrast. Note large linking vessels coursing perpendicular to the midline of the trunk. Linking vessels are parallel to the main axis of vascularity of the flap and maintain communication between adjacent perforators. Note multiple communicating branches between linking vessels. *Yellow arrow* shows direction of flow.

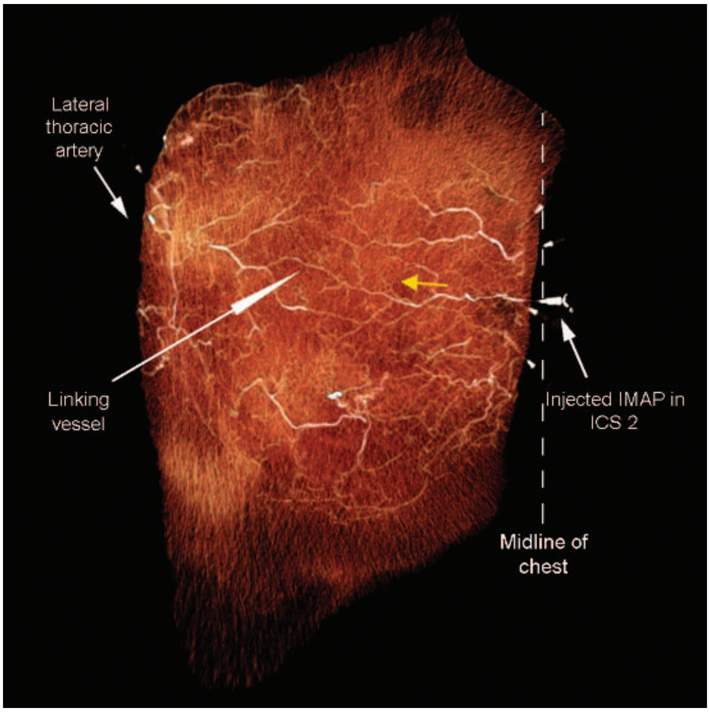

Fig. 12. Computed tomographic angiography scan (anteroposterior view) showing the skin from the anterior trunk (hemichest). An internal mammary artery perforator (*IMAP*) in the second intercostal space (*ICS*) was injected with contrast. Linking vessels are seen coursing perpendicular to the midline and away from the midline (seen here connecting with the lateral thoracic artery). *Yellow arrow* shows direction of flow.

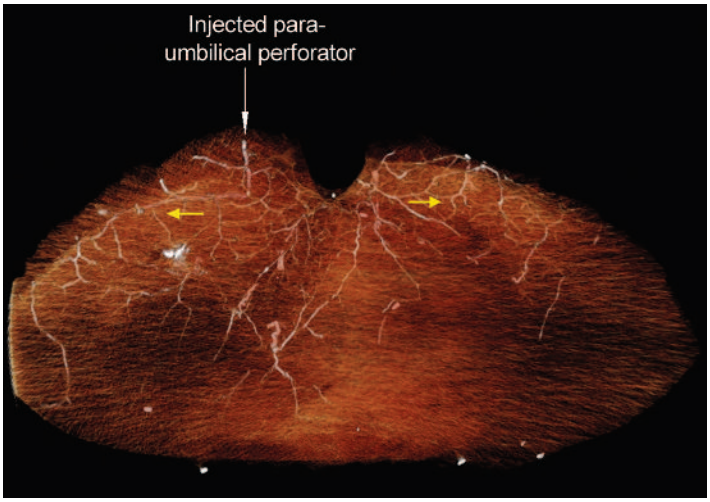

Fig. 13. Computed tomographic angiography scan (anteroposterior view) showing the lower transverse abdominal skin flap. A right paraumbilical artery perforator was injected with contrast. Flow is determined by linking vessels, which can be seen traveling perpendicular to the midline and away from the midline in a bidirectional fashion. *Yellow arrows* show direction of flow.

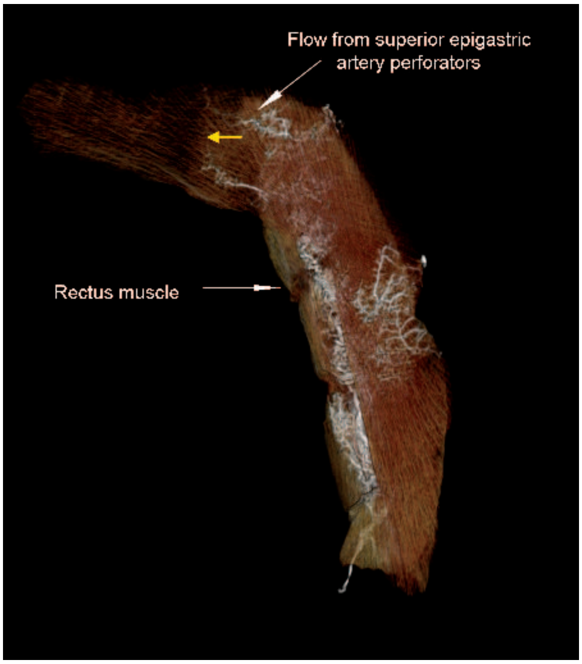

Fig. 14. Computed tomographic angiography scan (anteroposterior view) showing an extended vertical rectus myocutaneous flap, where the superior skin flap is extended to the region below the inframammary fold. The superior epigastric artery perforators were found to have linking vessels perpendicular to the midline, with flow directed away from the midline. *Yellow arrow* shows direction of flow.

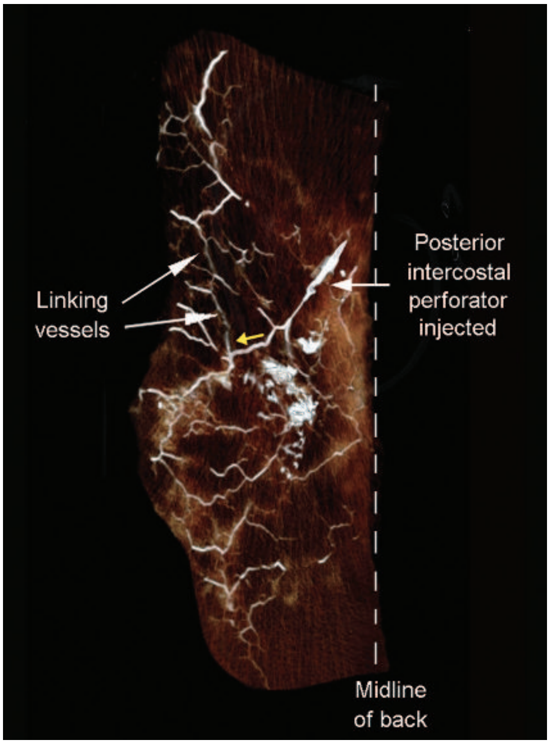

Fig. 15. Computed tomographic angiography scan (anteroposterior view) showing a hemiback flap where a posterior intercostal perforator was injected with contrast. *Yellow arrow* shows direction of flow.

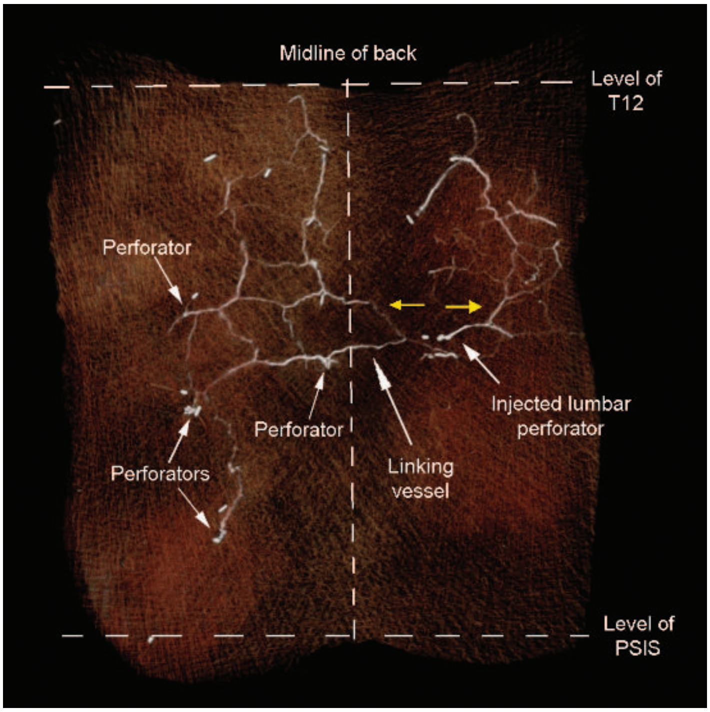

Fig. 16. Computed tomographic angiography scan (anteroposterior view) showing the entire lumbar skin from the T12 level to the posterior superior iliac spine (*PSIS*). The lumbar perforator was injected with contrast and found to perfuse across the midline and ipsilaterally in a transverse direction. Linking vessels can be seen crossing the midline and communicating with contralateral lumbar perforators. The axis of flow is directed along the axis of linking vessels, which are predominantly perpendicular to the trunk midline. *Yellow arrows* show direction of flow.

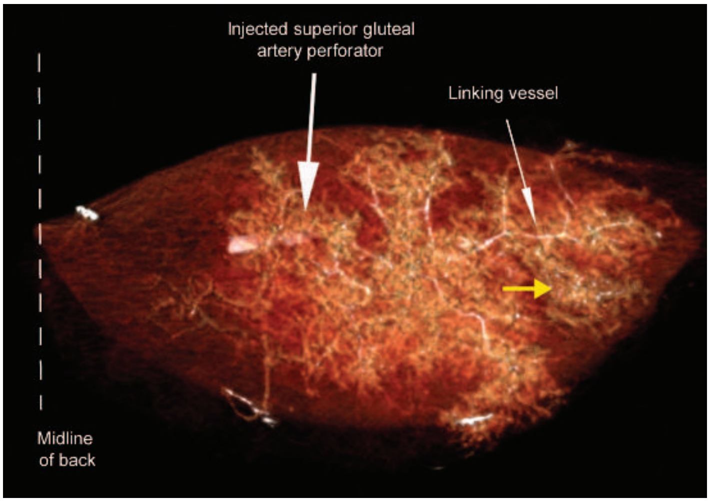

Fig. 17. Computed tomographic angiography scan (anteroposterior view) showing the gluteal region where a superior gluteal artery perforator close to the midline was injected with contrast. Note direction of linking vessel and overall axis of flow, which is perpendicular to the midline of the trunk. Note also the direction of flow, which is directed predominantly away from the midline. *Yellow arrow* shows direction of flow.

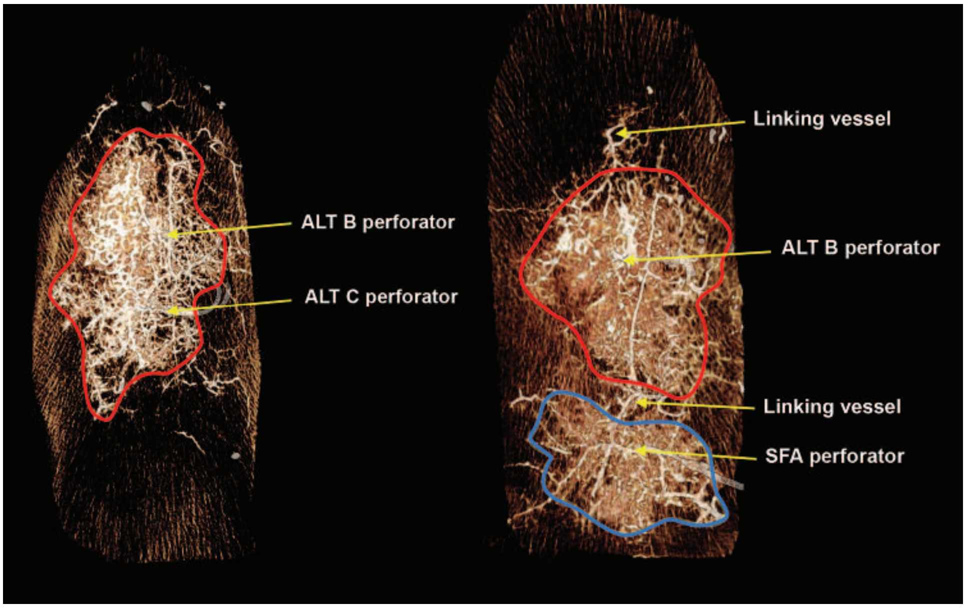

Fig. 18. Computed tomographic angiography scan (anteroposterior view) showing the anterior thigh skin. Preferential filling of perforators within the same source artery is demonstrated in this anterolateral thigh (*ALT*) flap, as perforators B and C from the descending branch of the lateral femoral circumflex artery are perfused before perforators from the superficial femoral artery (*SFA*).

whereas perforators found at a midpoint between two articulations (e.g., upper extremity) (Fig. 20) or at the midpoint in the trunk have a multidirectional flow distribution. Therefore, flap design should take into consideration perforator location (Fig. 21). Linking vessels found between two adjacent perforators have a bidirectional flow, which provides yet another mechanism of vascular protection against injury (**Supplemental Digital Content 1 through 4**).

DISCUSSION

Increased knowledge of vascular anatomy has played a critical role in increasing our understanding and use of perforator flaps in the clinical arena. As we shift toward increased use of single perforator–based flap reconstructions, knowledge of individual perforator vascular anatomy supersedes that of source artery vascular anatomy. Each perforator has its own vascular territory, called a perforasome, which carries a multidirectional flow pattern that is highly variable and complex. These perforasomes are linked to one another by both direct and indirect linking vessels, which themselves are linked by communicating branches. These numerous vascular connections confer further protection from ischemia and vascular injury in case of trauma. Linking vessels allow communication with adjacent perforasomes and follow a direction that is parallel to the direction of perforator flow. Therefore, perforator flap skin paddles should be parallel to the linking vessel orientation whenever possible. These linking vessels make it possible to harvest large perforator flaps based on a single perforator, such as the extended anterolateral thigh flap.[31] When a perforator flap is harvested, all muscle and cutaneous branches from the source artery are ligated, which results in hyperperfusion of the selected perforator. Increased vascular filling pressures clinically dilate the perforator itself and allow extensive interperforator flow by means of opening and recruitment of additional linking vessels. These linking vessels, both direct and indirect, are subject to higher than normal filling pressures and are able to capture additional adjacent perforator vascular territories (perforasomes).

Perforator flaps designed at a midpoint between two articulations can be designed in multiple fashions because of the multidirectional perforator flow distribution. Dense fibrous septae and ligamentous attachments can be found overlying each major articulation to maintain proper skin stability and draping during flexion and extension. Also, each articulation forms a boundary for a different vascular territory proximal and distal to that same articulation. Both of these factors might explain why perforators adjacent to an articulation will have flow directed away from it. Midline crossover of perforator flow was found in almost all

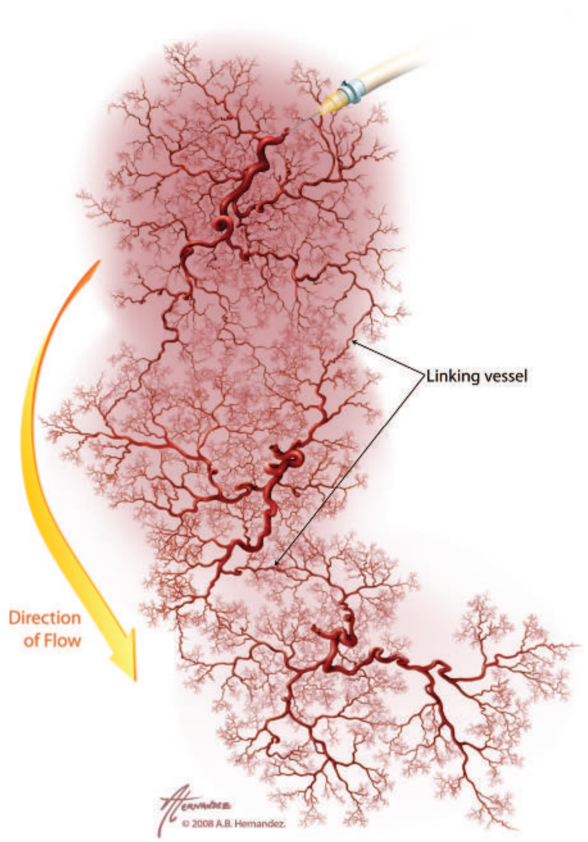

Fig. 19. Perfusion in multiple perforasomes via linking vessels. Vascular density is maximal within the cannulated perforator and its corresponding perforasome and decreases distally away from the midline of the trunk or an articulation. The orientation of linking vessels determines the orientation of vascular flow within the flap. Direction of flow is predominantly perpendicular to the trunk midline and parallel to the vertical axis of the limbs.

instances in the trunk by means of direct and indirect linking vessels. Indirect flow through the subdermal plexus becomes important when there is a paucity of subcutaneous tissue (less direct linking vessels) and where skin is intimately adherent over bone (e.g., sternum, anterior tibia).

CONCLUSIONS

Each perforator holds a unique vascular territory (perforasome). Perforator vascular supply is highly complex and follows some common guidelines. Both direct and indirect linking vessels play a critical part in perforator flap perfusion. Every perforator has the potential to become either a pedicle or a free perforator flap, depending on the size of the source artery. As a result, this allows a myriad of perforator flap designs that can be tailored to better reconstruct defects. The reconstructive surgeon now has more options in replacing like with like. Local flap alternatives become more plentiful and flap design is limited only by the availability of clinically relevant perforators close to the defect for pedicle perforator flaps. Free-style perforator flap options are limited only by the size and length of their respective source arteries and veins.

Hyperperfusion of a single perforator can capture multiple adjacent perforasomes. This explains why large perforator flaps can be harvested based on a single perforator (e.g., extended anterolateral thigh flap).[31] Additional adjacent perforasome territories can be captured through direct and indirect linking vessels by means of hyperperfusion. The perforasome theory described provides additional insight into the mech-

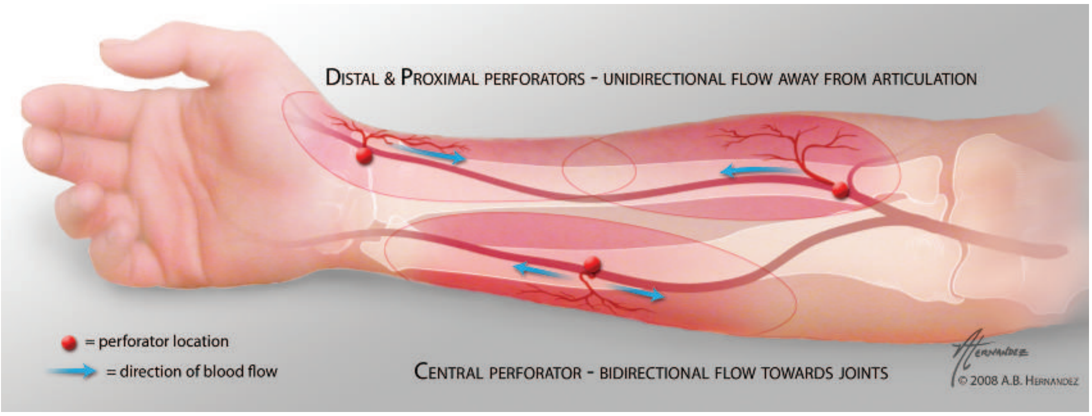

Fig. 20. Direction of perforator flow between articulations. Perforators in the extremities that are found close to an articulation will have preferential flow away from that articulation, whereas midpoint perforators will have bidirectional flow.

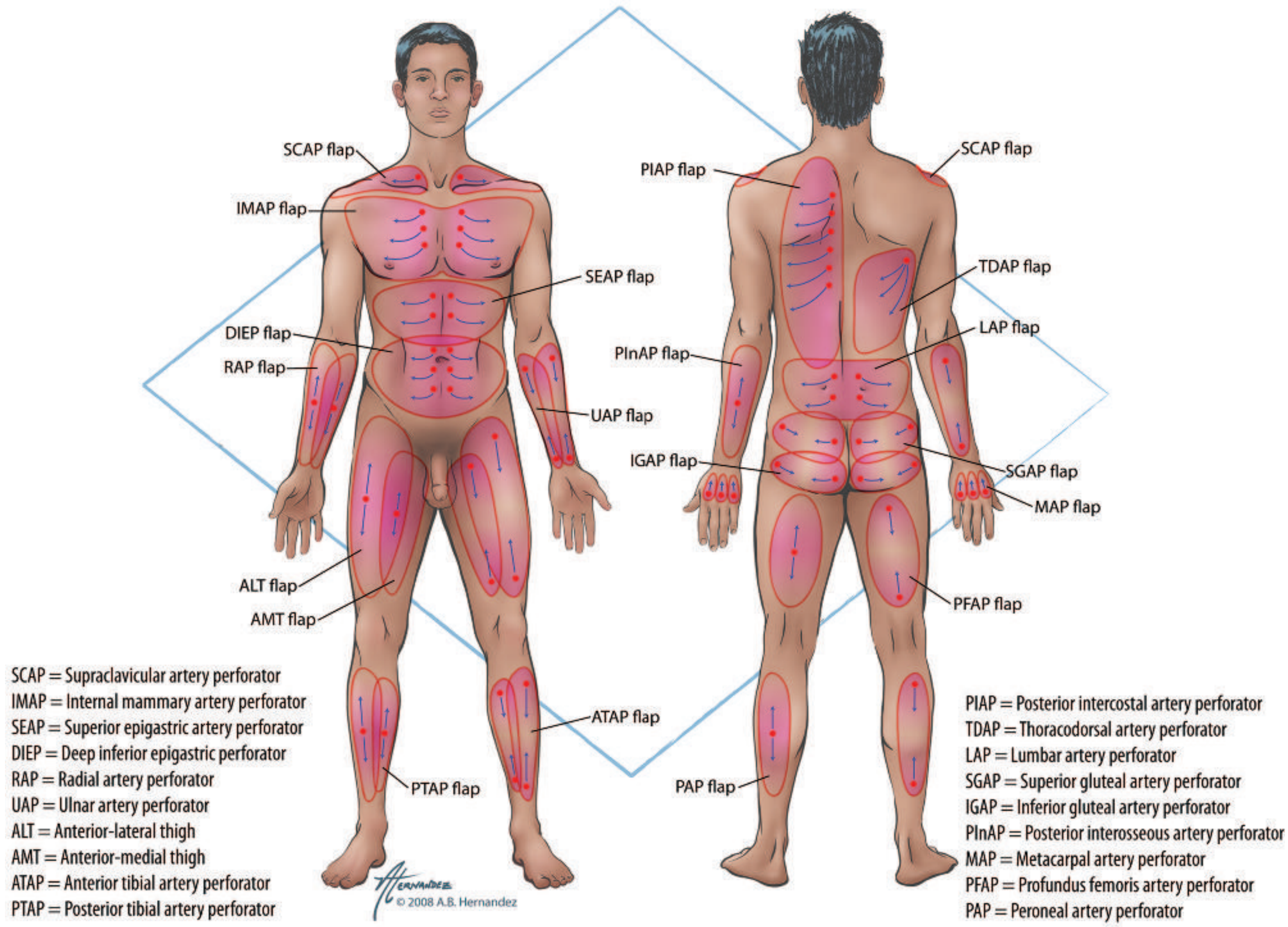

Fig. 21. Common perforasomes of the body demonstrating axis and direction of flow based on location.

anisms of perforator flap vascularity and serves to facilitate the understanding, design, and clinical use of both free and pedicle perforator flaps.

Michel Saint-Cyr, M.D.
Department of Plastic Surgery
University of Texas Southwestern Medical Center
1801 Inwood Road
Dallas, Texas 75390-9132
michel.saint-cyr@utsouthwestern.edu

REFERENCES

1. Manchot C. *The Cutaneous Arteries of the Human Body*. New York: Springer-Verlag; 1983.
2. Cormack GC, Lamberty BG. Fasciocutaneous vessels: Their distribution on the trunk and limbs, and their clinical application in tissue transfer. *Anat Clin.* 1984;6:121–131.
3. Taylor GI, Palmer JH. The vascular territories (angiosomes) of the body: Experimental study and clinical applications. *Br J Plast Surg.* 1987;40:113–141.
4. Salmon M. *Arteries of the Skin*. London: Churchill Livingstone; 1988.
5. Taylor GI, Caddy CM, Watterson PA, Crock JG. The venous territories (venosomes) of the human body: Experimental study and clinical implications. *Plast Reconstr Surg.* 1990;86:185–213.
6. Morris SF, Taylor GI. Predicting the survival of experimental skin flaps with a knowledge of the vascular architecture. *Plast Reconstr Surg.* 1993;92:1352–1361.
7. Tang M, Yin Z, Morris SF. A pilot study on three-dimensional visualization of perforator flaps by using angiography in cadavers. *Plast Reconstr Surg.* 2008;122:429–437.
8. Nakajima H, Minabe T, Imanishi N. Three-dimensional analysis and classification of arteries in the skin and subcutaneous adipofascial tissue by computer graphics imaging. *Plast Reconstr Surg.* 1998;102:748–760.
9. Koshima I, Soeda S. Inferior epigastric artery skin flaps without rectus abdominis muscle. *Br J Plast Surg.* 1989;42:645–648.
10. Koshima I, Moriguchi T, Fukuda H, Yoshikawa Y, Soeda S. Free, thinned, paraumbilical perforator-based flaps. *J Reconstr Microsurg.* 1991;7:313–316.
11. Koshima I, Soeda S. Free posterior tibial perforator-based flaps. *Ann Plast Surg.* 1991;26:284–288.
12. Koshima I, Moriguchi T, Soeda S, Kawata S, Ohta S, Ikeda A. The gluteal perforator-based flap for repair of sacral pressure sores. *Plast Reconstr Surg.* 1993;91:678–683.
13. Koshima I, Moriguchi T, Etoh H, Tsuda K, Tanaka H. The radial artery perforator-based adipofascial flap for dorsal hand coverage. *Ann Plast Surg.* 1995;35:474–479.
14. Koshima I, Urushibara K, Inagawa K, Hamasaki T, Moriguchi T. Free medial plantar perforator flaps for the resurfacing of

finger and foot defects. *Plast Reconstr Surg.* 2001;107:1753–1758.
15. Koshima I, Nanba Y, Tsutsui T, et al. Superficial circumflex iliac artery perforator flap for reconstruction of limb defects. *Plast Reconstr Surg.* 2004;113:233–240.
16. Koshima I, Narushima M, Mihara M, et al. New thoracodorsal artery perforator (TAPcp) flap with capillary perforators for reconstruction of upper limb. *J Plast Reconstr Aesthet Surg.* November 12, 2008 [ePub ahead of print].
17. Kroll SS, Rosenfield L. Perforator-based flaps for low posterior midline defects. *Plast Reconstr Surg.* 1988;81:561–566.
18. Allen RJ, Treece P. Deep inferior epigastric perforator flap for breast reconstruction. *Ann Plast Surg* 1994;32:32–38.
19. Angrigiani C, Grilli D, Siebert J. Latissimus dorsi musculocutaneous flap without muscle. *Plast Reconstr Surg.* 1995;96:1608–1614.
20. Wei FC, Jain V, Suominen S, Chen HC. Confusion among perforator flaps: What is a true perforator flap? *Plast Reconstr Surg.* 2001;107:874–876.
21. Hallock GG. Direct and indirect perforator flaps: The history and the controversy. *Plast Reconstr Surg.* 2003;111:855–865.
22. Wei FC, Celik N. Perforator flap entity. *Clin Plast Surg.* 2003;30:325–329.
23. Blondeel PN, Morris SF, Hallock GG, et al eds. *Perforator Flaps: Anatomy, Technique and Clinical Applications.* St. Louis: Quality Medical; 2006.
24. Taylor GI, Palmer JH. 'Angiosome theory'. *Br J Plast Surg.* 1992;45:327–328.
25. Saint-Cyr M, Schaverien M, Arbique G, Hatef D, Brown SA, Rohrich RJ. Three- and four-dimensional computed tomographic angiography and venography for the investigation of the vascular anatomy and perfusion of perforator flaps. *Plast Reconstr Surg.* 2008;121:772–780.
26. Schaverien M, Saint-Cyr M, Arbique G, Brown SA. Arterial and venous anatomies of the deep inferior epigastric perforator and superficial inferior epigastric artery flaps. *Plast Reconstr Surg.* 2008;121:1909–1919.
27. Schaverien M, Saint-Cyr M, Arbique G, Brown SA, Rohrich RJ. Three- and four-dimensional arterial and venous anatomies of the thoracodorsal artery perforator flap. *Plast Reconstr Surg.* 2008;121:1578–1587.
28. Schaverien M, Saint-Cyr M, Arbique G, Hatef D, Brown SA, Rohrich RJ. Three- and four-dimensional computed tomographic angiography and venography of the anterolateral thigh perforator flap. *Plast Reconstr Surg.* 2008;121:1685–1696.
29. Tan BK, Ng RT, Tay NS, Tan BS. Tissue microangiography using a simplified barium sulphate cadaver injection technique. *Ann Acad Med Singapore* 1999;28:152–154.
30. Mosahebi A, Disa JJ, Pusic AL, Cordeiro PG, Mehrara BJ. The use of the extended anterolateral thigh flap for reconstruction of massive oncologic defects. *Plast Reconstr Surg.* 2008;122:492–496.
31. Saint-Cyr M, Schaverien M, Wong C, et al. The extended anterolateral thigh flap: Anatomical basis and clinical experience. *Plast Reconstr Surg.* 2009;123:1245–1255.
32. Neligan PC, Lipa JE. Perforator flaps in head and neck reconstruction. *Semin Plast Surg.* 2006;20:56–63.
33. Yu P, Roblin P, Chevray P. Internal mammary artery perforator (IMAP) flap for tracheostoma reconstruction. *Head Neck* 2006;28:723–729.
34. Vesely MJ, Murray DJ, Novak CB, Gullane PJ, Neligan PC. The internal mammary artery perforator flap: An anatomical study and a case report. *Ann Plast Surg.* 2007;58:156–161.
35. Neligan PC, Gullane PJ, Vesely M, Murray D. The internal mammary artery perforator flap: New variation on an old theme. *Plast Reconstr Surg.* 2007;119:891–893.
36. Yu P. Characteristics of the anterolateral thigh flap in a Western population and its application in head and neck reconstruction. *Head Neck* 2004;26:759–769.